

Distributed Control of Networked Nonlinear Euler-Lagrange Systems

Ali Reza Mehrabian

PhD Thesis
in
The Department
of
Electrical and Computer Engineering

Presented in Partial Fulfillment of the Requirements
for the Degree of Doctor of Philosophy at
Concordia University
Montreal, Quebec, Canada

February 2013

© Ali Reza Mehrabian, 2013

**CONCORDIA UNIVERSITY
SCHOOL OF GRADUATE STUDIES**

This is to certify that the thesis prepared

By: **Alireza Mehrabian**

Entitled: **Distributed Control of Networked Nonlinear Euler-Lagrange Systems**

and submitted in partial fulfillment of the requirements for the degree of

DOCTOR OF PHILOSOPHY (Electrical and Computer Engineering)

complies with the regulations of the University and meets the accepted standards with respect to originality and quality.

Signed by the final examining committee:

_____ Chair
Dr. R. Zmeureanu

_____ External Examiner
Dr. A.K. Misra

_____ External to Program
Dr. Y.M. Zhang

_____ Examiner
Dr. A.G. Aghdam

_____ Examiner
Dr. S. Hashtrudi Zad

_____ Examiner
Dr. L. Rodrigues

_____ Thesis Co-Supervisor
Dr. K. Khorasani

_____ Thesis Co-Supervisor
Dr. S. Tafazoli

Approved by _____
Dr. J.X. Zhang, Graduate Program Director

January 10, 2013

Dr. Robin Drew, Dean
Faculty of Engineering and Computer Science

ABSTRACT

Distributed Control of Networked Nonlinear Euler-Lagrange Systems

Alireza Mehrabian, Ph.D.

Concordia University, 2013

Motivated by recent developments in formation and cooperative control of networked multi-agent systems, the main goal of this thesis is development of efficient synchronization and formation control algorithms for distributed control of networked nonlinear systems whose dynamics can be described by Euler-Lagrange (EL) equations. One of the main challenges in the design of the formation control algorithm is its optimality and robustness to parametric uncertainties, external disturbances and ability to reconfigure in presence of component, actuator, or sensor faults. Furthermore, the controller should be capable of handling switchings in the communication network topology.

In this work, nonlinear optimal control techniques are studied for developing distributed controllers for networked EL systems. An individual cost function is introduced to design a controller that relies on only local information exchanges among the agents. In the development of the controller, it is assumed that the communication graph is *not* fixed (in other words the topology is switching). Additionally, parametric uncertainties and faults in the EL systems are considered and two approaches, namely adaptive and robust techniques are introduced to compensate for the effects of uncertainties and actuator faults.

Next, a distributed H_∞ performance measure is considered to develop distributed robust controllers for uncertain networked EL systems. The developed

distributed controller is obtained through rigorous analysis and by considering an individual cost function to enhance the robustness of the controllers in presence of parametric uncertainties and external bounded disturbances. Moreover, a rigorous analysis is conducted on the performance of the developed controllers in presence of actuator faults as well as fault diagnostic and identification (FDI) imperfections.

Next, synchronization and set-point tracking control of networked EL systems are investigated in presence of three constraints, namely, (i) input saturation constraints, (ii) unavailability of velocity feedback, and (iii) lack of knowledge on the system parameters. It is shown that the developed distributed controllers can accomplish the desired requirements and specification under the above constraints.

Finally, a quaternion-based approach is considered for the attitude synchronization and set-point tracking control problem of formation flying spacecraft. Employing the quaternion in the control law design enables handling large rotations in the spacecraft attitude and, therefore, any singularities in the control laws are avoided. Furthermore, using the quaternion also enables one to guarantee boundedness of the control signals both with and without velocity feedback.

ACKNOWLEDGEMENTS

I would like to express my acknowledgements and thanks to all the people who helped me during my Ph.D. studies at Concordia University. Specifically, I would like to cordially thank *Nastaran* for her kindness, patience and continuous support during my good days and bad days in the past five years. In addition, I would like to sincerely thank both my supervisors, Professor K. Khorasani and Dr. S. Tafazoli, for their very kind support and guidance throughout my Ph.D. program. My special thanks belongs to Professor Khorasani for his prompt feedbacks on my reports, papers and thesis as well as his efforts to arrange my defence session in a timely manner.

I would also like to specially thank the members of my doctoral committee for reviewing my thesis and providing me valuable comments during my Ph.D. studies and the final version of my Ph.D. thesis.

I would like to thank all my friends, Concordia University staff and people who provided me a source of support and hospitality.

This thesis is dedicated to:

Nastaran,
Tahmineh and Hassan,
Ameneh and Rizwan.

TABLE OF CONTENTS

LIST OF FIGURES	x
LIST OF TABLES	xii
1 Introduction	1
1.1 Motivation	1
1.2 Literature Review	2
1.2.1 Formation Control	4
1.2.2 Consensus Algorithms	6
1.2.3 Synchronization Control of Networked EL systems	13
1.2.4 Spacecraft Formation Flying	14
1.2.5 FDI Approaches in Robotic Systems	18
1.3 General Problem Statement	25
1.4 Thesis Overview and Research Objectives	26
1.5 Thesis Contribution	30
2 Background, Preliminaries and Definitions	33
2.1 Multi-Agent Systems	33
2.2 Euler-Lagrange (EL) Systems	34
2.3 Examples of Nonlinear Euler-Lagrange Systems	38
2.3.1 Two-Link Robot Manipulator	38
2.3.2 Spacecraft Attitude Dynamics	40
2.4 The Kronecker Product	46
2.5 Vector/Matrix Calculus	47
2.6 Definition of a Saturation Function	48
2.7 Information Structure and Neighboring Set	49

2.8	Hamilton-Jacobi-Bellman (HJB) Equations	52
2.9	Stability Analysis and Theorems	53
2.9.1	Lyapunov Stability Theorem	55
2.9.2	Input to State Stability Theorem	57
2.9.3	Stability Analysis of Switched Systems	58
2.10	Concluding Remarks	62
3	Distributed Optimal Formation Control of Euler-Lagrange Systems	63
3.1	Introduction and Problem Statement	63
3.1.1	Communication Network Topology	64
3.1.2	Synchronization Error	65
3.1.3	Statement of the Problem	66
3.2	Optimal Synchronization Control of the EL Systems	67
3.2.1	Discussion on the Existence of a Solution	73
3.2.2	Stability Analysis	75
3.3	Synchronization Control of Uncertain EL Systems	77
3.3.1	Adaptive Control of Uncertain EL Systems	78
3.3.2	Robust Synchronization Control of Uncertain EL Systems	80
3.4	Control Recovery in Presence of Additive Actuator Faults	84
3.5	Simulation Studies: Distributed Control of Networked Spacecraft	88
3.5.1	Control of Networked Uncertain Spacecraft	91
3.5.2	Control of Networked Spacecraft Subject to Actuator Fault	92
3.6	Concluding Remarks	100
4	Distributed H_∞-Optimal Formation Control of EL Systems	105
4.1	Introduction and Problem Statement	105
4.1.1	Communication Network Topology and Synchronization Error	107

4.1.2	The \mathcal{L}_2 -Gain of General Networked Nonlinear Systems	107
4.1.3	ISS of General Networked Nonlinear Systems	108
4.1.4	Statement of the Problem	110
4.2	Distributed H_∞ State Synchronization Control of EL Systems	110
4.2.1	Discussions on Existence of a Solution	115
4.2.2	Stability Analysis of the Networked EL Systems	118
4.3	ISS of the Networked EL Systems	120
4.3.1	ISS with Switchings in the Communication Topology	121
4.4	Control Recovery in Presence of Additive Actuator Faults	123
4.4.1	Reconfiguration w/ Imperfection in the Fault Detection	124
4.4.2	Reconfiguration w/ Imperfection in the Fault Identification	126
4.4.3	Reconfiguration w/ Imperfection in the Fault Isolation	130
4.5	Simulation Studies: Distributed Control of Networked Spacecraft	131
4.5.1	Robust Distributed Control of Networked Spacecraft	131
4.5.2	Robust Reconfigurable Control of Networked Spacecraft	137
4.6	Concluding Remarks	144
5	Constrained Synchronization Control of Networked EL Systems	145
5.1	Introduction and Problem Statement	145
5.1.1	Communication Network Topology	146
5.1.2	Statement of the Problem	147
5.2	Distributed Constrained Nonlinear Control	148
5.2.1	Distributed State Synchronization w/ Bounded Input	150
5.3	Distributed Output Feedback Constrained Nonlinear Control	154
5.3.1	Output Feedback Synchronization w/ Bounded Input	155
5.4	Cooperative Reconfiguration w/ Actuator Saturation Faults	159

5.5	Simulation Results	167
5.5.1	Synchronization Control with Input Saturation Constraints . .	167
5.5.2	Cooperative Controller Reconfiguration	179
5.6	Concluding Remarks	182
6	Quaternion-Based Spacecraft Formation Control	186
6.1	Introduction and Problem Statement	186
6.1.1	Spacecraft Attitude Error Dynamics	187
6.2	Formation Attitude Synchronization and Tracking with Bounded Input	189
6.3	Formation Control with Bounded Input without Velocity Feedback .	193
6.4	Simulation Studies	198
6.5	Concluding Remarks	215
7	Conclusions and Future Work Directions	217
7.1	Conclusions	217
7.2	Suggestions for Future Research	220
A	Simulation Validation	223
A.1	Simulation Validation	224

LIST OF FIGURES

1.1	Applications for multi-agent coordinated control.	3
1.2	Hierarchical decomposition of a cooperative team design.	4
2.1	A space robot system with n manipulators.	38
2.2	Three sample communication network topologies.	51
3.1	The communication topologies considered in the simulations.	89
3.2	Attitude synchronization under the proposed adaptive controller.	93
3.3	Velocity synchronization under the proposed adaptive controller.	94
3.4	Attitude synchronization under the proposed robust controller.	95
3.5	Velocity synchronization under the proposed robust controller.	96
3.6	Control efforts under the proposed adaptive controller.	97
3.7	Control efforts under the proposed robust controller.	98
3.8	Spacecraft attitudes with additive actuator fault.	101
3.9	Spacecraft angular velocities with additive actuator fault.	102
3.10	Attitude synchronization recovery under the proposed algorithm.	103
3.11	Velocity synchronization recovery under the proposed algorithm.	104
4.1	The three communication graphs considered in the simulations.	132
4.2	Spacecraft attitudes under the proposed adaptive control law.	134
4.3	Spacecraft attitudes rates under the proposed control law.	135
4.4	Fault magnitude vs its estimate.	139
4.5	Spacecraft attitudes without controller reconfiguration.	140
4.6	Controller reconfiguration with imperfection in the fault identification.	142
4.7	Controller reconfiguration with imperfection in the fault isolation.	143

5.1	The communication network in the first two case studies	168
5.2	The communication network in the second part of the simulations .	171
5.3	The angular positions of the networked robots <i>w/o</i> velocity feedback	173
5.4	The angular velocities of the networked robots <i>w/o</i> velocity feedback	174
5.5	The control efforts of the networked robots <i>w/o</i> velocity feedback .	175
5.6	The angular positions.	176
5.7	The angular velocities.	177
5.8	The control efforts.	178
5.9	Reconfig. control of three robotic manipulators.	183
5.10	Scaled responses of three robotic manipulators.	184
6.1	The quaternions <i>w/</i> velocity feedback and the gains set #1	200
6.2	The angular velocities <i>w/</i> velocity feedback and the gains set #1 . .	201
6.3	The control efforts <i>w/</i> velocity feedback and the gains set #1	202
6.4	The quaternions <i>w/o</i> velocity feedback and the gains set #1	203
6.5	The angular velocities <i>w/o</i> velocity feedback and the gains set #1 . .	204
6.6	The control efforts <i>w/o</i> velocity feedback and the gains set #1	205
6.7	The quaternions <i>w/</i> velocity feedback and the gains set #2	206
6.8	The angular velocities <i>w/</i> velocity feedback and the gains set #2 . .	207
6.9	The control efforts <i>w/</i> velocity feedback and the gains set #2	208
6.10	The quaternions <i>w/o</i> velocity feedback and the gains set #2	209
6.11	The angular velocities <i>w/o</i> velocity feedback and the gains set #2 . .	210
6.12	The control efforts <i>w/o</i> velocity feedback and the gains set #2	211
A.1	Simulation software validation.	224

LIST OF TABLES

3.1	Physical parameters for each spacecraft in the network	90
3.2	Nominal physical parameters of the spacecraft in the network	90
3.3	Monte Carlo simulation results	99
4.1	The mean values for the control efforts	136
4.2	The state synchronization errors comparison	136
4.3	Comparing the synchronization errors w/ a controller in the literature	137
5.1	Physical parameters for each manipulator in the network	167
5.2	Performance of the state synchronization control strategies.	169
6.1	The two sets of selected controller gains	199
6.2	Performance of proposed constrained controllers	213
6.3	Performance of proposed constrained velocity-free controllers	213
6.4	Performance loss in absence of angular velocity feedback	214
6.5	Performance comparison and analysis.	216

LIST OF SYMBOLS

$(.)^T$	Matrix transpose
$(.)^{-1}$	Matrix inverse
$(.)^{-T}$	Transpose of an inverted matrix
$(.) \otimes (.)$	Kronecker product operator
\inf	Infimum
$\mathbf{C}(\cdot)$	The vector of Coriolis and centrifugal forces
$\mathbf{D}(\cdot)$	The general inertia matrix
$d_i(j)$	Indegree of the j -th node of a graph
$d_o(j)$	Outdegree of the j -th node of a graph
$\bar{E}(\cdot)$	A 3×3 matrix
\mathcal{E}	Graph edge set
$ \mathcal{E} $	The graph size (the number of edges of a graph)
\mathbf{e}	Euler axis
F	Force
\mathcal{F}	Rayleigh dissipation function
\mathcal{F}^I	The inertial frame
\mathcal{F}^B	The body frame of an spacecraft
$\mathfrak{F}(\cdot)$	A nonlinear function in the matrix format
$\bar{\mathfrak{F}}(\cdot)$	A nonlinear function in the matrix format
$\mathbf{F}(\cdot)$	A matrix
$\mathbf{F}_{jn,i}$	The interaction terms among the j -th and the n -th agent and according to the i -th communication graph
$f(\cdot)$	A function

$f(\cdot)$	A vector of functions
$\mathbf{G}(\cdot)$	The gravitational generalized force vector (GFV)
$\mathfrak{G}(\cdot)$	A nonlinear function in the matrix format
$\bar{\mathfrak{G}}(\cdot)$	A nonlinear function in the matrix format
\mathcal{G}	A directed-graph (digraph)
$g_i(\cdot)$	The i -th element of $\mathbf{G}(\cdot)$
g	The Earth's gravitational constant
\mathcal{H}	A set of h communication graphs
I_i	The moment of inertia about the center of mass of the i -th manipulator
\mathfrak{I}_n	An $n \times n$ identity matrix
\mathbf{J}	The moment of inertia matrix for an spacecraft
\mathcal{J}	The performance index (PI)
$\mathfrak{J}(\cdot)$	The Jacobian matrix
\mathcal{K}	A class of functions
\mathcal{K}_∞	A class of functions
\mathcal{KL}	A class of functions
$\mathcal{K}(\cdot)$	Kinetic energy function
\mathcal{L}	Laplacian matrix of a graph
$\mathcal{L}_{NC}(\cdot)$	<i>Non-conservative</i> Lagrangian function
l_i	The length of the i -th manipulator
l_{ci}	Distance from the center of the gravity of the i -th manipulators to its corresponding joint
\mathcal{N}_j	The neighboring set of the j -th node of a graph
$\mathcal{N}_{j,i}$	The neighboring set of the j -th node of the i -th graph
$ \mathcal{N}_j $	The number of neighbors of the j -th node of a graph

$ \mathcal{N}_j $	The number of neighbors of the j -th node of the i -th graph
$\mathcal{P}(\cdot)$	Potential energy function
\mathcal{P}_{NC}	<i>Non-conservative</i> potential energy function
\mathbf{p}	Momentum
$\bar{\mathbf{Q}}_{j,i}$	A symmetric positive semi-definite matrix
\mathbf{q}	Generalized coordinates
\mathbf{q}^*	The desired position
$\tilde{\mathbf{q}}_j$	The error vector for the j -th agent in the network
\mathbf{q}_{jn}	The synchronization error
\mathbf{q}_{jn}^b	A positive constant
$\vec{\mathbf{q}}$	Unit quaternions
$\vec{\mathbf{q}}_j^*$	the desired attitude of the spacecraft formation
$\bar{\mathbf{q}}$	Vector part of the quaternions
\hat{q}_4	Scalar part of the quaternions
$\vec{\mathbf{q}}_{jn}$	The attitude state error between the j -th and n -th spacecraft
$\bar{\mathbf{R}}$	Rotation matrix
\mathbb{R}	The set of real numbers
$\mathbf{R}_{j,i}$	A symmetric positive definite matrix
$\mathbf{S}(\cdot)$	An skew-symmetric matrix
s_j	Weighted error for the j -th agent in the network
s_{jn}	Weighted synchronization error between the j -th and n -th agents in the network
$\text{Sat}(\cdot)$	Saturation function
\mathbf{u}	The input vector
\mathbf{u}_j^s	The station-keeping controller

$\mathbf{u}_{j,i}^f$	The formation-keeping controller
$\bar{u}_r^{\max} _j$	Maximum control effort in the r -th input channel of the j -th agent
\mathcal{V}	The graph node set
\mathbf{w}	A vector
\mathbf{x}	The state vector
\mathbf{Y}	The <i>regressor matrix</i>
\mathcal{Y}	The value function
\mathbf{y}	A vector
$\nabla_{\mathbf{w}}(\cdot)$	Gradient with respect to vector \mathbf{w}
$\alpha_{j,i}$	A constant parameter for the j -th agent and i -th communication network topology
Θ	A vector for unknown but constant parameters
θ	Yaw angle
ϕ	Pitch angle
ψ	Roll angle
ω	angular velocity
ω_{jn}	The relative angular velocity vector between the j -th and n -th spacecraft
ρ	External torque (disturbance)
φ	Euler angle
$\delta(t)$	External signal (disturbance)
$\delta\mathbf{q}$	The virtual displacement corresponding to the variation of \mathbf{q}
δW	Virtual work
$\delta\vec{q}_j$	The station-keeping error for the j -th spacecraft in the network
$\delta\omega_j$	The station-keeping angular velocity error for the j -th spacecraft
Λ	Graph weighted adjacency matrix

$\Lambda_{jn,i}^p$	A positive definite matrix
Λ_j^p	A positive definite matrix
$\tau_{j,i}$	An auxiliary control input for the j -th agent under the i -th communication network topology
$\chi(x)$	A monotonically increasing odd function

Chapter 1

Introduction

1.1 Motivation

Synchronization and cooperative behavior in nature can be observed in several places. Examples of such behavior are the collective animal behavior, i.e. flocking of birds, shoaling and schooling fish, swarming behavior of insects, and herd behavior of land animals. Such behaviors happen in human societies as well. As an example, large stock market trends often begin and end with periods of frenzied buying (bubbles) and selling (crashes). Many observers cite these episodes as clear examples of herding behavior that is irrational and driven by emotion – greed in the bubbles, fear in the crashes, which is mainly due to the fact that individual investors join the crowd of others in a rush to get in or out of the market [1].

Researchers have studied these behaviors in different fields of science. For example, the phenomenon of herd behavior was among the first topics studied in social psychology [2]. Collective decision making and swarm intelligence of animals are also studied by several researchers (see [3, 4] and references therein). In addition, by studying and modeling swarm behavior of creatures, in recent years,

many optimization algorithms have been introduced [5, 6, 7].

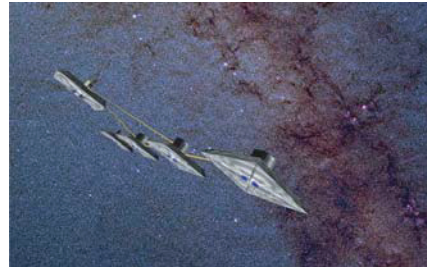
In recent years, there has been an increasing interest in the systems and control community for studying cooperative and distributed control of networked multi-agent systems. Networked multi-agent systems consist of several dynamically decoupled agents. However, these agents need to coordinate their states (or outputs) in order to accomplish missions that neither can do alone. This coordination and cooperation requires exchange of information between the agents' controllers, therefore, a network of agents is created. Networked multi-agent systems have many interesting applications. This new technology enables cooperation between agents in a network for completing complex tasks that cannot be accomplished alone. Examples of such tasks include cooperative control of multiple uninhabited (unmanned) ground, air or marine vehicles (UGVs, UAVs, or MAVs) for search, exploration, surveillance, rescue operations and mapping unknown or partially known environments (see Fig. 1.1(a)). In the space domain, this technology will enable one to design efficient control algorithms for control of multiple spacecraft (SC) or space robots in a formation for observation of distant planets/stars or on-orbit repairing and servicing (see Fig. 1.1(b)). Furthermore, this technology can be employed to move large objects, drill holes and pitch tents in tight coordination by using autonomous rovers on the Earth or other planets (see Figs. 1.1(c) and Fig. 1.1(d)).

1.2 Literature Review

Synchronization, cooperation and formation control in a network of uninhabited autonomous systems has been studied extensively in the past few years. Different frameworks and several approaches to formulating and solving this problem have



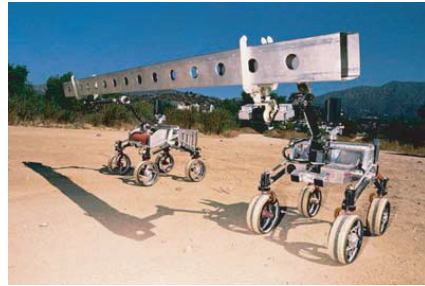
(a) Multi-agents for search, exploration, surveillance.



(b) Artist's concept of Terrestrial Planet Finder (TPF). Picture courtesy: JPL, NASA



(c) Cooperative object transportation using quad-rotors. Work done at GRASP Lab, University of Pennsylvania.



(d) Cooperative robots share the load. Picture courtesy: NASA

Figure 1.1: Possible applications for multi-agent synchronization and coordinated control.

been investigated and different information flow architectures have been considered [8, 9, 10, 11, 12]. Moreover, the problem of cooperation in a network has been considered at different levels. At the high-level, one may consider task assignment, timing and scheduling, navigation and path planning, as well as reconnaissance and map building [13, 14, 15] (see Fig. 1.2). In the mid-level, cooperative rendezvous, formation keeping, application of consensus algorithms, collective motion, and formal methods based on flocking/swarming ideas can be considered [8, 10, 12, 16, 17]. In low-level one can consider individual energy management, communication management, input/output management and data acquisition management.

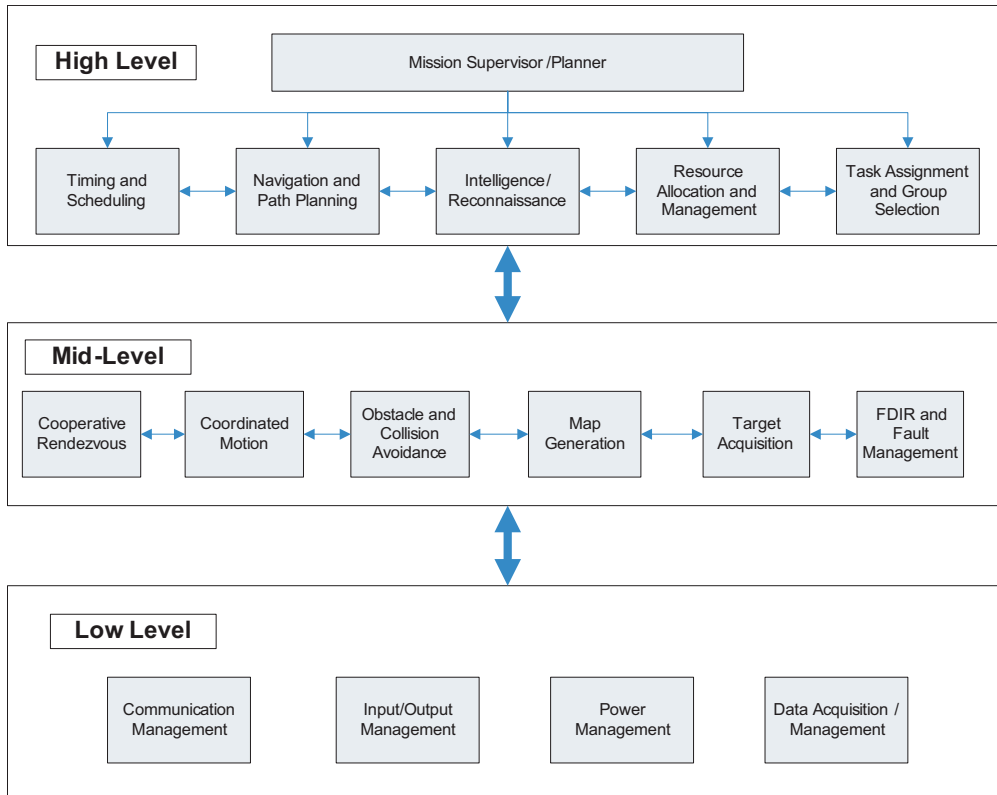


Figure 1.2: Hierarchical decomposition of a cooperative team design.

The present research work, only covers cooperation in the mid-level, therefore, the literature reviewed in this section are on the mid-level cooperation, i.e. formation control and consensus algorithms.

1.2.1 Formation Control

The main goal in formation control of a network of systems (agents) is to make sure that the agents in the network achieve a predefined and given geometry or posture and possibly follow a desired set-point or trajectory that is provided by a supervisor. This posture should be preserved during the mission, therefore, the agents in the network should, ideally, behave as a single rigid body. Based on this

property, a predefined trajectory is usually provided to the agents, e.g. in the form of a (virtual) leader command [12]. The agents in the network should follow this given and desired set-point or trajectory while the agents keep their relative positions and preserve the required posture, consequently, the stability of the entire formation should be guaranteed.

Reference [18] proposed the following five different architectures, which can be considered for the formation control of networked of agents, namely: (i) Multi-Input Multi-Output (MIMO) approach, (ii) leader-follower approach, (iii) virtual structure approach (or virtual leader), in which the entire formation is considered as a virtual structure, (iv) cyclic approach with non-hierarchical control architecture, and (v) behavioral approach.

In the MIMO architecture, the entire dynamics of the networked agents is considered as a single MIMO system. Hence, in this architecture any form of conventional control strategies, e.g. optimal, nonlinear, or robust control strategies can be implemented to achieve the formation objectives.

The most commonly employed approach in the literature is the leader-follower architecture [19, 20, 21]. In this approach a hierarchical control architecture is considered with one or more of the agents as the leader(s), and other agents as the followers. The followers receive leader information and should track their states. This structure can also be constructed in a tree form. The advantages of this approach are that it has a predictable and understandable behavior, the formation is preserved even if the leader is perturbed, and that group behavior can be inspected by properly setting the leader actions. However, lack of an explicit feedback to the formation, from the followers to the leader, is a disadvantage of this structure. Also, the failure of the leader implies the failure of the entire formation as mentioned in [8, 16].

In the virtual structure approach, the entire formation is treated as a single unit. Three steps are considered for a control design by using the virtual structure approach, i.e. (i) defining the desired dynamics of the virtual structure, (ii) transforming the states of the virtual structure into the states of individual agents, and (iii) designing the control laws for each agent accordingly. One can point out the following advantages for this approach, namely, its simplicity in defining the coordinated behavior of the group, keeping the formation during different maneuvers, and existence of a feedback from the agents to the virtual structure. The disadvantage of this structure is in its limitation in applications to time-varying or frequently changing formations.

In the cyclic architecture, the agents are connected to each other in a cyclic form rather than a hierarchical architecture [22]. In the behavioral approach several commands are combined to reach different and probably competing goals or several behaviors, e.g. collision avoidance, obstacle avoidance, and formation keeping for agents. The control law for each agent is a weighted average of the control for each behavior. Since competing behaviors are averaged, occasionally strange and unpredicted behaviors may occur. Despite the advantages of simple derivation of the control strategies, as well as an explicit feedback to the formation, and capability of decentralized implementation, there are some weaknesses as well. For example, in some scenarios, group behavior cannot be explicitly defined and mathematical stability analysis is not straightforward to accomplish as mentioned in [16].

1.2.2 Consensus Algorithms

An early study on decision making process in a team (or networked agents) has appeared in [23], which was followed by studies in [24, 25, 26]. More recently,

references [11, 12, 17, 19, 27, 28, 29, 30, 31, 32, 33, 34, 35, 36, 37, 38] considered this problem. In these studies, each agent in the network has access to limited information from other agents, or to information of its neighbors. The final state of the agents in the network is decided by the network members.

Consensus algorithms are one of the tools that are used for analysis of networked systems where the network information structure has a vital effect on the control law design where only part of the information is available to each agent. As discussed in [17], consensus problems deal with the agreement of a group of agents upon specific “quantities of interest”. In this configuration the agents try to decide and agree among themselves upon what the final state should be. The state where all the “quantities of interest” are the same is called the consensus state [12]. One can set the states of the agents (e.g. positions and velocities in the case of Euler-Lagrange systems) as the “quantities of interest”.

In [17], linear and nonlinear consensus protocols are applied to directed and undirected networks with fixed and switching topologies. A disagreement function was introduced as a Lyapunov function to provide a tool for convergence analysis of an agreement protocol in a switching network topology. The authors have shown that the maximum time-delay that can be tolerated by a network of integrators applying a linear consensus protocol is inversely proportional to the largest eigenvalue of the Laplacian of the information flow graph or the maximum degree of the nodes of the network.

In [19], the coordination problem is discussed for a team of agents using “nearest neighbor rule” for both leaderless and leader-follower configurations. The main focus of this work is on heading angle alignment in undirected graphs where the agents have simple integrator dynamics and the agents have the same speed but have different headings. In the leader-follower case, the leader can affect the

followers whenever it is in their neighboring set. However, there is no feedback from the followers to the leader. It is shown that the connectivity of the graph on average (connection of union of graphs) is sufficient for convergence of the heading angles of the agents. The neighboring set assignment is switching and so the team structure is dynamic. In [39], asynchronous protocols for consensus seeking are introduced. Some updating rules for the control input of agents with discrete-time dynamical equations are suggested so that the consensus state would take a desirable predefined value [12].

In [40], passivity is used as a tool to achieve network agreement (or consensus) for a class of agents with dynamics which can satisfy the passivity conditions. The group main goal is to reach at a predefined common velocity (or any other interpretation of the derivative of a state), while the relative positions (the difference between a common state in the group) converge to a desired compact set. Based on this method a Lyapunov function can be constructed for stability analysis in a distributed communication network with bidirectional links. The designed controller is a filter which has a nonlinear function of the relative states as its input and is designed based on passivity properties. The relation between the topology and the stability of the formation is provided. In [41], a wider class of systems, i.e. nonlinear dissipative systems are considered and synchronization in a strongly connected network of agents with this dynamical property is discussed.

In some references, the communication delay is considered in modeling of a network of agents with point-mass model. For an example, one can refer to [17] in which directed and undirected networks with fixed and switching topologies are considered. It is assumed that the delayed information from other agents is compared with the delayed value of the agent's own dynamics at each time step. On the other hand in [42] the delayed information of the neighbors are compared with the

current value of the agents' state. In this work, uniformly delayed communication links are analyzed for consensus algorithms.

Distributed consensus control of double-integrator systems is considered in [30, 31]. In [31] the authors consider both switching in the communication network topology with *constant* (fixed) communication network delay. The authors in [30] consider two general settings, namely, the setting where the interaction topologies for the position and velocity information flows is modeled by different graphs and the setting where the interaction topologies for the position and velocity information flows being modeled by the same graph. In the first setting, the authors have derived some sufficient conditions on the *fixed* communication topologies for the agents to achieve consensus. In the second setting, the consensus algorithm under both *fixed* and *time-varying* directed interaction topologies is investigated. Observed-based consensus control for linear multi-agent systems is considered in [32] and heading consensus of networked systems with communication time-delay is studied in [33]. Consensus control of a class of multi-agent nonlinear systems with sampled data information exchange is studied recently in [34], where the authors by constructing a Lyapunov-Krasovskii functional and using Finsler's lemma, we have theoretically proved that consensus with time-varying velocities in strongly connected networks can be achieved if the sampling interval is less than the maximal allowable sampling interval, which can be obtained by solving a feasible linear matrix inequality (LMI). A discrete-time second-order consensus algorithm for networks of agents with nonuniform and time-varying communication delays under dynamically changing communication network topologies in a sampled-data setting is investigated recently in [35]. Consensus control of *linear* systems with switching in the communication network topology is considered recently in [36].

Broadcast gossip algorithms are employed for development of quantized consensus in networked multi-agent systems recently in [37]. The authors in [38] studied consensus with Markovian switching topologies and data-sampled communication.

In reference [24] a Linear Quadratic Regulator (LQR) problem was solved by “using” a team of decision makers and not “in” a team of decision makers. In other words, each decision maker is responsible for design of an optimal control at one (or some) time instant where the other decision makers should decide what the best (optimal) actions for the next time instants are to minimize a common cost function. Therefore, although the problem is dynamic in the sense that at the outset an optimal controller is designed to minimize a cost function with a given dynamical constraint, none of the decision makers has an individual dynamics. This implies that each decision maker can be interpreted as the state of a discrete-time system at one time only and not as an independent dynamical system.

In more recent literature, an optimal approach to networked multi-agent systems is considered in [43, 44, 45, 46, 47] for formation control and in [12, 48, 49, 50, 51, 52, 53, 54, 55] for consensus seeking.

The approach in [45] is based on individual agent cost optimization for achieving team goals under the assumption that the states of the other team members are constant. The concepts of Nash equilibrium, penalty function as well as Pareto optimality are used for design of optimal controllers. In [47, 52] the effects of the amount of information on the value of the cost function is investigated. The authors have shown that the centralized architecture will result in the lowest cost value whereas the decentralized solution will increase the cost value. In order to solve an optimal consensus problem, the authors in [49] have assumed an individual agent cost for each team member. In evaluating the minimum value of each individual cost, the states of the other agents are assumed to be constant. For a switching

network structure the dwell-time that provides stability of the network subject to the switching structure is found. In [50] an H_2 optimal semi-stable methodology for stabilization of linear discrete-time systems is proposed. The authors then proposed a consensus algorithm and have shown that this protocol is a semi-stable controller which can solve the consensus seeking problem. The authors in [51] have shown that a specific type of graphs, i.e. de Bruijn's graph, is optimal for consensus seeking problem and with respect to a given cost function. An individual cost function is considered in [12] for obtaining a consensus protocol in a network of linear multi-agent systems, by considering two types of network structures, i.e. leader-less and leader-follower networks, where the leader receives feedback from the followers in the neighboring set. The authors in [53] consider nonlinear communication protocols for the consensus problem. Maximization of the second eigenvalue of the weighted graph Laplacian is considered in [54] to enhance robustness of the networked agents to disturbances.

In most of the referenced work in the previous paragraph, the optimal control problem is based on the individual cost definition for the team members. However, a single team cost function formulation has been proposed in only a few work [44, 46]. In [46], optimal control strategy is applied for formation keeping and a single team cost function is utilized. The authors in [44] assumed a distributed optimization technique for formation control in a leader-follower structure. The design is based on dual decomposition of local and global constraints. However, in this approach, the velocity and position commands are assumed to be available to the entire team. In [48], the dynamics of the entire network are decomposed into two components, namely one in the consensus space and the other in its orthogonal subspace. A set of Linear Matrix Inequalities (LMIs) are then used to guarantee the stability and consensus achievement using an H_2 design strategy. In [12] a team

cost function is defined and a min-max problem was solved to obtain a cooperative optimal solution for the consensus seeking problem based on game theory and using linear matrix inequalities (LMIs). It was shown that the results obtained by this approach yield a lower cost values when compared to the values obtained by the LMI-based optimal control technique.

The problem of team cooperation, and specifically consensus seeking with switching topologies, has received a wide attention in recent years and has been discussed in the literature from different perspectives [56, 57, 58, 59, 60, 61]. The work conducted in [56] can be considered as one of the pioneer work in this area in which algorithms for distributed computation in a network with a time-varying network structure are analyzed. Specifically, in [57] for a discrete-time model of processors and a given number of tasks, convergence of a consensus algorithm in a time-varying structure is discussed given that some restrictions are imposed on the frequency of availability of the inter-agent communication links. One of the underlying assumptions in many of the related work on switching networks is that the graph describing the information exchange structure is a balanced graph. The authors in [61] considered balanced information graphs and have shown the stability under switching time-delayed communication links. The analysis is performed by introducing a Lyapunov functional and then by showing the feasibility of a set of linear matrix inequalities (LMIs). In [11, 58] switching control laws are designed for a network of agents with undirected and connected underlying graphs whereas in [60], consensus in a directed, jointly connected and balanced network is discussed. The necessary conditions for achieving consensus in a network are discussed in [59]. The concept of “preleader-follower” is introduced as a new approach to achieve consensus in a network of discrete-time systems. The basic properties of stochastic matrices are used to guarantee consensus achievement in a network with

switching topology and time-delayed communication links.

1.2.3 Synchronization and Formation Control of Networked EL systems

Synchronization and formation control of multiple EL systems have attracted attention of several researchers recently [62, 63, 64, 65, 66, 67, 68, 69, 70, 71, 72, 73, 74, 75]. Reference [62] considered output and state synchronization of multi-agent EL systems. This study also considers communication delays and changes in the communication topology in the design of the synchronization controllers. However, it considers complete knowledge of the states (for state synchronization) and the EL systems structure and parameters. The author also provides a solution to the bilateral teleoperation problem (which considers one master robot and a single slave robot) in presence of parameter uncertainty and communication delays. Synchronization of networked EL systems in presence of control effort saturations is considered in [63] by considering full and partial state feedback. However, the algorithm introduced in [63] considers fixed communication network topology. Adaptive control algorithms are employed for distributed synchronization and formation control and state synchronization of networked EL systems in [64, 71, 72]. The authors in [64] proposed a formation control algorithm in presence of communication delays and parameter uncertainty. However, the communication topology is assumed to be fixed and full state measurements is required. In addition, the authors assume availability of the desired trajectory to all the agents in the formation. For development of the formation control law in [71], similar to [64], the authors assume availability of the desired trajectory to all the agents in the formation. State synchronization (consensus seeking) in presence of switchings in the communication

network topology is considered in [72]. The authors have shown that synchronization can be achieved in presence of constant communication time-delay. Reference [65] considers formation control in presence of multiple leaders on a directed graph. The parameters of the EL system are assumed to be constant and unknown.

The authors in [66, 67, 70, 75] employ potential functions to develop consensus and formation control algorithms, which allow the agents to avoid obstacles and collisions during the formation maneuver. Parameter uncertainties are handled by using adaptive control schemes in [67] and [75]. Nonholonomic constraints are considered in [68] and time-varying communication delays are handled similar to the scattering approach in [62]. Synchronization control of multiple robotic manipulators over a fixed and strongly connected communication graph with and without full state measurement is studied and validated experimentally in [69]. Distributed robust control in presence of parameter uncertainty is considered in [73] on strongly connected fixed graphs. Time-varying communication network topologies is considered in [74] for systems with parameter uncertainty.

1.2.4 Spacecraft Formation Flying

Spacecraft (SC) formation flying is a new technology which plays an important role in the future space missions such as NASA's Terrestrial Planet Finder (TPF) Mission and Space Telescope assembly [76, 77], the European Space Agency's (ESA) similar mission, called Darwin [78], among many others. Several algorithms have been proposed for the attitude and/or position synchronization and control of multiple SC in deep space and in low orbit [16, 79, 80, 81, 82, 83, 84, 85, 86, 87, 88, 89, 90, 91]. In this thesis, we consider attitude synchronization and tracking, therefore, we review recent literature on this topic in this subsection. Position synchronization

problem for spacecraft formation flying missions is not considered in this thesis.

The single SC attitude control and fault-tolerant attitude control with/without using angular velocity measurement is also studied in the literature [92, 93, 94, 95, 96]. Reference [79] is one of the earliest papers on coordinated attitude control of SC. This paper investigates the use of one-leader, multiple-leader, and barycenter coordination strategies. The one-leader coordination strategy requires that one SC serves as the reference SC, the leader, for the rest of the SC, the followers, in the formation. The followers then track the leader, possibly with a constant offset. The multiple-leader approach involves splitting the formation into two or more groups and assigning one or more fleet leaders. In this case, the fleet leaders act as the reference SC for the group leaders, which in turn, act as the reference SC for the group followers. This approach results in a hierarchical communication topology. The most interesting coordination strategy discussed is the barycenter strategy. In this strategy, the j -th SC uses the position information of the neighboring SC to determine the barycenter of their locations. The barycenter is then used as the desired location of the j -th SC. In a subsequent paper [80] the authors use the same type of formulation to develop one-leader based coordinated control laws for position and attitude control of a SC formation. The interesting addition of this paper is the application of the one leader coordinated control strategy to the problem of Michelson stellar interferometry.

The authors in [84] developed a distributed controller for the SC formation attitude control problem that they term the coupled dynamics controller. The coupled dynamics controller uses a ring communication topology, where each SC knows the state of two other SC in the formation. The desired state and the state of the two other SC are used to determine the appropriate control torque. A convergence proof

is provided; however the proof does not ensure global convergence of the formation attitude. It requires that the SC begin with no angular rate and that the initial formation error is below a certain limit.

In [86] the authors developed a passivity-based controller for the SC formation attitude control problem. The passivity-based controller uses only attitude information to determine control actions, thus alleviating the need for angular rate measurements. The authors also analytically determine the domain of attraction for the passivity-based controller and the coupled dynamics controller. Later in [16] a more general architecture for SC formation attitude control is introduced by the same authors. The architecture is designed to subsume the leader-follower, behavior-based, and virtual-structure coordination strategies. The authors claim that the architecture is “amenable to analysis via control theoretic methods.” A brief descriptive list of some formation control problems that can be analyzed using the architecture is given. The authors demonstrate the usefulness of the architecture by applying it to the practical problem of Michelson stellar interferometry.

In [97] the authors investigate a centralized implementation of virtual structure coordination strategy using the general architecture. The primary contribution of the paper is the addition of formation feedback to the SC formation. The authors prove the virtual structure control law guarantees the stability and convergence of the system.

A fundamentally difference approach is proposed in [82] for dealing with the SC formation control problems. In this paper, each SC in the formation uses its current desired state and state information communicated by the other SC to determine a quasi-desired state using the reference projection. The quasi-desired state is then used by the SCs attitude controller to determine the appropriate control action. Different types of coordination are possible using the appropriate reference projection.

In the paper, a reference projection is developed for the leader-follower, generalized leader-follower, and the virtual desired attitude coordination strategies. The leader-follower reference projection for the leader is the desired state of the formation, and the current state of the leader is the reference projection for the follower SC. The generalized leader-follower strategy differs in that the reference projection for the followers is a compromise between the desired state and the current state of the leader. The only truly decentralized coordination strategy is the virtual desired attitude strategy, where the reference projection for each SC is a compromise between the desired state and the average state of the SC in the formation. In a later paper [90], the authors discuss applying the idea of reference projections to tracking control and in [91] the authors investigate the idea further and present simulation results.

More recently, [98] introduce a distributed algorithm for SC formation attitude control. The authors consider unit-quaternion in their analysis, which enables large attitude maneuvers. However, the authors consider fixed communication network and full state measurement in their analysis. Communication delays are considered in [99], which extends the results in [98]. Modified Rodriguez Parameters (MRP) are also used in the controller design for SC formation flying in [100]. Communication time-delays are considered in [101]. However, when using MRP SC full attitude rotation maneuvers cannot be executed.

SC attitude synchronization and coordination control without requiring angular velocity feedback is very useful specially when this information is not available due to sensor failure. This problem is considered recently in the literature. Specifically, authors in [89] developed a velocity free attitude tracking algorithm for SC by using leader-follower approach. Consequently, failure of the leader SC will result in failure of the mission.

More recently, [88] developed an attitude synchronization and tracking algorithm for multiple SC formation by using MRP for attitude representation. The advantage of these two studies ([89] and [88]) is that they do not require sharing the estimate of the angular velocity among the SC in the formation, and this considerably reduces the communication load in the formation. Another recent study on velocity-free attitude control of SC formation is reported in [87]. In this paper, the authors use unit-quaternion to describe the SC attitude and extend the results reported in [94] for velocity control of a single SC to SC formation flying. However, in this algorithm it is required that an estimate of the angular velocity is shared among the SC in the formation. Therefore, the algorithm does not reduce the communication among the SC in the formation. However, it is interesting to note that in this algorithm boundedness of the control effort is guaranteed.

1.2.5 Fault Detection and Isolation (FDI) Approaches in Robotic Systems

As it was discussed earlier in this chapter, robotic systems play an important role in automation industries, including manufacturing, assembly, and biotechnology. In addition, there is a growing need for unmanned operation in different service and research sectors such as search and rescue, nuclear waste clean up, planetary exploration, and others where robotic manipulators play an equally important role. However, notwithstanding their widespread applicability and use, robotic systems are known to fail during normal operations due to various faults that include sensor and actuator faults, and component failure [102]. Hence, automated monitoring of the robotic systems and manipulators for any faults and effective accommodation of such faults play a crucial role in the use of robotic manipulators as autonomous

systems.

In this section we provide an overview of FDI approaches presented in the literature for robotic systems. It is, however, important to note that studying FDI algorithms for robots and EL systems is not the main focus of this thesis and it is discussed in this section for elaboration, presentation and introducing the reader to FDI algorithms available in the literature.

Model-based approaches for fault diagnosis of robotic manipulators

Implementation methods for model-based fault detection by using *analytical* redundancy (AR) can be classified into two groups: (1) indirect implementation, based on diagnostic observers for state or parameter estimation; and (2) direct implementation based on parity relation techniques [102, 103]. Early state estimation fault detection algorithms developed for robotic manipulators relied on the assumption that the process is linear (see for example [104]). However, it is shown later that the fault capability of the nonlinear observer-based fault detection approach is significantly better than the linear Luenberger observer based fault diagnosis approach. Various nonlinear diagnostic observer designs have been proposed and implemented on robotic manipulators to detect sensor and actuator faults [105, 106, 107, 108, 109]. Most of the studies on fault detection consider either a sensor fault or an actuator fault. A method based on generalized momenta for actuator fault detection is proposed in [105]. However, the proposed method could not detect sensor faults and was not robust in the presence of disturbance, noise and model-plant mismatch (MPM). The authors, however, presented an adaptive and robust scheme to encompass uncertain robot dynamics in [106, 109]. In [107], a model-based fault-detection approach was successfully demonstrated experimentally. This approach was based on the generation of residuals through a filtered torque estimate which

does not rely upon the measurement of acceleration quantities. Adaptive and robust detection algorithms were also developed in [107] to take into account possible uncertainty in the robot parameters. Sliding mode-based scheme for fault detection for robotic manipulators was also studied in [110].

Parameter estimation methods are used in [111] and [112] to monitor and identify changes in critical parameters due to faults in robotic systems. The method introduced in [111] was shown to be effective for certain types of faults. However the underlying dynamic model was highly simplified (constant inertias and coupling between joints was neglected), which implies again the need for either conservative thresholds, or probable false alarms [107]. A more rigorous approach to the synthesis of fault detection residuals was presented in [113], in which the theoretical maximum number of independent residuals were derived for a manipulator with redundant sensing, based on linearized dynamics for the robot. Dynamic thresholds were developed based on full (nonlinear) manipulator dynamics. The results were promising, however the thresholds required the measurement or estimation of manipulator acceleration which is problematic in practice [107].

Conceptually, direct implementation based on a parity relation is more straightforward than the observer based approach [114]. The literature on parity relation based fault detection of robotic manipulator is not rich. This is mainly due to lack of theoretical work on parity relations for nonlinear systems. Most research results on parity based fault detection techniques are for linear systems. The origin of parity relations based on AR can be found in [103] for linear systems. However, since a robotic manipulator is a nonlinear system, the above-mentioned results cannot be directly applied.

Model-free approaches for fault Diagnosis of robotic manipulators

Model-free approaches to manipulator fault detection include neural networks and fuzzy logic to generate residuals, which relies on the approximation capabilities of these approaches in presence of modeling uncertainty. In [115], a fuzzy logic approach is used to allow for such disturbances, however the approach remains somewhat heuristic. A neural network approach to manipulator fault detection was adopted in [116, 117]. However, the fault detection algorithms are based on a user defined bound on the modeling uncertainty. A comparison among three architectures for residual analysis for robotic manipulator is studied in [118]. Combinations of fuzzy logic and neural network are also employed for fault detection and isolation schemes for robot manipulators in [119]. A combination of H_∞ approach and Radial Basis Functions (RBFs) neural network is introduced in [120].

FDI approaches for single and networked mobile robots

Several FDI approaches have been proposed for mobile robots in the literature. One of the approaches to achieve FDI on mobile robots is based on multiple models and a bank of observers [121]. This fault detection algorithm is presented in [122] where only two possible faults are analyzed: a reduction in the radius of one tire and a periodic bump, without processing the information in the residuals extensively. In [123] the work in [122] is extended through the use of multiple hypotheses to isolate sensor faults. The probability of each hypothesis is calculated using the residuals of the corresponding Kalman filter, showing good results in FDI. Regretfully, in this work there is no description of the isolation criteria used to determine which fault has occurred. A similar bank of Kalman filters is used in [124] to determine

faults (on sensors and actuators) on a four-wheel robot, but in this case the residuals are processed through a neural network to isolate the faults. Similarly, two approaches based on extended Kalman filter and neural networks are developed for detection of two types of faults, namely the loss-of-effectiveness fault and locked-in-place fault in [125]. Another isolation method is presented in [126] where the bank of Kalman filters is combined with a Markov model representation to identify the faults through probability calculations. Another neural network-based model free fault detection algorithm for mobile robots is presented in [127].

Although these works present important advances in FDI, they detect faults only in speed related sensors (e.g., gyros and encoders), leaving behind other important sensors such as sonars, GPS, and magnetic compasses, where FDI is a more complex task [121]. However, in [128] a combination and integration of Kalman filter based sensor fusion and a parity equation based scheme is introduced to continuously monitor all the sensors used in the ground vehicle navigation to ensure the system's health, excluding Differential GPS. Authors in [129] consider non-linear dynamics for detection of change in the wheel radius fault and slipping or skidding faults, which is obtained by extension of the result reported in [107]. Fault detection in the robot navigation system by using hardware redundancy is considered in [130]. Additionally, detection and identification of control software faults for mobile robots is considered in [131]. Soft computing techniques have also been employed for mobile robot fault detection and isolation. For example, an execution monitoring algorithm for mobile robots has been proposed in [132]. An efficient new hybrid approach for multiple sensor fusion and fault detection is proposed in [133] addressing the problem with multiple faults, which is based on conventional fuzzy soft clustering and artificial immune systems. For this new approach, requires no prior knowledge or information about the sensors, or the system behavior, and

no learning processes are required.

Several researchers have proposed multiple approaches for FDI of networked mobile robots [113, 121, 134, 135, 136, 137, 138, 139]. In [134] the authors explain how the redundancy present in cooperative mobile robots can be used to increase the robustness of the group, thus improving the efficiency, but no fault detection system is described. The ALLIANCE architecture presented in [135] shows a simple fault detection system for cooperative robots based on behavioral programming, but fault detection process is limited to detect when a robot has suffered a fatal failure and the authors indicate that it presents a slow response. Using another approach, the work [136] shows a distributed localization scheme for resource limited mobile robots. The algorithm takes advantage of measurement redundancy to improve the localization of each robot and, at the same time, it is used to detect which localization measurements are incorrect, eliminating them from the system. Authors in [137, 138] present a cooperative approach for differential GPS fault detection in unmanned aerial vehicles (UAV). The proposed scheme uses artificial vision-based relative position measurements, aiming to detect wrong GPS absolute position measurements. The approach is based on the fact that in multi-UAV missions, it is possible to take advantage of the capabilities that the team of UAVs offers, to augment each of the individual FDI systems. In [113, 139] multiple layer approaches have been used to achieve FDI in different classes of robotic systems (systems with different levels of resources), so the FDI system can be adapted depending on the redundancy that exists, but the idea of having a cooperative layer within the architecture was not implemented. The result in [121] presents a layered architecture for FDI on cooperative robots that combines the advantages of single and multiple robots fault detection mechanisms, where the different layers can be implemented depending on capabilities and resources of the robots. The proposed architecture

combines existing methods for single robot FDI, where local information is used in order to detect the presence of faults, with the ideas present in cooperative robot FDI systems, where additional information obtained from multiple robots is used for detecting faults in any of the group members; yielding an architecture capable of detecting a wider range of faults in comparison with local information-based FDI systems. In addition, a distributed sensor fault detection for multiple mobile robots is presented in [140]. Also, a distributed, model-based, qualitative fault-diagnosis approach for formations of mobile robots is presented in [141]. This approach is based on a bond-graph modeling framework that can deal with multiple sensor types and isolate process, sensor, and actuator faults. The diagnosis scheme employs relative measurement orderings to discriminate among faults by exploiting the temporal order of measurement deviations.

FDI approaches for space mobile robots and robotic arms

Particle filter (also known as sequential Monte Carlo) is a promising approach for mobile robot fault diagnosis, and has received considerable attention in the past few years [142, 143, 144, 145, 146, 147, 148, 149]. Specifically, a combination of Unscented Kalman Filter (UKF) and the Variable Resolution Particle Filter (VRPF) is proposed in [146]. Decision-theoretic variable resolution particle filter is employed in [142] for fault detection of a six-wheel rocker-bogie rover. An adaptive particle filter is employed in [143]. Softcomputing techniques are also employed for mobile robot fault detection as well [144]. In addition, in [150] a combination of particle filters with Kalman filters is employed for fault detection.

Fault diagnostics and fault tolerant control of space robotic arms have been considered in the literature [151, 152, 153, 154]. A fault detection for robotic arms in presence of measurement noise without using velocity information is introduced

in [151]. A knowledge-based fault detection algorithm for a space robotic arm is presented in [154]. The notion of Variable Assignment Problem (VAP) is introduced in [153] as an abstract framework for characterizing fault diagnosis in space robots. In [152] a fault tolerant approach for space robots is introduced. An overview of recent research work on fault tolerant control of space robots at the University of Texas at Austin is provided in [155].

1.3 General Problem Statement

The main goal of this work is the development of efficient synchronization and formation control algorithms for distributed control of networked nonlinear systems whose dynamics can be described by EL equations. The formation controller must be able to guarantee several properties, including synchronization of their states and following a pre-defined position or trajectory. One of the main challenges in the design of formation control algorithm is its robustness and its ability to reconfigure in the presence of component faults. In other words, it is highly desirable to design a formation control algorithm which can maintain the group behavior and accomplish mission objectives in the presence of undesirable events such as component faults in the agents of the network. Therefore, the designed formation controller must have the capability of changing its gain or restructure in the presence of component faults. As a result, emphasis is put on the development of distributed control strategies that are easy to implement and can be reconfigured in the presence of component faults requiring minimum knowledge from the plant's dynamics. It is also important to make sure that the control algorithm requires minimum information exchange between the agents to accomplish its objectives in normal operation mode. Furthermore, the developed formation control algorithm, in the presence of

component faults should have the ability to reconfigure in order to accomplish mission objectives by requiring minimum information exchange between the agents. It is also highly desirable that the reconfiguration happen as soon as possible in the presence of component faults. Furthermore, there could be some constraints on the availability of information and hence other issues like unavailability of full state measurements must be considered in the design.

1.4 Thesis Overview and Research Objectives

The objectives that are pursued in this thesis are as follows. The organization of the thesis is also outlined below.

- In Chapter 2 basic assumptions and definitions for multi-agent and Euler-Lagrange (EL) systems are provided. We provide the basic assumptions and details on the class of EL systems that is considered in this thesis. We provide two examples of EL systems, which are the two-link manipulators and SC attitude kinematics and dynamics. Definition of the unit quaternions, which is a singularity-free attitude coordinate is also provided in this chapter. Next, we provide the definition of the Kronecker product, a saturation function as well as the information structure that will be used subsequently in this thesis. An overview of the Hamilton-Jacobi-Bellman (HJB) equations for minimization of a general nonlinear cost function is provided, which is followed by an overview on the stability analysis tools, such as Lyapunov theorem, invariance principle and Barbalat's lemma for autonomous and nonautonomous systems. Input-to-state stability (ISS) theorem as well as stability analysis tools for switched systems are provided at the end of this chapter.

- In Chapter 3 we consider distributed state synchronization (or consensus seeking) protocol and set-point tracking control of networked EL systems from optimal control point of view by introducing an objective function to minimize. The EL systems' dynamics are re-written in the state-space form and an optimal general solution is provided by employing HJB equations for switching network topology. A discussion on the existence of a solution to the optimal control problem is provided. Stability analysis of the closed-loop networked EL systems with switchings in the network topology is provided. Parameter uncertainties in the EL systems is also considered in this chapter. Specifically, we modify and amend the developed optimal control structure in order to compensate for the effects of parameter uncertainties. We also discuss and provide a controller reconfiguration strategy to deal with additive actuator fault (*both* intermittent and permanent) in the system is our last objective of this chapter.
- Parameter uncertainties and external disturbances always affect operation and performance of EL systems. Therefore, in Chapter 4, we consider H_∞ -optimal formation control of Euler-Lagrange systems. We formulate the problem of state synchronization (or consensus) protocol and set-point tracking control of multi-agent EL systems as an H_∞ optimal control problem in presence of parametric uncertainty, external disturbances, and actuator faults. We show that state synchronization protocol and set-point tracking controllers can be formally derived by employing our proposed analysis. In addition, we formally show that our proposed distributed control algorithm is input-to-state stable (ISS) where the input is considered to be the parameter uncertainty as well as external disturbances for *both* fixed and switching communication

network topologies. We also consider controller reconfiguration in presence of actuator faults. Note that the controller recovery algorithm that is proposed in Chapter 3 requires the knowledge of the fault bounds for controller reconfiguration. This information has to be provided by the fault detection, isolation and identification (FDI) algorithm that is working in parallel with the controller. However, in this chapter, we propose an adaptive distributed reconfigurable control algorithm, which has the capability of estimating the faults (*both* intermittent and permanent). We incorporate the information provided by the FDI module in the design of the adaptive controller. We consider three main types of imperfections in the FDI algorithm, namely, (1) *fault detection imperfection*, that is when fault is not detected by the FDI algorithm, (2) *fault isolation imperfection*, that is when the fault is detected in the wrong channel or in the wrong agent, and (3) *fault identification imperfection*, that is when the fault estimation is not exact. We show that our proposed distributed reconfigurable controller can maintain the closed-loop networked EL systems stability under these scenarios and can improve the performance of the closed-loop networked EL systems in the third case.

- In Chapter 5 we consider two constraints in the state synchronization control design protocol and set-point tracking control of multi-agent EL systems. Specifically, the first constraint is on the control input the second constraint is on availability of partial state feedback. Therefore, as our first contribution in this chapter, we develop bounded distributed synchronization and set-point tracking controllers with full state feedback. It is shown that boundedness of the control effort is guaranteed globally and independent of initial conditions. Our next contribution in this chapter is concerned with the design

of distributed output feedback controllers for synchronization and set-point tracking of networked EL systems. Our third main objective in this chapter is to design a reconfigurable controller for multi-agent networked EL system in presence of actuator saturation fault. Finally, our last objective of this chapter is to present a switching-based control reconfiguration strategy that is utilized in case of an actuator fault or an actuator saturation constraint to accomplish cooperative control of EL systems. Towards this end, we first introduce a class of distributed controller (denoted as the unconstrained *nominal* controller) that can be used for accomplishing cooperative state synchronization and set-point tracking control objectives. We then introduce a class of distributed constrained controller (denoted as the constrained *reconfigured* controller) that can be used to maintain the overall control objectives of the EL system in presence of actuator faults and actuator constraints. Finally, we introduce a procedure that can be employed to switch between the two distributed constrained controllers (namely, the constrained *nominal* and the constrained *reconfigured* controllers). In presence of actuator faults and actuator saturations, a switching mechanism is introduced to provide a reconfigurable controller for the networked EL system to ensure and maintain the overall mission objectives and requirements.

- In Chapter 6 we extend and modify our proposed controllers in Chapter 5 to introduce two quaternion-based attitude synchronization and set-point tracking controllers for networked SC. Our proposed control algorithms guarantee boundedness of the control efforts for all initial conditions. Furthermore, by using our proposed control laws, the desired attitude coordinates are only provided to a subset of the SC in the formation designated as the formation

leaders. This essentially increases flexibility in the design of the formation structure which increases robustness of the formation to component faults. We then propose a control law which does not require exchange of SC angular velocities (or their estimates) among the SC in the network. Furthermore, we use bidirectional communication between the agents, which increase robustness of the formation to component faults. In the simulations presented our proposed constrained attitude controllers are compared to the controller that is proposed recently in the literature and is shown through simulations that our proposed controller has a better performance.

- Finally, Chapter 7 concludes this thesis and provides guidelines for future research on distributed state synchronization protocol and set-point tracking control of networked EL systems.

1.5 Thesis Contribution

This thesis claims the following major contributions to the field of distributed control of networked multi-agent Euler-Lagrange systems:

1. The first main contribution of this thesis is systematic distributed controller synthesis for networked multi-agent EL systems. Unlike most of the controller design approaches in the literature for networked-multi-agent EL systems (cf. [62, 63, 64, 71, 156] and references therein), which only rely on stability analysis, in this thesis we provide a performance index for each EL system. This performance index is a suitable measure for expected performance of each EL system in the network. By minimizing this performance index we obtain a distributed controller for each agent that guarantees global

state synchronization and set-point tracking for EL systems in the network.

2. The second main contribution of this thesis is considering parameter uncertainty in networked EL systems and switchings in the communication network topology. Both of these problems have been considered separately in the literature, however, since in practice these two challenges may occur concurrently, new stability analysis based on switched systems theory is necessary to demonstrate stability of the entire EL systems network.
3. The third main contribution of this thesis is in the design of controller reconfiguration strategy for multi-agent EL systems subject to *both* intermittent and permanent additive actuator faults. Reconfigurable controller is a challenging problem which is being only considered for single EL systems in the literature. This problem for multi-agent EL systems with switchings in the communication network topology is considered for the first time.
4. The fourth contribution of this thesis is in the development of distributed control of networked EL systems in presence of parameter uncertainties and external disturbances based on H_∞ optimal control approach. Specifically, in this thesis for the first time in the literature we employ H_∞ synthesis to design the state synchronization and set-point tracking for networked EL systems. We also discuss input-to-state stability (ISS) of the networked EL systems for the first time in the literature.
5. The fifth contribution of this thesis is in the analysis and prediction of the performance of the networked EL systems in presence of actuator faults when the developed H_∞ controller is utilized. The following realistic scenarios are considered in our analysis: (1) *fault detection imperfection*, that is when fault

is not detected by the FDI algorithm, (2) *fault isolation imperfection*, that is when the fault is detected in the wrong channel or in the wrong agent, and (3) *fault identification imperfection*, that is when the fault estimation is not exact.

6. The sixth contribution of this thesis is in the development of controller reconfiguration strategy to improve the performance of our proposed H_∞ controller in presence of fault identification imperfection. To the best of our knowledge this realistic problem has not been considered before for single and multi-agent EL systems in the literature.
7. The seventh contribution of this thesis is in the development of distributed control algorithms for multi-agent EL systems in presence of both actuator saturation constraints and in absence of velocity measurements. We have shown in our simulations that our proposed controllers outperform the existing distributed constrained controllers for networked EL systems.
8. The eighth contribution of this thesis is in the development of controller reconfiguration strategy to compensate for the effects of actuator faults which results in a change in the available maximum control effort.
9. The ninth contribution of this thesis is in the extension and modification of our proposed constrained velocity-free controllers for EL systems to attitude control of SC formation flying missions. It is shown in the simulations that our proposed controller outperforms similar controllers in the literature.

Chapter 2

Background, Preliminaries and Definitions

2.1 Multi-Agent Systems

Multi-agent systems, in this thesis, refers to a network of multiple dynamical systems. The dynamics of these systems is not coupled individually, however, the system's dynamic states are coupled through a common (shared) control law. In this thesis we consider a class of nonlinear systems, which are known as Euler-Lagrange (EL) systems. The coupling among the agents of the network can be considered for all the states or only for parts of the states, e.g. outputs of the agents. The control law, which constitutes the connection among the agents in the network can be classified into three general types. The first type of the controllers, which are known as *centralized* controllers (e.g. Multi-Input Multi-Output controllers in [18]), receive the information from all of the agents in the network. The control command, in this case, is generated by a central controller and transmitted to all the agents in the network. The second type of controllers, known as *decentralized*

controllers [157], receive information only from the agent. In this type the communication among the controllers is not preplanned (or predefined) and the communication among the agents can be considered as an stochastic process. Therefore, the controller must make decisions based on the agent's own states. The third type of controllers, known as *distributed* controllers [12], receive information from the associated agent and the neighboring agents. The controller command is then generated based on the information the controller receives. Therefore, the controller needs to know the neighboring agent's states and must have a general knowledge of the network structure.

2.2 Euler-Lagrange (EL) Systems

Two basic approaches have been typically used for modeling physical systems with lumped parameters namely: (1) Derivation of the equations of motion using forces and torque laws, which is also known as the Newton-Euler equations; or (2) Application of variational principles to selected energy functions [158]. Generally speaking the link among different subsystems is that they transform energy within each other. Therefore, it seems natural and advantageous to formulate the modeling problem in terms of energy quantities. The starting point of the variational approach to modeling is the definition of energy functions in terms of sets of generalized coordinates, $\mathbf{q} \in \mathbb{R}^k$ (typically position and charges for mechanical and electrical systems, respectively), where k is the system's degree of freedom. This procedure leads to introduction of the Lagrangian function. In this thesis, it is assumed that the Lagrangian function has the following structure:

$$\mathcal{L}_{NC}(\mathbf{q}, \dot{\mathbf{q}}, t) = \mathcal{K}(\mathbf{q}, \dot{\mathbf{q}}) + \int_0^t \mathcal{F}(\dot{\mathbf{q}}) dt - (\mathcal{P}(\mathbf{q}) + \mathcal{P}_{NC}(\mathbf{q}, t)) \quad (2.1)$$

where $\mathcal{L}_{NC}(\mathbf{q}, \dot{\mathbf{q}}, t)$ is a *non-conservative* Lagrangian function, $\mathcal{K}(\mathbf{q}, \dot{\mathbf{q}})$ is the kinetic energy function, $\mathcal{P}(\mathbf{q})$ is the potential energy function, $\mathcal{P}_{NC}(\mathbf{q}, t)$ is a non-conservative energy function, and $\mathcal{F}(\dot{\mathbf{q}})$ is the Rayleigh dissipation function which satisfies $\dot{\mathbf{q}}^T \frac{\partial \mathcal{F}(\dot{\mathbf{q}})}{\partial \dot{\mathbf{q}}} \geq 0$ and $\frac{\partial \mathcal{F}}{\partial \dot{\mathbf{q}}}(0) = 0$.

Now, let $\delta \mathbf{q}$ denote the virtual displacement corresponding to the variation of \mathbf{q} . D'Alembert's principle indicates that the total virtual work of the total forces on a particle, augmented by the inertial forces, vanishes for reversible displacements [159]. This results in the following equation,

$$\delta W = \sum_j (F_j - \dot{\mathbf{p}}_j) \delta \mathbf{q}_j = 0 \quad (2.2)$$

where δW is the virtual work, F_j is the total force on the j -th particle, \mathbf{p}_j is the momentum of the j -th particle and is defined as $\mathbf{p}_j = m_j \dot{\mathbf{q}}_j$ [159, 160]. Consequently, by applying D'Alembert principle to the Lagrangian defined in (2.1) one obtains [160]:

$$\frac{d}{dt} \left(\frac{\partial \mathcal{K}(\mathbf{q}, \dot{\mathbf{q}})}{\partial \dot{\mathbf{q}}} \right) - \frac{\partial \mathcal{K}(\mathbf{q}, \dot{\mathbf{q}})}{\partial \mathbf{q}} = \zeta \quad (2.3)$$

where $\zeta(\mathbf{q}, \dot{\mathbf{q}}, t) = \int_0^t \mathcal{F}(\dot{\mathbf{q}}) dt - (\mathcal{P}(\mathbf{q}) + \mathcal{P}_{NC}(\mathbf{q}, t))$ is known as the generalized force.

We assume in this thesis that the non-conservative energy function has the following structure,

$$\mathcal{P}_{NC}(\mathbf{q}, t) = -(\mathbf{u} + \delta(t))^T \mathbf{q} \quad (2.4)$$

where $\delta(t) \in \mathbb{R}^k$ is an external signal (disturbance), which is a vector of uniformly bounded and piecewise continuous functions of time, i.e. $\sup_{t>0} \delta(t) < \infty$. Furthermore, it is further assumed that $\mathbf{u} \in \mathbb{R}^k$ is the input to the system. It is assumed

in this thesis that the number of inputs is equal to the number of generalized coordinates, i.e. the EL system is a fully actuated system. We further assume that the potential energy function \mathcal{P} is explicitly independent of time, that is $\mathcal{P} \equiv \mathcal{P}(\mathbf{q})$. Consequently, by noting (2.3), (2.4) the equations of motion can be expressed by the following equation,

$$\frac{d}{dt} \left(\frac{\partial \mathcal{L}(\mathbf{q}, \dot{\mathbf{q}})}{\partial \dot{\mathbf{q}}} \right) - \frac{\partial \mathcal{L}(\mathbf{q}, \dot{\mathbf{q}})}{\partial \mathbf{q}} + \frac{\partial \mathcal{F}(\dot{\mathbf{q}})}{\partial \dot{\mathbf{q}}} = \mathbf{u} + \delta(t) \quad (2.5)$$

where $\mathcal{L}(\mathbf{q}, \dot{\mathbf{q}}) = \mathcal{K}(\mathbf{q}, \dot{\mathbf{q}}) - \mathcal{P}(\mathbf{q})$ is known as a *conservative* Lagrangian. In this thesis, equation (2.5) is called the (first) differential equations of the EL or in short *EL equations*.

Euler-Lagrange systems with quadratic kinetic energy function

In this subsection, we consider a special class of Lagrangians. This class will be the basis of all the Lagrangians we will consider in this thesis. Note that for the development of the EL equation (2.5) it was assumed that the potential energy function \mathcal{P} is independent of time and $\dot{\mathbf{q}}$. We further assume in this thesis that the kinetic energy function is a quadratic function of the vector $\dot{\mathbf{q}}$ of the form:

$$\mathcal{K}(\mathbf{q}, \dot{\mathbf{q}}) = \frac{1}{2} \dot{\mathbf{q}}^T \mathbf{D}(\mathbf{q}) \dot{\mathbf{q}} \quad (2.6)$$

where $\mathbf{D}(\mathbf{q}) \in \mathbb{R}^{k \times k}$ is a symmetric positive definite matrix known as the general inertia matrix. In view of the above assumptions, equation (2.5) can be re-written in the following equivalent form [158]:

$$\mathbf{D}(\mathbf{q}) \ddot{\mathbf{q}} + \mathbf{C}(\mathbf{q}, \dot{\mathbf{q}}) \dot{\mathbf{q}} + \mathbf{G}(\mathbf{q}) + \frac{\partial \mathcal{F}(\dot{\mathbf{q}})}{\partial \dot{\mathbf{q}}} = \mathbf{u} + \delta \quad (2.7)$$

where $\mathbf{C}(\mathbf{q}, \dot{\mathbf{q}})\dot{\mathbf{q}}$ is the vector of Coriolis and centrifugal forces and

$$\mathbf{G}(\mathbf{q}) = \left[g_1(\mathbf{q}), \dots, g_k(\mathbf{q}) \right]^T \triangleq \frac{\partial}{\partial \mathbf{q}} \mathcal{P}(\mathbf{q})$$

which is denoted as the gravitational generalized force vector (GFV).

A space robot system is an example of a dynamic system satisfying the model (2.7) (refer to Fig. 2.1).

Additional properties and assumptions

In this thesis, we consider EL systems satisfying the following important additional properties. These properties will be used subsequently in the development of the control laws and our analysis [158].

Property 2.1.1: Boundedness: the general inertia matrix is bounded, specifically, $\exists \underline{k} > 0, \bar{k} > 0$ such that: $\underline{k} \mathcal{I}_k < \mathbf{D}(\mathbf{q}) < \bar{k} \mathcal{I}_k, \forall \mathbf{q}$, where \mathcal{I}_k is an $k \times k$ identity matrix. GFV is also upper bounded, that is, $0 \leq \sup_{\mathbf{q} \in \mathbb{R}^k} \{|g_i(\mathbf{q})|\} \leq \bar{g}_i, \forall i \in \{1, \dots, k\}$, where $g_i(\mathbf{q})$ denotes the elements of $\mathbf{G}(\mathbf{q})$.

Property 2.1.2: Skew symmetry property: $\dot{\mathbf{D}}(\mathbf{q}) - 2\mathbf{C}(\mathbf{q}, \dot{\mathbf{q}})$ is a skew-symmetric matrix, i.e. $\mathbf{x}^T [\dot{\mathbf{D}}(\mathbf{q}) - 2\mathbf{C}(\mathbf{q}, \dot{\mathbf{q}})] \mathbf{x} = 0$ for any nonzero vector \mathbf{x} .

Property 2.1.3: Linearity in the parameters: $\mathbf{D}(\mathbf{q})\mathbf{a} + \mathbf{C}(\mathbf{q}, \dot{\mathbf{q}})\mathbf{b} + \mathbf{G}(\mathbf{q}) + \frac{\partial \mathcal{F}(\dot{\mathbf{q}})}{\partial \dot{\mathbf{q}}} = \mathbf{Y}(\mathbf{q}, \dot{\mathbf{q}}, \mathbf{a}, \mathbf{b})\Theta$, for all vectors $\mathbf{a}, \mathbf{b} \in \mathbb{R}^k$, where $\mathbf{Y}(\mathbf{q}, \dot{\mathbf{q}}, \mathbf{a}, \mathbf{b})$ is the regressor matrix and Θ is a vector of unknown but constant parameters.

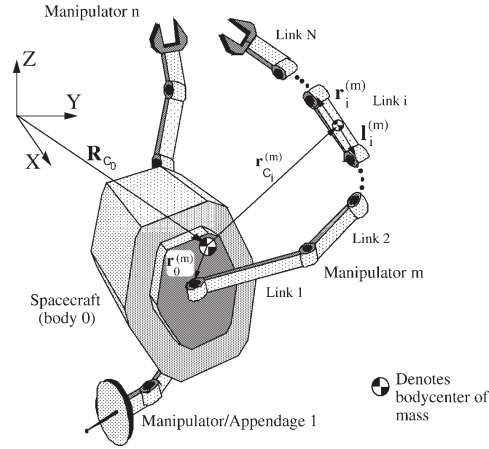


Figure 2.1: A space robotic system with n manipulators [161].

2.3 Examples of Nonlinear Euler-Lagrange Systems

2.3.1 Two-Link Robot Manipulator

A two-link planar robot manipulator has been selected as a representative example in nonlinear control theory and robotics research communities (refer to [162] for more details). This system has two degrees-of-freedom with $\mathbf{q} = [\theta_1, \theta_2]^T$. The moment of inertia about the center of mass of each manipulators is given by $I_i = \frac{1}{12}m_i l_i^2, i \in \{1, 2\}$, where l_1 and l_2 are the length of the first and the second manipulator and m_1 and m_2 denote the mass of the first and the second manipulators, respectively. The dynamics of this system can be expressed by using the EL

equation (2.7), as follows [162],

$$\begin{aligned}
\mathbf{D}(\mathbf{q}) &= \begin{bmatrix} I_1 + I_2 + m_1 l_{c1}^2 + m_2 (l_1^2 + l_{c2}^2 + 2l_1 l_{c2} \cos(\mathbf{q}_2)) & I_2 + m_2 (l_{c2}^2 + l_1 l_{c2} \cos(\mathbf{q}_2)) \\ I_2 + m_2 (l_{c2}^2 + l_1 l_{c2} \cos(\mathbf{q}_2)) & I_2 + m_2 l_{c2}^2 \end{bmatrix} \\
\mathbf{C}(\mathbf{q}, \dot{\mathbf{q}}) &= \begin{bmatrix} -m_2 l_1 l_{c2} \sin(\mathbf{q}_2) \dot{\mathbf{q}}_2 & -m_2 l_1 l_{c2} \sin(\mathbf{q}_2) (\dot{\mathbf{q}}_1 + \dot{\mathbf{q}}_2) \\ m_2 l_1 l_{c2} \sin(\mathbf{q}_2) \dot{\mathbf{q}}_1 & 0 \end{bmatrix} \\
\mathbf{G}(\mathbf{q}) &= \begin{bmatrix} (m_1 l_{c1} + m_2 l_1) g \cos(\mathbf{q}_1) + m_2 l_{c2} g \cos \mathbf{q}_1 + \mathbf{q}_2 \\ m_2 l_{c2} g \cos(\mathbf{q}_1 + \mathbf{q}_2) \end{bmatrix}
\end{aligned} \tag{2.8}$$

where g is the Earth's gravitational constant and l_{c1} and l_{c2} are the distances from the center of the gravity of the first and the second manipulators to their corresponding joints. In addition, for this system $\frac{\partial \mathcal{F}(\dot{\mathbf{q}})}{\partial \dot{\mathbf{q}}} = 0$.

It can be shown that the parameters of the two-link manipulator given above

satisfy **Properties 2.1.1–2.1.3**. Specifically, the parametrization of this robot according to **Property 2.1.3** is [162]:

$$\begin{aligned}
 \mathbf{Y}(\mathbf{q}, \dot{\mathbf{q}}, \mathbf{a}, \mathbf{b}) &= \begin{bmatrix} a_1 & 0 \\ a_1 + a_2 & a_1 + a_2 \\ \cos(q_2)(2a_1 + a_2) - \sin(q_2)(\dot{q}_1 b_2 + \dot{q}_2 b_2 + \dot{q}_2 b_1) & \cos(q_2)a_1 \\ g \cos(q_1) & 0 \\ g \cos(q_1) & 0 \\ g \cos(q_1 + q_2) & g \cos(q_1 + q_2) \end{bmatrix}^T \\
 \Theta &= \begin{bmatrix} m_1 l_{c1}^2 + m_2 l_1^2 + I_1 \\ m_2 l_{c2}^2 + I_2 \\ m_2 l_1 l_{c2} \\ m_1 l_{c1} \\ m_2 l_1 \\ m_2 l_{c2} \end{bmatrix}
 \end{aligned} \tag{2.9}$$

2.3.2 Spacecraft Attitude Dynamics

Sets of coordinates that completely describe the orientation (attitude) of a rigid body relative to some reference coordinate frame are known as the attitude coordinates. There are many different ways to describe the attitude of a rigid body in the 3D space. The four fundamental facts on the rigid body attitude coordinates are listed below [163]:

1. A minimum of three coordinates is required to describe the relative angular displacement between two reference frames.

2. Any minimal set of three attitude coordinates will contain at least one geometrical orientation where the coordinates are singular, at least two coordinates are undefined or not unique.
3. At or near such a geometric singularity, the corresponding kinematic differential equations are also singular.
4. The geometric singularities and associated numerical difficulties can be avoided altogether through a regularization. Redundant sets of four or more coordinates exist which are universally determined and contain no geometric singularities.

We review the two most commonly used attitude representations below. An interested reader can refer to [163] for more details.

Euler angles

The most commonly used sets of attitude parameters are the Euler angles. Aircraft and spacecraft orientations are commonly described through the Euler angles roll, pitch and yaw (ϕ , θ , ψ). The popularity of Euler angles stems from the fact that the relative attitude is easy to visualize.

The equations of motion of the spacecraft attitude dynamics are given by [163, 164],

$$\dot{\mathbf{q}} = \bar{\mathbf{R}}\boldsymbol{\omega} \quad (2.10a)$$

$$\mathbf{J}\dot{\boldsymbol{\omega}} = -\mathbf{S}(\boldsymbol{\omega})\mathbf{J}\boldsymbol{\omega} + \boldsymbol{\rho} \quad (2.10b)$$

where $\mathbf{q} = [\theta, \phi, \psi]^T$ is the vector of the Euler angles, $\boldsymbol{\omega} = [\omega_1, \omega_2, \omega_3]^T$ is the vector of spacecraft angular velocities in the body frame, $\boldsymbol{\rho} = [\rho_1, \rho_2, \rho_3]^T$ is the

vector of external torque inputs in the body frame, $\mathbf{J} = \mathbf{J}^T \in \mathbb{R}^{3 \times 3}$ is the spacecraft positive definite moment of inertia matrix, and $\bar{\mathbf{R}}$ is defined by,

$$\bar{\mathbf{R}} = \frac{1}{c_\theta} \begin{bmatrix} c_\theta & s_\phi s_\theta & c_\phi s_\theta \\ 0 & c_\phi c_\theta & -s_\phi c_\theta \\ 0 & s_\phi & c_\phi \end{bmatrix}$$

where c_θ stands for $\cos(\theta)$, s_θ stands for $\sin(\theta)$, s_ϕ stands for $\sin(\phi)$, and c_ϕ stands for $\cos(\phi)$. In addition, $\mathbf{S}(\mathbf{x})$ is the skew-symmetric matrix operator that is given by,

$$\mathbf{S}(\mathbf{x}) = \begin{bmatrix} 0 & -x_3 & x_2 \\ x_3 & 0 & -x_1 \\ -x_2 & x_1 & 0 \end{bmatrix}$$

From equation (2.10a), we have $\boldsymbol{\omega} = \bar{\mathbf{R}}^{-1} \dot{\mathbf{q}}$, which implies that $\dot{\boldsymbol{\omega}} = \dot{\bar{\mathbf{R}}}^{-1} \dot{\mathbf{q}} + \bar{\mathbf{R}}^{-1} \ddot{\mathbf{q}}$. Consequently, one can re-write equation (2.10b) as $\bar{\mathbf{R}}^{-T} \mathbf{J} \bar{\mathbf{R}}^{-1} \ddot{\mathbf{q}} + \bar{\mathbf{R}}^{-T} \dot{\mathbf{J}} \bar{\mathbf{R}}^{-1} \dot{\mathbf{q}} + \bar{\mathbf{R}}^{-T} \mathbf{S}(\bar{\mathbf{R}}^{-1} \dot{\mathbf{q}}) \mathbf{J} \bar{\mathbf{R}}^{-1} \dot{\mathbf{q}} = \bar{\mathbf{R}}^{-T} \boldsymbol{\rho}$. Therefore, the 3-degrees of freedom (DOF) attitude dynamics of a spacecraft can be written in the form of equation (2.7) with $g(\mathbf{q}) = \frac{\partial \mathcal{F}(\dot{\mathbf{q}})}{\partial \dot{\mathbf{q}}} = 0$, and where we specifically have,

$$\mathbf{D}(\mathbf{q}) = \bar{\mathbf{R}}^{-T} \mathbf{J} \bar{\mathbf{R}}^{-1} \tag{2.11a}$$

$$\mathbf{C}(\mathbf{q}, \dot{\mathbf{q}}) = \bar{\mathbf{R}}^{-T} \dot{\mathbf{J}} \bar{\mathbf{R}}^{-1} + \bar{\mathbf{R}}^{-T} \mathbf{S}(\bar{\mathbf{R}}^{-1} \dot{\mathbf{q}}) \mathbf{J} \bar{\mathbf{R}}^{-1} \tag{2.11b}$$

$$\mathbf{u} = \bar{\mathbf{R}}^{-T} \boldsymbol{\rho} \tag{2.11c}$$

When replacing the above terms in (2.7) one notices all the terms are left multiplied by $\bar{\mathbf{R}}^{-T}$. However, one should not cancel out this common term, which would then result in having a non-symmetric $\mathbf{D}(\mathbf{q})$.

Remark 2.3.1. Note that the Euler angle kinematic differential equations encounter a singularity at $\theta = \pm 90$ degrees for three successive rotations about the 3rd, 2nd and 1st body axis (labeled (3-2-1) set for short).

The spacecraft inertia matrix with a vector $\mathbf{a} = [a_1, a_2, a_3]^T$ can be written as [165],

$$\mathbf{J}\mathbf{a} = \mathcal{O}(\mathbf{a})\Theta \quad (2.12)$$

$$\text{where } \mathcal{O}(\mathbf{a}) = \begin{bmatrix} a_1 & 0 & 0 & 0 & a_3 & a_2 \\ 0 & a_2 & 0 & a_3 & 0 & a_1 \\ 0 & 0 & a_3 & a_2 & a_1 & 0 \end{bmatrix} \text{ and}$$

$$\Theta = \begin{bmatrix} J_{11,j} & J_{22,j} & J_{33,j} & J_{23,j} & J_{13,j} & J_{12,j} \end{bmatrix}^T$$

Consequently, we obtain

$$\begin{aligned} \mathbf{D}(\mathbf{q})\mathbf{a} + \mathbf{C}(\mathbf{q}, \dot{\mathbf{q}})\mathbf{b} &= \bar{\mathbf{R}}^{-T} \mathbf{J} \bar{\mathbf{R}}^{-1} \mathbf{a} + \bar{\mathbf{R}}^{-T} \mathbf{J} \dot{\bar{\mathbf{R}}}^{-1} \mathbf{b} + \bar{\mathbf{R}}^{-T} \mathbf{S}(\bar{\mathbf{R}}^{-1} \dot{\mathbf{q}}) \mathbf{J} \bar{\mathbf{R}}^{-1} \mathbf{b} \\ &\triangleq \mathbf{Y}(\mathbf{q}, \dot{\mathbf{q}}, \mathbf{a}, \mathbf{b}) \Theta \end{aligned} \quad (2.13)$$

$$\text{where } \mathbf{Y}(\mathbf{q}, \dot{\mathbf{q}}, \mathbf{a}, \mathbf{b}) = \bar{\mathbf{R}}^{-T} \left[\mathcal{O}(\bar{\mathbf{R}}^{-1} \mathbf{a}) + \mathcal{O}(\dot{\bar{\mathbf{R}}}^{-1} \mathbf{b}) + \mathbf{S}(\bar{\mathbf{R}}^{-1} \dot{\mathbf{q}}) \mathcal{O}(\bar{\mathbf{R}}^{-1} \mathbf{b}) \right].$$

The Euler angles provide a compact, three parameter attitude description whose coordinates are easy to visualize. One main drawback of these angles is that a rigid body or reference frame is never further than a 90 degree rotation away from a singular orientation. Therefore their use in describing large, and especially, arbitrary rotations is limited. One can use the unit quaternions to overcome this difficulty as described next.

Unit quaternions (Euler parameters)

Unit quaternions (also known as Euler parameters) are another popular set of attitude coordinates. They provide a redundant, nonsingular attitude description and are well-suited to describe arbitrary, large rotations [163]. The unit quaternion for the a spacecraft is defined as:

$$\vec{q} = \begin{bmatrix} \mathbf{e} \sin(\frac{\varphi}{2}) \\ \cos(\frac{\varphi}{2}) \end{bmatrix} = \begin{bmatrix} \bar{\mathbf{q}} \\ \hat{q}_4 \end{bmatrix} \quad (2.14)$$

where $\mathbf{e} = [e_1, e_2, e_3]^T \in \mathbb{R}^{3 \times 1}$ is the Euler axis, φ is the Euler angle, $\bar{\mathbf{q}}$ is the vector part, and \hat{q}_4 is the scalar part of the quaternion, satisfying the constraint

$$\hat{q}_4^2 + \bar{\mathbf{q}}^T \bar{\mathbf{q}} = 1 \quad (2.15)$$

Therefore, $\hat{q}_4 = \pm 1$ correspond to the same orientation in $SO(3)$. The matrix denoted by $\bar{\mathbf{R}}(\vec{q}) \in SO(3)$ represents the rotation from the inertial frame \mathcal{F}^I to the body frame of the spacecraft, \mathcal{F}^B . The rotation matrix is related to the quaternion through [164]:

$$\bar{\mathbf{R}}(\vec{q}) = (\hat{q}_4^2 - \bar{\mathbf{q}}^T \bar{\mathbf{q}}) \mathcal{I}_3 + 2\bar{\mathbf{q}}\bar{\mathbf{q}}^T - 2\hat{q}_4\bar{\mathbf{q}}^\times \quad (2.16)$$

where \mathcal{I}_n is an $n \times n$ identity matrix. In general, $+\vec{q}$ and $-\vec{q}$ both represent the same rotation matrix.

The equation of motion for the attitude dynamics and kinematics of a spacecraft is then given by [164]:

$$\begin{aligned}
\mathbf{J}\dot{\boldsymbol{\omega}} + \mathbf{C}(\bar{\mathbf{q}}, \boldsymbol{\omega})\boldsymbol{\omega} &= \mathbf{u} \\
\dot{\bar{\mathbf{q}}} - \frac{1}{2}\bar{\mathbf{E}}(\bar{\mathbf{q}})\boldsymbol{\omega} &= 0 \\
\dot{q}_4 + \frac{1}{2}\bar{\mathbf{q}}^T\boldsymbol{\omega} &= 0
\end{aligned} \tag{2.17}$$

where $\mathbf{u} = [u_1, u_2, u_3]^T \in \mathbb{R}^{3 \times 1}$ is the input vector and $\boldsymbol{\omega} = [\omega_1, \omega_2, \omega_3]^T \in \mathbb{R}^{3 \times 1}$ is the angular velocity of the spacecraft with respect to the inertial frame. In addition, the matrix $\bar{\mathbf{E}}(\bar{\mathbf{q}})$ is given by

$$\bar{\mathbf{E}}(\bar{\mathbf{q}}) = \hat{q}_4 \mathfrak{I}_{3 \times 3} + \bar{\mathbf{q}}^\times \tag{2.18}$$

When thrusters are used $\mathbf{C}(\bar{\mathbf{q}}, \boldsymbol{\omega})$ can be chosen as $\mathbf{C}(\bar{\mathbf{q}}, \boldsymbol{\omega}) = \boldsymbol{\omega}^\times \mathbf{J}$, and when momentum actuators (e.g. reaction wheels and control moment gyros) are chosen $\mathbf{C}(\bar{\mathbf{q}}, \boldsymbol{\omega})$ will be a function of the spacecraft rotation matrix and the angular momentum of actuators and the spacecraft in the body frame [166, 167]. In both cases, however, $\mathbf{C}(\bar{\mathbf{q}}, \boldsymbol{\omega})$ is a skew symmetric matrix [167].

Remark 2.3.2. Note that the parameters of the dynamic equation (2.17) satisfy the **Properties 2.1.1–2.1.4** that are provided in Section 2.2.

With reference to Remark 2.3.2 and by assuming that the spacecraft inertia matrix is expressed in the principal axis, one concludes that \mathbf{J} is a diagonal matrix.

2.4 The Kronecker Product

If \mathbf{A} is an m -by- n matrix and \mathbf{B} is a p -by- q matrix, then the Kronecker product $\mathbf{A} \otimes \mathbf{B}$ is the mp -by- nq block matrix [168]:

$$\mathbf{A} \otimes \mathbf{B} = \begin{bmatrix} a_{11}\mathbf{B} & \cdots & a_{1n}\mathbf{B} \\ \vdots & \ddots & \vdots \\ a_{m1}\mathbf{B} & \cdots & a_{mn}\mathbf{B} \end{bmatrix}$$

To be more precise, the above equation can be rewritten as:

$$\mathbf{A} \otimes \mathbf{B} = \begin{bmatrix} a_{11}b_{11} & a_{11}b_{12} & \cdots & a_{11}b_{1q} & \cdots & \cdots & a_{1n}b_{11} & a_{1n}b_{12} & \cdots & a_{1n}b_{1q} \\ a_{11}b_{21} & a_{11}b_{22} & \cdots & a_{11}b_{2q} & \cdots & \cdots & a_{1n}b_{21} & a_{1n}b_{22} & \cdots & a_{1n}b_{2q} \\ \vdots & \vdots & \ddots & \vdots & & & \vdots & \vdots & \ddots & \vdots \\ a_{11}b_{p1} & a_{11}b_{p2} & \cdots & a_{11}b_{pq} & \cdots & \cdots & a_{1n}b_{p1} & a_{1n}b_{p2} & \cdots & a_{1n}b_{pq} \\ \vdots & \vdots & & \vdots & \ddots & & \vdots & \vdots & & \vdots \\ \vdots & \vdots & & \vdots & & \ddots & \vdots & \vdots & & \vdots \\ a_{m1}b_{11} & a_{m1}b_{12} & \cdots & a_{m1}b_{1q} & \cdots & \cdots & a_{mn}b_{11} & a_{mn}b_{12} & \cdots & a_{mn}b_{1q} \\ a_{m1}b_{21} & a_{m1}b_{22} & \cdots & a_{m1}b_{2q} & \cdots & \cdots & a_{mn}b_{21} & a_{mn}b_{22} & \cdots & a_{mn}b_{2q} \\ \vdots & \vdots & \ddots & \vdots & & & \vdots & \vdots & \ddots & \vdots \\ a_{m1}b_{p1} & a_{m1}b_{p2} & \cdots & a_{m1}b_{pq} & \cdots & \cdots & a_{mn}b_{p1} & a_{mn}b_{p2} & \cdots & a_{mn}b_{pq} \end{bmatrix}$$

It can be shown that the Kronecker product has the following properties [168],

$$\mathbf{A} \otimes (\mathbf{B} + \mathbf{C}) = \mathbf{A} \otimes \mathbf{B} + \mathbf{A} \otimes \mathbf{C}$$

$$(\mathbf{A} + \mathbf{B}) \otimes \mathbf{C} = \mathbf{A} \otimes \mathbf{C} + \mathbf{B} \otimes \mathbf{C}$$

$$(k\mathbf{A}) \otimes \mathbf{B} = \mathbf{A} \otimes (k\mathbf{B}) = k(\mathbf{A} \otimes \mathbf{B})$$

$$(\mathbf{A} \otimes \mathbf{B}) \otimes \mathbf{C} = \mathbf{A} \otimes (\mathbf{B} \otimes \mathbf{C})$$

where \mathbf{A} , \mathbf{B} and \mathbf{C} are matrices and k is a scalar.

2.5 Vector/Matrix Calculus

In this thesis, we encounter problems with analysis of several variables. Vector/Matrix calculus extends calculus of one variable into that of a vector or a matrix of variables.

Definition 2.5.1. *Vector gradient* [169]: Let $\mathbf{w} \in \mathbb{R}^n$ and $f(\mathbf{w}) : \mathbb{R}^n \rightarrow \mathbb{R}$ be a differentiable scalar function of \mathbf{w} . Then the vector gradient of $f(\mathbf{w})$ with respect to \mathbf{w} is the n -dimensional vector of partial derivatives of $f(\mathbf{w})$, i.e.

$$\frac{\partial f(\mathbf{w})}{\partial \mathbf{w}} \triangleq \nabla_{\mathbf{w}} f = \begin{bmatrix} \frac{\partial f(\mathbf{w})}{\partial x_1} \\ \frac{\partial f(\mathbf{w})}{\partial x_2} \\ \vdots \\ \frac{\partial f(\mathbf{w})}{\partial x_n} \end{bmatrix}$$

□

Definition 2.5.2. *Jacobian matrix* [169]: Let $\mathbf{w} \in \mathbb{R}^n$ and $\mathbf{f}(\mathbf{w}) = (f_1(\mathbf{w}), f_2(\mathbf{w}), \dots, f_m(\mathbf{w})) : \mathbb{R}^n \rightarrow \mathbb{R}^m$ be a differentiable vector function of \mathbf{w} . Then the Jacobian matrix is defined as:

$$\frac{\partial \mathbf{f}(\mathbf{w})}{\partial \mathbf{w}} \triangleq \mathfrak{J}(\mathbf{f}(\mathbf{w})) = \begin{bmatrix} \frac{\partial f_1(\mathbf{w})}{\partial x_1} & \frac{\partial f_2(\mathbf{w})}{\partial x_1} & \dots & \frac{\partial f_m(\mathbf{w})}{\partial x_1} \\ \frac{\partial f_1(\mathbf{w})}{\partial x_2} & \frac{\partial f_2(\mathbf{w})}{\partial x_2} & \dots & \frac{\partial f_m(\mathbf{w})}{\partial x_2} \\ \vdots & \vdots & \ddots & \vdots \\ \frac{\partial f_1(\mathbf{w})}{\partial x_n} & \frac{\partial f_2(\mathbf{w})}{\partial x_n} & \dots & \frac{\partial f_m(\mathbf{w})}{\partial x_n} \end{bmatrix}$$

□

In the vector convention above, the columns of the Jacobian matrix are gradients of the corresponding components functions $f_i(\mathbf{w})$ with respect to the vector \mathbf{w} .

Definition 2.5.3. Let $\mathbf{w}, \mathbf{y} \in \mathbb{R}^n$, $\mathbf{f}(\mathbf{w}) = (f_1(\mathbf{w}), f_2(\mathbf{w}), \dots, f_n(\mathbf{w}))^T : \mathbb{R}^n \rightarrow \mathbb{R}^n$ be a differentiable vector function of \mathbf{w} and $\mathbf{F}(\mathbf{w}) = \begin{bmatrix} f_1(\mathbf{w}) & f_2(\mathbf{w}) & \dots & f_n(\mathbf{w}) \end{bmatrix}$ be a $n \times n$ matrix. Then we define:

$$\frac{\partial \mathbf{F}(\mathbf{w})}{\partial \mathbf{w}} \mathbf{y} = \begin{bmatrix} \mathfrak{J}(f_1(\mathbf{w}))\mathbf{y} & \mathfrak{J}(f_2(\mathbf{w}))\mathbf{y} & \dots & \mathfrak{J}(f_n(\mathbf{w}))\mathbf{y} \end{bmatrix}$$

□

Based on the definition provided above, $\frac{\partial \mathbf{F}(\mathbf{w})}{\partial \mathbf{w}} \mathbf{y}$ is a $n \times n$ matrix.

2.6 Definition of a Saturation Function

Definition 2.6.1. [158] A saturation function denoted by $\text{Sat}(x) : \mathbb{R} \rightarrow \mathbb{R}$, is an odd function with the following properties $\forall x \in \mathbb{R}$, namely, (i) $\text{Sat}(x) = 0$, if and only if $x = 0$; (ii) $|\text{Sat}(x)| \leq 1$; (iii) $\text{Sat}(-x) = -\text{Sat}(x)$; (iv) $\frac{\partial}{\partial x} \text{Sat}(x) \geq 0$ and $\frac{\partial \text{Sat}(x)}{\partial x} \neq 0$, when $x = 0$; and (v) there exists a constant $b > 0$ such that $\forall x \in [-b, b]$, we have $\text{Sat}(x) = \gamma x$, where $\gamma > 0$. □

The following lemma will be used subsequently in this thesis.

Lemma 2.6.1. *The saturation function defined above has the following property,*

$$\int_0^{x_1} \text{sat}(x) dx \geq \frac{1}{2} \text{sat}(x_1) x_1 \geq 0, \quad x_1 \in \mathbb{R}$$

Proof: Proof can be found in [158]. ■

2.7 Information Structure and Neighboring Set

In this thesis, the information exchanges among the m EL systems is represented by a graph. We provide here some basic terminologies and definitions from graph theory in order to facilitate understanding of the subsequent analyses and developments. An interested reader can refer to [170, 171] for more details.

A directed-graph (digraph) \mathcal{G} consists of a node set $\mathcal{V} = \{1, \dots, m\}$, an edge set $\mathcal{E} \subseteq \mathcal{V} \times \mathcal{V}$, and a weighted adjacency matrix $\Lambda = [\lambda_{jn}] \in \mathbb{R}^{m \times m}$. The m agents in the network are considered as nodes of a digraph. The communication links among the agents are considered as the digraph edge set, where self-connection is not allowed.

Two vertices j and n are called adjacent if at least one edge exists between them i.e. $(j, n) \in \mathcal{E}$, which is also denoted by $j \downarrow n$. If $j \downarrow n$ then node j is the parent of node n and node n is the child of node j . The weighted adjacency matrix $\Lambda = [\lambda_{jn}]$ is defined such that λ_{jn} is a positive weight if $n \downarrow j$, while $\lambda_{jn} = 0$, otherwise. The indegree and outdegree of node j are given by $d_i(j) = \sum_n \lambda_{nj}$ and $d_o(j) = \sum_n \lambda_{jn}$ respectively. Associated with Λ we introduce a matrix known as the Laplacian matrix $\mathcal{L} = [l_{jn}] \in \mathbb{R}^{m \times m}$ such that $l_{jj} = \sum_{n=1, n \neq j}^m \lambda_{jn}$ and $l_{jn} = -\lambda_{jn}$, where $k \neq j$. This implies that \mathcal{L} is a zero row sum matrix. A path of length l_p in a digraph is a sequence (j_0, \dots, j_l) of l_p distinct vertices such that for every $i \in \{0, \dots, l_p - 1\}$, (j_i, j_{i+1}) is an edge. A digraph is *strongly connected* if for any pair of distinct vertices j and n , there is a directed path from j to n . Furthermore, if the digraph is strongly connected, \mathcal{L} has a simple eigenvalue 0 with an associated right eigenvector of $\bar{k}\mathbf{1}_m$, where $\mathbf{1}_m$ is an $m \times 1$ column vector of ones and \bar{k} is a positive number, i.e. $\mathcal{L}\mathbf{1}_m = 0$. All the other eigenvalues of \mathcal{L} are positive if and only if the digraph \mathcal{G} is strongly connected [171]. For a given node j , the set of

agents from which it can receive information is called a neighboring set \mathcal{N}_j , that is $\forall j = 1, \dots, n : \mathcal{N}_j = \{n | (n, j) \in \mathcal{E}\}$. In addition, the number of neighbors of the j -th node is denoted by $|\mathcal{N}_j|$ (which is also known as the cardinality of the j -th node). Also, the graph size $|\mathcal{E}|$ is the number of edges.

An undirected-graph is a digraph with an additional property, i.e. $j \downarrow n \Leftrightarrow n \downarrow j$. This implies that $\lambda_{jn} = \lambda_{nj}$ and $d_i(j) = d_o(j)$ for all $j, n \in \mathcal{V}$. An undirected-graph is connected if and only if it is strongly connected. Let us denote $(\mathcal{L} \otimes \mathfrak{I}_p)x$ as a column stack vector of all $\sum_{j=1}^m \lambda_{nj}(\mathbf{x}_n - \mathbf{x}_j)$, $n \in \mathcal{V}$ with $\mathbf{x} = [\mathbf{x}_1^T, \dots, \mathbf{x}_m^T]^T \in \mathbb{R}^{p \cdot m \times 1}$. It can be shown that $\mathbf{x}^T (\mathcal{L} \otimes \mathfrak{I}_p) \mathbf{x} = \frac{1}{2} \sum_{n=1}^m \sum_{j=1}^m \lambda_{nj} \|\mathbf{x}_n - \mathbf{x}_j\|^2$.

We next define two general communication network topologies, which will be used subsequently in this thesis.

Definition 2.7.1. A finite set of h communication graphs $\mathcal{G} = \{\mathcal{G}_1, \dots, \mathcal{G}_h\}$ are characterized by having the same node set, i.e. $\mathcal{V}_1 = \dots = \mathcal{V}_h = \mathcal{V}$. Furthermore, the edge set for each communication graph is different from the others, i.e. $\mathcal{E}_1 \neq \dots \neq \mathcal{E}_h$. This results in a different weighted adjacency matrix for each communication graph, specifically, $\Lambda_1 \neq \dots \neq \Lambda_h$. Consequently, the Laplacian matrix associated with each $j \in \mathcal{H}$, where $\mathcal{H} = \{1, \dots, h\}$, communication graph denoted by \mathcal{L}_j , will also be different. All the h communication graphs are assumed to be *connected*, therefore, \mathcal{L}_j is a positive semi-definite matrix $\forall j \in \mathcal{H}$. \square

Definition 2.7.2. A finite set of h connected communication graphs is denoted by $\bar{\mathcal{G}} = \{\mathcal{G}_1, \dots, \mathcal{G}_h\}$ and is characterized by having the same node set, i.e. $\mathcal{V}_1 = \dots = \mathcal{V}_h$. Furthermore, the edge set for h communication graphs are different from the others, i.e. $\mathcal{E}_1 \neq \dots \neq \mathcal{E}_h$. However, it is assumed that the indegree and the number of neighbors for each node are the same for all graphs. This will result in a different weighted adjacency matrix for each communication graph. Consequently,

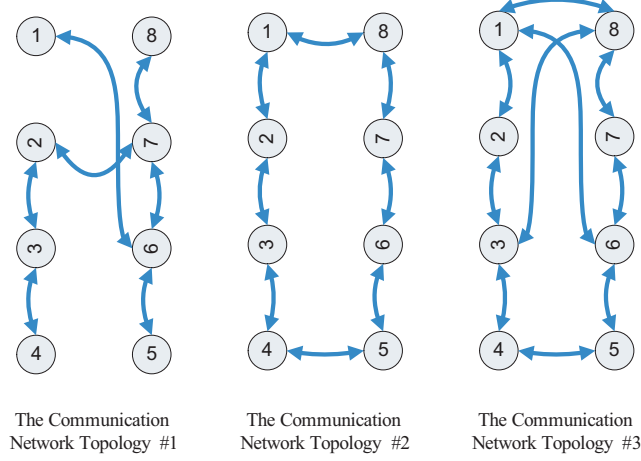


Figure 2.2: The three communication network topologies that are considered in this work according to the Definition 2.7.1.

the Laplacian matrix associated with each $i \in \mathcal{H}$, where $\mathcal{H} = \{1, \dots, h\}$, communication graph, denoted by \mathcal{L}_j , will also be different. Due to the fact that the communication digraphs are strongly connected, \mathcal{L}_j is a positive semi-definite matrix $\forall j \in \mathcal{H}$. □

An example of the communication graph \mathcal{G} is depicted in Fig. 2.2. All the three networks are strongly connected and the connections are bi-directional.

The following lemma will be used subsequently in this thesis.

Lemma 2.7.1. *Consider a symmetric matrix $\Lambda = \Lambda^T \in \mathbb{R}^{k \times k}$. Let us denote λ_{ij} as the ij -th element of this matrix. The following equality then holds:*

$$\frac{1}{2} \sum_{i=1}^k \sum_{j=1}^k \lambda_{ij} (y_i - y_j) \chi(x_i - x_j) = \sum_{i=1}^k \sum_{j=1}^k \lambda_{ij} y_i \chi(x_i - x_j) \quad (2.19)$$

where $\chi(x)$ is any odd function.

Proof: The left hand side of (2.19) can be written as:

$$\begin{aligned}
& \frac{1}{2} \sum_{i=1}^k \sum_{j=1}^k \lambda_{ij} (y_i - y_j) \chi(x_i - x_j) \\
&= \frac{1}{2} \sum_{i=1}^k \sum_{j=1}^k \lambda_{ij} y_i \chi(x_i - x_j) - \frac{1}{2} \sum_{i=1}^k \sum_{j=1}^k \lambda_{ij} y_j \chi(x_i - x_j) \\
&= \frac{1}{2} \sum_{i=1}^k \sum_{j=1}^k \lambda_{ij} y_i \chi(x_i - x_j) - \frac{1}{2} \sum_{j=1}^k \sum_{i=1}^k \lambda_{ji} y_i \chi(x_j - x_i)
\end{aligned}$$

By noting $\lambda_{ij} = \lambda_{ji}$ and $\chi(x_i - x_j) = -\chi(x_j - x_i)$ one obtains (2.19). This completes the proof of the lemma. ■

2.8 Hamilton-Jacobi-Bellman (HJB) Equations

Minimization of a general nonlinear cost function, either unconstrained or subject to certain constraints, may be solved by using the HJB equations. In this thesis unconstrained minimization problem is considered. The HJB equations in the general form for an infinite horizon scenario are provided below [172, 173]. Assume that the model of a dynamical system is given by

$$\dot{\mathbf{x}} = f(t, \mathbf{x}, \mathbf{u}) \tag{2.20}$$

where $f : [0, \infty) \times \mathbb{R}^n \times \mathbb{R}^m \rightarrow \mathbb{R}^n$ is continuous in t and Lipschitz in \mathbf{x} and \mathbf{u} . The solution to the following optimization problem

$$\begin{aligned}
& \min_{\mathbf{u}} \mathcal{J} = \int_0^{\infty} g(t, \mathbf{x}, \mathbf{u}) dt \\
& \text{subject to } \dot{\mathbf{x}} = f(t, \mathbf{x}, \mathbf{u}) \\
& \mathbf{x}(0) = \mathbf{x}_0
\end{aligned} \tag{2.21}$$

where \mathcal{J} is denoted as the performance index (PI) is obtained if the following HJB equations with appropriate boundary conditions have a solution:

$$\begin{aligned} -\frac{\partial \mathcal{Y}(\mathbf{x}, t)}{\partial t} &= \min_{\mathbf{u}} \Phi(t, \mathbf{x}, \mathbf{u}) \\ \Phi(t, \mathbf{x}, \mathbf{u}) &= \frac{\partial \mathcal{Y}(\mathbf{x}, t)}{\partial \mathbf{x}} \dot{\mathbf{x}} + g(t, \mathbf{x}, \mathbf{u}) \end{aligned} \quad (2.22)$$

where $\Phi(t, \mathbf{x}, \mathbf{u})$ is denoted as the Hamiltonian and $\mathcal{Y}(\mathbf{x}, t)$ is referred to as the value function and is chosen such that the above Partial Differential Equation (PDE) is satisfied.

2.9 Stability Analysis and Theorems

In this section, we present theorems for stability analysis of general smooth nonlinear systems as well as switched nonlinear systems. These theorems will be used frequently in this thesis to analyze the stability of the closed-loop networked systems. Our first definition is provided below from [174].

Definition 2.9.1. A continuous function $\alpha : [0, a) \rightarrow [0, \infty)$ is said to belong to class \mathcal{K} if it is strictly increasing and $\alpha(0) = 0$. It is said to belong to class \mathcal{K}_∞ if $a = \infty$ and $\alpha(r) \rightarrow \infty$ as $r \rightarrow \infty$. \square

Definition 2.9.2. A continuous function $\beta : [0, a) \times [0, \infty) \rightarrow [0, \infty)$ is said to belong to class \mathcal{KL} if, for each fixed s , the mapping $\beta(r, s)$ belongs to class \mathcal{K} with respect to r and, for each fixed r , the mapping $\beta(r, s)$ is decreasing with respect to s and $\beta(r, s) \rightarrow 0$ and $s \rightarrow \infty$. \square

We present the following additional definitions.

Definition 2.9.3. A real-valued function $\alpha : \mathbb{R} \rightarrow \mathbb{R}$ is said to be smooth if it has continuous derivatives of arbitrary order. We denote its k -th derivative by $\alpha^k(\cdot)$. \square

Given $\mathcal{W} : \mathbb{R}^n \rightarrow \mathbb{R}$ and $f : \mathbb{R}^n \rightarrow \mathbb{R}^n$, we use the following notation:

$$\begin{aligned}\mathfrak{L}_f^1 \mathcal{W}(\mathbf{x}) &= \mathfrak{L}_f \mathcal{W}(\mathbf{x}) \triangleq \frac{\partial \mathcal{W}}{\partial \mathbf{x}} f(\mathbf{x}) \\ \mathfrak{L}_f^{i+1} \mathcal{W}(\mathbf{x}) &\triangleq \mathfrak{L} \left(\mathfrak{L}_f^i \mathcal{W}(\mathbf{x}) \right), \quad i \in \mathfrak{N}\end{aligned}$$

Definition 2.9.4. A function $\mathcal{W}(\mathbf{x}) : \mathbb{R}^n \rightarrow [0, \infty)$ is said to be positive definite if $\mathcal{W}(0) = 0$ and $\mathcal{W}(\mathbf{x}) > 0$ for all $\mathbf{x} \neq 0$. It is said to be positive semi-definite if $\mathcal{W}(0) = 0$ and $\mathcal{W}(\mathbf{x}) \geq 0$ for all $\mathbf{x} \neq 0$. \square

Definition 2.9.5. A function $\mathcal{W}(\mathbf{x}) : \mathbb{R}^n \rightarrow [0, \infty)$ is said to be negative definite (semi-definite) if $-\mathcal{W}(\mathbf{x})$ is positive definite (semi-definite). \square

Definition 2.9.6. A function $\mathcal{W}(\mathbf{x})$ is said to be radially unbounded if $\|\mathbf{x}\| \rightarrow \infty \Rightarrow \mathcal{W}(\mathbf{x}) \rightarrow \infty$. \square

The following additional definition, which will be used subsequently, is taken from [174].

Definition 2.9.7. The space L_r^m for $1 \leq r < \infty$ is defined as the set of all piecewise continuous functions $u : [0, \infty) \rightarrow \mathbb{R}^m$ such that

$$\|u\|_{L_r} = \left(\int_0^\infty \|u(t)\|^r dt \right)^{1/r} < \infty$$

The subscript r in L_r^m refers to the type of r -norm that is used to define the space, while the superscript m denotes the dimension of u . \square

Remark 2.9.1. It follows from Definition 2.9.7 that for a given scalar function $e(t)$, we have $e(t) \in \mathfrak{L}_1$ if and only if $\|e\|_{\mathfrak{L}_1} = \int_0^\infty |e(t)| dt < \infty$.

2.9.1 Lyapunov Stability Theorem

We consider autonomous systems of the form

$$\dot{\mathbf{x}} = f(\mathbf{x}) \tag{2.23}$$

where $f(\mathbf{x})$ is a smooth continuous and Lipschitz function over \mathbb{R}^n .

Definition 2.9.8. A smooth function $\mathcal{W}(\mathbf{x}) : \mathbb{R}^n \rightarrow [0, \infty)$ is a *weak* Lyapunov function for the system (2.23) if it is positive definite and

$$\dot{\mathcal{W}}(\mathbf{x}) = \mathcal{L}_f \mathcal{W}(\mathbf{x}) \leq 0, \mathbf{x} \in \mathbb{R}^n$$

□

Definition 2.9.9. A smooth function $\mathcal{W}(\mathbf{x}) : \mathbb{R}^n \rightarrow [0, \infty)$ is a *strong* Lyapunov function for the system (2.23) if it is positive definite and

$$\dot{\mathcal{W}}(\mathbf{x}) = \mathcal{L}_f \mathcal{W}(\mathbf{x}) < 0, \mathbf{x} \in \mathbb{R}^n$$

□

We use the standard definitions of exponential, global exponential, asymptotic, and global asymptotic stability for general nonlinear systems (see Definition 4.4, Lemma 4.5 and Definition 4.5 in [174] for details).

The following theorem, provided without proof, considers stability of a general autonomous system. The proof can be found in [174].

Theorem 2.9.1. *Let $\mathbf{x} = 0$ be an equilibrium point of the system (2.23) and $D \subset \mathbb{R}^n$ be a domain containing $\mathbf{x} = 0$. Let $\mathcal{W}(\mathbf{x}) : D \rightarrow \mathbb{R}$ be a continuously differentiable*

unbounded function. If the function $\mathcal{W}(\mathbf{x})$ is a weak Lyapunov function, then $\mathbf{x} = 0$ is stable. Moreover, if the function $\mathcal{W}(\mathbf{x})$ is a strong Lyapunov function, then $\mathbf{x} = 0$ is asymptotically stable. If the Lyapunov function is radially unbounded, i.e. $D = \mathbb{R}^n$, and $\mathbf{x} = 0$ is the unique equilibrium point of the system (2.23), then the stability results are global.

In the next theorem we show that if in a domain about the origin we can find a weak Lyapunov function and we can establish that no trajectory can stay identically at points where $\dot{\mathcal{W}}(\mathbf{x}) = 0$, except at the origin, then the origin is asymptotically stable. This idea follows from LaSalle's invariance principle. We first define positively invariant sets and then state LaSalle's theorem.

Definition 2.9.10. A set \mathcal{S} is said to be a positively invariant set with respect to $\dot{\mathbf{x}} = f(\mathbf{x})$, if $\mathbf{x}(0) \in \mathcal{S} \Rightarrow \mathbf{x}(t) \in \mathcal{S}, \forall t \geq 0$. □

We are now ready to state LaSalle's theorem [174].

Theorem 2.9.2. Let $\Omega \in D$ be a compact set that is positively invariant with respect to the system (2.23). Let $\mathcal{W}(\mathbf{x}) : D \rightarrow \mathbb{R}$ be a continuously differentiable function such that $\dot{\mathcal{W}}(\mathbf{x}) \leq 0$ in Ω . Let E be the set of all points in Ω where $\dot{\mathcal{W}}(\mathbf{x}) = 0$. Let \mathcal{S} be the largest invariant set in E . Then, every solution starting in Ω approaches to \mathcal{S} as $t \rightarrow \infty$.

The following lemma, which is known as Barbashin–Krasovskii lemma [174], can be employed for stability analysis of nonlinear autonomous systems.

Lemma 2.9.1. Let $\mathbf{x} = 0$ be an equilibrium point of the system (2.23) and $D \subset \mathbb{R}^n$ be a domain containing $\mathbf{x} = 0$. Let $\mathcal{W}(\mathbf{x}) : D \rightarrow \mathbb{R}$ be a continuously differentiable unbounded function such that $\dot{\mathcal{W}}(\mathbf{x}) \leq 0$. Let $\mathcal{S} = \{\mathbf{x} \in D | \dot{\mathcal{W}}(\mathbf{x}) = 0\}$ and suppose that no solution can stay identically in \mathcal{S} , other than the trivial solution $\mathbf{x}(t) = 0$.

Then, the origin is asymptotically stable. Furthermore, if the Lyapunov function is radially unbounded, i.e. $D = \mathbb{R}^n$, and $\mathbf{x} = 0$ is the unique equilibrium point of the system (2.23), then the stability results are global.

Let us now consider nonautonomous systems of the form

$$\dot{\mathbf{x}} = f(t, \mathbf{x}) \quad (2.24)$$

where $f(t, \mathbf{x})$ is a smooth continuous and Lipschitz function. Theorem 2.9.2 and Lemma 2.9.1 are not valid for nonautonomous systems. Therefore, analysis of asymptotic stability of nonautonomous systems is generally more difficult than that of autonomous systems. The following lemma, which is known as Barbalat's lemma, can be employed in these cases. The proof of this lemma can be found on page 323 of [174].

Lemma 2.9.2. *Let $\alpha : \mathbb{R} \rightarrow \mathbb{R}$ be a uniformly continuous function on $[0, \infty)$. Suppose that $\lim_{t \rightarrow \infty} \int_0^t \alpha(\tau) d\tau$ exists and is finite. Then, $\alpha(t) \rightarrow 0$ as $t \rightarrow \infty$.*

2.9.2 Input to State Stability Theorem

The following definition is provided from [174].

Definition 2.9.11. The system (2.20) is said to be input-to-state stable (ISS) if there exist a class \mathcal{KL} function β and a class \mathcal{K} function γ such that for any initial state $\mathbf{x}(t_0)$ and any bounded input $\mathbf{u}(t)$, the solution $\mathbf{x}(t)$ exists for all $t \geq t_0$ and satisfies

$$\|\mathbf{x}(t)\| \leq \beta(\|\mathbf{x}(t_0)\|, t - t_0) + \gamma\left(\sup_{t_0 \leq \tau \leq t} \|\mathbf{u}(\tau)\|\right) \quad (2.25)$$

The above inequality guarantees that for any bounded input $\mathbf{u}(t)$, the state $\mathbf{x}(t)$ will be bounded. Furthermore, as t increases, the state $\mathbf{x}(t)$ will be ultimately bounded

by class \mathcal{K} function of $\sup_{t \geq t_0} \|\mathbf{u}(t)\|$. Input-to-state stability implies that the origin of the unforced system with $\mathbf{u}(t) = 0$ is globally uniformly asymptotically stable. \square

The following Lyapunov-like theorem gives a sufficient condition for input-to-state stability [174].

Theorem 2.9.3. *Let $\mathcal{W}(t, \mathbf{x}) : [0, \infty) \times \mathbb{R}^n \rightarrow \mathbb{R}$ be a continuously differentiable function such that*

$$\begin{aligned} \alpha_1(\|\mathbf{x}\|) &\leq \mathcal{W}(t, \mathbf{x}) \leq \alpha_2(\|\mathbf{x}\|) \\ \frac{\partial \mathcal{W}}{\partial t} + \frac{\partial \mathcal{W}}{\partial \mathbf{x}} f(t, \mathbf{x}, \mathbf{u}) &\leq \mathcal{W}_0(\mathbf{x}), \quad \forall \|\mathbf{x}\| \geq \rho(\|\mathbf{u}\|) > 0 \end{aligned}$$

$\forall (t, \mathbf{x}, \mathbf{u}) \in [0, \infty) \times \mathbb{R}^n \times \mathbb{R}^m$, where α_1, α_2 are class \mathcal{K}_∞ functions, ρ is a class \mathcal{K} function, and $\mathcal{W}_0(\mathbf{x})$ is a continuous positive definite function on \mathbb{R}^n . Then, the system (2.20) is input-to-state stable.

Proof: Is the same as in Theorem 4.19 in [174], and is, therefore omitted. \blacksquare

2.9.3 Stability Analysis of Switched Systems

In this subsection, we briefly define switched systems that will be used subsequently in the thesis. We consider a family of systems [175],

$$\dot{\mathbf{x}} = f_p(\mathbf{x}, t), \quad p \in \mathfrak{P} \tag{2.26}$$

where $\mathbf{x} \in \mathbb{R}^n$ is the state vector, $\mathfrak{P} = \{1, \dots, N\}$ and each $f_p(\mathbf{x}, t) : \mathbb{R}^n \times [0, \infty) \rightarrow \mathbb{R}^n$ is smooth and Lipschitz over \mathbb{R}^n with $f_p(0, t) = 0$. We define the switching signal $\sigma(t) : [0, \infty) \rightarrow \mathfrak{P}$, which is a piecewise constant function of time, with a finite number of discontinuities over every bounded time interval, which are denoted as

the switching times. The switching signal takes a constant value on every interval between two consecutive switching times. The role of σ is to specify, at each time instant t , the index $\sigma(t) \in \mathfrak{P}$ of the active subsystem.

The following two definitions and lemma are taken from [176].

Definition 2.9.12. There is a *non-vanishing dwell-time* for a given switched system if there exists a sequence $\{\tau_k\}$ of switching times such that $\inf_k \{\tau_{k+1} - \tau_k\} \geq \bar{\tau}$. Any value of $\bar{\tau} > 0$ for which this inequality holds is denoted as the *non-vanishing dwell-time*. \square

Definition 2.9.13. There is an *average dwell-time* for a given switched system, denoted by $\tau_{ad} > 0$, if the number of switchings on an arbitrary interval (t_1, t_2) , which is denoted by N_{sw} , satisfies,

$$N_{sw} \leq \frac{t_2 - t_1}{\tau_{ad}}$$

This implies that there exists a $\tau_{ad} > 0$ such that no switching occurs on any interval smaller than τ_{ad} . \square

Lemma 2.9.3. [176] *If a switched system has an average dwell-time τ_{ad} , then it has a non-vanishing dwell-time, $\bar{\tau} \in (0, \tau_{ad})$.* \square

The following two definitions will be used subsequently in the thesis.

Definition 2.9.14. [177] A smooth decrescent function $\mathscr{W}(\mathbf{x}, t) : \mathbb{R}^n \times [0, \infty) \rightarrow [0, \infty)$ is a *weak common* Lyapunov function for the switched system (2.26) if it is positive definite, $\mathscr{V}_1(\mathbf{x}) \leq \mathscr{W}(\mathbf{x}, t) \leq \mathscr{V}_2(\mathbf{x})$, where $\mathscr{V}_1(\mathbf{x})$ and $\mathscr{V}_2(\mathbf{x})$ are continuous positive definite functions, and

$$\dot{\mathscr{W}}(\mathbf{x}, t) = \frac{\partial \mathscr{W}}{\partial t} + \frac{\partial \mathscr{W}}{\partial \mathbf{x}} f_p(\mathbf{x}, t) \leq 0, \mathbf{x} \in \mathbb{R}^n, p \in \mathfrak{P}$$

□

Definition 2.9.15. [177] A smooth decrescent function $\mathcal{W}(\mathbf{x}, t) : \mathbb{R}^n \times [0, \infty) \rightarrow [0, \infty)$ is a *strong common* Lyapunov function for the switched system (2.26) if it is positive definite, $\mathcal{V}_1(\mathbf{x}) \leq \mathcal{W}(\mathbf{x}, t) \leq \mathcal{V}_2(\mathbf{x})$, where $\mathcal{V}_1(\mathbf{x})$ and $\mathcal{V}_2(\mathbf{x})$ are continuous positive definite functions, and

$$\dot{\mathcal{W}}(\mathbf{x}, t) = \frac{\partial \mathcal{W}}{\partial t} + \frac{\partial \mathcal{W}}{\partial \mathbf{x}} f_p(\mathbf{x}, t) < 0, \mathbf{x} \in \mathbb{R}^n, p \in \mathfrak{P}$$

□

The first lemma on stability of switched systems is provided next.

Lemma 2.9.4. *Let $\mathbf{x} = 0$ be an equilibrium point of the switched system (2.26) and $D \subset \mathbb{R}^n$ be a domain containing $\mathbf{x} = 0$. Let $\mathcal{W}(\mathbf{x}, t) : D \times [0, \infty) \rightarrow \mathbb{R}$ be a continuously differentiable, decrescent and unbounded function. If the function $\mathcal{W}(\mathbf{x}, t)$ is a weak common Lyapunov function (as per Definition 2.9.14), then $\mathbf{x} = 0$ is uniformly stable. Moreover, if the function $\mathcal{W}(\mathbf{x}, t)$ is a strong common Lyapunov function (as per Definition 2.9.15), then $\mathbf{x} = 0$ is uniformly asymptotically stable. If $\mathcal{V}_1(\mathbf{x})$ is radially unbounded, i.e. $\mathcal{V}_1(\mathbf{x}) \rightarrow \infty$ as $\|\mathbf{x}\| \rightarrow \infty$, and $D = \mathbb{R}^n$, then $\mathbf{x} = 0$ is globally uniformly asymptotically stable.*

Proof: Is similar to that of the Proposition 2.6 in [177], and is, therefore omitted. ■

Next, we present a result that will be employed for stability analysis of nonautonomous switched systems, which is similar to Barbalat's lemma ¹.

Lemma 2.9.5. *Let us define a switched signal $\mathcal{S}(t) = \xi_p(t)$, $p \in \mathfrak{P}$, where $\xi_p(t)$ is a uniformly continuous function and assume $\xi_p(t)$ is upper bounded, i.e. $\sup_t \{\xi_p(t)\} <$*

¹A similar argument has appeared in the proof of Theorem 7 in [176].

∞ . This consequently implies $\sup_t \{\mathcal{S}(t)\} < \infty$. Let $\dot{\xi}_p(t) \leq 0$. Then, $\mathcal{S}(t) \rightarrow 0$ as $t \rightarrow \infty$ provided that there exists a non-vanishing dwell-time between two sequential switchings.

Proof: Without loss of generality, consider any two consecutive switching of the p -th and the \bar{p} -th systems, where $p, \bar{p} \in \mathfrak{P}, p \neq \bar{p}$. Let t_{h_1}, t_{h_2}, \dots denote an infinite sequence of switching times for the p -th system, and $t_{h_1+1}, t_{h_2+1}, \dots$, denote another infinite sequence of switching times for the \bar{p} -th system. The difference between any two consecutive time intervals, namely, $[t_{h_e}, t_{h_e+1}), e = 1, 2, \dots$ is not less than $\bar{\tau}$. We denote the union of these intervals by $\bar{\mathcal{E}}$, i.e. $\bar{\mathcal{E}} \triangleq \bigcup_{e=1}^{\infty} [t_{h_e}, t_{h_e+1})$. Now let us introduce a new function,

$$y_{\bar{\mathcal{E}}}(t) = \begin{cases} -\frac{d}{dt} \xi_p(t) & \text{if } t \in \bar{\mathcal{E}} \\ 0 & \text{otherwise} \end{cases} \quad (2.27)$$

Note that we have $\sup\{\xi_p(t)\} < \infty$ and $\dot{\xi}_p \leq 0$. Consequently, we have $y_{\bar{\mathcal{E}}}(t) = |y_{\bar{\mathcal{E}}}(t)|, \forall t \geq 0$, and therefore, from Definition 2.9.7 and Remark 2.9.1 we have $y_{\bar{\mathcal{E}}}(t) \in \mathfrak{L}_1$. Next, we show that $y_{\bar{\mathcal{E}}}(t) \rightarrow 0$ as $t \rightarrow \infty$. Let us suppose that $y_{\bar{\mathcal{E}}}(t) \not\rightarrow 0$ as $t \rightarrow \infty$. Then, there exists a sequence $t_{\bar{n}}$ in $[0, \infty)$ such that $t_{\bar{n}} \rightarrow \infty$ as $\bar{n} \rightarrow \infty$, and $\|y_{\bar{\mathcal{E}}}(t_{\bar{n}})\| \geq \varepsilon > 0$ for all \bar{n} , where $\bar{n} \in \mathbb{N}$. Note that $y_{\bar{\mathcal{E}}}(t)$ is uniformly continuous on $\bar{\mathcal{E}}$. Non-compactness of $\bar{\mathcal{E}}$ would not impact our analysis since $-\frac{d}{dt} \xi_p(t)$ is properly defined and is uniformly continuous (refer to the Continuous Extension Theorem on page 165 of [178] for more information). By the uniform continuity of $y_{\bar{\mathcal{E}}}(t)$ on $\bar{\mathcal{E}}$, it follows that there exists a $\delta > 0$ such that for all \bar{n} and all $0 \leq t \in \bar{\mathcal{E}}$, we have $\|t_{\bar{n}} - t\| \leq \delta \Rightarrow \|y_{\bar{\mathcal{E}}}(t_{\bar{n}}) - y_{\bar{\mathcal{E}}}(t)\| \leq \frac{\varepsilon}{2}$.

In other words, for all $t \in [t_{\bar{n}}, t_{\bar{n}} + \delta]$ and for all \bar{n} we have (recall that the

length of each interval in $\bar{\mathcal{E}}$ is bounded from below by $\bar{\tau} > 0$):

$$\|y_{\bar{\mathcal{E}}}(t)\| = \|y_{\bar{\mathcal{E}}}(t_{\bar{n}}) - (y_{\bar{\mathcal{E}}}(t_{\bar{n}}) - y_{\bar{\mathcal{E}}}(t))\| \geq \|y_{\bar{\mathcal{E}}}(t_{\bar{n}})\| - \|y_{\bar{\mathcal{E}}}(t_{\bar{n}}) - y_{\bar{\mathcal{E}}}(t)\| \geq \varepsilon - \frac{\varepsilon}{2} = \frac{\varepsilon}{2}$$

This contradicts the assertion stated earlier that $y_{\bar{\mathcal{E}}}(t) \in \mathfrak{L}_1$. Therefore, $y_{\bar{\mathcal{E}}}(t) \rightarrow 0$ as $t \rightarrow \infty$, and therefore, we have $\mathcal{S}(t) \rightarrow 0$ as $t \rightarrow \infty$. This completes the proof of the lemma. ■

2.10 Concluding Remarks

This chapter summarized basic assumptions and theorems that will be employed subsequently in this thesis. We provided definitions of multi-agent systems as well as Euler-Lagrange (EL) dynamical systems. As it is discussed in this chapter, spacecraft attitude dynamics can be described by using EL formulation. Furthermore, we review basic assumptions and preliminaries from graph theory and optimal control theory. Finally, stability theorems for nonlinear and switched systems are provided.

Chapter 3

Distributed Optimal Formation

Control of Euler-Lagrange Systems

3.1 Introduction and Problem Statement

The general objective of this thesis is to study synchronization and set-point tracking control of a network of Euler-Lagrange (EL) systems. To be more specific, our objective is to design a distributed control law for each EL system in the network (which is equivalently called as the *agent*) to guarantee the states of the agents reach to a common value with possibility of pre-defined distances (which is also denoted as the *consensus state*, *consensus value* or *formation-keeping behavior* in this thesis) and the agents follow a desired common set-point signal (if it is provided), which is equivalently denoted as the *station-keeping behavior* in this thesis. We consider several practical constraints in the design of the controllers, including parameter uncertainties, external disturbances, actuator faults and input saturation constraints. Therefore, we use controller design and synthesis techniques, such as optimal control techniques, robust and adaptive approaches to meet our objectives.

Our objective in this chapter is to employ synthesis-based control techniques to satisfy formation-keeping as well as station-keeping objectives by employing optimal control techniques to guarantee satisfaction of a performance index. Additionally, we consider parameter uncertainty in this chapter and propose two approaches, namely, adaptive and robust, to compensate for the effects of parameter uncertainty in the system. It is important to note that in this chapter we assume the communication network topology, which will be defined subsequently, is not fixed and it is *switching*. In other words, we assume that the number of the neighbors of an agent are not fixed and the agents are allowed to communicate with different agents in different times.

3.1.1 Communication Network Topology

In this chapter, it is assumed that information exchanges among the m EL systems can be represented by a graph \mathcal{G} . This graph consists of a node set \mathcal{V} , an edge set $\mathcal{E} \subseteq \mathcal{V} \times \mathcal{V}$, and a weighted adjacency matrix $\Lambda = [\lambda_{jn}] \in \mathbb{R}^{m \times m}$. The m agents in the network are considered as nodes of this graph. The communication links among the agents are considered as the graph edge set. In the following, we provide the definition of the communication network topology that is considered in this chapter.

Definition 3.1.1. A finite set of h communication graphs is denoted by $\bar{\mathcal{G}} = \{\mathcal{G}_1, \dots, \mathcal{G}_h\}$ which is characterized by having the same node set, i.e. $\mathcal{V}_1 = \dots = \mathcal{V}_h$. Furthermore, the edge set for f ($f \leq h$) communication graphs are different from the others, i.e. $\mathcal{E}_1 \neq \dots \neq \mathcal{E}_f$. In addition, $h - f \geq 0$ communication graphs with the same node set and edge set(s) have different weighted adjacency matrices. This results in a different weighted adjacency matrix for each communication graph, specifically, $\Lambda_1 \neq \dots \neq \Lambda_h$. Consequently, the Laplacian matrix associated with each $i \in \mathcal{H}$

communication graph, that is denoted by \mathcal{L}_i , where $\mathcal{H} = \{1, \dots, h\}$, is also different. All the h communication graphs are assumed to be *connected*, therefore, \mathcal{L}_i is positive semi-definite $\forall i \in \mathcal{H}$. \square

3.1.2 Synchronization Error

Let us denote the *position synchronization error* between the j -th and the n -th EL system agents as,

$$\mathbf{q}_{jn}(t) = \mathbf{q}_j(t) - \mathbf{q}_n(t) - \mathbf{q}_{jn}^b, \quad j \in \mathcal{V}, n \in \mathcal{N}_j \quad (3.1)$$

where \mathbf{q}_{jn}^b is a positive constant added to allow non-zero distances among the agents in the steady-state. The *velocity synchronization error*, which is the time derivative of $\mathbf{q}_{jn}(t)$, is given by $\dot{\mathbf{q}}_{jn}(t) = \dot{\mathbf{q}}_j(t) - \dot{\mathbf{q}}_n(t)$, $j \in \mathcal{V}, n \in \mathcal{N}_j$.

Let us now designate s_{jn} as a “*weighted*” *synchronization error* according to,

$$s_{jn} = \dot{\mathbf{q}}_{jn} + \bar{\mathbf{K}}_j \mathbf{q}_{jn} \quad (3.2)$$

where $\bar{\mathbf{K}}_j \in \mathbb{R}^{k \times k}$ is a positive definite diagonal matrix.

One can decompose the term \mathbf{q}_{jn}^b as follows $\mathbf{q}_{jn}^b = \mathbf{q}_j^b - \mathbf{q}_n^b$, $j, n \in \mathcal{V}, j \neq n$, where \mathbf{q}_j^b and \mathbf{q}_n^b are constant positive numbers that are provided to the j -th and the n -th EL systems by the command and control center to avoid the agents collision. Furthermore, let us denote the desired constant position for the networked EL systems to be \mathbf{q}^* .

Definition 3.1.2. The EL systems that receive the desired position, \mathbf{q}^* , are defined as the *leaders*. The other EL systems, which do not have access to this desired position are denoted as the *followers*. We label, without loss of generality, the EL

systems 1 to ‘ l ’ as the leaders and the EL systems ‘ $l + 1$ ’ to ‘ m ’ as the followers. \square

Let us now define the error vectors for the leaders, $\tilde{\mathbf{q}}_j(t)$, according to:

$$\tilde{\mathbf{q}}_j(t) = \mathbf{q}_j(t) - \mathbf{q}_j^b - \mathbf{q}^*, \quad j \in \{1, \dots, l\} \quad (3.3)$$

The error vectors for the followers are defined according to

$$\tilde{\mathbf{q}}_j(t) = \mathbf{q}_j(t) - \mathbf{q}_j^b, \quad j \in \{l + 1, \dots, m\} \quad (3.4)$$

Consequently, one can designate s_j as a “*weighted*” error according to: $s_j = \dot{\tilde{\mathbf{q}}}_j + \bar{\mathbf{K}}_j \tilde{\mathbf{q}}_j, j \in \mathcal{V}$. One can then show that $s_{jn} = s_j - s_n$ for the j -th and the n -th EL systems in the network. It can also be shown that the weighted synchronization error can be re-written as: $s_{jn} = \dot{\tilde{\mathbf{q}}}_{jn} + \bar{\mathbf{K}}_j \tilde{\mathbf{q}}_{jn}$, where $\dot{\tilde{\mathbf{q}}}_{jn} = \dot{\tilde{\mathbf{q}}}_j - \dot{\tilde{\mathbf{q}}}_n$ and $\tilde{\mathbf{q}}_{jn} = \tilde{\mathbf{q}}_j - \tilde{\mathbf{q}}_n$.

Remark 3.1.1. It should be noted that the constant term \mathbf{q}_{jn}^b is introduced to effectively avoid the EL system agents from colliding at the steady-state. However, during the transient phase of the mission one needs to consider an obstacle avoidance penalty function and add an extra term to the controllers in order to avoid collision among the agents. This aspect is, however, beyond the scope of this chapter. An interested reader can refer to [21, 179] for more details. It should be noted that in applications such as spacecraft attitude synchronization for formation flying missions, which is considered in this chapter, adding a collision avoidance term is not required since the spacecraft attitude do not collide with one another.

3.1.3 Statement of the Problem

Consider a network of ‘ m ’ heterogeneous nonlinear EL systems with a set of ‘ h ’ communication graphs as per Definition 3.1.1. The j -th EL system in the network,

$j \in \mathcal{V}$, is governed by the dynamic equation (2.7). Our objective is to design and develop distributed optimal control laws which can guarantee state synchronization of the networked EL systems as well as position tracking. In other words, we employ optimal control techniques to develop distributed control laws which guarantee the following requirements: (r1) stability of the closed-loop networked EL systems, (r2) synchronization of the EL system coordinates (which is also denoted as the consensus seeking or the formation-keeping), that is $\mathbf{q}_{jn} \rightarrow 0$ and $\dot{\mathbf{q}}_{jn} \rightarrow 0$ as $t \rightarrow \infty$, and (r3) tracking of the desired position by the networked EL systems (which is also denoted as the station-keeping), i.e. $\tilde{\mathbf{q}}_j \rightarrow 0$ and $\dot{\tilde{\mathbf{q}}}_j \rightarrow 0$ as $t \rightarrow \infty$. The above requirements will guarantee that the EL systems reach, at the steady-state, the same relative posture. The controller that guarantees the requirements (r1) and (r2) is denoted as the *formation-keeping controller* and the controller that guarantees the requirements (r1) and (r3) is denoted as the *station-keeping controller*.

The constraints that we consider for the development of our optimal control laws are as follows: (c1) the communication network topology is *not* fixed and is *switching*, and (c2) the EL systems parameters are not known *a priori*.

Remark 3.1.2. In this chapter $\delta(t)$ in (2.7) is used to represent additive actuator faults in Section 3.4. It is therefore, assumed to be equal to zero in this chapter, unless otherwise stated.

3.2 Optimal Synchronization Control of the Heterogeneous Euler-Lagrange Systems

Our goal in this section is to introduce an optimal distributed control law which satisfies the three requirements (r1), (r2) and (r3) and the first constraint (c1) as

introduced in Section 3.1.3.

We employ the following modified computed-torque control law to the j -th EL system for the corresponding i -th communication network topology, i.e.,

$$\mathbf{u}_{j,i} = \mathbf{D}_j(\mathbf{q}_j)\dot{\mathbf{r}}_j + \mathbf{C}_j(\mathbf{q}_j, \dot{\mathbf{q}}_j)\mathbf{r}_j + \mathbf{G}_j(\mathbf{q}_j) + \frac{\partial \mathcal{F}(\dot{\mathbf{q}}_j)}{\partial \dot{\mathbf{q}}_j} + \tau_{j,i}, \quad j \in \mathcal{V}, i \in \mathcal{H} \quad (3.5)$$

where $\tau_{j,i}$ is an auxiliary control input and $\mathbf{r}_j = -\bar{\mathbf{K}}_j \tilde{\mathbf{q}}_j$. The dynamics of the closed-loop system (2.7) and (3.5) is now reduced to

$$\mathbf{D}_j(\mathbf{q}_j)(\ddot{\tilde{\mathbf{q}}}_j + \bar{\mathbf{K}}_j \dot{\tilde{\mathbf{q}}}_j) + \mathbf{C}_j(\mathbf{q}_j, \dot{\tilde{\mathbf{q}}}_j)(\dot{\tilde{\mathbf{q}}}_j + \bar{\mathbf{K}}_j \tilde{\mathbf{q}}_j) = \tau_{j,i} \quad (3.6)$$

which can be written in the following *nonlinear* state-space form ¹,

$$\dot{\mathbf{x}}_j = \mathfrak{F}_j(\mathbf{x}_j)\mathbf{x}_j + \mathfrak{G}_j(\mathbf{x}_j)\tau_{j,i} \quad (3.7)$$

where $\mathbf{x}_j = [\tilde{\mathbf{q}}_j^T, \dot{\tilde{\mathbf{q}}}_j^T]^T$, and

$$\mathfrak{F}_j(\mathbf{x}_j) = \begin{bmatrix} 0 & \mathfrak{J}_k \\ -\mathbf{D}_j^{-1}\mathbf{C}_j\bar{\mathbf{K}}_j & -\mathbf{D}_j^{-1}\mathbf{C}_j - \bar{\mathbf{K}}_j \end{bmatrix},$$

$$\mathfrak{G}_j(\mathbf{x}_j) = \begin{bmatrix} 0 \\ \mathbf{D}_j^{-1} \end{bmatrix}$$

The auxiliary control input $\tau_{j,i}$ is now decomposed into,

$$\tau_{j,i} = \bar{\tau}_j + \sum_{n \in \mathcal{N}_{j,i}} \mathbf{F}_{jn,i} \mathbf{x}_n \quad (3.8)$$

¹This is obtained by re-writing (3.6) in the following form: $\ddot{\tilde{\mathbf{q}}}_j = \mathbf{D}_j^{-1}(\mathbf{q}_j)\tau_{j,i} - \mathbf{D}_j^{-1}(\mathbf{q}_j)\mathbf{C}_j(\mathbf{q}_j, \dot{\tilde{\mathbf{q}}}_j)\bar{\mathbf{K}}_j\tilde{\mathbf{q}}_j - (\mathbf{D}_j^{-1}(\mathbf{q}_j)\mathbf{C}_j(\mathbf{q}_j, \dot{\tilde{\mathbf{q}}}_j) + \bar{\mathbf{K}}_j)\dot{\tilde{\mathbf{q}}}_j$.

where $\mathbf{F}_{jn,i}$ represents the interaction terms among the agents and is to be selected according to the i -th communication graph, $i \in \mathcal{H}$, and $\bar{\tau}_j$ represents the dependence of the agent j control input on its local information.

To derive an optimal feedback control law for $\bar{\tau}_j$, the following quadratic performance index (PI) for the j -th EL system is introduced corresponding to the i -th communication network topology,

$$\mathcal{J}_{j,i} = \int_0^\infty \left[\frac{1}{2} \mathbf{x}_j^T \mathbf{Q}_{j,i} \mathbf{x}_j + \bar{\tau}_j^T \mathbf{R}_{j,i} \bar{\tau}_j + \frac{1}{4} \sum_{n \in \mathcal{N}_{j,i}} (\mathbf{x}_j - \mathbf{x}_n)^T \mathbf{Q}_{jn,i} (\mathbf{x}_j - \mathbf{x}_n) \right] dt \quad (3.9)$$

where $\mathbf{R}_{j,i}$ is a symmetric positive definite matrix and

$$\mathbf{Q}_{j,i} = (1 - \alpha_{j,i}) \bar{\mathbf{Q}}_{j,i}$$

and $\sum_{n \in \mathcal{N}_{j,i}} \mathbf{Q}_{jn,i} = \alpha_{j,i} \bar{\mathbf{Q}}_{j,i}$, and $\bar{\mathbf{Q}}_{j,i}$ is a symmetric positive semi-definite matrix. We further assume that $\sum_{n \in \mathcal{N}_{j,i}} \mathbf{Q}_{jn,i} = \sum_{j \in \mathcal{N}_{n,i}} \mathbf{Q}_{nj,i}$. For the leader EL system PI the parameter $\alpha_{j,i}$ is selected as $0 < \alpha_{j,i} < 1$ and for the follower EL system PI this parameter is set to $\alpha_{j,i} = 1$. The parameter $\alpha_{j,i}$ plays an important role in weighting two specific criteria for the leader EL system. Specifically, the smaller the value of $\alpha_{j,i}$, the less emphasis is placed on the state synchronization over the set-point tracking requirement. On the other hand, by selecting higher values for $\alpha_{j,i}$ one can put more emphasis on the state synchronization requirement and less on the set-point tracking. By minimizing $\mathcal{J}_{j,i}$ for the follower EL system ($\alpha_{j,i} = 1$), one can guarantee $(\mathbf{x}_j - \mathbf{x}_n) \rightarrow 0$ and $\bar{\tau}_j \rightarrow 0$ in the steady state, which is defined as the state synchronization (consensus seeking or formation-keeping). Consequently, by minimizing the cost function (3.9) our goal is to guarantee that all the agents in a neighboring set would synchronize their states and all the agents follow the desired

position despite the fact that this information is only available to the leaders.

Our objective is to find the control law $\bar{\tau}_j$ that minimizes (3.9) subject to the constraints that are imposed on (3.7). This optimal control law is denoted by $\bar{\tau}_j^*$. By invoking arguments that are presented in Section 2.8, one can show that a sufficient condition for existence of a smooth control input $\bar{\tau}_j^*$ that minimizes (3.9) and satisfies the constraint (3.7) is that there exists a function $\mathcal{Y}_{j,i}(\mathbf{x}_j, t)$ such that the following Hamilton-Jacobi-Bellman (HJB) equation is satisfied,

$$\begin{aligned} -\frac{\partial \mathcal{Y}_{j,i}(\mathbf{x}_j, t)}{\partial t} &= \min_{\bar{\tau}_j} \Phi_{j,i}(t, \mathbf{x}_j, \bar{\tau}_j) \\ \Phi_{j,i}(t, \mathbf{x}_j, \bar{\tau}_j) &= \frac{\partial \mathcal{Y}_{j,i}(\mathbf{x}_j, t)}{\partial \mathbf{x}_j} \dot{\mathbf{x}}_j + \bar{\tau}_j^T \mathbf{R}_{j,i} \bar{\tau}_j + \frac{1}{2} \mathbf{x}_j^T \mathbf{Q}_{j,i} \mathbf{x}_j \\ &\quad + \frac{1}{4} \sum_{n \in \mathcal{N}_{j,i}} (\mathbf{x}_j - \mathbf{x}_n)^T \mathbf{Q}_{jn,i} (\mathbf{x}_j - \mathbf{x}_n) \end{aligned} \quad (3.10)$$

where $\Phi_{j,i}(t, \mathbf{x}_j, \bar{\tau}_j)$ is known as the Hamiltonian. Since the matrix $\frac{\partial^2 \Phi_{j,i}(t, \mathbf{x}_j, \bar{\tau}_j)}{\partial \bar{\tau}_j^2} = \mathbf{R}_{j,i}$ is positive definite and is independent of \mathbf{x}_j , then the smooth input $\bar{\tau}_j$ that satisfies $\frac{\partial \Phi_{j,i}(t, \mathbf{x}_j, \bar{\tau}_j)}{\partial \bar{\tau}_j} = \mathbf{R}_{j,i} \bar{\tau}_j + \frac{\partial \mathcal{Y}_{j,i}(\mathbf{x}_j, t)}{\partial \mathbf{x}_j} \mathfrak{G}_j(\mathbf{x}_j) = 0$ is the solution to the optimal control problem. In the above formulation, $\mathcal{Y}_{j,i}(\mathbf{x}_j, t)$ is referred to as the value function for the i -th communication network topology. Our first main result is now presented below.

Theorem 3.2.1. *Consider the PI (3.9) for ‘ m ’ heterogeneous nonlinear EL systems where the j -th agent dynamics is governed by (3.7) subject to the corresponding i -th network topology, $i \in \mathcal{H}$. Suppose there exists a symmetric positive definite matrix $\mathbf{P}_{j,i}(\mathbf{x}_j) \in \mathbb{R}^{2k \times 2k}$ that is only a function of $\tilde{\mathbf{q}}_j$ such that the following dynamic*

Riccati equation is satisfied

$$\begin{aligned} \dot{\mathbf{P}}_{j,i}(\mathbf{x}_j) + \mathbf{P}_{j,i}(\mathbf{x}_j)\mathfrak{F}_j(\mathbf{x}_j) + \mathfrak{F}_j^T(\mathbf{x}_j)\mathbf{P}_{j,i}(\mathbf{x}_j) + \mathbf{Q}_{j,i} + \sum_{n \in \mathcal{N}_{j,i}} \mathbf{Q}_{jn,i} \\ - \mathbf{P}_{j,i}(\mathbf{x}_j)\mathfrak{G}_j(\mathbf{x}_j)\mathbf{R}_{j,i}^{-1} \times \mathfrak{G}_j^T(\mathbf{x}_j)\mathbf{P}_{j,i}(\mathbf{x}_j) = 0 \end{aligned} \quad (3.11)$$

The distributed control law for the j -th system that is given by

$$\tau_{j,i} \triangleq \underbrace{-\frac{1}{2}\mathbf{R}_{j,i}^{-1}\mathfrak{G}_j^T \left[\frac{\partial \mathcal{Y}_{j,i}(\mathbf{x}_j, t)}{\partial \mathbf{x}_j} \right]^T}_{\bar{\tau}_j^*} + \sum_{n \in \mathcal{N}_{j,i}} \mathbf{F}_{jn,i} \mathbf{x}_n \quad (3.12)$$

where $\mathbf{F}_{jn,i}$ is chosen such that $\mathbf{P}_{j,i}\mathfrak{G}_j \sum_{n \in \mathcal{N}_{j,i}} \mathbf{F}_{jn,i} = \frac{1}{2} \sum_{n \in \mathcal{N}_{j,i}} \mathbf{Q}_{jn,i}$ is an optimal controller in the sense that it minimizes the PI (3.9).

Proof: Let us introduce the following value function for the j -th EL system corresponding to the i -th communication network topology,

$$\mathcal{Y}_{j,i}(\mathbf{x}_j) = \frac{1}{2} \mathbf{x}_j^T \mathbf{P}_{j,i}(\mathbf{x}_j) \mathbf{x}_j \quad (3.13)$$

Consequently, the HJB equation (3.10) can be written as:

$$\frac{d}{dt} \mathcal{Y}_{j,i}(\mathbf{x}_j) + \bar{\tau}_j^T \mathbf{R}_{j,i} \bar{\tau}_j + \frac{1}{2} \mathbf{x}_j^T \mathbf{Q}_{j,i} \mathbf{x}_j + \frac{1}{4} \sum_{n \in \mathcal{N}_{j,i}} (\mathbf{x}_j - \mathbf{x}_n)^T \mathbf{Q}_{jn,i} (\mathbf{x}_j - \mathbf{x}_n) = 0$$

Since $\frac{d}{dt} \mathcal{Y}_{j,i}(\mathbf{x}_j) = \mathbf{x}_j^T \mathbf{P}_{j,i}(\mathbf{x}_j) \dot{\mathbf{x}}_j + \frac{1}{2} \mathbf{x}_j^T \dot{\mathbf{P}}_{j,i}(\mathbf{x}_j) \mathbf{x}_j$, we obtain,

$$\begin{aligned} \frac{1}{2} \mathbf{x}_j^T (\dot{\mathbf{P}}_{j,i} + \mathbf{P}_{j,i}\mathfrak{F}_j + \mathfrak{F}_j^T \mathbf{P}_{j,i} + \mathbf{Q}_{j,i}) \mathbf{x}_j + \mathbf{x}_j^T \mathbf{P}_{j,i} \mathfrak{G}_j \left(\bar{\tau}_j^* + \sum_{n \in \mathcal{N}_{j,i}} \mathbf{F}_{jn,i} \mathbf{x}_n \right) \\ + (\bar{\tau}_j^*)^T \mathbf{R}_{j,i} \bar{\tau}_j^* + \frac{1}{4} \sum_{n \in \mathcal{N}_{j,i}} (\mathbf{x}_j - \mathbf{x}_n)^T \mathbf{Q}_{jn,i} (\mathbf{x}_j - \mathbf{x}_n) = 0 \end{aligned} \quad (3.14)$$

Next we show that $\frac{\partial \mathcal{V}_{j,i}(\mathbf{x}_j,t)}{\partial \mathbf{x}_j} \mathfrak{G}_j = \mathbf{x}_j^T \mathbf{P}_{j,i} \mathfrak{G}_j$. Given the fact that $\frac{\partial \mathcal{V}_{j,i}(\mathbf{x}_j,t)}{\partial \mathbf{x}_j} = \frac{1}{2} \mathbf{x}_j^T \frac{\partial \mathbf{P}_{j,i}}{\partial \mathbf{x}_j} \mathbf{x}_j + \mathbf{x}_j^T \mathbf{P}_{j,i}^2$ and since $\mathbf{P}_{j,i}(\mathbf{x}_j)$ is only a function of $\tilde{\mathbf{q}}_j$ we have: $\frac{\partial \mathcal{V}_{j,i}(\mathbf{x}_j,t)}{\partial \mathbf{x}_j} = \left[\frac{1}{2} \mathbf{x}_j^T \frac{\partial \mathbf{P}_{j,i}}{\partial \tilde{\mathbf{q}}_j^T} \mathbf{x}_j \quad 0 \right] + \mathbf{x}_j^T \mathbf{P}_{j,i}$. Therefore, $\frac{\partial \mathcal{V}_{j,i}(\mathbf{x}_j,t)}{\partial \mathbf{x}_j} \mathfrak{G}_j$ can be written as $\frac{\partial \mathcal{V}_{j,i}(\mathbf{x}_j,t)}{\partial \mathbf{x}_j} \mathfrak{G}_j = \left[\frac{1}{2} \mathbf{x}_j^T \frac{\partial \mathbf{P}_{j,i}}{\partial \tilde{\mathbf{q}}_j^T} \mathbf{x}_j \quad 0 \right] \mathfrak{G}_j + \mathbf{x}_j^T \mathbf{P}_{j,i} \mathfrak{G}_j$, which reduces to: $\frac{\partial \mathcal{V}_{j,i}(\mathbf{x}_j,t)}{\partial \mathbf{x}_j} \mathfrak{G}_j = \mathbf{x}_j^T \mathbf{P}_{j,i} \mathfrak{G}_j$. Noting this and by using (3.12), expression (3.14), can be re-written as,

$$\begin{aligned} & \sum_{j=1}^m \frac{1}{2} \mathbf{x}_j^T \left(\dot{\mathbf{P}}_{j,i} + \mathbf{P}_{j,i} \tilde{\mathfrak{F}}_j + \tilde{\mathfrak{F}}_j^T \mathbf{P}_{j,i} + \mathbf{Q}_{j,i} - \mathbf{P}_{j,i} \mathfrak{G}_j \mathbf{R}_{j,i}^{-1} \mathfrak{G}_j^T \mathbf{P}_{j,i} \right) \mathbf{x}_j \\ & + \sum_{j=1}^m \mathbf{x}_j^T \mathbf{P}_{j,i} \mathfrak{G}_j \sum_{n \in \mathcal{N}_{j,i}} \mathbf{F}_{jn,i} \mathbf{x}_n + \frac{1}{4} \sum_{j=1}^m \sum_{n \in \mathcal{N}_{j,i}} (\mathbf{x}_j - \mathbf{x}_n)^T \mathbf{Q}_{jn,i} (\mathbf{x}_j - \mathbf{x}_n) = 0 \end{aligned}$$

which can be further simplified to

$$\begin{aligned} & \sum_{j=1}^m \frac{1}{2} \mathbf{x}_j^T \left(\dot{\mathbf{P}}_{j,i} + \mathbf{P}_{j,i} \tilde{\mathfrak{F}}_j + \tilde{\mathfrak{F}}_j^T \mathbf{P}_{j,i} + \mathbf{Q}_{j,i} - \mathbf{P}_{j,i} \mathfrak{G}_j \mathbf{R}_{j,i}^{-1} \mathfrak{G}_j^T \mathbf{P}_{j,i} \right) \mathbf{x}_j \\ & + \frac{1}{2} \sum_{j=1}^m \mathbf{x}_j^T \sum_{n \in \mathcal{N}_{j,i}} \mathbf{Q}_{jn,i} \mathbf{x}_n + \frac{1}{2} \sum_{j=1}^m \sum_{n \in \mathcal{N}_{j,i}} \mathbf{x}_j^T \mathbf{Q}_{jn,i} (\mathbf{x}_j - \mathbf{x}_n) = 0 \end{aligned} \quad (3.15)$$

Consequently, one obtains

$$\sum_{j=1}^m \frac{1}{2} \mathbf{x}_j^T \left(\dot{\mathbf{P}}_{j,i} + \mathbf{P}_{j,i} \tilde{\mathfrak{F}}_j + \tilde{\mathfrak{F}}_j^T \mathbf{P}_{j,i} + \mathbf{Q}_{j,i} + \sum_{n \in \mathcal{N}_{j,i}} \mathbf{Q}_{jn,i} - \mathbf{P}_{j,i} \mathfrak{G}_j \mathbf{R}_{j,i}^{-1} \mathfrak{G}_j^T \mathbf{P}_{j,i} \right) \mathbf{x}_j = 0$$

Therefore, by satisfying the dynamic Riccati equation (3.11), one can conclude that the above expression is also satisfied and $\mathbf{P}_{j,i}(\mathbf{x}_j)$ can be employed to obtain the value function (3.13). Hence, the control law (3.12) is a solution to the optimal control problem and this completes the proof of the theorem. \blacksquare

²For the definition of $\frac{\partial \mathbf{P}_{j,i}}{\partial \mathbf{x}_j} \mathbf{x}_j$ refer to Definition 2.5.3.

3.2.1 Discussion on the Existence of a Solution

It is not straightforward, in general, to obtain a solution to the *nonlinear* Riccati equation (3.11) for an arbitrary selection of the matrices $\mathbf{P}_{j,i}$, $\mathbf{Q}_{j,i}$, $\mathbf{Q}_{jn,i}$ and $\mathbf{R}_{j,i}$. Therefore, in order to guarantee existence of a solution to this Riccati equation, we assign specific structures to the matrices $\mathbf{P}_{j,i}$, $\mathbf{Q}_{j,i}$, $\mathbf{Q}_{jn,i}$ and $\mathbf{R}_{j,i}$. Specifically, inspired from [180], let $\mathbf{P}_{j,i}$ and $\mathbf{R}_{j,i}$ be chosen as follows,

$$\mathbf{P}_{j,i}(\mathbf{x}_j) \triangleq \begin{bmatrix} \bar{\mathbf{K}}_j \mathbf{D}_j \bar{\mathbf{K}}_j + \bar{\mathbf{K}}_j \mathbf{K}_{j,i} & \bar{\mathbf{K}}_j \mathbf{D}_j \\ \bar{\mathbf{K}}_j \mathbf{D}_j & \mathbf{D}_j \end{bmatrix} \text{ and } \mathbf{R}_{j,i} = \mathbf{K}_{j,i}^{-1}$$

where $\mathbf{K}_{j,i} \in \mathbb{R}^{k \times k}$ is a positive definite diagonal matrix. One can now show that

according to Property 2.1.2 we have $\dot{\mathbf{P}}_{j,i} + \mathbf{P}_{j,i} \bar{\mathfrak{F}}_j + \bar{\mathfrak{F}}_j^T \mathbf{P}_{j,i} = \begin{bmatrix} 0 & \bar{\mathbf{K}}_j \mathbf{K}_{j,i} \\ \bar{\mathbf{K}}_j \mathbf{K}_{j,i} & 0 \end{bmatrix}$.

In addition, we obtain $\mathbf{P}_{j,i} \mathfrak{G}_j \mathbf{R}_{j,i}^{-1} \mathfrak{G}_j^T \mathbf{P}_{j,i} \equiv \mathbf{P}_{j,i} \mathfrak{G}_j \mathbf{K}_{j,i} \mathfrak{G}_j^T \mathbf{P}_{j,i} = \begin{bmatrix} \bar{\mathbf{K}}_j^2 \mathbf{K}_{j,i} & \bar{\mathbf{K}}_j \mathbf{K}_{j,i} \\ \bar{\mathbf{K}}_j \mathbf{K}_{j,i} & \mathbf{K}_{j,i} \end{bmatrix}$.

Consequently, we have $\mathbf{Q}_{j,i} + \sum_{n \in \mathcal{N}_{j,i}} \mathbf{Q}_{jn,i} = \bar{\mathbf{Q}}_{j,i} \triangleq \begin{bmatrix} \bar{\mathbf{K}}_j^2 \mathbf{K}_{j,i} & 0 \\ 0 & \mathbf{K}_{j,i} \end{bmatrix}$. This guarantees that the Riccati equation has a solution. By using the above parameterizations,

one now obtains $\sum_{n \in \mathcal{N}_{j,i}} \mathbf{F}_{jn,i} = \frac{1}{2} [\bar{\mathbf{K}}_j \mathbf{K}_{j,i} \quad \mathbf{K}_{j,i}]$.

One can further assume that $\mathbf{Q}_{jn,i} = \mathbf{Q}_{jk,i}$ where $n \neq k$ and $n, k \in \mathcal{N}_{j,i}, i \in \mathcal{H}$.

It can then be shown according to (3.12) and using the parameterizations provided above that the control law for the j -th *leader* EL system that is corresponding to the

i -th communication network topology is obtained as,

$$\begin{aligned}
\tau_{j,i}^{\text{leader}} &\triangleq -\frac{1}{2}\mathbf{K}_{j,i}(\dot{\tilde{\mathbf{q}}}_j + \bar{\mathbf{K}}_j\tilde{\mathbf{q}}_j) + \frac{\alpha_{j,i}}{2}\mathbf{K}_{j,i} \sum_{n \in \mathcal{N}_{j,i}} \frac{1}{|\mathcal{N}_{j,i}|} (\dot{\tilde{\mathbf{q}}}_n + \bar{\mathbf{K}}_j\tilde{\mathbf{q}}_n) \\
&= -\frac{1}{2}(1 - \alpha_{j,i})\mathbf{K}_{j,i}(\dot{\tilde{\mathbf{q}}}_j + \bar{\mathbf{K}}_j\tilde{\mathbf{q}}_j) \\
&\quad - \frac{\alpha_{j,i}}{2}\mathbf{K}_{j,i} \sum_{n \in \mathcal{N}_{j,i}} \frac{1}{|\mathcal{N}_{j,i}|} \left[(\dot{\tilde{\mathbf{q}}}_j + \bar{\mathbf{K}}_j\tilde{\mathbf{q}}_j) - (\dot{\tilde{\mathbf{q}}}_n + \bar{\mathbf{K}}_j\tilde{\mathbf{q}}_n) \right]
\end{aligned} \tag{3.16}$$

and the control law for the j -th follower EL system that is corresponding to the i -th communication network topology is obtained as,

$$\begin{aligned}
\tau_{j,i}^{\text{follower}} &\triangleq -\frac{1}{2}\mathbf{K}_{j,i}(\dot{\tilde{\mathbf{q}}}_j + \bar{\mathbf{K}}_j\tilde{\mathbf{q}}_j) + \frac{1}{2}\mathbf{K}_{j,i} \sum_{n \in \mathcal{N}_{j,i}} \frac{1}{|\mathcal{N}_{j,i}|} (\dot{\tilde{\mathbf{q}}}_n + \bar{\mathbf{K}}_j\tilde{\mathbf{q}}_n) \\
&= -\frac{1}{2}\mathbf{K}_{j,i} \sum_{n \in \mathcal{N}_{j,i}} \frac{1}{|\mathcal{N}_{j,i}|} \left[(\dot{\tilde{\mathbf{q}}}_j + \bar{\mathbf{K}}_j\tilde{\mathbf{q}}_j) - (\dot{\tilde{\mathbf{q}}}_n + \bar{\mathbf{K}}_j\tilde{\mathbf{q}}_n) \right]
\end{aligned} \tag{3.17}$$

The following lemma summarizes our results in this subsection.

Lemma 3.2.1. *Consider a network of ‘ m ’ heterogeneous EL systems whose dynamics are governed by (3.7) and subject to the control law (3.16) for the j -th leader and the control law (3.17) for the j -th follower corresponding to the i -th communication network topology ($i \in \mathcal{H}$). The control law (3.16) is optimal in the sense*

that it minimizes the PI (3.9) with $\mathbf{R}_{j,i} = \mathbf{K}_{j,i}^{-1}$, $\sum_{n \in \mathcal{N}_{j,i}} \mathbf{Q}_{jn,i} = \alpha_{j,i} \begin{bmatrix} \bar{\mathbf{K}}_j^2 \mathbf{K}_{j,i} & 0 \\ 0 & \mathbf{K}_{j,i} \end{bmatrix}$,

$\mathbf{Q}_{j,i} = (1 - \alpha_{j,i}) \begin{bmatrix} \bar{\mathbf{K}}_j^2 \mathbf{K}_{j,i} & 0 \\ 0 & \mathbf{K}_{j,i} \end{bmatrix}$, and $0 < \alpha_{j,i} < 1$, and the control law (3.17) is

optimal in the sense that it minimizes the PI (3.9) with $\mathbf{R}_{j,i} = \mathbf{K}_{j,i}^{-1}$, $\sum_{n \in \mathcal{N}_{j,i}} \mathbf{Q}_{jn,i} = \begin{bmatrix} \bar{\mathbf{K}}_j^2 \mathbf{K}_{j,i} & 0 \\ 0 & \mathbf{K}_{j,i} \end{bmatrix}$, and $\mathbf{Q}_{j,i} = 0$, where $\mathbf{K}_{j,i}$, $\bar{\mathbf{K}}_j$ are positive definite diagonal matrices.

Proof: Follows along the constructive lines that are derived above. ■

3.2.2 Stability Analysis

In this subsection, we demonstrate the global stability of the networked heterogeneous EL systems under the distributed control laws (3.5) and (3.16) for the j -th leader and the control laws (3.5) and (3.17) for the j -th follower. Our second main result is formally stated below.

Theorem 3.2.2. *Consider a network of ‘ m ’ heterogeneous EL systems where agents are governed by the dynamics (2.7) with $\delta = 0$ and subject to the distributed control laws (3.5) and (3.16) for the j -th leader and the distributed control laws (3.5) and (3.17) for the j -th follower, corresponding to the i -th communication network topology, where $\mathbf{K}_{j,i}$, $\bar{\mathbf{K}}_j$ are positive definite diagonal matrices. It then follows that the closed-loop EL system satisfies the requirements (r1)–(r3) as specified in Section 3.1.3 in presence of average dwell-time switchings in the communication network topologies.*

Proof: Let us consider the following radially unbounded Lyapunov function candidate for the networked closed-loop system (2.7), (3.5), (3.16) and (3.17),

$$\mathcal{X}_1 \triangleq \mathcal{W}_i = \sum_{j=1}^m \mathcal{W}_j = \frac{1}{2} \sum_{j=1}^m s_j^T \mathbf{D}_j(\mathbf{q}_j) s_j = \frac{1}{2} \sum_{j=1}^m \mathbf{x}_j^T \begin{bmatrix} \bar{\mathbf{K}}_j \mathbf{D}_j \bar{\mathbf{K}}_j & \bar{\mathbf{K}}_j \mathbf{D}_j \\ \bar{\mathbf{K}}_j \mathbf{D}_j & \mathbf{D}_j \end{bmatrix} \mathbf{x}_j \quad (3.18)$$

The above function is positive definite since $\underline{k} \mathfrak{I}_k < \mathbf{D}(\mathbf{q}) < \bar{k} \mathfrak{I}_k, \forall \mathbf{q}$ according to property **Property 2.1.1**.

The time derivative of the above Lyapunov function candidate along the trajectories of the closed-loop system is given by

$$\begin{aligned}
\dot{\mathcal{X}}_1 &= \sum_{j=1}^m \frac{1}{2} \mathbf{s}_j^T \dot{\mathbf{D}}_j \mathbf{s}_j + \sum_{j=1}^m \mathbf{s}_j^T \mathbf{D}_j \dot{\mathbf{s}}_j \\
&= \sum_{j=1}^m \frac{1}{2} (\dot{\mathbf{q}}_j + \bar{\mathbf{K}}_j \tilde{\mathbf{q}}_j)^T \dot{\mathbf{D}}_j (\dot{\mathbf{q}}_j + \bar{\mathbf{K}}_j \tilde{\mathbf{q}}_j) + \sum_{j=1}^m (\dot{\mathbf{q}}_j + \bar{\mathbf{K}}_j \tilde{\mathbf{q}}_j)^T \times \\
&\quad \left[\boldsymbol{\tau}_{j,i} - \mathbf{C}_j(\mathbf{q}_j, \dot{\mathbf{q}}_j) (\dot{\mathbf{q}}_j + \bar{\mathbf{K}}_j \tilde{\mathbf{q}}_j) \right] \\
&= \sum_{j=1}^m (\dot{\mathbf{q}}_j + \bar{\mathbf{K}}_j \tilde{\mathbf{q}}_j)^T \left[\frac{1}{2} \dot{\mathbf{D}}_j - \mathbf{C}_j(\mathbf{q}_j, \dot{\mathbf{q}}_j) \right] (\dot{\mathbf{q}}_j + \bar{\mathbf{K}}_j \tilde{\mathbf{q}}_j) \\
&\quad + \sum_{j=1}^l (\dot{\mathbf{q}}_j + \bar{\mathbf{K}}_j \tilde{\mathbf{q}}_j)^T \left[-\frac{1}{2} (1 - \alpha_{j,i}) \mathbf{K}_{j,i} (\dot{\mathbf{q}}_j + \bar{\mathbf{K}}_j \tilde{\mathbf{q}}_j) \right. \\
&\quad \left. - \frac{\alpha_{j,i}}{2} \mathbf{K}_{j,i} \sum_{n \in \mathcal{N}_{j,i}} \frac{(\dot{\mathbf{q}}_j + \bar{\mathbf{K}}_j \tilde{\mathbf{q}}_j) - (\dot{\mathbf{q}}_n + \bar{\mathbf{K}}_j \tilde{\mathbf{q}}_n)}{|\mathcal{N}_{j,i}|} \right] + \sum_{j=l+1}^m (\dot{\mathbf{q}}_j + \bar{\mathbf{K}}_j \tilde{\mathbf{q}}_j)^T \times \\
&\quad \left[-\frac{1}{2} \mathbf{K}_{j,i} \sum_{n \in \mathcal{N}_{j,i}} \frac{(\dot{\mathbf{q}}_j + \bar{\mathbf{K}}_j \tilde{\mathbf{q}}_j) - (\dot{\mathbf{q}}_n + \bar{\mathbf{K}}_j \tilde{\mathbf{q}}_n)}{|\mathcal{N}_{j,i}|} \right]
\end{aligned}$$

The above can be simplified to

$$\begin{aligned}
\dot{\mathcal{X}}_1 &= -\frac{1}{2} \sum_{j=1}^l (1 - \alpha_{j,i}) \mathbf{s}_j^T \mathbf{K}_{j,i} \mathbf{s}_j - \sum_{j=1}^l \frac{\alpha_{j,i}}{4} \sum_{n \in \mathcal{N}_{j,i}} \frac{1}{|\mathcal{N}_{j,i}|} \mathbf{s}_{jn}^T \mathbf{K}_{j,i} \mathbf{s}_{jn} \\
&\quad - \sum_{j=l+1}^m \frac{1}{4} \sum_{n \in \mathcal{N}_{j,i}} \frac{1}{|\mathcal{N}_{j,i}|} \mathbf{s}_{jn}^T \mathbf{K}_{j,i} \mathbf{s}_{jn} \leq 0
\end{aligned} \tag{3.19}$$

where $\mathbf{s}_{jn} = \mathbf{s}_j - \mathbf{s}_n \triangleq (\dot{\mathbf{q}}_j + \bar{\mathbf{K}}_j \tilde{\mathbf{q}}_j) - (\dot{\mathbf{q}}_n + \bar{\mathbf{K}}_j \tilde{\mathbf{q}}_n)$ and $\mathbf{K}_{j,i}$, $\bar{\mathbf{K}}_j$ are positive definite diagonal matrices.

Given the fact that the Lyapunov function candidate is identical for all the communication topologies one notes that the Lyapunov function \mathcal{X}_1 is a *weak* common Lyapunov function for the considered switched system (refer to Definition 2.9.14). Note that since the Lyapunov function is radially unbounded and $\dot{\mathcal{X}}_1 \leq 0$,

all the signals remain globally bounded and the closed-loop EL system is globally stable. Note that Lemma 2.9.3 implies that there exists a non-vanishing dwell time $\bar{\tau} \in (0, \tau_{ad})$ among each switchings in the communication network topologies.

Now given that \mathcal{X}_1 is upper bounded and $\dot{\mathcal{X}}_1 \leq 0$, by invoking Lemma 2.9.5 one can conclude that under non-vanishing dwell-time we have $s_{jn} \rightarrow 0$ as $t \rightarrow \infty$. This implies that $s_{jn} \in \mathcal{L}_2, \forall j, n \in \mathcal{V}, j \neq n$. By invoking Lemma A.12 in [158], one can also conclude that $\mathbf{q}_{jn} \rightarrow 0$ and $\dot{\mathbf{q}}_{jn} \rightarrow 0$ as $t \rightarrow \infty$. In addition, by invoking Lemma 2.9.5 one can conclude that under non-vanishing dwell-time we have $s_j \rightarrow 0, j \in \{1, \dots, l\}$ as $t \rightarrow \infty$. Consequently, due to the fact that the communication network topology is connected, boundedness and asymptotic stability of $s_j, \forall j$ are also guaranteed. Therefore, the requirements (r1)–(r3) are formally shown to be satisfied. This completes the proof of the theorem. ■

3.3 Synchronization Control of Uncertain EL Systems

In the development of the optimal control laws in the previous section it was assumed that an exact knowledge of the EL system parameters is available. In this section, the control laws are generalized by taking into account that parameter uncertainties are present. In other words, our goal is now to solve the problem under *both* constraints (c1) and (c2) as stated in Section 3.1.3. We first introduce an *adaptive control* approach to compensate for the effects of parametric uncertainties. Our second result involves design of a *robust control* approach to compensate for these uncertainties.

3.3.1 Adaptive Control of Uncertain EL Systems

In developing our control algorithms in this subsection we assume no *a priori* knowledge on the system *constant* parameters. Instead of the controller (3.5), we propose the following adaptive law to compensate for the effects of the parametric uncertainties in the EL systems,

$$\mathbf{u}_{j,i} = \mathbf{Y}_j(\mathbf{q}_j, \dot{\mathbf{q}}_j, \dot{\mathbf{r}}_j, \mathbf{r}_j) \bar{\Theta}_j + \boldsymbol{\tau}_{j,i}, \quad j \in \mathcal{V}, i \in \mathcal{H} \quad (3.20a)$$

$$\dot{\bar{\Theta}}_j = -\Sigma_j \mathbf{Y}_j(\mathbf{q}_j, \dot{\mathbf{q}}_j, \dot{\mathbf{r}}_j, \mathbf{r}_j) \mathbf{s}_j \quad (3.20b)$$

where $\mathbf{Y}_j(\mathbf{q}_j, \dot{\mathbf{q}}_j, \dot{\mathbf{r}}_j, \mathbf{r}_j)$ denotes the regressor function as per property **2.1.3**, $\bar{\Theta}_j$ denotes an estimate of the parameters of the j -th EL system, Σ_j is a positive definite diagonal matrix, and $\boldsymbol{\tau}_{j,i}$ is given by equation (3.16) for the j -th leader and by (3.17) for the j -th follower. Using the Property **2.1.3**, it follows that the dynamics of the closed-loop system (2.7), (3.16), (3.17), (3.20a) and (3.20b) is reduced to $\mathbf{D}_j(\mathbf{q}_j) \dot{\mathbf{s}}_j + \mathbf{C}_j(\mathbf{q}_j, \dot{\mathbf{q}}_j) \mathbf{s}_j = \mathbf{Y}_j(\mathbf{q}_j, \dot{\mathbf{q}}_j, \dot{\mathbf{r}}_j, \mathbf{r}_j) \check{\Theta}_j + \boldsymbol{\tau}_{j,i}$, where $\check{\Theta}_j = \bar{\Theta}_j - \Theta_j$ and with Θ_j denoting the actual but unknown constant parameters of the EL systems. Our third main result is provided in the following theorem.

Theorem 3.3.1. *Consider a network of ‘m’ heterogeneous EL systems, where the j -th system is governed by the dynamics (2.7) with $\delta = 0$ and is subject to the distributed control laws (3.16), (3.20a) and (3.20b) for the j -th leader, and the distributed control laws (3.17), (3.20a) and (3.20b) for the j -th follower corresponding to the i -th communication network topology. It then follows that the closed-loop EL system satisfies the requirements (r1)–(r3) as specified in Section 3.1.3 as well as the global boundedness of the update parameters $\bar{\Theta}_j$ in presence of average dwell-time switchings in the communication network topologies.*

Proof: Let us consider the following positive definite radially unbounded Lyapunov function candidate for the networked closed-loop system (2.7), (3.16), (3.17), (3.20a) and (3.20b),

$$\mathcal{X}_2 \triangleq \mathcal{W}_i = \frac{1}{2} \sum_{j=1}^m \left(\mathbf{s}_j^T \mathbf{D}_j(\mathbf{q}_j) \mathbf{s}_j + \check{\Theta}_j^T \Sigma_j^{-1} \check{\Theta}_j \right) \quad (3.21)$$

The time derivative of the above function along the trajectories of the closed-loop system is given by,

$$\begin{aligned} \dot{\mathcal{X}}_2 &= \sum_{j=1}^m \frac{1}{2} \mathbf{s}_j^T \dot{\mathbf{D}}_j \mathbf{s}_j + \sum_{j=1}^m \mathbf{s}_j^T \mathbf{D}_j \dot{\mathbf{s}}_j + \sum_{j=1}^m \check{\Theta}_j^T \Sigma_j^{-1} \dot{\check{\Theta}}_j \\ &= \sum_{j=1}^m \frac{1}{2} \mathbf{s}_j^T \dot{\mathbf{D}}_j \mathbf{s}_j + \sum_{j=1}^m \mathbf{s}_j^T \left[\mathbf{Y}_j \check{\Theta}_j + \boldsymbol{\tau}_{j,i} - \mathbf{C}_j \mathbf{s}_j \right] - \sum_{j=1}^m \check{\Theta}_j^T \mathbf{Y}_j \mathbf{s}_j \end{aligned}$$

which can be simplified to

$$\begin{aligned} \dot{\mathcal{X}}_2 &= -\frac{1}{2} \sum_{j=1}^l (1 - \alpha_{j,i}) \mathbf{s}_j^T \mathbf{K}_{j,i} \mathbf{s}_j - \sum_{j=1}^l \frac{\alpha_{j,i}}{4} \sum_{n \in \mathcal{N}_{j,i}} \frac{1}{|\mathcal{N}_{j,i}|} \mathbf{s}_{jn}^T \mathbf{K}_{j,i} \mathbf{s}_{jn} \\ &\quad - \sum_{j=l+1}^m \frac{1}{4} \sum_{n \in \mathcal{N}_{j,i}} \frac{1}{|\mathcal{N}_{j,i}|} \mathbf{s}_{jn}^T \mathbf{K}_{j,i} \mathbf{s}_{jn} \leq 0 \end{aligned} \quad (3.22)$$

Consequently, the Lyapunov function \mathcal{X}_2 is a *weak* common Lyapunov function for the considered switched system. Since \mathcal{X}_2 is radially unbounded, all the signals of the closed-loop system remain globally bounded, i.e. the states $\tilde{\mathbf{q}}_j$, $\check{\mathbf{q}}_j$, and $\bar{\Theta}_j$ are globally stable. Note that Lemma 2.9.3 implies that there exists a non-vanishing dwell time $\bar{\tau} \in (0, \tau_{ad})$ among each switchings in the communication network topologies.

Since \mathcal{X}_2 is upper bounded and $\dot{\mathcal{X}}_2 \leq 0$, by invoking Lemma 2.9.5 one can conclude that under the non-vanishing dwell-time we have $\mathbf{s}_{jn} \rightarrow 0$ as $t \rightarrow \infty$. This

implies that $s_{jn} \in \mathcal{L}_2$, $\forall j, n \in \mathcal{V}, j \neq n$. By invoking Lemma A.12 in [158], one can further conclude that $\mathbf{q}_{jn} \rightarrow 0$ and $\dot{\mathbf{q}}_{jn} \rightarrow 0$ as $t \rightarrow \infty$. In addition, by invoking Lemma 2.9.5 one can conclude that under non-vanishing dwell-time we have $s_j \rightarrow 0, j \in \{1, \dots, l\}$ as $t \rightarrow \infty$. Consequently, due to the fact that the communication network topology is connected, boundedness and asymptotic stability of $s_j, \forall j$ are also guaranteed. Consequently, the requirements (r1)–(r3) are formally shown to hold. This completes the proof of the theorem. \blacksquare

3.3.2 Robust Synchronization Control of Uncertain EL Systems

In the previous subsection, an adaptive control approach was introduced to compensate for the effects of parametric uncertainties in the networked EL systems. In the development of the adaptive control laws no *a priori* knowledge of the *constant* parameters of the system was assumed. In this subsection, we assume certain *a priori* knowledge of the *nominal* EL system's parameters. However, to generalize our results we now assume and allow that the system's parameters could be *time-varying*, although the exact values of the parameters are not known precisely. However, the bounds on the parameters are assumed to be known *a priori*. We make this assumption explicit as indicated below.

Let the j -th *nominal* EL system be governed by the *nonlinear* dynamic equation,

$$\hat{\mathbf{D}}_j(\mathbf{q}_j)\ddot{\mathbf{q}}_j + \hat{\mathbf{C}}_j(\mathbf{q}_j, \dot{\mathbf{q}}_j)\dot{\mathbf{q}}_j + \hat{\mathbf{G}}_j(\mathbf{q}_j) + \hat{\mathcal{F}}_j \triangleq \mathbf{Y}_j(\mathbf{q}_j, \dot{\mathbf{q}}_j, \dot{\mathbf{r}}_j, \mathbf{r}_j)\hat{\Theta}_j = \mathbf{u}_j \quad (3.23)$$

where $\hat{\Theta}_j$ denotes the vector of *constant* parameters of the *nominal* EL system. The parameters $\hat{\Theta}_j$ could represent the designer's best knowledge or estimate of the actual parameters of the EL system. Let the difference between the *nominal*

values of the j -th EL system's parameters $\hat{\Theta}_j$ and the *actual* values of the j -th EL system's parameters that are denoted by $\Theta_j(t)$ and that are unknown and *possibly time-varying* be given by $\tilde{\Theta}_j(t) = \Theta_j(t) - \hat{\Theta}_j$. We make the following assumption on $\tilde{\Theta}_j(t)$.

Assumption 3.3.1. Let the difference between the nominal values of the EL system's parameters and the actual values of the EL system's parameters be upper bounded and let this upper bound be known *a priori*. Specifically, $\|\tilde{\Theta}_j(t)\| \leq \rho_j$, where $\rho_j > 0$ is a known constant parameter.

We propose the following robust control law to compensate for the effects of the parametric uncertainties in the EL systems,

$$\mathbf{u}_{j,i} = \mathbf{Y}_j(\mathbf{q}_j, \dot{\mathbf{q}}_j, \dot{\mathbf{r}}_j, \mathbf{r}_j)(\hat{\Theta}_j + \mathbf{v}_j) + \boldsymbol{\tau}_{j,i} \quad (3.24)$$

where \mathbf{v}_j is to be specified subsequently.

By using the Property 2.1.3, the dynamics of the closed-loop system (2.7), (3.16), (3.17) and (3.24) is reduced to $\mathbf{D}_j(\mathbf{q}_j)\dot{\mathbf{s}}_j + \mathbf{C}_j(\mathbf{q}_j, \dot{\mathbf{q}}_j)\mathbf{s}_j = \mathbf{Y}_j(\mathbf{q}_j, \dot{\mathbf{q}}_j, \dot{\mathbf{r}}_j, \mathbf{r}_j)(\hat{\Theta}_j + \mathbf{v}_j) + \boldsymbol{\tau}_{j,i}$. Our fourth main result is provided in the following theorem.

Theorem 3.3.2. Consider a network of ' m ' heterogeneous EL systems, where the j -th EL system is governed by the dynamics (2.7) with $\delta = 0$ and is subject to the distributed control laws (3.16) and (3.24) for the j -th leader and the distributed control laws (3.17) and (3.24) for the j -th follower corresponding to the i -th communication network topology. Let the control input \mathbf{v}_j be selected as

$$\mathbf{v}_j = \begin{cases} -\rho_j \text{sgn}(\mathbf{Y}_j \mathbf{s}_j) & \text{if } \|\mathbf{Y}_j \mathbf{s}_j\| > \varepsilon_j \\ -\frac{\rho_j}{\varepsilon_j} \mathbf{Y}_j \mathbf{s}_j & \text{if } \|\mathbf{Y}_j \mathbf{s}_j\| < \varepsilon_j \end{cases} \quad (3.25)$$

where ε_j is a small positive constant. It then follows that the closed-loop system is: (A1) globally stable, and (A2) the state synchronization and set-point tracking errors remain globally bounded under average dwell-time switchings in the communication network topologies, where the bound is a function of ε_j .

Proof: Let us consider a positive definite radially unbounded decrescent Lyapunov function candidate (3.18) for the networked closed-loop EL system (2.7), (3.16), (3.17), (3.24) and (3.25). The time derivative of this function along the trajectories of the closed-loop system is given by,

$$\begin{aligned} \dot{\mathcal{X}}_1 = & \sum_{j=1}^l \mathbf{s}_j^T \left[-\frac{1}{2}(1 - \alpha_{j,i})\mathbf{K}_{j,i}\mathbf{s}_j - \frac{\alpha_{j,i}}{2}\mathbf{K}_{j,i} \sum_{n \in \mathcal{N}_{j,i}} \frac{\mathbf{s}_{jn}}{|\mathcal{N}_{j,i}|} + \mathbf{Y}_j(\mathbf{q}_j, \dot{\mathbf{q}}_j, \dot{\mathbf{r}}_j, \mathbf{r}_j)(\hat{\Theta}_j + \mathbf{v}_j) \right] \\ & + \sum_{j=l+1}^m \mathbf{s}_j^T \left[-\frac{1}{2}\mathbf{K}_{j,i} \sum_{n \in \mathcal{N}_{j,i}} \frac{\mathbf{s}_{jn}}{|\mathcal{N}_{j,i}|} + \mathbf{Y}_j(\mathbf{q}_j, \dot{\mathbf{q}}_j, \dot{\mathbf{r}}_j, \mathbf{r}_j)(\hat{\Theta}_j + \mathbf{v}_j) \right] \end{aligned} \quad (3.26)$$

Let us first assume that $\|\mathbf{Y}_j \mathbf{s}_j\| > \varepsilon_j$. Given the control law (3.25), it can be shown that $\dot{\mathcal{X}}_1$ in equation (3.26) satisfies,

$$\begin{aligned} \dot{\mathcal{X}}_1 \leq & \sum_{j=1}^l \mathbf{s}_j^T \left(-\frac{1}{2}(1 - \alpha_{j,i})\mathbf{K}_{j,i}\mathbf{s}_j - \frac{\alpha_{j,i}}{2}\mathbf{K}_{j,i} \sum_{n \in \mathcal{N}_{j,i}} \frac{\mathbf{s}_{jn}}{|\mathcal{N}_{j,i}|} \right) \\ & + \sum_{j=l+1}^m \mathbf{s}_j^T \left(-\frac{1}{2}\mathbf{K}_{j,i} \sum_{n \in \mathcal{N}_{j,i}} \frac{\mathbf{s}_{jn}}{|\mathcal{N}_{j,i}|} \right) \\ & + \sum_{j=1}^m \left(\|\mathbf{s}_j^T \mathbf{Y}_j \hat{\Theta}_j\| - \rho_j \|\mathbf{s}_j^T \mathbf{Y}_j\| \right) \\ \leq & \sum_{j=1}^l \mathbf{s}_j^T \left(-\frac{1}{2}(1 - \alpha_{j,i})\mathbf{K}_{j,i}\mathbf{s}_j - \frac{\alpha_{j,i}}{2}\mathbf{K}_{j,i} \sum_{n \in \mathcal{N}_{j,i}} \frac{\mathbf{s}_{jn}}{|\mathcal{N}_{j,i}|} \right) \\ & + \sum_{j=l+1}^m \mathbf{s}_j^T \left(-\frac{1}{2}\mathbf{K}_{j,i} \sum_{n \in \mathcal{N}_{j,i}} \frac{\mathbf{s}_{jn}}{|\mathcal{N}_{j,i}|} \right) \end{aligned}$$

It follows along similar lines and arguments that were invoked in the proof of Theorem 3.2.2 that the properties (A1) and (A2) hold. Now let $\|\mathbf{Y}_j \mathbf{s}_j\| < \varepsilon_j$. Given the control law (3.25) we obtain

$$\begin{aligned} \dot{\mathcal{X}}_1 &\leq \sum_{j=1}^l \mathbf{s}_j^T \left(-\frac{1}{2}(1 - \alpha_{j,i}) \mathbf{K}_{j,i} \mathbf{s}_j - \frac{\alpha_{j,i}}{2} \mathbf{K}_{j,i} \sum_{n \in \mathcal{N}_{j,i}} \frac{\mathbf{s}_{jn}}{|\mathcal{N}_{j,i}|} \right) \\ &\quad + \sum_{j=l+1}^m \mathbf{s}_j^T \left(-\frac{1}{2} \mathbf{K}_{j,i} \sum_{n \in \mathcal{N}_{j,i}} \frac{\mathbf{s}_{jn}}{|\mathcal{N}_{j,i}|} \right) \\ &\quad + \sum_{j=1}^m \|\mathbf{s}_j^T \mathbf{Y}_j (\hat{\Theta}_j + \mathbf{v}_j)\| \end{aligned}$$

Following along the similar lines as those used in [162], it follows that the term $\|\mathbf{s}_j^T \mathbf{Y}_j (\hat{\Theta}_j + \mathbf{v}_j)\|$ is upper bounded by $\varepsilon_j \rho_j / 4$. Therefore, the above inequality is reduced to,

$$\begin{aligned} \dot{\mathcal{X}}_1 &\leq - \sum_{j=1}^l \mathbf{s}_j^T \left(\frac{1}{2}(1 - \alpha_{j,i}) \mathbf{K}_{j,i} \mathbf{s}_j + \frac{\alpha_{j,i}}{2} \mathbf{K}_{j,i} \sum_{n \in \mathcal{N}_{j,i}} \frac{\mathbf{s}_{jn}}{|\mathcal{N}_{j,i}|} \right) \\ &\quad - \sum_{j=l+1}^m \mathbf{s}_j^T \left(\frac{1}{2} \mathbf{K}_{j,i} \sum_{n \in \mathcal{N}_{j,i}} \frac{\mathbf{s}_{jn}}{|\mathcal{N}_{j,i}|} \right) \\ &\quad + \sum_{j=1}^m \varepsilon_j \rho_j / 4 \end{aligned} \tag{3.27}$$

It then follows that

$$\dot{\mathcal{X}}_1 \leq - \sum_{j=1}^l k_{1,i}(\mathbf{s}_j) - \sum_{j=1}^m k_{2,i} \left(\sum_{n=1}^m \mathbf{s}_{jn} \right) + \sum_{j=1}^m \varepsilon_j \rho_j / 4 \leq - \sum_{j=1}^m k_{2,i} \left(\sum_{n=1}^m \mathbf{s}_{jn} \right) + \sum_{j=1}^m \varepsilon_j \rho_j / 4$$

for some class \mathcal{K}_∞ functions $k_{1,i}(\cdot)$ and $k_{2,i}(\cdot)$. Note that the inequality (3.27) is satisfied irrespective of the value of $\|\mathbf{Y}_j \mathbf{s}_j\|$. Let $k_{3,i}(\varepsilon_j) = k_{2,i}^{-1}(\sum_{j=1}^m \varepsilon_j \rho_j / 2)$. Let us define the region $D = \{\mathbf{s}_{jn} | k_{3,i}(\varepsilon_j) \leq \sum_{j=1}^m \sum_{n=1}^m \|\mathbf{s}_{jn}\|, \mathcal{X}_1 \leq \bar{l}\}$, where \bar{l} is a

sufficiently large number. In this region we have,

$$\dot{\mathcal{X}}_1 < -\frac{1}{4} \sum_{j=1}^m k_{2,i} \left(\sum_{n=1}^m \|s_{jn}\| \right) \leq 0$$

which implies that $\dot{\mathcal{X}}_1$ is decreasing in D . Therefore, any solution starting in D will remain in D and cannot leave it.

Since \mathcal{X}_1 is upper bounded, by invoking Lemma 2.9.5 one can conclude that $\dot{\mathcal{X}}_1 \rightarrow 0$ as $t \rightarrow \infty$ under the condition of average dwell-time switchings on D . This essentially implies that $\sum_{j=1}^l k_{1,i}(\|s_j\|) + \sum_{j=1}^m k_{2,i}(\sum_{n=1}^m \|s_{jn}\|)$ is upper bounded by $\sum_{j=1}^m \rho_j \frac{\varepsilon_j}{4}$ in the steady-state under the condition of average dwell-time switchings $\forall i \in \mathcal{H}$. This from the definition of s_{jn} implies that $\dot{\mathbf{q}}_{jn}$ and \mathbf{q}_{jn} are also bounded in the steady-state. In addition, in this region we have $\|Y_j s_j\| < \varepsilon_j$. Consequently, $\dot{\tilde{\mathbf{q}}}_j$ and $\tilde{\mathbf{q}}_j$ are also bounded in the steady-state as $t \rightarrow \infty$. Therefore, the properties (A1) and (A2) are formally shown to hold and this completes the proof of the theorem. ■

Remark 3.3.1. The constant ε_j should be chosen such that a good performance in the closed-loop system response is obtained. However, to avoid any numerical problems one should not this constant too small.

3.4 Synchronization Control Recovery in Presence of Additive Actuator Faults

In this section, we introduce a controller reconfiguration strategy for state synchronization of networked EL systems in presence of additive actuator faults. Our objective is to reconfigure the “nominal” controller (which is given by equations (3.5) and (3.16) for the j -th leader and given by (3.5) and (3.17) for the j -th follower)

such that state synchronization of the EL system is achieved subject to the constraint (c1) that was stated in Section 3.1.3. To accomplish this goal, we add a term $\bar{\mathbf{v}}_j$ to the nominal control law, i.e., $\mathbf{u}_j = \mathbf{u}_j^{\text{nom}} + \bar{\mathbf{v}}_j$.

Let δ in equation (2.7) represent an additive actuator fault in this section. We impose the following assumption on the magnitude of the actuator fault $\delta_{r|j}(t, \mathbf{q}_j, \dot{\mathbf{q}}_j, \mathbf{u}_j)$, namely

$$\|\delta_{r|j}(t, \mathbf{q}_j, \dot{\mathbf{q}}_j, \mathbf{u}_j)\| \leq \rho_{r|j}(t, \mathbf{q}_j, \dot{\mathbf{q}}_j, \mathbf{q}_n, \dot{\mathbf{q}}_n) + \sigma_{r|j}(t) \|\bar{\mathbf{v}}_j\| \quad (3.28)$$

for all $r \in \{1, \dots, k\}$, $j \in \mathcal{V}$ and $n \in \mathcal{N}_j$. In addition, $\rho_{r|j}: [0, \infty) \times (2k + 2k|\mathcal{N}_j|) \rightarrow \mathfrak{R}$ represents a non-negative continuous function, which can be either linear or non-linear depending on the fault and we have $0 \leq \sigma_{r|j}(t) < 1$. It is important to emphasize that the functions $\rho_{r|j}(t, \mathbf{q}_j, \dot{\mathbf{q}}_j, \mathbf{q}_n, \dot{\mathbf{q}}_n)$ and $\sigma_{r|j}(t)$ are the only information that one needs regarding the fault. Note that $\rho_{r|j}$ can be an arbitrary function of states and time, which is more complex than the representation that is employed in [181] in which $\rho_{r|j}$ is assumed to be *only* a linear function of the states of the j -th agent. Also note that unlike [182] we do not make any assumption on the magnitude and the structure of the function $\rho_{r|j}$. One can invoke an appropriate fault detection and identification (FDI) scheme (as in for example [183, 184, 185, 186, 187, 188, 189]) to estimate the functions and parameters in equation (3.28), although a formal discussion on this is beyond the scope of this thesis.

We are now in a position to introduce the main result of this section.

Theorem 3.4.1. *Consider a network of ‘ m ’ heterogeneous EL systems where each agent is governed by the dynamics (2.7) subject to additive faults under the following distributed control law for the i -th communication network topology*

$$\mathbf{u}_{j,i} = \mathbf{u}_{j,i}^{\text{nom}} + \bar{\mathbf{v}}_{j,i}, \quad j \in \mathcal{V}, i \in \mathcal{H} \quad (3.29)$$

where $\mathbf{u}_{j,i}^{\text{nom}}$ is defined according to

$$\begin{aligned} \mathbf{u}_{j,i}^{\text{nom}} = & \mathbf{D}_j(\mathbf{q}_j)\dot{\mathbf{r}}_j + \mathbf{C}_j(\mathbf{q}_j, \dot{\mathbf{q}}_j)\mathbf{r}_j + \mathbf{G}_j(\mathbf{q}_j) + \frac{\partial \mathcal{F}(\dot{\mathbf{q}}_j)}{\partial \dot{\mathbf{q}}_j} \\ & - \frac{1}{2}(1 - \alpha_{j,i})\mathbf{K}_{j,i}(\dot{\mathbf{q}}_j + \bar{\mathbf{K}}_j\tilde{\mathbf{q}}_j) \\ & - \frac{\alpha_{j,i}}{2}\mathbf{K}_{j,i} \sum_{n \in \mathcal{N}_{j,i}} \frac{1}{|\mathcal{N}_{j,i}|} \left[(\dot{\mathbf{q}}_j + \bar{\mathbf{K}}_j\tilde{\mathbf{q}}_j) - (\dot{\mathbf{q}}_n + \bar{\mathbf{K}}_j\tilde{\mathbf{q}}_n) \right] \end{aligned} \quad (3.30)$$

for the j -th leader and according to

$$\begin{aligned} \mathbf{u}_{j,i}^{\text{nom}} = & \mathbf{D}_j(\mathbf{q}_j)\dot{\mathbf{r}}_j + \mathbf{C}_j(\mathbf{q}_j, \dot{\mathbf{q}}_j)\mathbf{r}_j + \mathbf{G}_j(\mathbf{q}_j) + \frac{\partial \mathcal{F}(\dot{\mathbf{q}}_j)}{\partial \dot{\mathbf{q}}_j} \\ & - \frac{1}{2}\mathbf{K}_{j,i} \sum_{n \in \mathcal{N}_{j,i}} \frac{1}{|\mathcal{N}_{j,i}|} \left[(\dot{\mathbf{q}}_j + \bar{\mathbf{K}}_j\tilde{\mathbf{q}}_j) - (\dot{\mathbf{q}}_n + \bar{\mathbf{K}}_j\tilde{\mathbf{q}}_n) \right] \end{aligned} \quad (3.31)$$

for the j -th follower, with

$$\bar{\mathbf{v}}_j = -\eta_j(t, \mathbf{q}_j, \dot{\mathbf{q}}_j, \mathbf{q}_n, \dot{\mathbf{q}}_n) \text{sgn}(\mathbf{s}_j) \quad (3.32)$$

where $\text{sgn}(\mathbf{s}_j) = \begin{cases} 1 & \text{if } \mathbf{s}_j > 0 \\ 0 & \text{if } \mathbf{s}_j = 0 \\ -1 & \text{if } \mathbf{s}_j < 0 \end{cases}$. In addition, $\eta_j(\mathbf{q}_j, \dot{\mathbf{q}}_j, \mathbf{q}_n, \dot{\mathbf{q}}_n)$ satisfies the following inequality

$$\eta_r|_j(t, \mathbf{q}_j, \dot{\mathbf{q}}_j, \mathbf{q}_n, \dot{\mathbf{q}}_n) \geq \frac{\rho_r|_j(t, \mathbf{q}_j, \dot{\mathbf{q}}_j, \mathbf{q}_n, \dot{\mathbf{q}}_n)}{1 - \sigma_r|_j(t)} \quad (3.33)$$

where $r \in \{1, \dots, k\}, n \in \mathcal{N}_j$ and the set of ‘h’ communication graphs satisfies the properties that are stated in Definition 3.1.1. Provided that there exists an average dwell-time (refer to Definition 2.9.13) when switching between any of the communication graphs and any switchings from the nominal controller to the reconfigured

controller and vice versa, one can guarantee that all the closed-loop system signals remain globally bounded, and moreover the requirements (r1)–(r3) are satisfied.

Proof: Consider \mathcal{X}_1 as a radially unbounded continuously differentiable Lyapunov function candidate for the i -th communication topology. The time derivative of this function along the trajectories of the closed-loop system (3.30) and (3.31) is governed by

$$\begin{aligned} \dot{\mathcal{X}}_1 = & -\frac{1}{2} \sum_{j=1}^l (1 - \alpha_{j,i}) \mathbf{s}_j^T \mathbf{K}_{j,i} \mathbf{s}_j - \sum_{j=1}^l \frac{\alpha_{j,i}}{4} \sum_{n \in \mathcal{N}_{j,i}} \frac{1}{|\mathcal{N}_{j,i}|} \mathbf{s}_{jn}^T \mathbf{K}_{j,i} \mathbf{s}_{jn} \\ & - \sum_{j=l+1}^m \frac{1}{4} \sum_{n \in \mathcal{N}_{j,i}} \frac{1}{|\mathcal{N}_{j,i}|} \mathbf{s}_{jn}^T \mathbf{K}_{j,i} \mathbf{s}_{jn} - \sum_{j=1}^m \eta_j(t, \mathbf{q}_j, \dot{\mathbf{q}}_j) \|\mathbf{s}_j\| + \sum_{j=1}^m \mathbf{s}_j^T \boldsymbol{\delta}_j \end{aligned}$$

which can be re-written as

$$\begin{aligned} \dot{\mathcal{X}}_1 \leq & -\frac{1}{2} \sum_{j=1}^l (1 - \alpha_{j,i}) \mathbf{s}_j^T \mathbf{K}_{j,i} \mathbf{s}_j - \sum_{j=1}^l \frac{\alpha_{j,i}}{4} \sum_{n \in \mathcal{N}_{j,i}} \frac{1}{|\mathcal{N}_{j,i}|} \mathbf{s}_{jn}^T \mathbf{K}_{j,i} \mathbf{s}_{jn} \\ & - \sum_{j=l+1}^m \frac{1}{4} \sum_{n \in \mathcal{N}_{j,i}} \frac{1}{|\mathcal{N}_{j,i}|} \mathbf{s}_{jn}^T \mathbf{K}_{j,i} \mathbf{s}_{jn} + \sum_{j=1}^m \|\mathbf{s}_j\| (-\eta_j(1 - \sigma_j) + \rho_j) \end{aligned}$$

From (3.33) it now follows that

$$\begin{aligned} \dot{\mathcal{X}}_1 \leq & -\frac{1}{2} \sum_{j=1}^l (1 - \alpha_{j,i}) \mathbf{s}_j^T \mathbf{K}_{j,i} \mathbf{s}_j - \sum_{j=1}^l \frac{\alpha_{j,i}}{4} \sum_{n \in \mathcal{N}_{j,i}} \frac{1}{|\mathcal{N}_{j,i}|} \mathbf{s}_{jn}^T \mathbf{K}_{j,i} \mathbf{s}_{jn} \\ & - \sum_{j=l+1}^m \frac{1}{4} \sum_{n \in \mathcal{N}_{j,i}} \frac{1}{|\mathcal{N}_{j,i}|} \mathbf{s}_{jn}^T \mathbf{K}_{j,i} \mathbf{s}_{jn} \leq 0 \end{aligned} \tag{3.34}$$

which is a decrescent negative semi-definite function for all $i \in \mathcal{H}$. By invoking an argument similar to the argument presented in Theorem 3.2.2 one can conclude that the requirements (r1)–(r3) are satisfied. This completes the proof of the theorem. ■

The discontinuity of the control laws (3.29) and (3.32) can cause complications for the numerical solvers in simulations. It also can lead to chattering phenomenon (high-frequency actuation and vibration) in practice. This is due to the fact that the discontinuity term, $\text{sgn}(s_j)$, keeps switching from a positive s_j to a negative s_j that can be damaging to the actuators. To avoid chattering, alternatively we can use the following

$$\bar{v}_j = \begin{cases} -\eta_j(t, \mathbf{q}_j, \dot{\mathbf{q}}_j) \text{sgn}(s_j) & \text{if } \eta_j(t, \mathbf{q}_j, \dot{\mathbf{q}}_j) \|s_j\| \geq \varepsilon_j \\ -\frac{\eta_j^2(t, \mathbf{q}_j, \dot{\mathbf{q}}_j)}{\varepsilon_j} s_j & \text{otherwise} \end{cases} \quad (3.35)$$

where $\varepsilon_j > 0$. By application of the modified control law (3.35) to the networked EL system (2.7) one can guarantee that the synchronization errors approach to a neighborhood of the origin. In other words, one can guarantee that the synchronization errors remain ultimately bounded.

3.5 Simulation Studies: Distributed Control of Networked Spacecraft

In the simulations that are conducted in this section we consider a network of eight (8) spacecraft, with two leaders (to ensure “hardware” redundancy in case one leader is “lost” due to a severe and catastrophic fault) and six followers. The actual values of each spacecraft moment of inertia matrix are provided in Table 3.1 and the *nominal* physical parameters that are assumed to be known to the controllers are provided in Table 3.2. The initial angular velocities are selected randomly in the interval ± 0.005 (rad/sec) and the initial angular positions are chosen randomly between 0 and 0.4 (rad) for conducting the simulations.

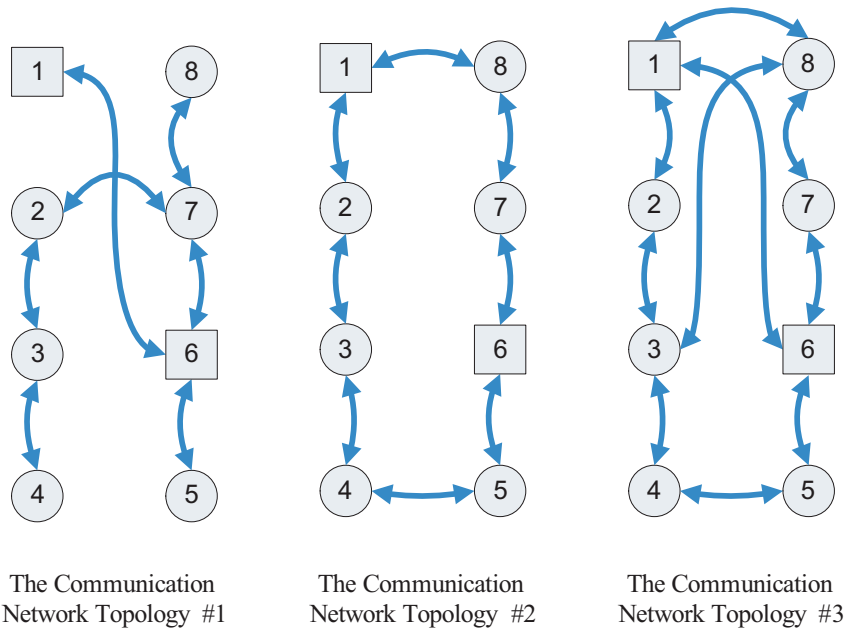


Figure 3.1: The three communication topologies that are considered in the simulations according to the Definition 3.1.1. The EL systems that are shown by a square are the *leaders* and the ones that are shown by a circle are the *followers*.

Table 3.1: Physical parameters for each spacecraft in the network

Spacecraft #	J_{11} ($kg \cdot m^2$)	J_{22} ($kg \cdot m^2$)	J_{33} ($kg \cdot m^2$)	J_{23} ($kg \cdot m^2$)	J_{13} ($kg \cdot m^2$)	J_{12} ($kg \cdot m^2$)
1	30	15	17	4	4	5
2	28	12	14	4	4	5
3	32	18	15	4	4	5
4	35	22	20	4	4	5
5	38	12	22	4	4	5
6	30	16	17	4	4	5
7	26	18	20	4	4	5
8	30	18	20	4	4	5

Table 3.2: Nominal physical parameters of the spacecraft in the network

Spacecraft #	J_{11} ($kg \cdot m^2$)	J_{22} ($kg \cdot m^2$)	J_{33} ($kg \cdot m^2$)	J_{23} ($kg \cdot m^2$)	J_{13} ($kg \cdot m^2$)	J_{12} ($kg \cdot m^2$)
1-8	32	14	15	2	3	8

We consider three communication graphs ($h = 3$ according to Definition 3.1.1) as depicted in Fig. 3.1. All the three networks are strongly connected and the connections are bi-directional. In the simulations we randomly switch among these communication graphs every 10 seconds.

3.5.1 Control of Networked Uncertain Spacecraft

We demonstrate the performance of our proposed controllers for achieving synchronization control of networked spacecraft in this subsection. The parameters of the controller (3.16) are set to $\alpha_{j,i} = 0.8$, $\mathbf{K}_{j,i} = 62.5\mathfrak{J}_3$, and $\bar{\mathbf{K}}_j = 0.1\mathfrak{J}_3$. This results in the following parameters for the PI (3.9) of the j -th leader EL system, namely, $\mathbf{R}_j = \frac{1}{62.5}\mathfrak{J}_3$, $\mathbf{Q}_j = \text{diag}([0.125, 0.125, 0.125, 62.5, 62.5, 62.5])$, and $\sum_{n \in \mathcal{N}_{j,i}} \mathbf{Q}_{jn} = \text{diag}([0.5, 0.5, 0.5, 50, 50, 50])$, $j \in \{1, 6\}$, $i \in \{1, 2, 3\}$. Furthermore, the parameters of the controller (3.17) is set to $\mathbf{K}_{j,i} = 50\mathfrak{J}_3$ and $\bar{\mathbf{K}}_j = 0.1\mathfrak{J}_3$. This results in the following parameters for the PI (3.9) of the j -th follower EL system $\mathbf{R}_j = \frac{1}{50}\mathfrak{J}_3$ and $\sum_{n \in \mathcal{N}_{j,i}} \mathbf{Q}_{jn} = \text{diag}([0.5, 0.5, 0.5, 50, 50, 50])$, $j \in \{2, 3, 4, 5, 7, 8\}$, $i \in \{1, 2, 3\}$. According to the above controller gains selection, more emphasis will be placed on the angular velocity synchronization as compared to the attitude synchronization. The gains for the adaptive controller (3.20b) is set to $\Sigma_j = 1 \mathfrak{J}_3$. The parameters of the robust controllers as given by (3.24) and (3.25) are set according to $\rho_j = 20$ and $\varepsilon_j = 1$. Note that depending on the mission requirements by selecting proper controller gains one can put more weight on attitude synchronization as compared to angular velocity synchronization. This is a trade-off and the choice is made by the designer.

The response of the closed-loop system states using our proposed adaptive and robust controllers with the same initial conditions are depicted in Figures 3.2,

3.3, 3.4, and 3.5 respectively. One can observe from these figures that the state synchronization and set-point tracking are achieved by using both control strategies. It is also observed that the state synchronization is achieved prior to the set-point tracking in simulations. The control efforts for the spacecraft are depicted in Figures 3.6 and 3.7 by using our proposed adaptive and robust controllers, respectively. One can observe that the control efforts are reasonable for both control strategies. The discontinuities in the robust control efforts are due to the switching in the control law.

In order to compare the performance of the two proposed controllers, we executed 10 Monte Carlo simulation runs, and the results are reported in Table 3.3. In this table we consider synchronization and set point-tracking errors as well as the control efforts for the spacecraft #1 (as a leader) and the spacecraft #8 (as a follower) in order to compare the performance of our proposed controllers. From this table, one can conclude that our proposed adaptive controller outperforms the robust controller in all cases. The only case when the robust controller is superior to the adaptive controller is in following the reference velocity of the spacecraft #1. One can also conclude from this table that the leader spacecraft #1 requires more control effort as compared to the follower spacecraft #8. Furthermore, the spacecraft #1 has a higher synchronization error, and at the same time it has a lower set-point tracking error when compared to the spacecraft #8.

3.5.2 Control of Networked Spacecraft Subject to Actuator Fault

In this subsection, we consider state synchronization control of the networked spacecraft with actuator faults. We consider the following scenario. Assume that an additive fault occurs in the first input channel of the spacecraft #2 at $t = 22$ seconds,

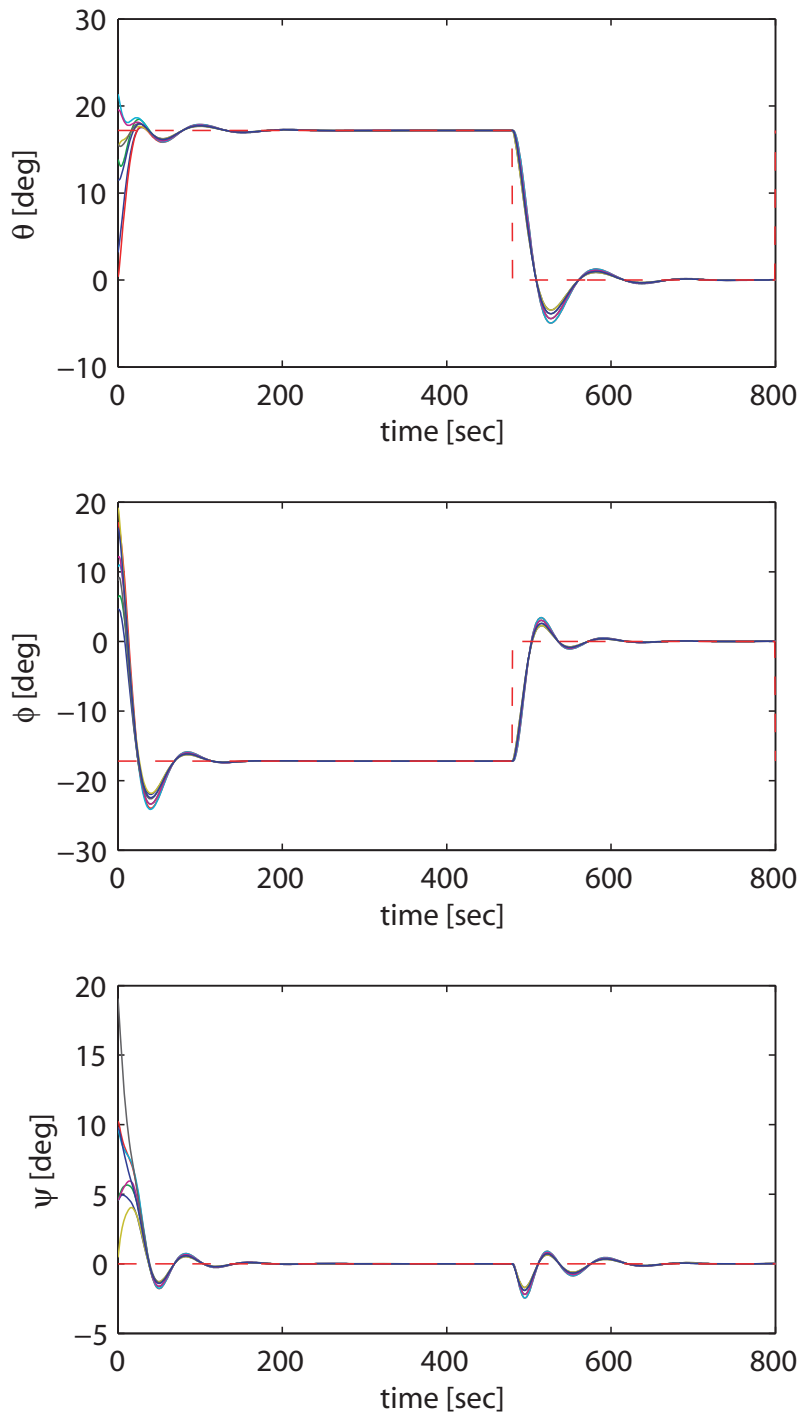


Figure 3.2: The attitudes of the eight networked spacecraft under our proposed adaptive synchronization controller. The dotted line represents the reference set-point that is only available to the network leaders, i.e. the spacecraft #1 and #6.

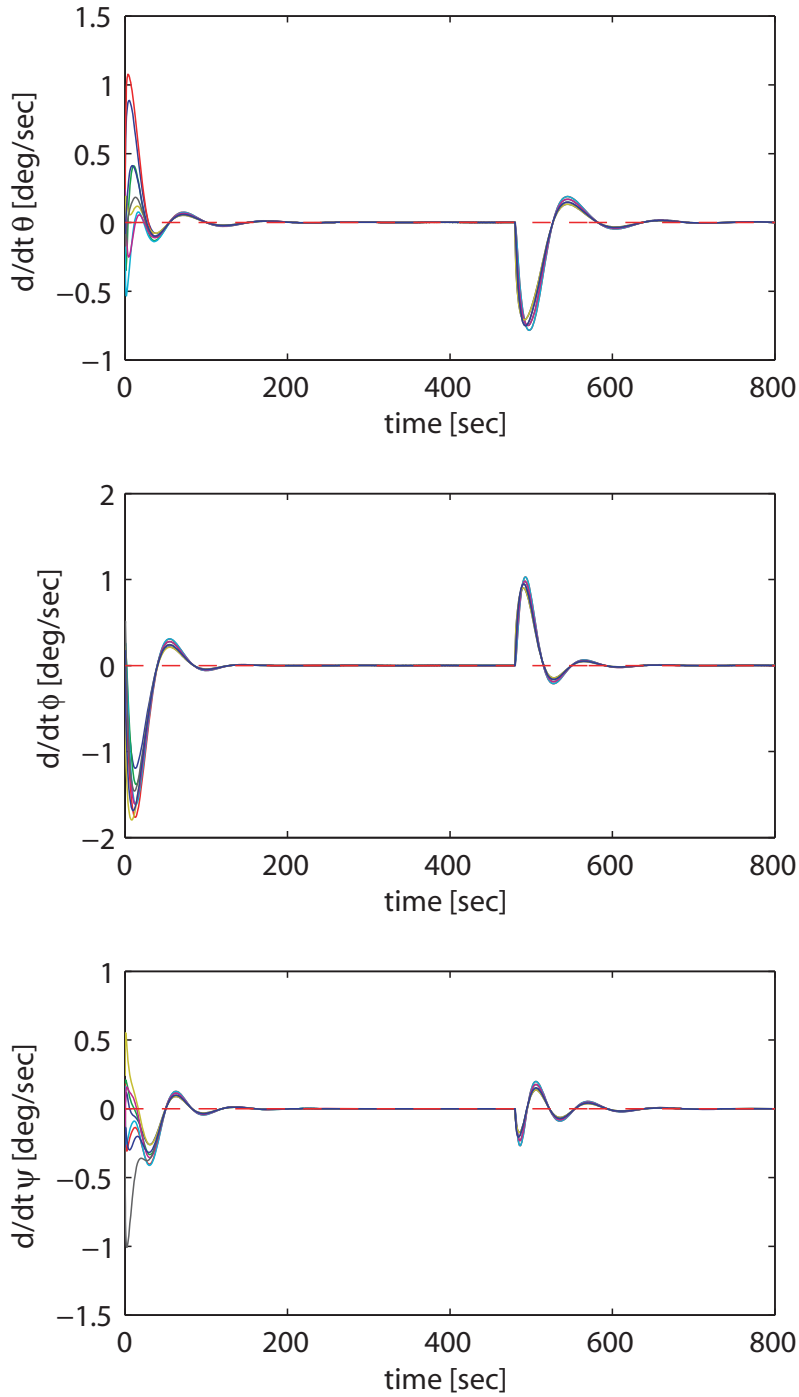


Figure 3.3: The angular velocities of the eight networked spacecraft under our proposed adaptive synchronization controller. The dotted line represents the reference set-point.

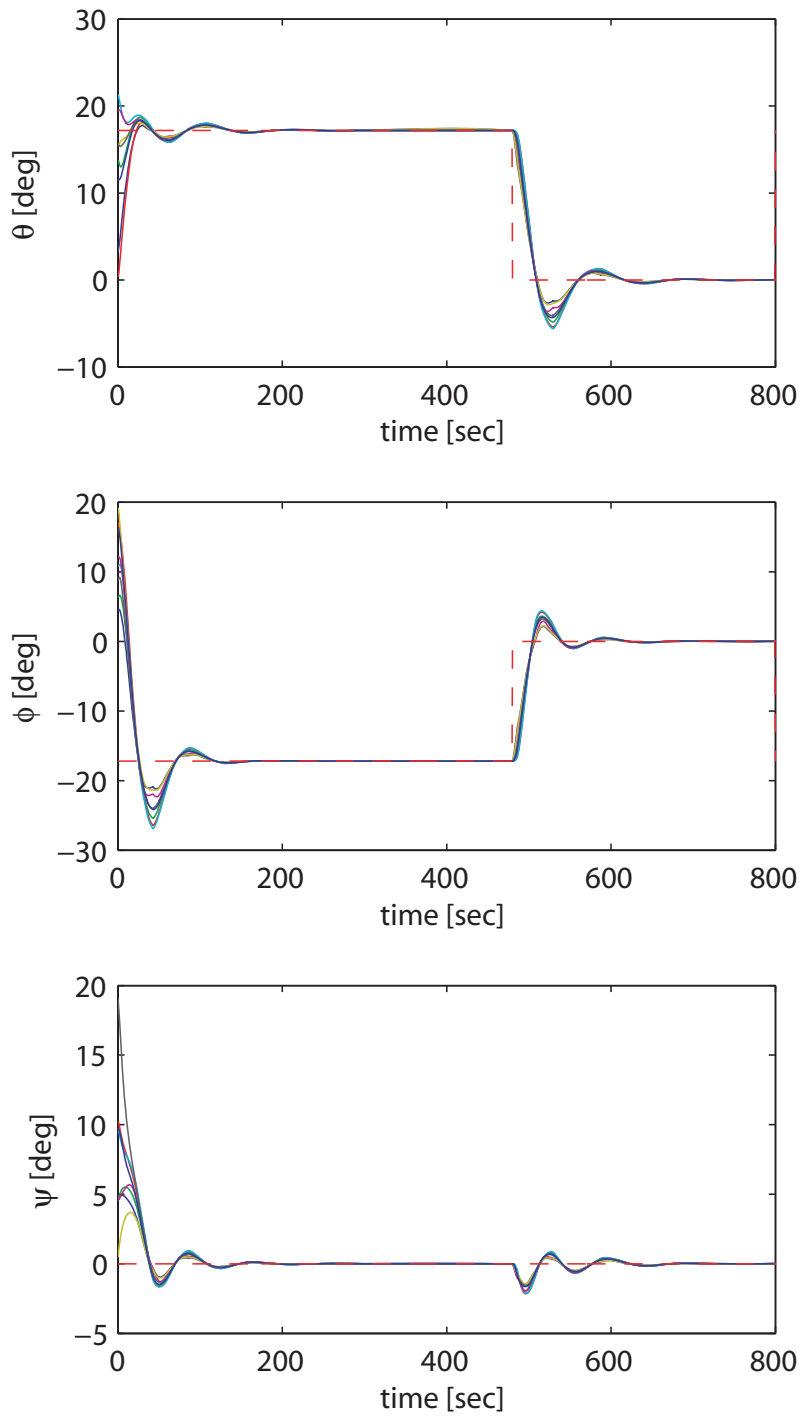


Figure 3.4: The attitudes of the eight networked spacecraft under our proposed robust synchronization controller. The dotted line represents the reference set-point that is only available to the network leaders, i.e. the spacecraft #1 and #6.

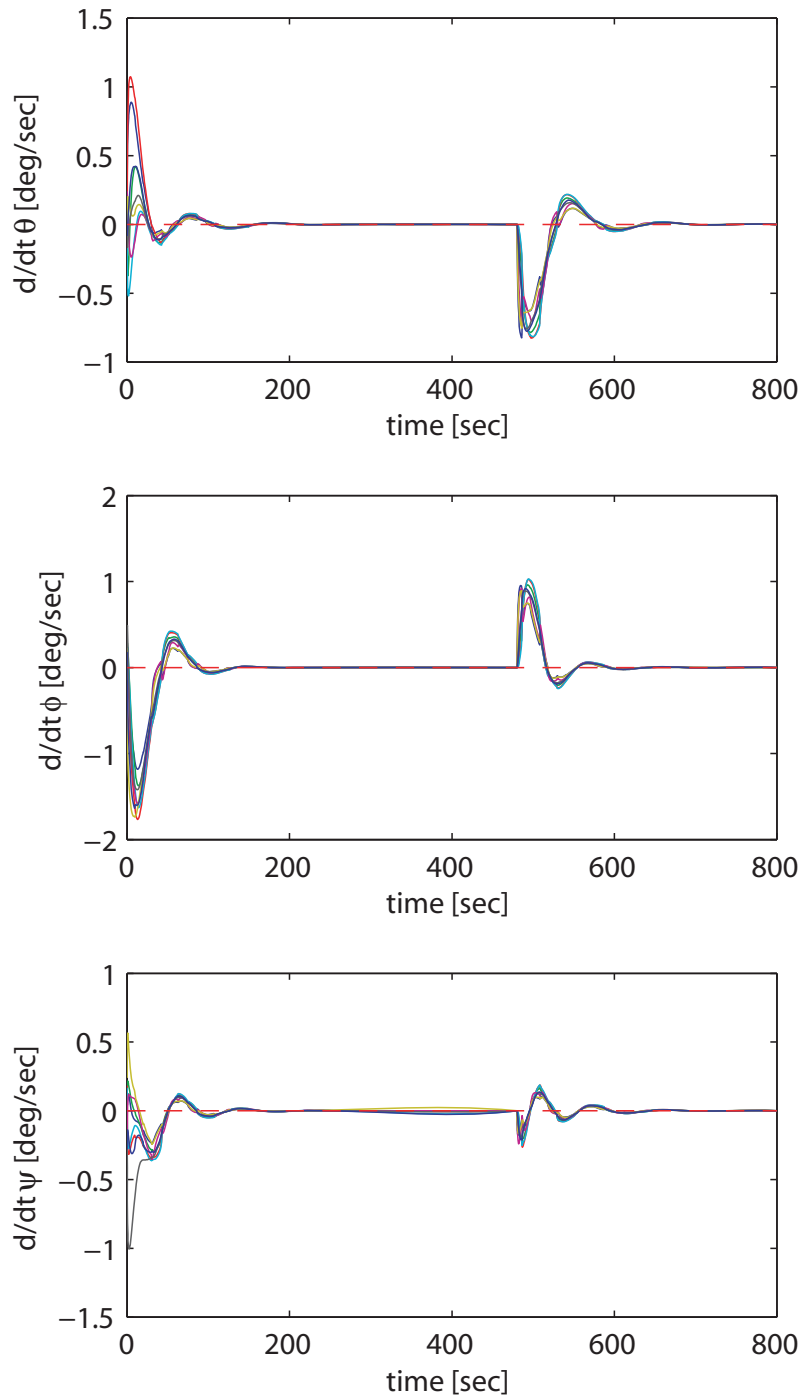


Figure 3.5: The angular velocities of the eight networked spacecraft under our proposed robust synchronization controller. The dotted line represents the reference set-point.

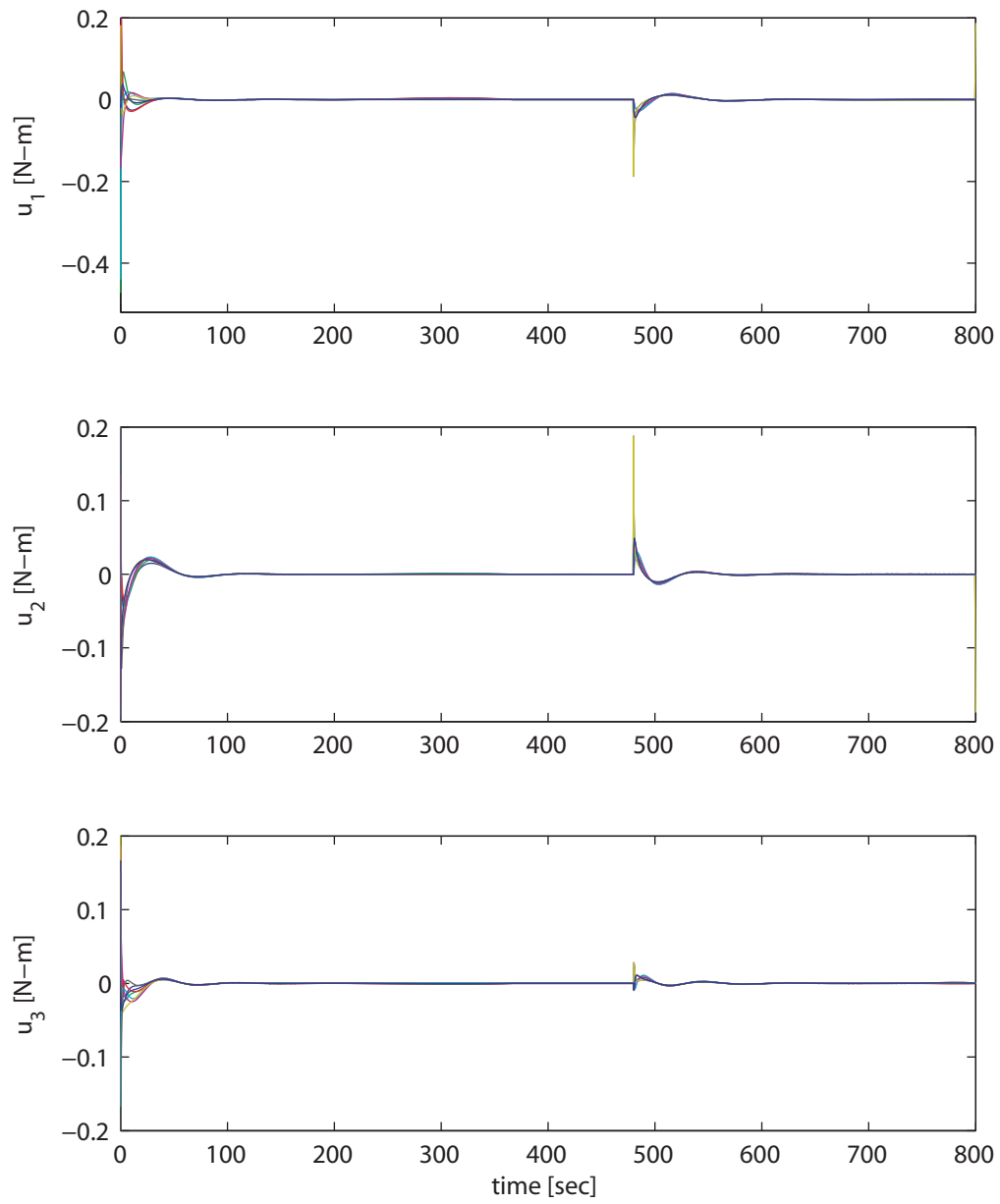


Figure 3.6: The control efforts of the eight networked spacecraft under our proposed adaptive synchronization controller.

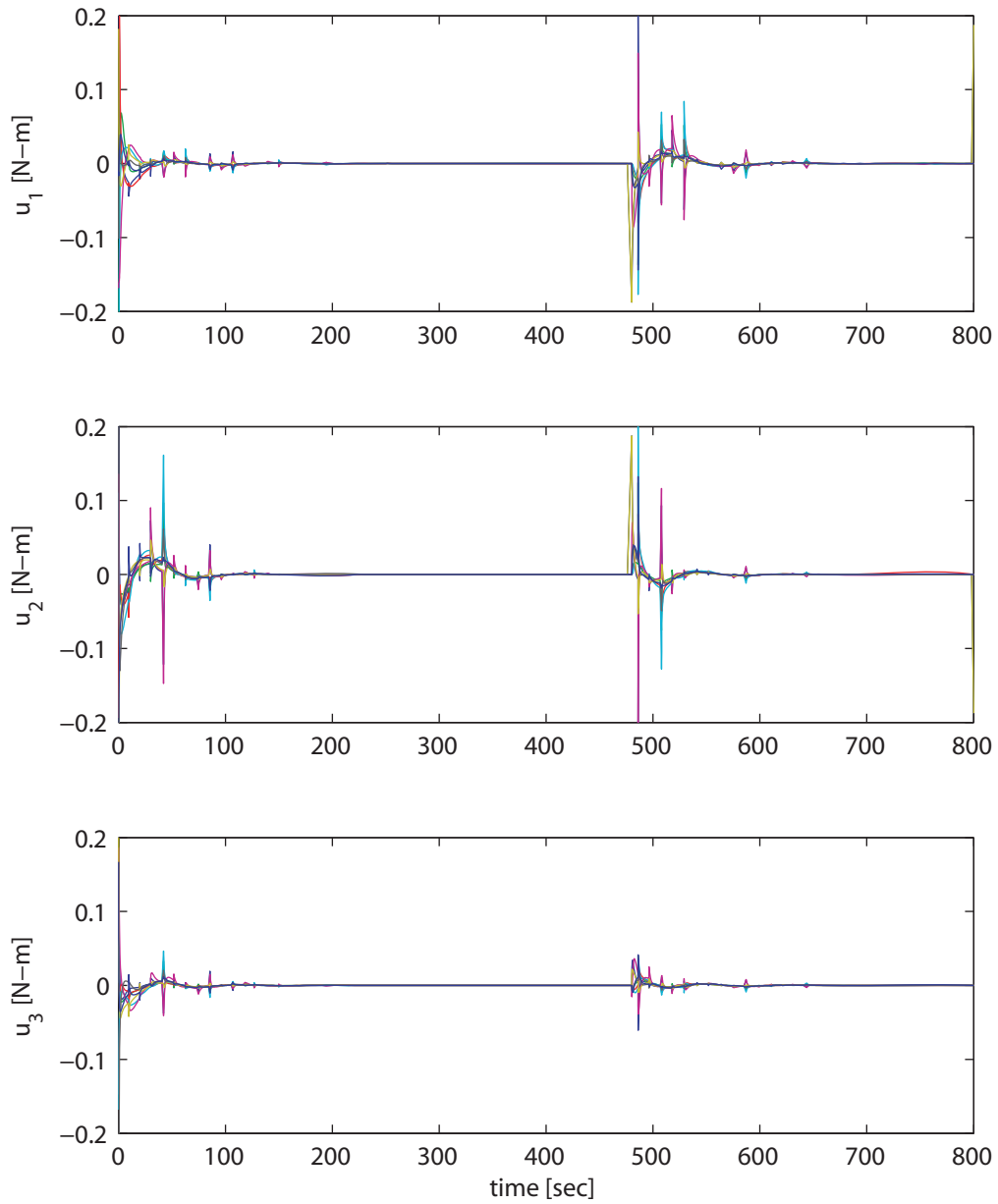


Figure 3.7: The control efforts of the eight networked spacecraft under our proposed robust synchronization controller.

Table 3.3: Monte Carlo simulation results

Performance measure	Adaptive control algorithm	Robust control algorithm
$\int_0^{800} \ \mathbf{u}_1\ ^2 dt$	0.213	0.22
$\sum_{j=2,\dots,8} \int_0^{800} \ \mathbf{q}_{1j}\ ^2 dt$	3.058	4.42
$\sum_{j=2,\dots,8} \int_0^{800} \ \dot{\mathbf{q}}_{1j}\ ^2 dt$	0.031	0.042
$\int_0^{800} \ \tilde{\mathbf{q}}_1\ ^2 dt$	4.582	4.169
$\int_0^{800} \ \dot{\tilde{\mathbf{q}}}_1\ ^2 dt$	0.024	0.02
$\int_0^{800} \ \mathbf{u}_8\ ^2 dt$	0.133	0.167
$\sum_{j=1,\dots,7} \int_0^{800} \ \mathbf{q}_{8j}\ ^2 dt$	2.577	3.14
$\sum_{j=1,\dots,7} \int_0^{800} \ \dot{\mathbf{q}}_{8j}\ ^2 dt$	0.026	0.031
$\int_0^{800} \ \tilde{\mathbf{q}}_8\ ^2 dt$	5.131	5.877
$\int_0^{800} \ \dot{\tilde{\mathbf{q}}}_8\ ^2 dt$	0.025	0.025

and the fault is removed at $t = 530$ seconds. The fault magnitude is assumed to be represented by $\delta_2 = [0.4 \times q_{1,2} + 0.6 \times \dot{q}_{1,2} + 0.8 \times \tilde{q}_{1,3}, 0, 0]^T$ and $\sigma_1(t) = 0$. Note that the above fault corresponds to an *intermittent* actuator fault.

We first demonstrate the performance of our proposed optimal controllers (3.16) and (3.16) in presence of the actuator faults defined above. The attitude responses of the eight spacecraft are shown in Figures 3.8 and 3.9 for the first 50 seconds. One can easily observe that the state synchronization and set-point tracking requirements can *no longer* be achieved. One can also note that $\theta(t)$ grows and produces a very undesirable response in presence of the additive actuator faults.

We now demonstrate the performance of our proposed reconfigurable controllers (3.29), (3.30), (3.31) and (3.32). It is assumed that it takes 20 seconds for the fault detection and identification module to detect and estimate the severity of the fault and to *automatically* reconfigure the controllers, i.e. the controller for the spacecraft #2 is *reconfigured* at $t = 42$ seconds. In the simulations conducted we have set $\eta_j = [1.6 \times |q_{1,2}| + 2.8 \times |\dot{q}_{1,2}| + 1.2 \times |\tilde{q}_{1,3}|, 0, 0]^T$. It is also assumed that

after removal of the fault, the reconfigured controllers are *automatically changed* to the nominal controllers at $t = 580$ seconds for the spacecraft #2 (that is, with a delay of 50 seconds after the removal of the faults).

The closed-loop EL system positions are depicted in Figures 3.10 and 3.11 for the first 800 seconds. It follows from this figure that subsequent to the initiation of the reconfigurable controllers at $t = 42$ seconds the eight spacecraft states do remain bounded and the state synchronization and set-point tracking objectives are indeed achieved despite the presence of additive actuator faults. In addition, after removal of the fault at $t = 530$ seconds and consequent removal of the controller re-configuration part at $t = 580$ seconds, the performance of the networked spacecraft is preserved and state-synchronization and set-point tracking is guaranteed.

3.6 Concluding Remarks

In this chapter optimal control techniques are employed in this paper to formally design a distributed controller which addresses state synchronization and set-point tracking of a team of multi-agent nonlinear EL systems. In addition, we consider adaptive and robust control approaches to compensate the effects of parametric uncertainty. Additive actuator faults are also considered in this chapter. We introduce a robust distributed control technique to compensate effect of the faults in the network. Several simulation studies on the control of networked spacecraft in deep space are conducted to demonstrate merits of our proposed control algorithms.

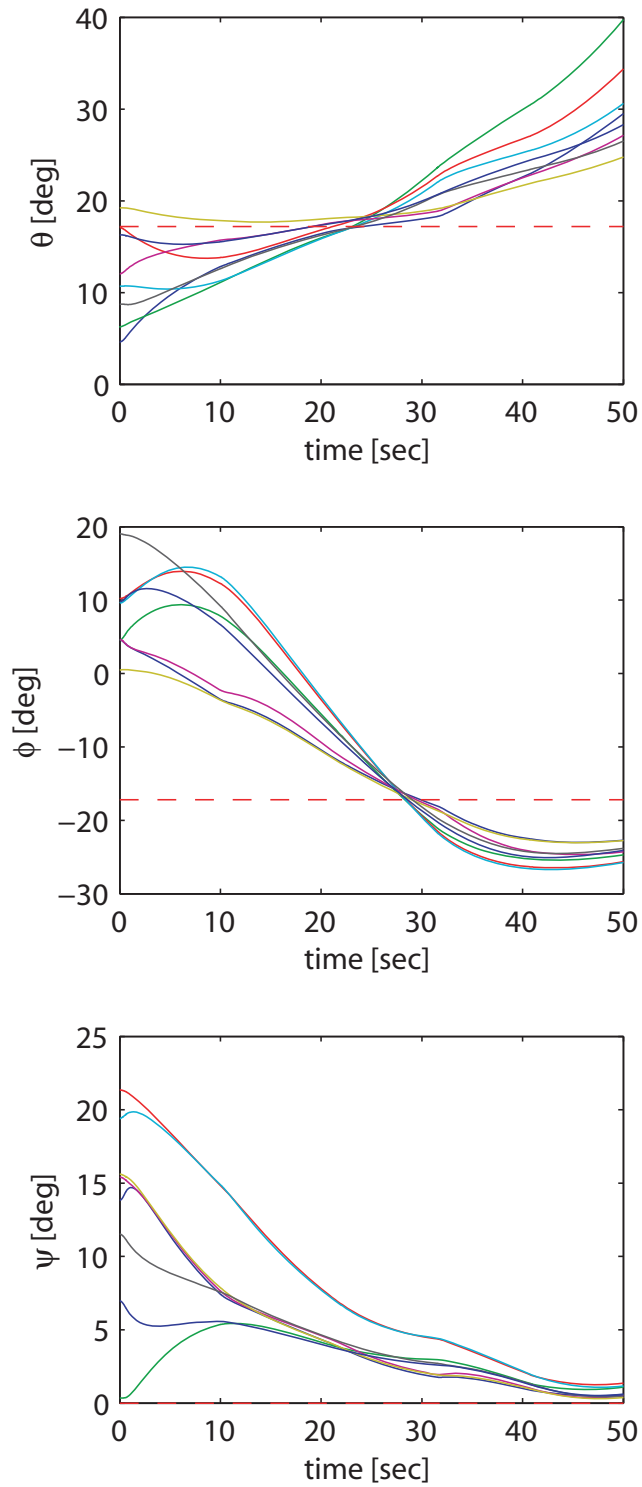


Figure 3.8: The attitudes of the eight networked spacecraft in presence of additive actuator fault for the first 50 seconds.

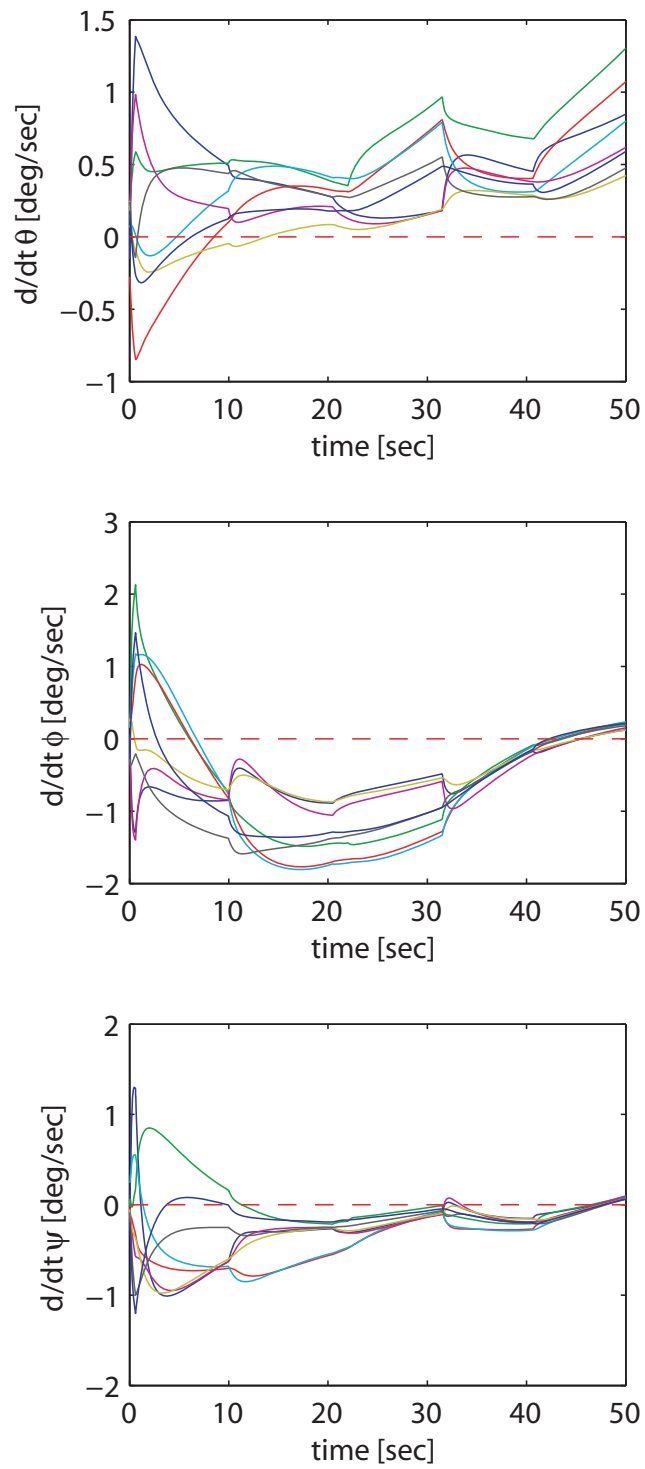


Figure 3.9: The angular velocities of the eight networked spacecraft in presence of additive actuator fault for the first 50 seconds.

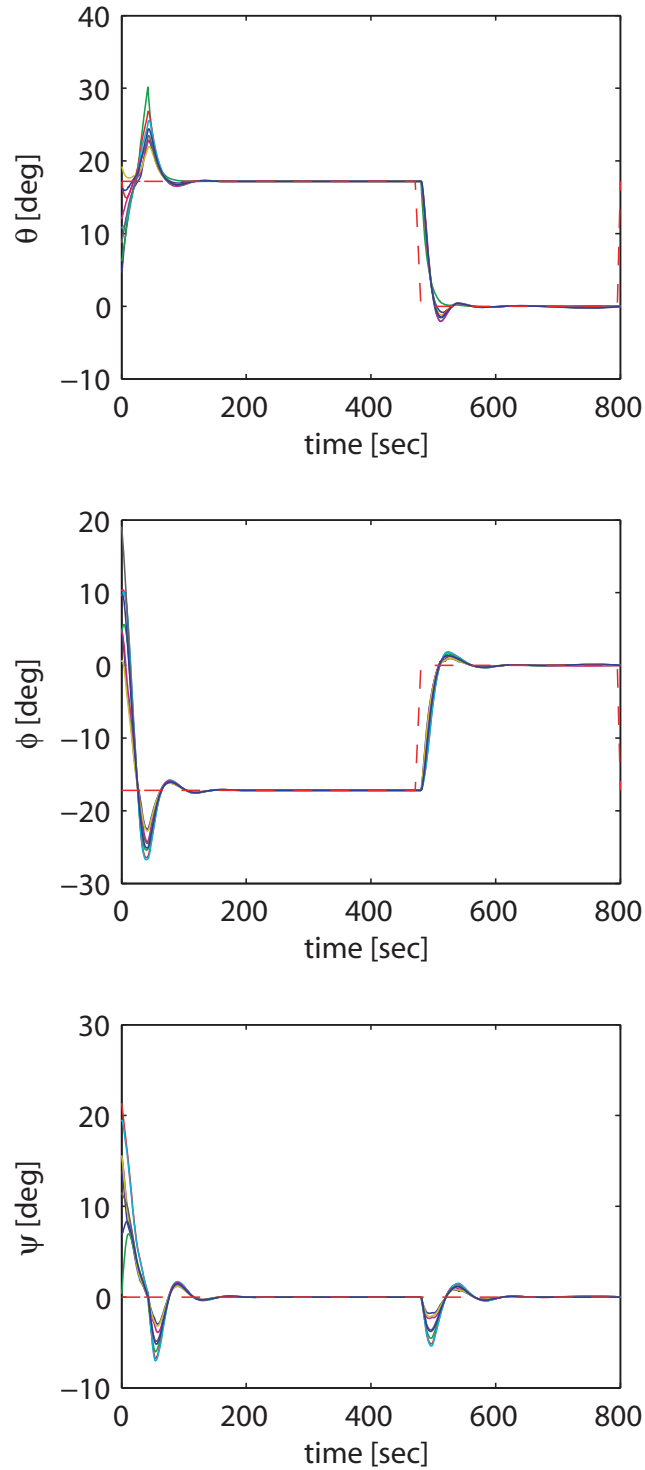


Figure 3.10: The attitudes of the eight networked spacecraft in presence of additive actuator fault under our proposed controller reconfiguration algorithm. The dotted line represents the reference set-point that is only available to the network leaders, i.e. the spacecraft #1 and #6.

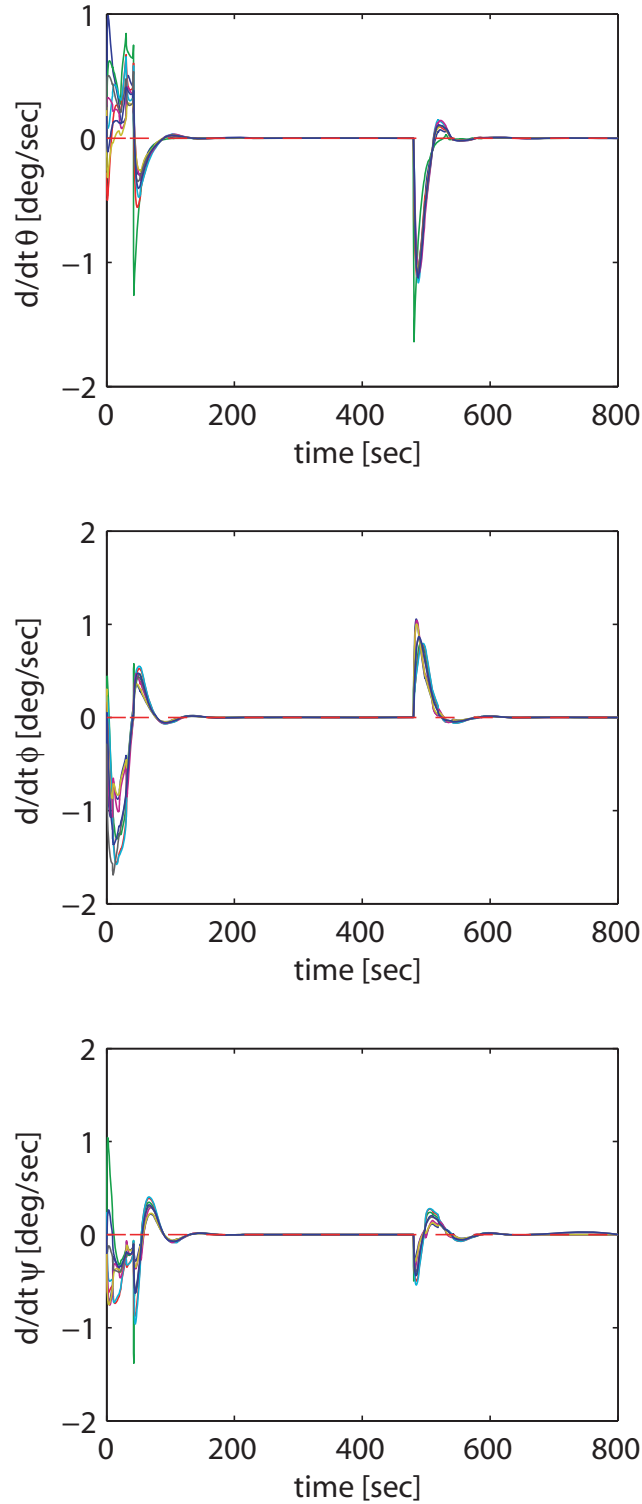


Figure 3.11: The angular velocities of the eight networked spacecraft in presence of additive actuator fault under our proposed controller reconfiguration algorithm. The dotted line represents the reference set-point.

Chapter 4

Distributed H_∞ -Optimal Formation Control of Euler-Lagrange Systems

4.1 Introduction and Problem Statement

In this chapter, we formulate the problem of state synchronization (or consensus) protocol and set-point tracking control of multi-agent EL systems as an H_∞ optimal control problem in presence of parametric uncertainty, external disturbances, and actuator faults. We show that the state synchronization (or consensus) protocol and set-point tracking controllers can be formally derived by employing our proposed analysis. This implies that our proposed method is indeed a formal approach to derive distributed and robust set-point tracking control and state synchronization (or consensus) protocols for networked nonlinear EL systems. This can be considered as one of the key features of the work presented in this chapter when compared to the other approaches that are reported in the literature. In addition, we formally show that our proposed distributed control algorithm is input-to-state stable (ISS) where the input is considered to be subject to the parameter uncertainty as well as

external disturbances for *both* fixed and switching communication network topologies.

We also consider controller reconfiguration in presence of actuator faults in this chapter. Note that, the controller recovery algorithm that is proposed in the previous chapter requires the knowledge of fault bounds for controller reconfiguration. This information has to be provided by the fault detection, isolation and identification (FDI) algorithm that is working in parallel with the controller. However, in the present chapter, we propose an adaptive distributed reconfigurable control algorithm, which has the capability of estimating the faults (*both* intermittent and permanent). We incorporate the information provided by the FDI module in the design of the adaptive controller. We consider three main types of imperfections in the FDI algorithm, namely, (1) *fault detection imperfection*, that is when the fault is not detected by the FDI algorithm, (2) *fault isolation imperfection*, that is when the fault is detected in the wrong channel or in the wrong agent, and (3) *fault identification imperfection*, that is when the fault estimation is not exact. We show that our proposed distributed reconfigurable controller can maintain the closed-loop networked EL systems stability under these scenarios and can improve the performance of the closed-loop networked EL systems in the third case.

Simulation results for the attitude control of a network of spacecraft demonstrate the effectiveness and capabilities of our proposed distributed control algorithms.

4.1.1 Communication Network Topology and Synchronization Error

In this chapter we consider a communication network topology according to Definition 3.1.1. Let the position synchronization error between the j -th and the n -th EL system agents be represented by (3.1). We assume in this chapter that the desired constant position for the networked EL systems, \mathbf{q}^* , is available to all the EL systems in the network. Consequently, the set-point tracking error is defined according to (3.3) for all $j \in \mathcal{V}$.

4.1.2 The \mathcal{L}_2 -Gain of General Networked Nonlinear Systems

Definition 4.1.1. [190] Consider the following nonlinear system

$$\begin{aligned}\dot{\mathbf{x}}_j &= f_j(\mathbf{x}_j) + g_j(\mathbf{x}_j)\mathbf{u}_j + \bar{g}_j(\mathbf{x}_j)\mathbf{w}_j \\ \mathbf{y}_j &= h_j(\mathbf{x}_j)\end{aligned}\tag{4.1}$$

where $\mathbf{x}_j \in \mathbb{R}^{\bar{n}}$, $\mathbf{u}_j \in \mathbb{R}^{\bar{m}}$, $\mathbf{y}_j \in \mathbb{R}^p$, $\mathbf{w}_j \in \mathbb{R}^l$, $g_j(\mathbf{x}_j) \in \mathbb{R}^{\bar{n} \times \bar{m}}$, and $\bar{g}_j(\mathbf{x}_j) \in \mathbb{R}^{\bar{n} \times l}$. Let $\bar{\gamma}_j \geq 0$ and $\mathbf{w}_j(t) = 0, \forall t \geq 0$. The above nonlinear system is said to have \mathcal{L}_2 -gain from the input $\mathbf{u}_j(t)$ to the output $\mathbf{y}_j(t)$ less than or equal to $\bar{\gamma}_j$ if

$$\int_0^T \|\mathbf{y}_j(t)\|^2 dt \leq \bar{\gamma}_j^2 \int_0^T \|\mathbf{u}_j(t)\|^2 dt$$

is satisfied for all the initial conditions $T \geq 0$ and all $\mathbf{y}_j(t), \mathbf{u}_j(t) \in [0, T)$. \square

Definition 4.1.2. Consider a network of ‘ m ’ heterogeneous nonlinear systems where the dynamics of the j -th agent can be expressed by (4.1). The nonlinear state-feedback H_∞ control problem is to find the control $\mathbf{u}_j = K_j(\mathbf{x}_j) + K_{jn}(\mathbf{x}_{jn})$, where $\mathbf{x}_{jn} = \mathbf{x}_j - \mathbf{x}_n$, for the j -th nonlinear system with $K_j(0) = 0$ and $K_{jn}(0) = 0$, such that

the \mathcal{L}_2 gain from the disturbance $\mathbf{u}_j(t)$ to the block vector of outputs $\mathbf{y}_j(t)$, $\mathbf{y}_{jn}(t)$, where $n \in \mathcal{N}_j$ and $\mathbf{y}_{jn}(t) = \mathbf{y}_j(t) - \mathbf{y}_n(t)$, and the input $\mathbf{u}_j(t)$ is less than $\bar{\gamma}_j \geq 0$. In other words, there exists functions $K_j(\mathbf{x}_j) \succeq 0$ and $K_{jn}(\mathbf{x}_{jn}) \succeq 0$ such that,

$$\begin{aligned} & \int_0^\infty \left(k_1 \|\mathbf{y}_j(t)\|^2 + k_2 \sum_{n \in \mathcal{N}_j} \|\mathbf{y}_{jn}(t)\|^2 + k_3 \|\mathbf{u}_j(t)\|^2 \right) dt \\ & \leq k_4 \bar{\gamma}_j^2 \int_0^\infty \|\mathbf{w}_j(t)\|^2 dt, \quad j \in \mathcal{V}, n \in \mathcal{N}_j \end{aligned} \quad (4.2)$$

is satisfied for some weighting parameters $k_i > 0$, $i = \{1, \dots, 4\}$, all initial conditions and all $\mathbf{y}_j(t), \mathbf{u}_j(t), \mathbf{w}_j(t) \in [0, \infty)$. The H_∞ optimal control problem is to find, if it exists, the smallest value $\bar{\gamma}_j^*$ of the \mathcal{L}_2 gains $\bar{\gamma}_j$. \square

4.1.3 Input-to-State Stability of General Networked Nonlinear Systems

In this subsection, we extend the standard definition (Definition 2.9.11) of the input-to-state stability (ISS) of general nonlinear systems to general *networked* nonlinear systems.

Definition 4.1.3. Consider a network of ‘ m ’ heterogeneous nonlinear systems where the dynamics of the j -th agent can be expressed by (4.1). A nonlinear state-feedback control law $\mathbf{u}_j = K_j(\mathbf{x}_j) + K_{jn}(\mathbf{x}_{jn})$ for the j -th nonlinear system, with $\mathbf{x}_{jn} = \mathbf{x}_j - \mathbf{x}_n$, $j \in \mathcal{V}, n \in \mathcal{N}_j$, $K_j(0) = 0$ and $K_{jn}(0) = 0$, is said to be ISS if for the closed-loop system there exists a class \mathcal{KL} function $\bar{\beta}_j$ and a class \mathcal{K} function $\bar{\gamma}_j$ such that for any initial conditions $\mathbf{x}_j(0)$ and $\mathbf{x}_{jn}(0)$, where $n \in \mathcal{N}_j$, and any bounded input $\mathbf{w}_j(t)$, the solutions $\mathbf{x}_j(t)$ and $\mathbf{x}_{jn}(t)$ exist for all $t \geq 0$ and satisfy,

$$\|\mathbf{x}_j(t)\| + \|\mathbf{x}_{jn}(t)\| \leq \bar{\beta}_j \left(\|\mathbf{x}_j(0)\| + \|\mathbf{x}_{jn}(0)\|, t \right) + \bar{\gamma}_j \left(\sup_{0 \leq \xi \leq t} \|\mathbf{w}_j(\xi)\| \right) \quad (4.3)$$

The above inequality guarantees that for any bounded disturbance $\mathbf{w}_j(t)$, the states $\mathbf{x}_j(t)$ and $\mathbf{x}_{jn}(t)$ will remain bounded. In addition, as time evolves (t increases) the states $\mathbf{x}_j(t)$ and $\mathbf{x}_{jn}(t)$ will remain ultimately bounded by a class \mathcal{K} function of $\sup_{0 \leq \xi \leq t} \|\mathbf{w}_j(\xi)\|$. One can further show that if $\mathbf{w}_j(t) \rightarrow 0$ as $t \rightarrow \infty$, then, $\mathbf{x}_j(t) \rightarrow 0$ and $\mathbf{x}_{jn}(t) \rightarrow 0$ as $t \rightarrow \infty$. \square

The ISS can be shown by using a Lyapunov-like theorem as discussed below.

Lemma 4.1.1. *Consider a network of ‘ m ’ heterogeneous nonlinear systems where the dynamics of the j -th agent can be expressed by (4.1). Suppose there exists a nonlinear state-feedback control law $\mathbf{u}_j = \mathbf{K}_j(\mathbf{x}_j) + \mathbf{K}_{jn}(\mathbf{x}_{jn})$ for the j -th nonlinear system, with $\mathbf{K}_j(0) = 0$ and $\mathbf{K}_{jn}(0) = 0$, and a continuously differentiable positive definite radially unbounded Lyapunov function \mathcal{W} for the networked heterogeneous nonlinear system such that for the closed-loop system we have,*

$$\begin{aligned} \dot{\mathcal{W}} &\leq -\bar{\gamma}(\|\mathbf{x}_j(t)\| + \|\mathbf{x}_{jn}(t)\|) + \underline{\gamma}\|\mathbf{w}_j(t)\|, \text{ and} \\ \dot{\mathcal{W}} &\leq -\underline{\underline{\gamma}}(\|\mathbf{x}_j(t)\| + \|\mathbf{x}_{jn}(t)\|) \Leftrightarrow \|\mathbf{x}_j(t)\| + \|\mathbf{x}_{jn}(t)\| \geq \rho(\|\mathbf{w}_j(t)\|) \end{aligned} \quad (4.4)$$

for all $\mathbf{x}_j(t)$, $\mathbf{x}_{jn}(t)$, and $\mathbf{w}_j(t)$, where $\bar{\gamma}$, $\underline{\gamma}$, and $\underline{\underline{\gamma}}$ are class \mathcal{K}_∞ functions and ρ is a class \mathcal{K} function. Then the system is ISS.

Proof: The proof is similar to the proof of Theorem 4.19 in [174] and is therefore omitted. \blacksquare

Definition 4.1.4. Any positive definite radially unbounded Lyapunov function \mathcal{W} which satisfies (4.4) is denoted as the *ISS-Lyapunov function*. \square

4.1.4 Statement of the Problem

Consider a network of ‘ m ’ heterogeneous nonlinear EL systems with a set of ‘ h ’ communication graphs as per Definition 3.1.1. The j -th EL system in the network, $j \in \mathcal{V}$, is governed by the dynamic equation (2.7). Our objective is to design and develop distributed robust control laws which can guarantee boundedness of state synchronization and set-point tracking for the networked EL systems in presence of external disturbances and parameter uncertainties. In other words, we employ robust control techniques to develop distributed control laws which guarantee the following requirements in presence of external disturbances: (r1) boundedness of synchronization error of the EL system coordinates, and (r2) boundedness of set-point tracking errors of the networked EL systems.

The constraints that we consider for the development of our optimal control laws are as follows: (c1) the EL systems parameters are not exactly known, and (c2) the communication network topology is *not* fixed and is *switching*.

Remark 4.1.1. In this chapter $\delta(t)$ in equation (2.7) is used to represent external disturbances in Sections 4.2 and 4.3. It is used to represent additive actuator faults in Section 4.4.

4.2 Distributed H_∞ State Synchronization Control of Networked Euler-Lagrange Systems

We employ the following modified computed-torque control input, i.e.,

$$\mathbf{u}_j = \hat{\mathbf{D}}_j(\mathbf{q}_j)\dot{\mathbf{r}}_j + \hat{\mathbf{C}}_j(\mathbf{q}_j, \dot{\mathbf{q}}_j)\mathbf{r}_j + \hat{\mathbf{g}}_j(\mathbf{q}_j) + \frac{\partial \hat{\mathcal{F}}(\dot{\mathbf{q}}_j)}{\partial \dot{\mathbf{q}}_j} + \boldsymbol{\tau}_j \quad (4.5)$$

where $\hat{\mathbf{D}}_j(\mathbf{q}_j)$, $\hat{\mathbf{C}}_j(\mathbf{q}_j, \dot{\mathbf{q}}_j)$, $\hat{g}_j(\mathbf{q}_j)$ and $\hat{\mathcal{F}}_j$ are estimations of $\mathbf{D}_j(\mathbf{q}_j)$, $\mathbf{C}_j(\mathbf{q}_j, \dot{\mathbf{q}}_j)$, $g_j(\mathbf{q}_j)$ and \mathcal{F}_j , respectively. In addition, τ_j is an auxiliary control input vector and $\mathbf{r}_j = -\bar{\mathbf{K}}_j \tilde{\mathbf{q}}_j - \bar{\bar{\mathbf{K}}}_j \int_0^t \tilde{\mathbf{q}}(\xi) d\xi$, where $\bar{\mathbf{K}}_j$ and $\bar{\bar{\mathbf{K}}}_j$ are positive definite diagonal matrices. Then the dynamics of system (2.7) is reduced to

$$\mathbf{D}_j(\mathbf{q}_j)(\ddot{\tilde{\mathbf{q}}}_j + \bar{\mathbf{K}}_j \dot{\tilde{\mathbf{q}}}_j + \bar{\bar{\mathbf{K}}}_j \tilde{\mathbf{q}}) + \mathbf{C}_j(\mathbf{q}_j, \dot{\tilde{\mathbf{q}}}_j)(\dot{\tilde{\mathbf{q}}}_j + \bar{\mathbf{K}}_j \tilde{\mathbf{q}}_j + \bar{\bar{\mathbf{K}}}_j \int_0^t \tilde{\mathbf{q}}(\xi) d\xi) = \tau_j + \mathbf{w}_j(t) \quad (4.6)$$

where $\mathbf{w}_j(t)$ is a new disturbance applied to the system and it is defined below,

$$\begin{aligned} \mathbf{w}_j = & \tilde{\mathbf{D}}_j(\mathbf{q}_j)(\ddot{\tilde{\mathbf{q}}}_j + \bar{\mathbf{K}}_j \dot{\tilde{\mathbf{q}}}_j + \bar{\bar{\mathbf{K}}}_j \tilde{\mathbf{q}}) + \tilde{\mathbf{C}}_j(\mathbf{q}_j, \dot{\tilde{\mathbf{q}}}_j)(\dot{\tilde{\mathbf{q}}}_j + \bar{\mathbf{K}}_j \tilde{\mathbf{q}}_j + \bar{\bar{\mathbf{K}}}_j \int_0^t \tilde{\mathbf{q}}(\xi) d\xi) \\ & + \tilde{g}_j(\mathbf{q}_j) + \tilde{\mathcal{F}}_j + \delta(t) \end{aligned} \quad (4.7)$$

where $\tilde{\mathbf{D}}_j = \mathbf{D}_j - \hat{\mathbf{D}}_j$, $\tilde{\mathbf{C}}_j = \mathbf{C}_j - \hat{\mathbf{C}}_j$, $\tilde{g}_j = g_j - \hat{g}_j$, and $\tilde{\mathcal{F}}_j = \frac{\partial \mathcal{F}(\dot{\mathbf{q}}_j)}{\partial \dot{\mathbf{q}}_j} - \frac{\partial \hat{\mathcal{F}}(\dot{\mathbf{q}}_j)}{\partial \dot{\mathbf{q}}_j}$.

The dynamics system (4.6) can be written in the following state-space form,

$$\dot{\mathbf{x}}_j = \tilde{\mathfrak{J}}_j(\mathbf{x}_j, t) \mathbf{x}_j + \tilde{\mathfrak{G}}_j \tau_j + \tilde{\mathfrak{B}}_j(\mathbf{x}_j, t) \mathbf{w}_j \quad (4.8)$$

where $\mathbf{x}_j = [\int_0^t \tilde{\mathbf{q}}_j^T d\xi, \tilde{\mathbf{q}}_j^T, \dot{\tilde{\mathbf{q}}}_j^T]^T \in \mathbb{R}^{3k}$, and

$$\tilde{\mathfrak{J}}_j(\mathbf{x}_j, t) = \begin{bmatrix} 0 & \mathfrak{I}_k & 0 \\ 0 & 0 & \mathfrak{I}_k \\ -\mathbf{D}_j^{-1} \mathbf{C}_j \bar{\bar{\mathbf{K}}}_j & -\mathbf{D}_j^{-1} \mathbf{C}_j \bar{\mathbf{K}}_j - \bar{\bar{\mathbf{K}}}_j & -\mathbf{D}_j^{-1} \mathbf{C}_j - \bar{\mathbf{K}}_j \end{bmatrix}$$

$$\tilde{\mathfrak{B}}_j(\mathbf{x}_j, t) = \begin{bmatrix} 0 \\ 0 \\ \mathbf{D}_j^{-1} \end{bmatrix}$$

The auxiliary control input vector τ_j can be decomposed as:

$$\tau_j = \bar{\tau}_j + \sum_{n \in \mathcal{N}_j} \mathbf{F}_{jn} \mathbf{x}_n \quad (4.9)$$

where \mathbf{F}_{jn} represents interaction among the agents and $\bar{\tau}_j$ represents the dependence of the control input of the agent j on its local information. To derive the H_∞ feedback control law for the control input vector $\bar{\tau}_j$, we introduce the following inequality for the networked EL systems,

$$\begin{aligned} \sum_{j=1}^m \int_0^\infty \left[\frac{1}{2} \mathbf{x}_j^T \mathbf{Q}_j \mathbf{x}_j + \bar{\tau}_j^T \mathbf{R}_j \bar{\tau}_j + \frac{1}{4} \sum_{n \in \mathcal{N}_j} (\mathbf{x}_j - \mathbf{x}_n)^T \mathbf{Q}_{jn} (\mathbf{x}_j - \mathbf{x}_n) \right] dt \\ \leq \sum_{j=1}^m \frac{1}{2} \bar{\gamma}_j^2 \int_0^\infty \mathbf{w}_j^T \mathbf{w}_j dt \end{aligned} \quad (4.10)$$

where $\mathbf{Q}_j \succeq 0$, $\mathbf{R}_j \succ 0$ and $\mathbf{Q}_{jn} \succeq 0$ are diagonal matrices. We further assume that \mathbf{Q}_{jn} is chosen such that $\sum_{n \in \mathcal{N}_j} \mathbf{Q}_{jn} = \sum_{j \in \mathcal{N}_n} \mathbf{Q}_{nj}$, $j, n \in \mathcal{V}$, $j \neq n$.

Our first result is concerned with a network of general nonlinear systems whose dynamic equations can be written in the state-space form (4.8).

Lemma 4.2.1. *Consider a network of ‘m’ heterogeneous nonlinear EL systems with the state-space dynamics governed by (4.8). Let $\bar{\gamma}_j > 0$. Suppose there exist smooth functions $\mathcal{Y}_j(\mathbf{x}_j, t)$ in class \mathcal{KL} with $\mathcal{Y}_j(0, t) = 0$, $\forall j \in \{0, \dots, m\}$ such that the following Hamilton-Jacobi-Isaacs (HJI) partial differential inequality is satisfied*

$$\begin{aligned} \frac{\partial \mathcal{Y}_j(\mathbf{x}_j, t)}{\partial t} + \frac{\partial \mathcal{Y}_j(\mathbf{x}_j, t)}{\partial \mathbf{x}_j} \tilde{\mathfrak{F}}_j(\mathbf{x}_j, t) \mathbf{x}_j + \frac{1}{2} \frac{\partial \mathcal{Y}_j^T(\mathbf{x}_j, t)}{\partial \mathbf{x}_j} \left[\frac{1}{\bar{\gamma}_j^2} \bar{\mathfrak{G}}_j^T \bar{\mathfrak{G}}_j \right. \\ \left. - \frac{1}{2} \bar{\mathfrak{G}}_j^T \mathbf{R}_j^{-1} \bar{\mathfrak{G}}_j \right] \frac{\partial \mathcal{Y}_j(\mathbf{x}_j, t)}{\partial \mathbf{x}_j} + \frac{1}{2} \mathbf{x}_j^T \left(\mathbf{Q}_j + \sum_{n \in \mathcal{N}_j} \mathbf{Q}_{jn} \right) \mathbf{x}_j \leq 0 \end{aligned} \quad (4.11)$$

Now consider the following distributed control law for the j -th system

$$\tau_j \triangleq \underbrace{-\frac{1}{2}\mathbf{R}_j^{-1}\bar{\tau}_j^*}_{\bar{\tau}_j} + \underbrace{\frac{1}{2}\sum_{n \in \mathcal{N}_j} \Upsilon_j \mathbf{Q}_{jn} \mathbf{x}_n}_{\sum_{n \in \mathcal{N}_j} \mathbf{F}_{jn}} \quad (4.12)$$

where $\bar{\tau}_j^* = \bar{\mathfrak{G}}_j^T \frac{\partial \mathcal{Y}_j^T(\mathbf{x}_j, t)}{\partial \mathbf{x}_j}$, and Υ_j is chosen such that $\frac{\partial \mathcal{Y}_j(\mathbf{x}_j, t)}{\partial \mathbf{x}_j} \bar{\mathfrak{G}}_j \Upsilon_j = \mathbf{x}_j$. Then by choosing the distributed control law (4.12) for the j -th EL system it is guaranteed that the expression (4.10) is satisfied for all $t \geq 0$.

Proof: Let us introduce the following value function for the j -th nonlinear system,

$$\mathcal{Y}_j(\mathbf{x}_j) = \frac{1}{2} \mathbf{x}_j^T \mathbf{P}_j \mathbf{x}_j \quad (4.13)$$

where $\mathbf{P}_j(\tilde{\mathbf{q}}_j) \in \mathbb{R}^{3k}$, $\mathbf{P}_j = \mathbf{P}_j^T \succ 0$. Consequently, by noting (4.11) and (4.12) we

have

$$\begin{aligned}
\frac{d}{dt} \mathcal{Y}_j &= \frac{\partial \mathcal{Y}_j}{\partial \mathbf{x}_j} \bar{\mathfrak{S}}_j(\mathbf{x}_j, t) \mathbf{x}_j + \frac{\partial \mathcal{Y}_j}{\partial \mathbf{x}_j} \bar{\mathfrak{S}}_j \tau_j + \frac{\partial \mathcal{Y}_j}{\partial \mathbf{x}_j} \bar{\mathfrak{S}}_j \mathbf{w}_j \\
&\leq \frac{1}{4} \frac{\partial \mathcal{Y}_j^T}{\partial \mathbf{x}_j} \bar{\mathfrak{S}}_j^T \mathbf{R}_j^{-1} \bar{\mathfrak{S}}_j \frac{\partial \mathcal{Y}_j}{\partial \mathbf{x}_j} \\
&\quad - \frac{1}{2} \frac{1}{\bar{\gamma}_j^2} \frac{\partial \mathcal{Y}_j^T}{\partial \mathbf{x}_j} \bar{\mathfrak{S}}_j^T \bar{\mathfrak{S}}_j \frac{\partial \mathcal{Y}_j}{\partial \mathbf{x}_j} - \frac{1}{2} \mathbf{x}_j^T \mathbf{Q}_j \mathbf{x}_j - \frac{1}{2} \mathbf{x}_j^T \sum_{n \in \mathcal{N}_j} \mathbf{Q}_{jn} \mathbf{x}_j \\
&\quad + \underbrace{(\bar{\tau}_j^*)^T}_{\frac{\partial \mathcal{Y}_j}{\partial \mathbf{x}_j} \bar{\mathfrak{S}}_j} \left[-\frac{1}{2} \mathbf{R}_j^{-1} \bar{\tau}_j^* + \frac{1}{2} \sum_{n \in \mathcal{N}_j} \Upsilon_j \mathbf{Q}_{jn} \mathbf{x}_n \right] + \frac{\partial \mathcal{Y}_j}{\partial \mathbf{x}_j} \bar{\mathfrak{S}}_j \mathbf{w}_j \\
&\leq -\frac{1}{2} \bar{\gamma}_j^2 \left\| \mathbf{w}_j - \frac{1}{\bar{\gamma}_j^2} \bar{\mathfrak{S}}_j^T \frac{\partial \mathcal{Y}_j^T}{\partial \mathbf{x}_j} \right\|^2 - \frac{1}{2} \mathbf{x}_j^T \mathbf{Q}_j \mathbf{x}_j - \frac{1}{2} \mathbf{x}_j^T \sum_{n \in \mathcal{N}_j} \mathbf{Q}_{jn} (\mathbf{x}_j - \mathbf{x}_n) \\
&\quad + \frac{1}{2} \bar{\gamma}_j^2 \|\mathbf{w}_j\|^2 - \bar{\tau}_j^T \mathbf{R}_j \bar{\tau}_j \\
&\leq -\frac{1}{2} \mathbf{x}_j^T \mathbf{Q}_j \mathbf{x}_j - \frac{1}{2} \mathbf{x}_j^T \sum_{n \in \mathcal{N}_j} \mathbf{Q}_{jn} (\mathbf{x}_j - \mathbf{x}_n) + \frac{1}{2} \bar{\gamma}_j^2 \|\mathbf{w}_j\|^2 - \bar{\tau}_j^T \mathbf{R}_j \bar{\tau}_j
\end{aligned}$$

Consequently,

$$\begin{aligned}
\frac{d}{dt} \mathcal{Y} &\leq \sum_{j=1}^m \left[-\frac{1}{2} \mathbf{x}_j^T \mathbf{Q}_j \mathbf{x}_j - \frac{1}{2} \mathbf{x}_j^T \sum_{n \in \mathcal{N}_j} \mathbf{Q}_{jn} (\mathbf{x}_j - \mathbf{x}_n) + \frac{1}{2} \bar{\gamma}_j^2 \|\mathbf{w}_j\|^2 - \bar{\tau}_j^T \mathbf{R}_j \bar{\tau}_j \right] \\
&\leq \sum_{j=1}^m \left[-\frac{1}{2} \mathbf{x}_j^T \mathbf{Q}_j \mathbf{x}_j - \frac{1}{4} \sum_{n \in \mathcal{N}_j} (\mathbf{x}_j - \mathbf{x}_n)^T \mathbf{Q}_{jn} (\mathbf{x}_j - \mathbf{x}_n) + \frac{1}{2} \bar{\gamma}_j^2 \|\mathbf{w}_j\|^2 - \bar{\tau}_j^T \mathbf{R}_j \bar{\tau}_j \right]
\end{aligned} \tag{4.14}$$

where $\mathcal{Y} \triangleq \sum_{j=1}^m \mathcal{Y}_j$. By integrating from $t \in [0, \infty)$ we obtain,

$$\begin{aligned}
&\int_0^\infty \sum_{j=1}^m \left[\frac{1}{2} \mathbf{x}_j^T \mathbf{Q}_j \mathbf{x}_j + \bar{\tau}_j^T \mathbf{R}_j \bar{\tau}_j + \frac{1}{4} \sum_{n \in \mathcal{N}_j} (\mathbf{x}_j - \mathbf{x}_n)^T \mathbf{Q}_{jn} (\mathbf{x}_j - \mathbf{x}_n) \right] dt \\
&\leq \frac{1}{2} \sum_{j=1}^m \bar{\gamma}_j^2 \int_0^\infty \|\mathbf{w}_j\|^2 dt + \mathcal{Y}(0) - \mathcal{Y}(\infty)
\end{aligned} \tag{4.15}$$

Since \mathcal{V} is non-increasing with time, the results follows. This completes the proof. ■

4.2.1 Discussions on Existence of a Solution

Our next result provides a solution to the value function (4.13) for general nonlinear EL systems.

Lemma 4.2.2. *Consider a network of ‘m’ heterogeneous EL systems with dynamics governed by (4.8). Select the value function (4.13) for the j-th system, with,*

$$\mathbf{P}_j = \begin{bmatrix} \bar{\bar{\mathbf{K}}}_j \mathbf{D}_j \bar{\bar{\mathbf{K}}}_j + \bar{\bar{\mathbf{K}}}_j \bar{\mathbf{K}}_j \mathbf{K}_j & \bar{\bar{\mathbf{K}}}_j \mathbf{D}_j \bar{\bar{\mathbf{K}}}_j + \bar{\bar{\mathbf{K}}}_j \mathbf{K}_j & \bar{\bar{\mathbf{K}}}_j \mathbf{D}_j \\ \bar{\mathbf{K}}_j \mathbf{D}_j \bar{\bar{\mathbf{K}}}_j + \bar{\bar{\mathbf{K}}}_j \mathbf{K}_j & \bar{\mathbf{K}}_j \mathbf{D}_j \bar{\bar{\mathbf{K}}}_j + \bar{\bar{\mathbf{K}}}_j \mathbf{K}_j & \bar{\mathbf{K}}_j \mathbf{D}_j \\ \mathbf{D}_j \bar{\bar{\mathbf{K}}}_j & \mathbf{D}_j \bar{\bar{\mathbf{K}}}_j & \mathbf{D}_j \end{bmatrix} \quad (4.16)$$

where \mathbf{K}_j is a positive definite symmetric matrix and $\bar{\bar{\mathbf{K}}}_j^2 > 2\bar{\bar{\mathbf{K}}}_j$. This selection of the matrices guarantees positive definiteness of the matrix \mathbf{P}_j . One can show that the HJI inequality (4.11) for this system is satisfied if the following Riccati equation is satisfied,

$$\dot{\mathbf{P}}_j + \mathbf{P}_j \bar{\mathfrak{F}}_j + \bar{\mathfrak{F}}_j^T \mathbf{P}_j + \mathbf{Q}_j + \sum_{n \in \mathcal{N}_j} \mathbf{Q}_{jn} - \mathbf{P}_j \bar{\mathfrak{G}}_j \mathbf{R}_j^{-1} \bar{\mathfrak{G}}_j^T \mathbf{P}_j + \frac{1}{\bar{\gamma}_j^2} \mathbf{P}_j \bar{\mathfrak{G}}_j \bar{\mathfrak{G}}_j^T \mathbf{P}_j = 0 \quad (4.17)$$

.

Proof: One can show that $\frac{\partial \mathcal{V}_j}{\partial t} + \frac{\partial \mathcal{V}_j}{\partial \mathbf{x}_j} \bar{\mathfrak{F}}_j(\mathbf{x}_j, t) \mathbf{x}_j = \frac{1}{2}(\dot{\mathbf{P}}_j + \mathbf{P}_j \bar{\mathfrak{F}}_j + \bar{\mathfrak{F}}_j^T \mathbf{P}_j)$. One can also show that $\frac{\partial \mathcal{V}_j}{\partial \mathbf{x}_j} \bar{\mathfrak{G}}_j = \mathbf{x}_j^T \mathbf{P}_j \bar{\mathfrak{G}}_j$ [180]. Consequently, the HJI equation (4.11) can be written as (4.17). This completes the proof. ■

It is not straight-forward to solve the Riccati equation (4.17) for an arbitrary selection of the weighting matrices \mathbf{Q}_j , \mathbf{Q}_{jn} and \mathbf{R}_j . In our next result, we provide

a guideline for selecting the weighting matrices in order to guarantee existence of a solution for the Riccati equation (4.17).

Lemma 4.2.3. *For a given $\tilde{\gamma}_j > 0$ choose \mathbf{K}_j such that $\mathbf{K}_j - \frac{1}{\tilde{\gamma}_j^2} \mathfrak{J}_3 \succ 0$. Let the weighting matrix \mathbf{R}_j to be designed as*

$$\mathbf{R}_j = \left(\mathbf{K}_j - \frac{1}{\tilde{\gamma}_j^2} \mathfrak{J}_3 \right)^{-1} \quad (4.18)$$

and the weighting matrices \mathbf{Q}_j , and \mathbf{Q}_{jn} to be selected as follows,

$$\mathbf{Q}_j + \sum_{n \in \mathcal{N}_j} \mathbf{Q}_{jn} = \begin{bmatrix} \bar{\bar{\mathbf{K}}}_j^2 \mathbf{K}_j & 0 & 0 \\ 0 & \mathbf{K}_j (\bar{\bar{\mathbf{K}}}_j^2 - 2\bar{\bar{\mathbf{K}}}_j) & 0 \\ 0 & 0 & \mathbf{K}_j \end{bmatrix} \quad (4.19)$$

Then the Riccati equation (4.17) is satisfied along with (4.13) and (4.16).

Proof: By noting (4.18) one can simplify (4.17) as,

$$\dot{\mathbf{P}}_j + \mathbf{P}_j \tilde{\mathfrak{F}}_j + \tilde{\mathfrak{F}}_j^T \mathbf{P}_j + \mathbf{Q}_j + \sum_{n \in \mathcal{N}_j} \mathbf{Q}_{jn} - \mathbf{P}_j \tilde{\mathfrak{G}}_j \mathbf{K}_j \tilde{\mathfrak{G}}_j^T \mathbf{P}_j = 0 \quad (4.20)$$

One can show by noting the Property 2.1.2 that

$$\dot{\mathbf{P}}_j + \mathbf{P}_j \tilde{\mathfrak{F}}_j + \tilde{\mathfrak{F}}_j^T \mathbf{P}_j = \begin{bmatrix} 0 & \bar{\bar{\mathbf{K}}}_j \bar{\bar{\mathbf{K}}}_j \mathbf{K}_j & \bar{\bar{\mathbf{K}}}_j \mathbf{K}_j \\ \bar{\bar{\mathbf{K}}}_j \bar{\bar{\mathbf{K}}}_j \mathbf{K}_j & 2\bar{\bar{\mathbf{K}}}_j \mathbf{K}_j & \bar{\bar{\mathbf{K}}}_j \mathbf{K}_j \\ \bar{\bar{\mathbf{K}}}_j \mathbf{K}_j & \bar{\bar{\mathbf{K}}}_j \mathbf{K}_j & 0 \end{bmatrix} \quad (4.21)$$

In addition, one can show that

$$\mathbf{P}_j \bar{\mathcal{G}}_j \mathbf{K}_j \bar{\mathcal{G}}_j^T \mathbf{P}_j = \begin{bmatrix} \bar{\mathbf{K}}_j^2 \mathbf{K}_j & \bar{\mathbf{K}}_j \bar{\mathbf{K}}_j \mathbf{K}_j & \bar{\mathbf{K}}_j \mathbf{K}_j \\ \bar{\mathbf{K}}_j \bar{\mathbf{K}}_j \mathbf{K}_j & \bar{\mathbf{K}}_j^2 \mathbf{K}_j & \bar{\mathbf{K}}_j \mathbf{K}_j \\ \bar{\mathbf{K}}_j \mathbf{K}_j & \bar{\mathbf{K}}_j \mathbf{K}_j & \mathbf{K}_j \end{bmatrix} \quad (4.22)$$

Consequently, by adding (4.21) and (4.22) and noting (4.20) one obtains (4.19).

This completes the proof. \blacksquare

Now define $0 < \alpha_j < 1$ such that $(1 - \alpha_j) \bar{\mathbf{K}}_j^2 - 2 \bar{\mathbf{K}}_j \succ 0$. Consequently, one obtains

$$\sum_{n \in \mathcal{N}_j} \mathbf{Q}_{jn} = \alpha_j \begin{bmatrix} \bar{\mathbf{K}}_j^2 \mathbf{K}_j & 0 & 0 \\ 0 & \bar{\mathbf{K}}_j^2 \mathbf{K}_j & 0 \\ 0 & 0 & \mathbf{K}_j \end{bmatrix} \quad (4.23)$$

As a result, one gets

$$\mathbf{Q}_j = (1 - \alpha_j) \begin{bmatrix} \bar{\mathbf{K}}_j^2 \mathbf{K}_j & 0 & 0 \\ 0 & \bar{\mathbf{K}}_j^2 \mathbf{K}_j & 0 \\ 0 & 0 & \mathbf{K}_j \end{bmatrix} - \begin{bmatrix} 0 & 0 & 0 \\ 0 & 2 \bar{\mathbf{K}}_j \mathbf{K}_j & 0 \\ 0 & 0 & 0 \end{bmatrix} \quad (4.24)$$

We also assume that $\mathbf{Q}_{jn} = \mathbf{Q}_{jk}$ where $n \neq k$ and $n, k \in \mathcal{N}_j$. The parameter α_j plays an important weighting role. Specifically, smaller values of α_j ($\alpha_j \rightarrow 0$) put more weight on the trajectory tracking control law over the state synchronization control law (follows from (4.23) and (4.24) and the ‘‘cost’’ function in (4.10)). On the other hand, by selecting larger values for α_j ($\alpha_j \rightarrow 1$) one can put more emphasis on the state synchronization of the agents and less emphasis on the trajectory tracking.

It can be shown by noting (4.12) and (4.18) with the parameterizations provided above that one obtains the following control law for the j -th EL system in the

network:

$$\begin{aligned} \tau_j \triangleq & -\frac{1}{2} \left(\mathbf{K}_j - \frac{1}{\bar{\gamma}_j^2} \mathfrak{J}_3 \right) (\dot{\mathbf{q}}_j + \bar{\mathbf{K}}_j \tilde{\mathbf{q}}_j + \bar{\bar{\mathbf{K}}}_j \int_0^t \tilde{\mathbf{q}}_j d\xi) \\ & + \frac{\alpha_j}{2} \mathbf{K}_j \sum_{n \in \mathcal{N}_j} \frac{1}{|\mathcal{N}_j|} (\dot{\mathbf{q}}_n + \bar{\mathbf{K}}_j \tilde{\mathbf{q}}_n + \bar{\bar{\mathbf{K}}}_j \int_0^t \tilde{\mathbf{q}}_n d\xi) \end{aligned} \quad (4.25)$$

4.2.2 Stability Analysis of the Networked Euler-Lagrange Systems

The purpose of this section is to demonstrate global asymptotic stability of the networked EL systems (4.8) under the distributed control law (4.25) in absence of modeling uncertainty and external disturbances.

Theorem 4.2.1. *Consider a network of ‘m’ heterogeneous EL systems that are governed by the dynamics (4.8) and subject to the distributed control law (4.25) for the j-th system. Suppose for a given $\bar{\gamma}_j > 0$ the controller gains, $\bar{\mathbf{K}}_j$, $\bar{\bar{\mathbf{K}}}_j$, \mathbf{K}_j , and α_j are selected such that the following conditions are satisfied,*

$$\bar{\mathbf{K}}_j \succ 0, \bar{\bar{\mathbf{K}}}_j \succ 0, \mathbf{K}_j - \frac{1}{\bar{\gamma}_j^2} \mathfrak{J}_3 \succ 0, \quad (4.26)$$

$$1 > \alpha_j > 0 \quad (4.27)$$

$$(1 - \alpha_j) \bar{\mathbf{K}}_j^2 - 2\bar{\bar{\mathbf{K}}}_j \succ 0 \quad (4.28)$$

Consequently, \mathbf{P}_j , \mathbf{Q}_j , \mathbf{R}_j , and \mathbf{Q}_{jn} are positive definite matrices $\forall j \in \{1, \dots, m\}$, $j \neq n$. Then, in absence of modeling uncertainty and external disturbances the closed-loop system is globally asymptotically stable and the networked EL systems synchronize their states and follow the desired trajectory, i.e. $\int_0^t \mathbf{q}_{jn}(\xi) d\xi \rightarrow 0$, $\mathbf{q}_{jn} \rightarrow 0$, and $\dot{\mathbf{q}}_{jn} \rightarrow 0$, as $t \rightarrow \infty$, and $\int_0^t \mathbf{q}_j(\xi) d\xi \rightarrow 0$, $\mathbf{q}_j \rightarrow 0$, and $\dot{\mathbf{q}}_j \rightarrow 0$, as $t \rightarrow \infty$.

Proof: Consider the following function as the positive definite, radially unbounded, Lyapunov function candidate for the networked system,

$$\mathcal{W} = \frac{1}{2} \sum_{j=1}^m \mathbf{s}_j^T \mathbf{D}_j \mathbf{s}_j \quad (4.29)$$

where $\mathbf{s}_j = \dot{\mathbf{q}}_j + \bar{\mathbf{K}}_j \tilde{\mathbf{q}}_j + \bar{\mathbf{K}}_j \int_0^t \tilde{\mathbf{q}}(\xi) d\xi$. The time derivative of the Lyapunov function candidate along the trajectories of the closed-loop system (2.7), (4.5), and (4.25) is given by $\dot{\mathcal{W}} = \sum_{j=1}^m \frac{1}{2} \dot{\mathbf{s}}_j^T \mathbf{D}_j \mathbf{s}_j + \sum_{j=1}^m \mathbf{s}_j^T \mathbf{D}_j \dot{\mathbf{s}}_j$. This by noting (4.6) can be written as:

$$\begin{aligned} \dot{\mathcal{W}} &= \sum_{j=1}^m \frac{1}{2} \dot{\mathbf{s}}_j^T (\mathbf{D}_j - 2\mathbf{C}_j) \mathbf{s}_j + \sum_{j=1}^m \mathbf{s}_j^T (\boldsymbol{\tau}_j + \mathbf{w}_j) \\ &= \sum_{j=1}^m \mathbf{s}_j^T \left[-\frac{1}{2} \left(\mathbf{K}_j - \frac{1}{\tilde{\gamma}_j^2} \mathcal{J}_3 \right) \mathbf{s}_j + \frac{\alpha_j}{2} \mathbf{K}_j \sum_{n \in \mathcal{N}_j} \frac{1}{|\mathcal{N}_j|} \mathbf{s}_n \right] + \mathbf{s}_j^T \mathbf{w}_j \\ &\leq -\frac{1}{2} \sum_{j=1}^m \mathbf{s}_j^T \left(\mathbf{K}_j - \frac{\alpha_j}{\tilde{\gamma}_j^2} \mathcal{J}_3 \right) \mathbf{s}_j - \frac{\alpha_j}{2} \mathbf{s}_j^T \mathbf{K}_j \left[\sum_{n \in \mathcal{N}_j} \frac{1}{|\mathcal{N}_j|} (\mathbf{s}_j - \mathbf{s}_n) \right] \\ &\quad + \|\mathbf{s}_j\| \|\mathbf{w}_j\| \\ &\leq -\frac{1}{2} \sum_{j=1}^m \mathbf{s}_j^T \left(\mathbf{K}_j - \frac{\alpha_j}{\tilde{\gamma}_j^2} \mathcal{J}_3 \right) \mathbf{s}_j - \frac{\alpha_j}{4} (\mathbf{s}_j - \mathbf{s}_n)^T \mathbf{K}_j \left[\sum_{n \in \mathcal{N}_j} \frac{1}{|\mathcal{N}_j|} \mathbf{s}_{jn} \right] \\ &\quad + \|\mathbf{s}_j\| \|\mathbf{w}_j\| \end{aligned} \quad (4.30)$$

where $\mathbf{s}_{jn} = \mathbf{s}_j - \mathbf{s}_n$. When $\|\mathbf{w}_j\| = 0$ for all $t \geq 0$, i.e. no disturbance is applied to the system and there is no modeling uncertainty, then by noting (4.26) and (4.27) one can conclude that (4.30) is a negative definite decrescent function; this by noting that the Lyapunov function \mathcal{W} (in (4.29)) is radially unbounded, implies that all the signals remain globally bounded. By invoking Theorem 2.9.1 one can conclude that the closed-loop system is globally asymptotically stable in absence of external disturbances, i.e. $\mathbf{s}_j \rightarrow 0$, and $\mathbf{s}_{jn} \rightarrow 0$ as $t \rightarrow \infty$. By invoking Lemma A.12 in

[158] one can conclude that $\int_0^t \mathbf{q}_{jn}(\xi) d\xi \rightarrow 0$, $\mathbf{q}_{jn} \rightarrow 0$, and $\dot{\mathbf{q}}_{jn} \rightarrow 0$, as $t \rightarrow \infty$, and $\int_0^t \tilde{\mathbf{q}}_j(\xi) d\xi \rightarrow 0$, $\tilde{\mathbf{q}}_j \rightarrow 0$, and $\dot{\tilde{\mathbf{q}}}_j \rightarrow 0$, as $t \rightarrow \infty$. This completes the proof of the theorem. ■

4.3 Input-to-State Stability (ISS) of the Networked Euler-Lagrange Systems

The purpose of this section is to demonstrate that the networked EL systems (4.8) under the distributed control law (4.25) in presence of the modeling uncertainty and external disturbances is ISS.

Theorem 4.3.1. *Consider a network of ‘m’ heterogeneous EL systems that are governed by the dynamics (4.8) and subject to the distributed control law (4.25) for the j-th system. Suppose for a given $\bar{\gamma}_j > 0$ the controller gains, $\bar{\mathbf{K}}_j$, $\bar{\mathbf{K}}_j$, \mathbf{K}_j , and α_j are selected such that the conditions (4.26), (4.27), and (4.28) are satisfied. Consequently, \mathbf{P}_j , \mathbf{Q}_j , \mathbf{R}_j , and \mathbf{Q}_{jn} are positive definite matrices $\forall j \in \{1, \dots, m\}$, $j \neq n$. Then, in presence of the modeling uncertainty and external disturbances (nonzero $\mathbf{w}_j(t)$) the closed-loop system is input-to-state stable (cf. Definition 4.1.3) and the synchronization and tracking trajectory errors remain globally ultimately bounded.*

Proof: Consider (4.13) as the positive definite, radially unbounded, Lyapunov function candidate for the j-th system. Let $\mathcal{V} \triangleq \sum_{j=1}^m \mathcal{V}_j$ be the Lyapunov function candidate for the network. One can show, similar to (4.14), that the time derivative of the Lyapunov function candidate \mathcal{V} along the trajectories of the

closed-loop system (4.8), (4.18), (4.23), (4.24) and (4.25) can be written as

$$\begin{aligned} \dot{\mathcal{Y}} \leq & -\frac{1}{2} \sum_{j=1}^m \mathbf{x}_j^T \left[\mathbf{Q}_j + \frac{1}{2} \mathbf{P}_j \bar{\mathfrak{G}}_j \mathbf{R}_j \bar{\mathfrak{G}}_j^T \mathbf{P}_j \right] \mathbf{x}_j \\ & - \frac{1}{4} \sum_{j=1}^m \sum_{n \in \mathcal{N}_j} (\mathbf{x}_j - \mathbf{x}_n)^T \mathbf{Q}_{jn} (\mathbf{x}_j - \mathbf{x}_n) + \frac{1}{2} \sum_{j=1}^m \bar{\gamma}_j^2 \|\mathbf{w}_j\|^2 \end{aligned} \quad (4.31)$$

Positive definite matrices \mathbf{Q}_j , \mathbf{R}_j , and $\mathbf{Q}_{jn} \forall j \in \{1, \dots, m\}$, $n \in \mathcal{N}_j$ imply that the first two terms on the right hand side of the inequality (4.31) are \mathcal{H}_∞ function of \mathbf{x}_j and $(\mathbf{x}_j - \mathbf{x}_n)$, respectively. Define the bounded region \mathfrak{B}_r that includes the origin, that is

$$\begin{aligned} \mathfrak{B}_r = & \left\{ \mathbf{x}_j, (\mathbf{x}_j - \mathbf{x}_n) \mid \frac{1}{2} \mathbf{x}_j^T \left[\mathbf{Q}_j + \frac{1}{2} \mathbf{P}_j \bar{\mathfrak{G}}_j \mathbf{R}_j \bar{\mathfrak{G}}_j^T \mathbf{P}_j \right] \mathbf{x}_j \right. \\ & \left. + \frac{1}{4} \sum_{n \in \mathcal{N}_j} (\mathbf{x}_j - \mathbf{x}_n)^T \mathbf{Q}_{jn} (\mathbf{x}_j - \mathbf{x}_n) \leq \frac{1}{2} \bar{\gamma}_j^2 \|\mathbf{w}_j\|^2 \right\} \end{aligned}$$

For all \mathbf{x}_j and \mathbf{x}_{jn} outside of this region we have $\frac{d}{dt} \mathcal{Y} < 0$. Consequently, by invoking Lemma 4.1.1 one can conclude that the closed-loop networked EL systems under the distributed control law (4.25) for the j -th system is ISS and the synchronization and tracking trajectory errors remain globally ultimately bounded. This completes the proof of the theorem. \blacksquare

4.3.1 ISS with Switchings in the Communication Topology

Finally, we now consider the situation for switchings in the communication network topology.

Lemma 4.3.1. *Consider a network of ‘ m ’ heterogeneous EL systems that is governed by the dynamics (4.8) and is subject to the distributed control law for the j -th*

system and the i -th communication network topology as given by

$$\tau_{j,i} \triangleq -\frac{1}{2} \left(\mathbf{K}_j - \frac{1}{\bar{\gamma}_{j,i}^2} \mathfrak{J}_3 \right) \mathbf{s}_j + \frac{\alpha_{j,i}}{2} \mathbf{K}_j \sum_{n \in \mathcal{N}_{j,i}} \frac{1}{|\mathcal{N}_{j,i}|} \mathbf{s}_n \quad (4.32)$$

Suppose that for a given $\bar{\gamma}_{j,i} > 0$ the controller gains $\bar{\bar{\mathbf{K}}}_j$, $\bar{\mathbf{K}}_j$, \mathbf{K}_j , and $\alpha_{j,i}$ are selected such that the conditions (4.26) and (4.27) are satisfied for all $i \in \{1, \dots, h\}$. Consequently, $\mathbf{P}_j(\mathbf{x}_j)$, $\mathbf{Q}_{j,i}$, $\mathbf{R}_{j,i}$, and $\mathbf{Q}_{jn,i}$ are positive definite matrices $\forall j \in \mathcal{V}$, $j \neq n$ and for all $i \in \{1, \dots, h\}$. It then follows that in presence of modeling uncertainty and external disturbances the closed-loop system is ISS stable and the synchronization and the tracking trajectory errors remain globally ultimately bounded for arbitrary switchings in the communication network topologies.

Proof: The proof is based on the existence of a common ISS-Lyapunov function (as per Definition 4.1.4) for the considered switched system. Let $\mathcal{Y} \triangleq \sum_{j=1}^m \mathcal{Y}_j$ be the Lyapunov function candidate for the EL system network. It follows from Theorem 4.3.1 that the closed-loop networked system is ISS for the i -th communication network topology that is given in Definition 3.1.1. In addition, note that $\mathbf{P}_j(\mathbf{x}_j)$ is the same for all the communication network topologies. Consequently, the function \mathcal{Y} is a common ISS-Lyapunov function. By invoking Theorem 3.1 in [191] one can conclude that the closed-loop system is ISS under *arbitrary* switching in the communication network topologies. This completes the proof of the lemma. ■

4.4 Control Recovery in Presence of Additive Actuator Faults

In this section, we consider $m > 1$ Euler-Lagrange (EL) systems, where the j -th system is governed by the following *nonlinear* dynamic equations,

$$\mathbf{D}_j(\mathbf{q}_j)\ddot{\mathbf{q}}_j + \mathbf{C}_j(\mathbf{q}_j, \dot{\mathbf{q}}_j)\dot{\mathbf{q}}_j + \mathbf{G}_j(\mathbf{q}_j) + \frac{\partial \mathcal{F}_j(\dot{\mathbf{q}}_j)}{\partial \dot{\mathbf{q}}_j} = \text{DI}_j(\mathbf{u}_j) + \delta_j \quad (4.33)$$

where $\text{DI}_j(\cdot)$ is a nonlinear function of inputs, i.e. $\text{DI}_j(\mathbf{u}_j) \triangleq \bar{\mathbf{u}}_j(t) + \mathbf{u}_j(t)$, where

$$\bar{\mathbf{u}}_j(t) = [\bar{\mathbf{u}}_{j,1}(t), \dots, \bar{\mathbf{u}}_{j,k}(t)]^T \in \mathbb{R}^k$$

The vector $\bar{\mathbf{u}}_j(t)$ represents additive actuator faults and the corresponding FDI imperfections.

We make the following assumption explicit.

Assumption 4.4.1. The function $\bar{\mathbf{u}}_{j,1}(t)$ is defined as $\bar{\mathbf{u}}_{j,1}(t) = \bar{\mathbf{u}}_{j,1,l}(t)$, for $t_{l-1} \leq t < t_l$, $l = 1, 2, \dots$, where $\bar{\mathbf{u}}_{j,1,l}(t) \in \mathcal{C}^1$ (class of continuously differentiable functions). This implies that $\bar{\mathbf{u}}_j(t)$ is a vector of piecewise bounded continuous functions of time. The time derivative of $\bar{\mathbf{u}}_j(t)$ is well-defined everywhere except at time t_l where $\frac{d}{dt}\bar{\mathbf{u}}_j(t)$ consists of a Dirac delta function.

The input imperfection $\bar{\mathbf{u}}_j(t)$ considered in Assumption 4.4.1 is a function of time. Therefore, through this formulation one can represent *both* intermittent and permanent actuator faults.

Assumption 4.4.2. The disturbance signal $d(t) \in \mathbb{R}^k$ is a vector of uniformly bounded and piecewise continuous functions of time, i.e. $\sup_{t>0} d(t) < \infty$.

We also assume that an FDI unit is operating in parallel with the distributed controller (4.5) and (4.25). In presence of a fault the term Γ_j is added to the distributed control law (4.25) to compensate for the effects of a fault and recover, as much as possible, the performance of the closed-loop system. In reality, however, no FDI algorithm is 100% perfect and reliable. Consequently, the controller must be robust to imperfections in the FDI algorithm. Let the fault in the j -th system satisfy Assumption 4.4.1. We now consider the following three cases.

Case 1. The FDI algorithm is not capable of detecting the fault. Consequently, the controller for the j -th system will not reconfigure itself in presence of the fault. This is designated as *imperfection in the fault detection*.

Case 2. The FDI algorithm has detected the fault in an incorrect input channel or an incorrect agent. Consequently, the controller is reconfigured in an inappropriate channel or agent. This is designated as *imperfection in the fault isolation*.

Case 3. The FDI algorithm has detected the fault in the correct input channel or agent. However, the magnitude or the severity of the fault is not correctly identified. In other words, the FDI algorithm provides a piecewise continuous estimation of the vector $\bar{\mathbf{u}}_j(t)$, which is denoted by $\bar{\mathbf{u}}_j^*(t)$ such that $\|\bar{\mathbf{u}}_j^* - \bar{\mathbf{u}}_j\|$ is always bounded, i.e. $\sup_{t>0} \|\bar{\mathbf{u}}_j^* - \bar{\mathbf{u}}_j\| < \infty$. This is designated as *imperfection in the fault identification*.

4.4.1 Control Reconfiguration Subject to Imperfections in the Fault Detection Module

In presence of imperfection in the fault detection module the controller is not reconfigured appropriately. However, one can still guarantee boundedness of the synchronization and the trajectory tracking errors in presence of the fault. Our next

result is provided in the following lemma.

Lemma 4.4.1. *Consider a network of ‘m’ heterogeneous nonlinear EL systems (2.7) under the distributed control laws (4.5) and (4.25). Suppose for a given $\bar{\gamma}_j > 0$ the controller gains, $\bar{\bar{\mathbf{K}}}_j$, $\bar{\mathbf{K}}_j$, \mathbf{K}_j , and α_j are selected such that the conditions (4.26), (4.27), and (4.28) are satisfied. Then under Assumption 4.4.1 the closed-loop networked system remains globally bounded under Case 1 for $t \geq 0$.*

Proof: When no fault recovery is invoked one can combine the actuator fault signal $\bar{\mathbf{u}}_j(t)$ as part of the disturbance $\delta(t)$. Consequently, let $\bar{\delta}(t) = \bar{\mathbf{u}}_j(t) + \delta(t)$. Now, consider the expression (4.13) as the positive definite, radially unbounded, ISS-Lyapunov function candidate for the j -th system.

Let $\mathcal{V} \triangleq \sum_{j=1}^m \mathcal{V}_j$ be the ISS-Lyapunov function candidate for the networked EL systems. One can show that the time derivative of the ISS-Lyapunov function candidate \mathcal{V} along the trajectories of the closed-loop system (2.7), (4.5), (4.18), (4.23), (4.24), and (4.25) can be written as

$$\begin{aligned} \dot{\mathcal{V}} \leq & -\frac{1}{4} \sum_{j=1}^m \mathbf{x}_j^T \left[\mathbf{P}_j(\mathbf{x}_j) \bar{\mathfrak{G}}_j(\mathbf{x}_j) \mathbf{R}_j \bar{\mathfrak{G}}_j^T(\mathbf{x}_j) \mathbf{P}_j(\mathbf{x}_j) \right] \mathbf{x}_j \\ & - \frac{1}{2} \sum_{j=1}^m \mathbf{x}_j^T \mathbf{Q}_j \mathbf{x}_j - \frac{1}{4} \sum_{j=1}^m \sum_{n \in \mathcal{N}_j} \mathbf{x}_{jn}^T \mathbf{Q}_{jn} \mathbf{x}_{jn} + \frac{1}{2} \sum_{j=1}^m \bar{\gamma}_j^2 \|\bar{\delta}_j\|^2 \end{aligned} \quad (4.34)$$

The positive definite matrices \mathbf{Q}_j , \mathbf{R}_j , and $\mathbf{Q}_{jn} \forall j \in \mathcal{V}, n \in \mathcal{N}_j$ imply that the first two terms in the right hand side of the inequality (6.16) are \mathcal{K}_∞ function of \mathbf{x}_j and \mathbf{x}_{jn} , respectively. Define the bounded region \mathfrak{B}_r that includes the origin, that is

$$\begin{aligned} \mathfrak{B}_r = & \left\{ \mathbf{x}_j, (\mathbf{x}_j - \mathbf{x}_n) \mid \frac{1}{2} \mathbf{x}_j^T \left[\mathbf{Q}_j + \frac{1}{2} \mathbf{P}_j(\mathbf{x}_j) \bar{\mathfrak{G}}_j(\mathbf{x}_j) \mathbf{R}_j \bar{\mathfrak{G}}_j^T(\mathbf{x}_j) \mathbf{P}_j(\mathbf{x}_j) \right] \mathbf{x}_j \right. \\ & \left. + \frac{1}{4} \sum_{n \in \mathcal{N}_j} \mathbf{x}_{jn}^T \mathbf{Q}_{jn} \mathbf{x}_{jn} \leq \frac{1}{2} \bar{\gamma}_j^2 \|\bar{\delta}_j\|^2 \right\} \end{aligned}$$

For all \mathbf{x}_j and \mathbf{x}_{jn} outside this region we have $\frac{d}{dt} \mathcal{Y} < 0$. Consequently, by invoking Lemma 4.1.1, one can conclude that the closed-loop networked EL system under the distributed control laws (4.5) and (4.25) is ISS and the synchronization and the tracking trajectory errors remain globally ultimately bounded. ■

Lemma 4.4.1 guarantees boundedness of the synchronization and the trajectory tracking errors in presence of a fault. However, in presence of actuator faults and without invoking a controller reconfiguration, this bound may be too large and may exceed the mission specifications (as shown in the simulations in Section 4.5). Therefore, one may need to appropriately adjust the controller to recover the performance of the networked EL systems as described in the next subsection.

4.4.2 Control Reconfiguration Subject to Imperfections in the Fault Identification Module

Consider that Case 3 described in Section 4.4 holds. The purpose of this subsection is to design $\Gamma_j = \text{diag}(\gamma_{1,j}, \dots, \gamma_{k,j}) \in \mathbb{R}^k$ in order to compensate for the effects of the FDI imperfections and actuator faults. Our result is now presented below.

Theorem 4.4.1. *Consider a network of ‘m’ heterogeneous EL systems that are governed by the dynamics (2.7) and subject to the distributed control laws (4.5) and (4.25) for the the j-th system. Given that the conditions in Case 3 hold, let us set $\gamma_{p,j}$ according to,*

$$\gamma_{p,j} = -\text{sgn}(\mathbf{s}_{p,j}) \hat{\mathbf{u}}_{p,j}(t), p \in \{1, \dots, k\}, j \in \{1, \dots, m\} \quad (4.35)$$

where $\hat{\mathbf{u}}_{p,j}(t)$ is an estimate of $\bar{\mathbf{u}}_{p,j}(t)$ and is governed by

$$\dot{\hat{\mathbf{u}}}_{p,j}(t) = \bar{\sigma}_{p,j} \mathbf{s}_{p,j} - \bar{e}_{p,j} [\hat{\mathbf{u}}_{p,j}(t) - \bar{\mathbf{u}}_{p,j}^*(t)] \quad (4.36)$$

where $\bar{\sigma}_{p,j} > 0$, $\bar{\mathbf{u}}_{p,j}^*$ denotes the estimate of the fault severity that is provided by the FDI algorithm, and $\bar{e}_{p,j} > 0$, $p \in \{1, \dots, k\}$ are diagonal elements of the positive definite matrix $\bar{\mathbf{E}}_j \succ 0$. Then under Assumption 4.4.1 and by application of the distributed adaptive control law (4.36) the closed-loop states of the j -th nonlinear EL system, i.e. $\bar{\mathbf{x}}_j = [\bar{\mathbf{x}}_j^T \ \bar{\mathbf{u}}_j^T]^T$, with $\bar{\mathbf{u}}_j = \hat{\mathbf{u}}_j - \bar{\mathbf{u}}_j$ remain globally bounded under Case 3 for all $t \geq 0$.

Proof: The time derivative of the estimation error $\tilde{\mathbf{u}}_{p,j}(t)$ defined as $\tilde{\mathbf{u}}_{p,j}(t) = \hat{\mathbf{u}}_{p,j}(t) - \bar{\mathbf{u}}_{p,j}(t)$, along the trajectories of (4.36) is given by

$$\begin{aligned} \dot{\tilde{\mathbf{u}}}_{p,j}(t) &= \dot{\hat{\mathbf{u}}}_{p,j}(t) - \dot{\bar{\mathbf{u}}}_{p,j}(t) \\ &= \bar{\sigma}_{p,j} \mathbf{s}_{p,j} - \bar{e}_j [\hat{\mathbf{u}}_{p,j}(t) - \bar{\mathbf{u}}_{p,j}^*(t)] - \dot{\bar{\mathbf{u}}}_{p,j}(t) \\ &= \bar{\sigma}_{p,j} \mathbf{s}_{p,j} - \bar{e}_j \tilde{\mathbf{u}}_{p,j}(t) + \bar{e}_j [\bar{\mathbf{u}}_{p,j}^*(t) - \bar{\mathbf{u}}_{p,j}(t)] - \dot{\bar{\mathbf{u}}}_{p,j}(t) \end{aligned}$$

Consider the following positive definite radially unbounded function as the ISS-Lyapunov function candidate for the closed-loop networked EL system

$$\mathcal{W}(\bar{\mathbf{x}}_j) = \sum_{j=1}^m \left[\mathcal{Y}_j(\mathbf{x}_j) + \sum_{p=1}^k \frac{1}{2\bar{\sigma}_{p,j}} \tilde{\mathbf{u}}_{p,j}^2 \right] \quad (4.37)$$

where $\bar{\mathbf{x}}_j = [\bar{\mathbf{x}}_j^T, \bar{\mathbf{u}}_j^T]^T$ and $\mathcal{Y}_j(\mathbf{x}_j)$ is given by (4.13) and

$$\mathbf{P}_j(\mathbf{x}_j) = \begin{bmatrix} \bar{\bar{\mathbf{K}}}_j \mathbf{D}_j \bar{\bar{\mathbf{K}}}_j + \bar{\bar{\mathbf{K}}}_j \bar{\mathbf{K}}_j \mathbf{K}_j & \bar{\bar{\mathbf{K}}}_j \mathbf{D}_j \bar{\mathbf{K}}_j + \bar{\bar{\mathbf{K}}}_j \mathbf{K}_j & \bar{\bar{\mathbf{K}}}_j \mathbf{D}_j \\ \bar{\bar{\mathbf{K}}}_j \mathbf{D}_j \bar{\bar{\mathbf{K}}}_j + \bar{\bar{\mathbf{K}}}_j \mathbf{K}_j & \bar{\bar{\mathbf{K}}}_j \mathbf{D}_j \bar{\mathbf{K}}_j + \bar{\bar{\mathbf{K}}}_j \mathbf{K}_j & \bar{\bar{\mathbf{K}}}_j \mathbf{D}_j \\ \mathbf{D}_j \bar{\bar{\mathbf{K}}}_j & \mathbf{D}_j \bar{\mathbf{K}}_j & \mathbf{D}_j \end{bmatrix} \quad (4.38)$$

where $\mathbf{P}_j(\mathbf{x}_j)$ is a positive definite matrix provided that the conditions (4.26), (4.27), and (4.28) are satisfied. This essentially implies that there exist positive scalars k_0 and \bar{k}_0 such that $k_0 \|\bar{\mathbf{x}}_j\|^2 \leq \mathcal{W}(\bar{\mathbf{x}}_j) \leq \bar{k}_0 \|\bar{\mathbf{x}}_j\|^2$. Therefore, $\mathcal{W}(\bar{\mathbf{x}}_j)$ is a positive definite radially unbounded function.

The time derivative of the ISS-Lyapunov function candidate along the trajectories of the closed-loop system is obtained as,

$$\begin{aligned}
\frac{d}{dt} \mathcal{W} &= \sum_{j=1}^m \left[\frac{\partial \mathcal{Y}_j}{\partial \mathbf{x}_j} \tilde{\mathfrak{F}}_j(\mathbf{x}_j) \mathbf{x}_j + \frac{\partial \mathcal{Y}_j}{\partial \mathbf{x}_j} \tilde{\mathfrak{G}}_j(\mathbf{x}_j) \boldsymbol{\tau}_j + \frac{\partial \mathcal{Y}_j}{\partial \mathbf{x}_j} \tilde{\mathfrak{G}}_j(\mathbf{x}_j) \boldsymbol{\delta}_j + \tilde{\mathbf{u}}_j^T \bar{\Sigma}_j^{-1} \dot{\tilde{\mathbf{u}}}_j \right] \\
&= \sum_{j=1}^m \left[\frac{1}{2} \mathbf{x}_j^T [\mathbf{P}_j(\mathbf{x}_j) + \mathbf{P}_j(\mathbf{x}_j) \tilde{\mathfrak{F}}_j(\mathbf{x}_j) + \tilde{\mathfrak{F}}_j^T(\mathbf{x}_j) \mathbf{P}_j(\mathbf{x}_j)] \mathbf{x}_j + \mathbf{x}_j^T \mathbf{P}_j(\mathbf{x}_j) \tilde{\mathfrak{G}}_j(\mathbf{x}_j) \boldsymbol{\tau}_j \right. \\
&\quad \left. + \mathbf{x}_j^T \mathbf{P}_j(\mathbf{x}_j) \tilde{\mathfrak{G}}_j(\mathbf{x}_j) \boldsymbol{\delta}_j + \tilde{\mathbf{u}}_j^T \bar{\Sigma}_j^{-1} \dot{\tilde{\mathbf{u}}}_j \right] \\
&\leq -\frac{1}{4} \sum_{j=1}^m \mathbf{x}_j^T \mathbf{P}_j \tilde{\mathfrak{G}}_j \mathbf{R}_j^{-1} \tilde{\mathfrak{G}}_j^T \mathbf{P}_j \mathbf{x}_j - \frac{1}{2} \sum_{j=1}^m \mathbf{x}_j^T \mathbf{Q}_j \mathbf{x}_j - \frac{1}{4} \sum_{j=1}^m \sum_{n \in \mathcal{N}_j} \mathbf{x}_{jn}^T \mathbf{Q}_{jn} \mathbf{x}_{jn} \\
&\quad - \sum_{j=1}^m \tilde{\mathbf{u}}_j^T \bar{\Sigma}_j^{-\frac{1}{2}} \bar{\mathbf{E}}_j \bar{\Sigma}_j^{-\frac{1}{2}} \tilde{\mathbf{u}}_j + \sum_{j=1}^m \tilde{\mathbf{u}}_j^T \bar{\Sigma}_j^{-\frac{1}{2}} \bar{\mathbf{E}}_j \bar{\Sigma}_j^{-\frac{1}{2}} (\bar{\mathbf{u}}_j^* - \bar{\mathbf{u}}_j) \\
&\quad - \sum_{j=1}^m \tilde{\mathbf{u}}_j^T \bar{\Sigma}_j^{-1} \dot{\tilde{\mathbf{u}}}_{p,j} + \sum_{j=1}^m \|s_j\| \|\boldsymbol{\delta}_j\|
\end{aligned} \tag{4.39}$$

where $\bar{\Sigma}_j = \text{diag}(\bar{\sigma}_{1,j}, \dots, \bar{\sigma}_{k,j}) \in \mathbb{R}^k$. Consequently, we obtain,

$$\begin{aligned}
\frac{d}{dt} \mathcal{W} &\leq -\frac{1}{4} \sum_{j=1}^m \mathbf{x}_j^T \mathbf{P}_j \tilde{\mathfrak{G}}_j \mathbf{R}_j \tilde{\mathfrak{G}}_j^T \mathbf{P}_j \mathbf{x}_j - \frac{1}{2} \sum_{j=1}^m \mathbf{x}_j^T \mathbf{Q}_j \mathbf{x}_j - \frac{1}{4} \sum_{j=1}^m \sum_{n \in \mathcal{N}_j} \mathbf{x}_{jn}^T \mathbf{Q}_{jn} \mathbf{x}_{jn} \\
&\quad - \sum_{j=1}^m \tilde{\mathbf{u}}_j^T \bar{\Sigma}_j^{-\frac{1}{2}} \bar{\mathbf{E}}_j \bar{\Sigma}_j^{-\frac{1}{2}} \tilde{\mathbf{u}}_j + \sum_{j=1}^m \tilde{\mathbf{u}}_j^T \bar{\Sigma}_j^{-\frac{1}{2}} \bar{\mathbf{E}}_j \bar{\Sigma}_j^{-\frac{1}{2}} (\bar{\mathbf{u}}_j^* - \bar{\mathbf{u}}_j) \\
&\quad - \sum_{j=1}^m \tilde{\mathbf{u}}_j^T \bar{\Sigma}_j^{-1} \dot{\tilde{\mathbf{u}}}_{p,j} + \sum_{j=1}^m \|s_j\| \|\boldsymbol{\delta}_j\|
\end{aligned} \tag{4.40}$$

which implies that there exists constant positive scalars k_i , $i \in \{1, \dots, 8\}$, such that

$$\begin{aligned} \frac{d}{dt} \mathcal{W} &\leq \sum_{j=1}^m \left[-k_1 \|\mathbf{x}_j\|^2 - k_2 \|\tilde{\mathbf{u}}_j\|^2 - k_3 \|\mathbf{x}_{jn}\|^2 + k_4 \|\tilde{\mathbf{u}}_j\| \|\tilde{\mathbf{u}}_j^* - \tilde{\mathbf{u}}_j\| \right. \\ &\quad \left. + k_5 \|\tilde{\mathbf{u}}_j\| \|\dot{\tilde{\mathbf{u}}}_j\| + k_6 \|\delta_j\|^2 \right] \\ &\leq \sum_{j=1}^m \left[-k_7 \|\bar{\mathbf{x}}_j\|^2 + k_5 \|\bar{\mathbf{x}}_j\| \|\dot{\tilde{\mathbf{u}}}_j\| + k_8 \|\bar{\mathbf{x}}_j\| \|\bar{\mathbf{v}}_j\| \right] \end{aligned}$$

where $\|\bar{\mathbf{v}}_j\| = \|\tilde{\mathbf{u}}_j^* - \tilde{\mathbf{u}}_j\| + \|\delta_j\|^2$. Consequently,

$$k_0 \sum_{j=1}^m \frac{d}{d\xi} \|\bar{\mathbf{x}}_j\|^2 \leq -k_7 \sum_{j=1}^m \|\bar{\mathbf{x}}_j\|^2 + k_5 \sum_{j=1}^m \|\bar{\mathbf{x}}_j\| \|\dot{\tilde{\mathbf{u}}}_j\| + k_8 \sum_{j=1}^m \|\bar{\mathbf{x}}_j\| \|\bar{\mathbf{v}}_j\|$$

Therefore, when $\|\bar{\mathbf{x}}_j\| \neq 0$ one obtains,

$$\sum_{j=1}^m \frac{d}{d\xi} \|\bar{\mathbf{x}}_j\| \leq -\frac{k_7}{k_0} \sum_{j=1}^m \|\bar{\mathbf{x}}_j\| + \frac{k_5}{k_0} \sum_{j=1}^m \|\dot{\tilde{\mathbf{u}}}_j\| + \frac{k_8}{k_0} \sum_{j=1}^m \|\bar{\mathbf{v}}_j\|$$

By integrating the above inequality we obtain

$$\begin{aligned} \sum_{j=1}^m \|\bar{\mathbf{x}}_j(t)\| &\leq \sum_{j=1}^m \|\bar{\mathbf{x}}_j(0)\| e^{-\frac{k_7}{k_0} t} + \sum_{j=1}^m \int_0^t \frac{k_5}{k_0} e^{\frac{k_7}{k_0} \xi} \|\dot{\tilde{\mathbf{u}}}_j(\xi)\| d\xi \\ &\quad + \sum_{j=1}^m \int_0^t \frac{k_8}{k_0} e^{\frac{k_7}{k_0} \xi} \|\bar{\mathbf{v}}_j\| d\xi \\ &\leq \sum_{j=1}^m \|\bar{\mathbf{x}}_j(0)\| e^{-\frac{k_7}{k_0} t} + k_9 + \frac{k_8}{k_7} \sum_{j=1}^m \bar{\mathbf{v}}_{j,0} \end{aligned} \tag{4.41}$$

where $\bar{\mathbf{v}}_{j,0} = \sup_{t \geq 0} \|\bar{\mathbf{v}}_j\|$ and $k_9 = \sum_{j=1}^m \int_0^t \frac{k_5}{k_0} e^{\frac{k_7}{k_0} \xi} \|\dot{\tilde{\mathbf{u}}}_j(\xi)\| d\xi$. Assumption 4.4.2 implies that $\bar{\mathbf{v}}_{j,0} < \infty$. Consequently, in view of Assumption 4.4.1 one can conclude that the states of the j -th closed-loop system, $\bar{\mathbf{x}}_j(t)$, are globally uniformly bounded.

This completes the proof of the theorem. ■

The overall distributed adaptive control law can be written in the following form,

$$\begin{aligned} \mathbf{u}_j = & \mathbf{D}_j(\mathbf{q}_j)\dot{\mathbf{r}}_j + \mathbf{C}_j(\mathbf{q}_j, \dot{\mathbf{q}}_j)\mathbf{r}_j + g_j(\mathbf{q}_j) - \frac{1}{2}\mathbf{s}_j^T \left(\mathbf{K}_j - \frac{\alpha_j}{\tilde{\gamma}_j^2} \mathcal{J}_3 \right) \mathbf{s}_j \\ & - \frac{\alpha_j}{4} \mathbf{s}_{jn}^T \mathbf{K}_j \sum_{n \in \mathcal{N}_j} \frac{1}{|\mathcal{N}_j|} \mathbf{s}_{jn} - \text{sgn}(\mathbf{s}_j)^T \hat{\mathbf{u}}_j(t) \end{aligned} \quad (4.42)$$

with

$$\hat{\mathbf{u}}_j(t) = \bar{\Sigma}_j \mathbf{s}_j - \bar{\mathbf{E}}_j [\hat{\mathbf{u}}_j(t) - \bar{\mathbf{u}}_j^*(t)] \quad (4.43)$$

where $\bar{\mathbf{u}}_j^*(t)$ is an estimate of $\bar{\mathbf{u}}_j(t)$ provided by the FDI module.

4.4.3 Control Reconfiguration Subject to Imperfections in the Fault Isolation Module

In presence of an imperfection in the fault isolation, the controller is reconfigured according to (4.42) and (4.43) but for an incorrect agent or an incorrect input channel. The stability of the networked EL system, however, can still be guaranteed. Our specific result is now given in the following lemma.

Lemma 4.4.2. *Consider a network of ‘m’ heterogeneous EL systems that are governed by the dynamics (2.7) and subject to (4.5) and (4.25) for the j-th system. Let conditions of Case 2 hold. For the p-th input channel of the j-th agent, which is fault-free, let us set $\gamma_{p,j}$ according to (4.35) and let the time derivative of $\hat{\mathbf{u}}_{p,j}(t)$ be chosen according to (4.36), where $\bar{\sigma}_{p,j} > 0$, and $\bar{e}_{p,j} > 0$, $p \in \{1, \dots, k\}$ are diagonal elements of the positive definite matrix $\bar{\mathbf{E}}_j \succ 0$. Then under Assumption 4.4.1 and by application of the distributed adaptive control law the closed-loop system*

states of the j -th nonlinear EL system, i.e. $\bar{\mathbf{x}}_j = [\mathbf{x}_j^T \tilde{\mathbf{u}}_j^T]^T$, remain globally bounded under Case 2 for all $t \geq 0$.

Proof: The proof is straightforward and can be carried out similar to the proofs of Lemma 4.4.1 and Theorem 4.4.1, and is therefore omitted. ■

Remark 4.4.1. The discontinuity of the distributed adaptive control law (4.42) can cause complications for the numerical solvers in performing simulations. It also can lead to chattering phenomenon of the system (high-frequency actuation and vibration) in practice. This chattering is due to the fact that the variables s_j are never exactly zero in control calculations. Therefore, the discontinuous term keeps switching from a small positive s_j to a small negative s_j . To avoid chattering, a saturation function can replace the sign function in the control law (4.42). The saturation function is continuous around the surface $s_j = 0$, which allows s_j to smoothly converge to a neighborhood of origin.

4.5 Simulation Studies: Distributed Control of Networked Spacecraft

4.5.1 Robust Distributed Control of Networked Spacecraft

In this section, our proposed distributed control strategy is applied to attitude synchronization for the spacecraft formation flying problem. As discussed in Section 2.3.2, the 3-degrees of freedom (DOF) attitude dynamics of a spacecraft can be written in the form of (2.7).

We consider three communication graphs as depicted in Fig. 4.1 with 8 spacecraft. Note that all the three networks are strongly connected and the connections

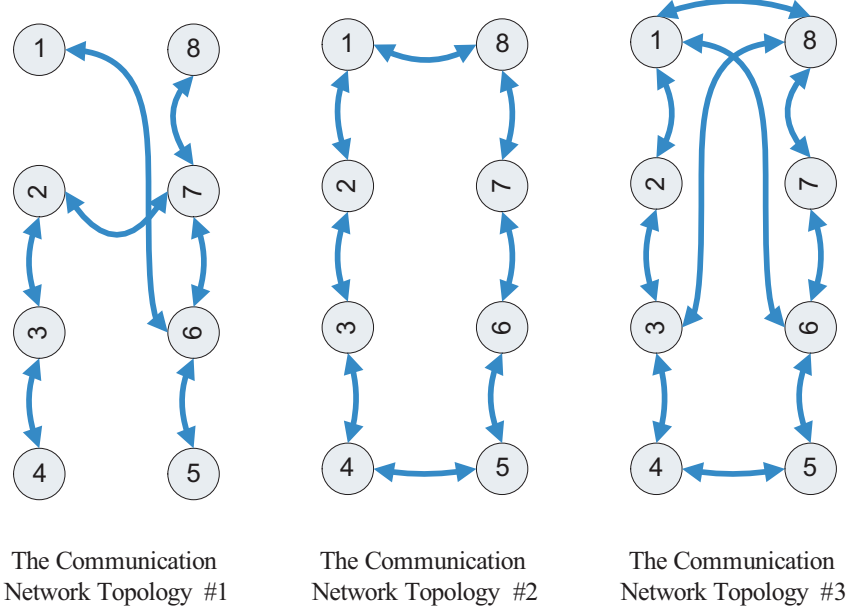


Figure 4.1: The three communication network graphs considered in the simulations.

are bi-directional. Furthermore, we randomly switch among the three communication graphs every 10 seconds.

For simulations we set $\bar{\gamma}_{j,i} = 0.6$, $\alpha_{j,i} = 0.86$, $\forall j \in \{1, \dots, 8\}, i \in \{1, 2, 3\}$. In addition, in view of (4.26) and (4.27) the distributed controller (4.32) gains are selected as: $\mathbf{K}_j = 20\mathcal{J}_3$, $\bar{\mathbf{K}}_j = 0.4\mathcal{J}_3$, and $\bar{\mathbf{K}}_j = 0.02\mathcal{J}_3$. This studies in the following parameters for the j -th EL system, namely, $\mathbf{R}_{j,i} = 13.75\mathcal{J}_3$, $\sum_{n \in \mathcal{N}_j} \mathbf{Q}_{jn,i} = \text{diag}([5.5e-3, 5.5e-3, 5.5e-3, 2.2, 2.2, 2.2, 13.75, 13.75, 13.75])$, and $\mathbf{Q}_{j,i} = \text{diag}([2.5e-3, 2.5e-3, 2.5e-3, 0.2, 0.2, 0.2, 6.25, 6.25, 6.25])$. The above selection of the controller gains puts more emphasis on the state synchronization specification of the spacecraft attitudes and their attitude rates and considerably less emphasis on the state regulation specification. Our desired objective is to keep the spacecraft states in the close to zero. Note that depending on the mission requirements by selecting proper controller gains one can put more weight on attitude regulation as compared to attitude synchronization.

In all of the simulation scenarios the initial attitudes of the spacecraft are selected randomly between zero to 60 degrees and the disturbance $\delta_j(t)$ is considered to be a Rayleigh distributed noise with the fading envelope of 0.09 and sampling time of 0.5 seconds.

In the first part of the simulation results in this subsection, we consider $\pm 10\%$ uncertainty in the inertia matrices of the 8 spacecraft in the network. The spacecraft attitudes with the above-mentioned initial conditions and disturbances are depicted in Fig. 4.2 for the first 200 seconds. The corresponding attitude rates are depicted in Fig. 4.3.

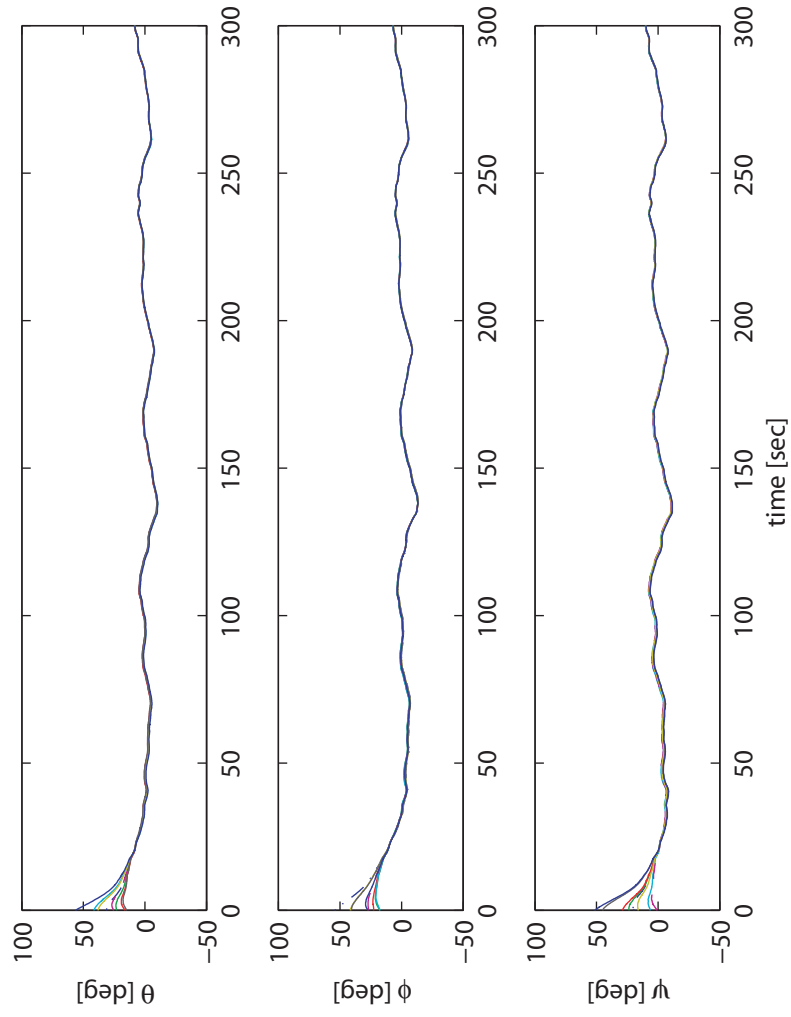


Figure 4.2: Spacecraft attitudes under the distributed control law (4.32) for the first 300 seconds.

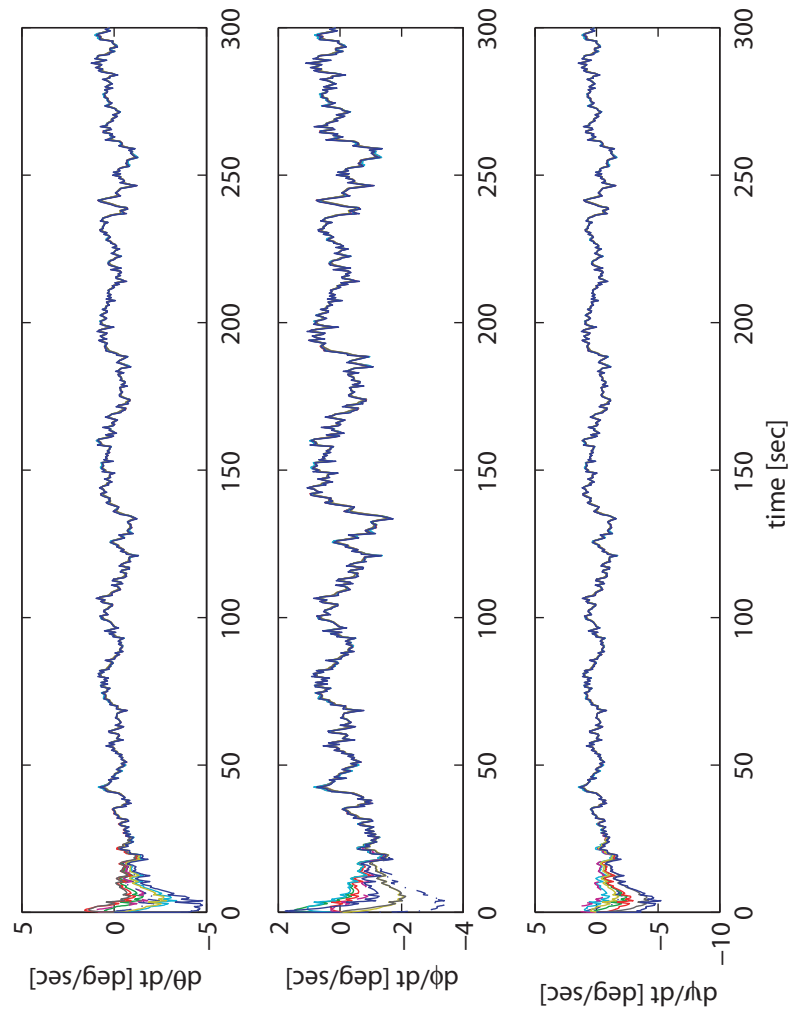


Figure 4.3: Spacecraft attitude rates under the distributed control law (4.32) for the first 300 seconds.

Table 4.1: The mean values for the control efforts for spacecraft #1 under the controllers (4.5) and (4.25) versus the controller in [63] for the first 200 seconds.

	u_1 [N.m]	u_2 [N.m]	u_3 [N.m]
W/ 10% uncertainty in \mathbf{J}_j	-0.3494	-0.3416	-0.3399
W/ 50% uncertainty in \mathbf{J}_j	-0.3494	-0.3414	-0.3407
Equation (7) in [63]	-0.3495	-0.3417	-0.3459

Table 4.2: The mean values for the state synchronization errors for spacecraft #1 under the controllers (4.5) and (4.25) versus the controller in [63] for the first 200 seconds.

	$q_1(\theta)$	$q_2(\phi)$	$q_3(\psi)$
W/ 10% uncertainty in \mathbf{J}_j	6.1940	5.4541	6.0248
W/ 50% uncertainty in \mathbf{J}_j	8.6281	8.3233	7.6036
Equation (7) in [63]	9.8578	10.0208	9.4797

One can conclude from Figs. 4.2 and 4.3 that the state synchronization is achieved by using our proposed robust controller in presence of parameter uncertainties and external disturbances.

In the second part of the simulations in this subsection, we compare the performance of our proposed distributed controllers (4.5) and (4.25) without switchings in the communication network topologies with the distributed controller that is proposed in [63] (see (7) in [63]), which does not require the numerical values of the matrices \mathbf{D}_j and \mathbf{C}_j . In order to make the comparison fair, the controller gains are selected such that the mean values of the control efforts for both controllers are almost the same under the communication network topology #1 (cf. Table 4.1) over 10 simulation runs. The mean values for the state synchronization errors for spacecraft #1 are provided in Table 4.2 over 10 simulation runs. The results in this table show that our proposed distributed controller produces lower state synchronization errors.

Table 4.3: The mean values for the state synchronization errors for spacecraft #1 under the controllers (4.5) and (4.32) versus the controller in [62] for the first 200 seconds.

	$\mathbf{q}_1(\theta)$	$\mathbf{q}_2(\phi)$	$\mathbf{q}_3(\psi)$
W/ 50% uncertainty in \mathbf{J}_j	7.1742	7.5310	6.9247
Equation (3.23) in [62]	10.4092	11.2602	12.0256

Finally, we would like to compare the performance of our proposed robust distributed controller with the distributed controller that proposed in [62] (refer to equation (3.23) in [62]) with *switchings* in the communication network topologies. In order to make the comparison fair, the controller gains are selected such that the mean values for the control efforts for both controllers are almost the same for the spacecraft #1 over corresponding to 10 simulation runs. The mean values for the state synchronization errors for the spacecraft #1 are provided in Table 4.3. The results in this table show that our proposed distributed controller produces lower state synchronization errors.

4.5.2 Distributed Robust Reconfigurable Control of Networked Spacecraft

In this subsection, we demonstrate the performance of our proposed reconfigurable control strategy in presence of actuator faults for the spacecraft formation flying missions.

In the simulations in this subsection, we set $\gamma_j = 0.6$, $\alpha_j = 0.86$, $\forall j \in \{1, \dots, 8\}$. In addition, in view of (4.26), (4.27), and (4.28) the distributed controllers (4.42) and (4.43) gains are selected as: $\mathbf{K}_j = 20\mathcal{J}_3$, $\bar{\mathbf{K}}_j = 0.16\mathcal{J}_3$, and $\bar{\bar{\mathbf{K}}}_j = 0.001\mathcal{J}_3$. This

results in the following parameters for the j -th EL system, namely, $\mathbf{R}_j = 17.22\mathbf{I}_3$

$$\sum_{n \in \mathcal{N}_j} \mathbf{Q}_{jn} = \text{diag}([0.17e-4, 0.17e-4, 0.17e-4, 0.44, 0.44, 0.44, 17.22, 17.22, 17.22])$$

and $\mathbf{Q}_j = \text{diag}([0.27e-5, 0.27e-5, 0.27e-5, 0.031e-3, 0.031e-3, 0.031e-3, 2.78, 2.78, 2.78])$. The above selection of the controller gains imposes more emphasis on the synchronization of the spacecraft attitudes and their attitude rates and considerably less emphasis on the state regulation. Our desired objective is to keep the spacecraft attitude states close to the origin. Note that depending on the mission requirements by selecting proper controller gains one can put more weight on attitude regulation as compared to attitude synchronization. This is a trade-off and the choice made by the designer.

In this subsection, we assume that the inertia matrix of the spacecraft in the network is known within a $\pm 10\%$ accuracy, i.e. $\mathbf{J}_j = \hat{\mathbf{J}}_j \pm 0.10\hat{\mathbf{J}}_j$, where \mathbf{J}_j is the actual spacecraft inertia matrix and $\hat{\mathbf{J}}_j$ is its nominal value. The disturbance $d(t)$ is considered to be a Gaussian distributed noise with the mean value of zero and variance of 0.001. The initial attitudes of the spacecraft are selected randomly between zero to 60 degrees.

An additive actuator fault occurs in the third input channel of the first spacecraft, i.e. $\bar{u}_{1,3}(t) = 0.05 \sin(0.02t) + 0.6$ for $40 \leq t \leq 240$. The fault and its estimate, which is provided by a typical FDI algorithm (which is beyond the scope of this work) are depicted in Fig. 4.4. One can observe from this figure that there exists an error in the fault identification by the FDI algorithm.

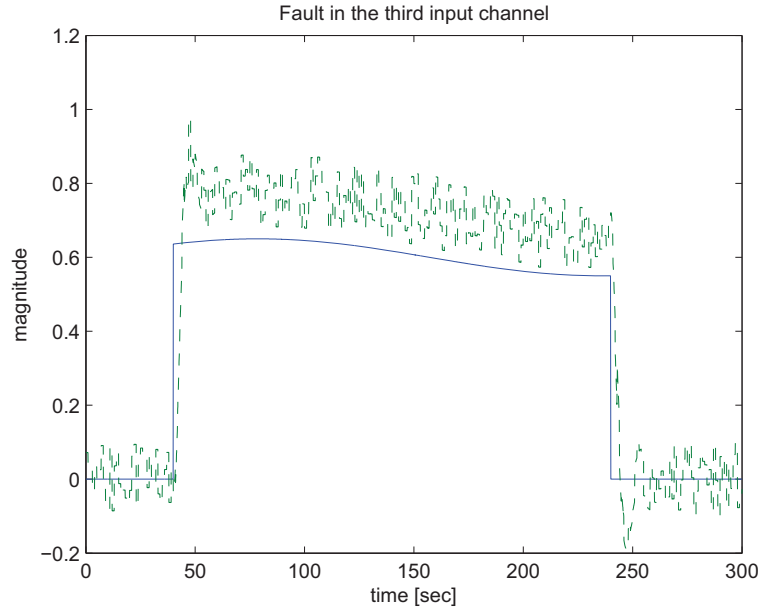


Figure 4.4: Fault magnitude in the third input channel of the spacecraft # 1 (blue line) versus its estimate obtained from the FDI algorithm (dashed green line).

Distributed Control of Spacecraft Formation Subject to Imperfections in the Fault Detection Module and without Controller Reconfiguration

In the first part of our simulation results we assume imperfections in the fault detection module where the controller is *not* reconfigured in presence of the actuator fault, i.e. $\Gamma_j(t) = 0, \forall j \in 1, \dots, 8, t \geq 0$. Attitudes of the spacecraft in this scenario are shown in Fig. 4.5 for the first 300 seconds.

Fig. 4.5 shows that without controller reconfiguration the attitude synchronization is not achieved. However, in view of the fact that the proposed controller is robust to input disturbances and actuator faults (refer to Lemma 4.4.1), the states remain bounded and stable.

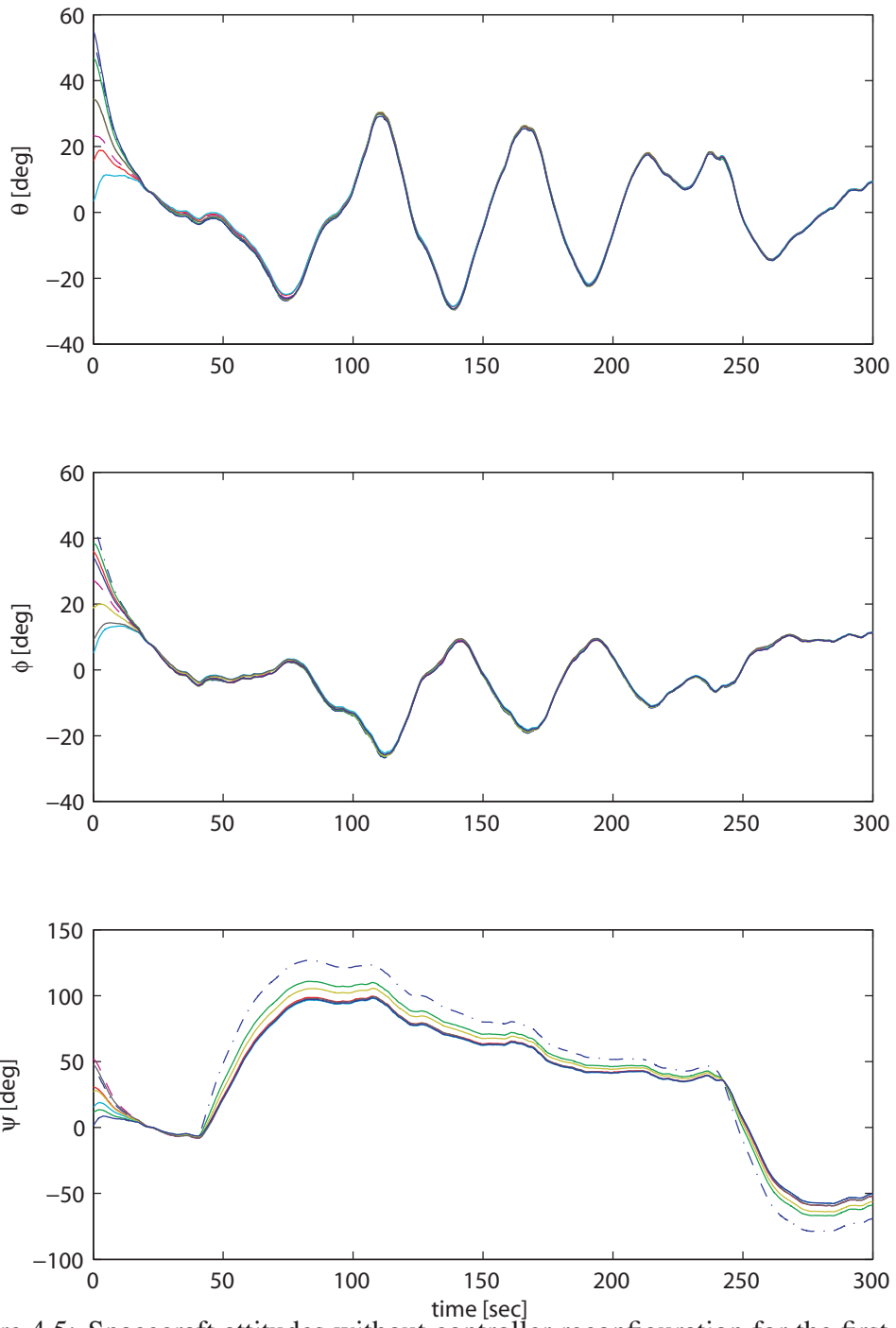


Figure 4.5: Spacecraft attitudes without controller reconfiguration for the first 300 seconds. The dash-dotted line represents the spacecraft # 1.

Distributed Control of Spacecraft Formation with Controller Reconfiguration Subject to Imperfections in the Fault Identification Module

In this part of simulations we assume that the adaptive reconfiguration part of the controller is present. The parameters of the controller (4.42) and (4.43) are selected as: $\bar{\Sigma}_j = 0.5\mathfrak{J}_3$ and $\bar{\mathbf{E}}_j = \mathfrak{J}_3$. Furthermore, it is assumed that it takes 5 seconds for the FDI algorithm to detect the fault and activates the controller reconfiguration.

Fig. 4.6 depicts the attitudes of the eight spacecraft in the formation under the distributed adaptive control laws (4.42) and (4.43) for the first 300 seconds. By comparing Fig. 4.6 with Fig. 4.5 one notices a great improvement in the synchronization and tracking performance of the closed-loop networked EL systems. Specifically, the synchronization error is considerably decreased by employing the adaptive controller. In addition, the attitudes are closer to zero when compared with those obtained in Fig. 4.5.

Distributed Control of Spacecraft Formation with Controller Reconfiguration Subject to Imperfections in the Fault Isolation Module

In the last part of our simulation results we consider imperfections in the fault isolation module. Specifically, we assume that the FDI algorithm detects the fault, however, it incorrectly reconfigures the second input channel of the first spacecraft.

Attitudes of the networked eight spacecraft are shown in Fig. 4.7. By comparing the results presented in Fig. 4.6 with those of Fig. 4.7 the degradations in the synchronization of the roll angle, $\phi(t)$ can be observed. This is in addition to the performance degradations in the third channel, ψ . This, however, confirms our analysis (refer to Lemma 4.4.2) which guarantees boundedness of the closed-loop signals in presence of imperfections in the fault isolation module.

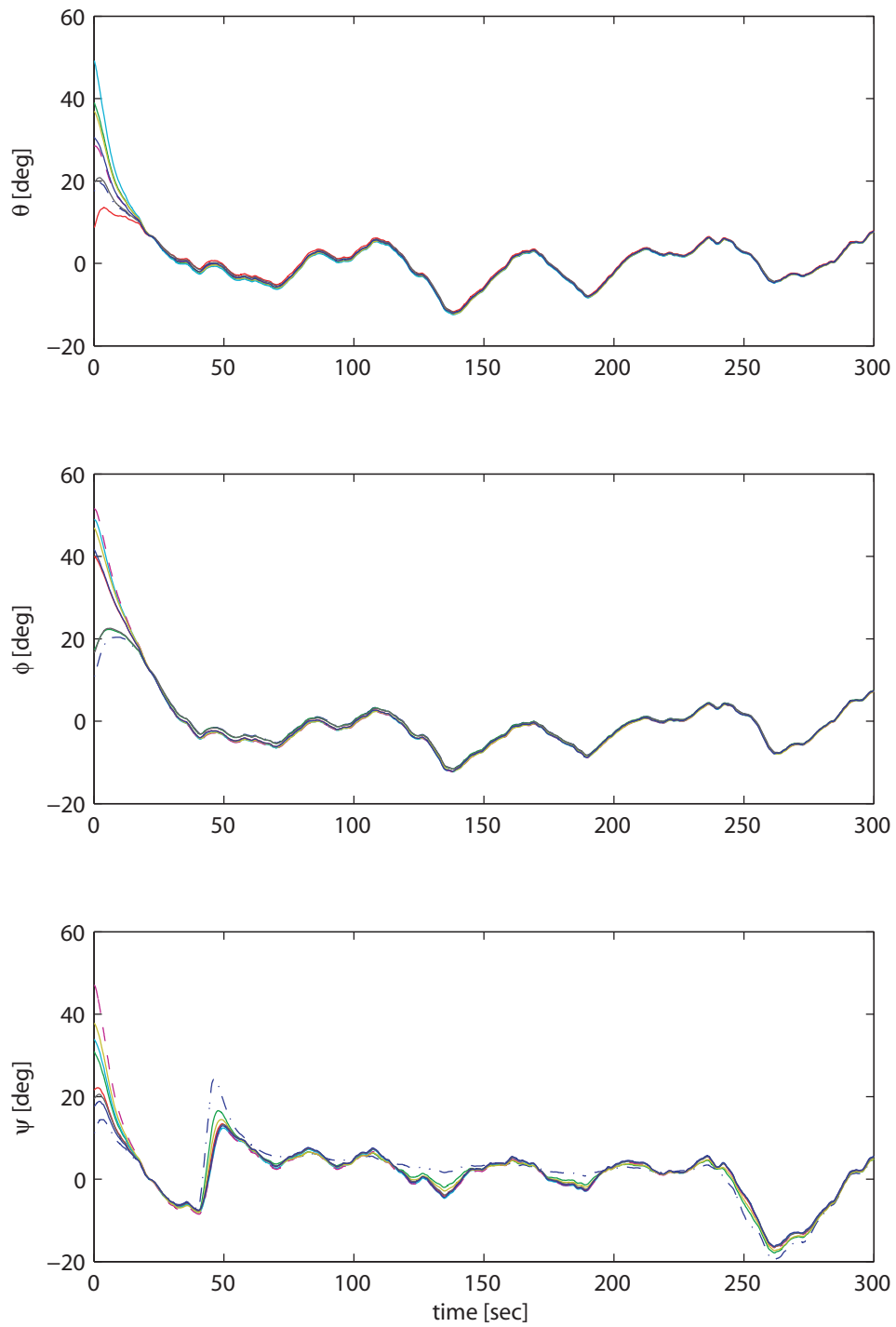


Figure 4.6: Spacecraft attitudes with the the controller reconfiguration for the first 300 seconds subject to imperfection in the fault identification. The dash-dotted line represents the spacecraft # 1.

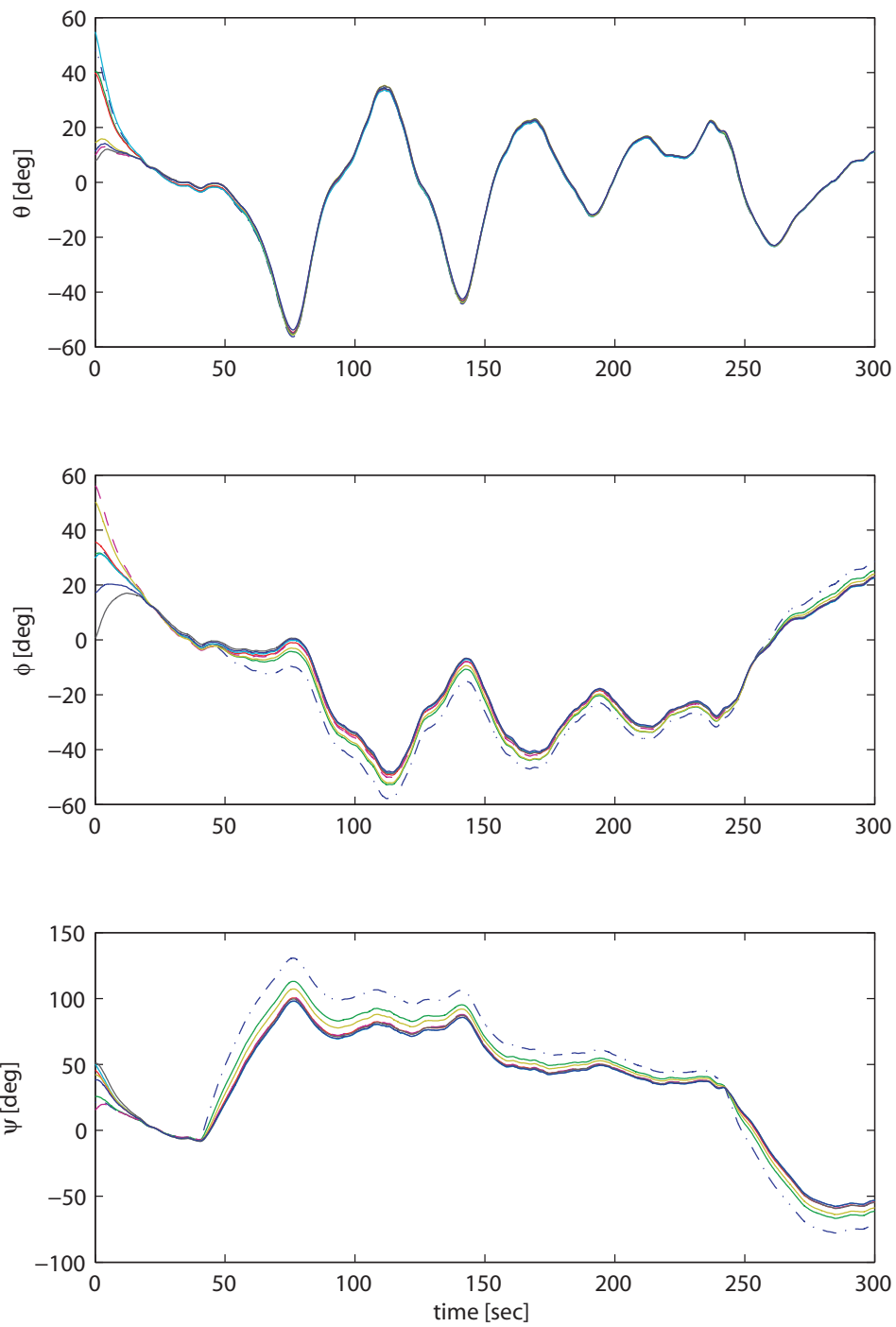


Figure 4.7: Spacecraft attitudes with the controller reconfiguration for the first 300 seconds subject to imperfection in the fault isolation. The dash-dotted line represents the spacecraft # 1.

In other words, despite the incorrect application of the controller reconfiguration to a healthy actuator and no controller reconfiguration to a faulty actuator, the overall closed-loop networked EL system still remains stable.

4.6 Concluding Remarks

This chapter provided formal development of distributed state synchronization and tracking control laws for nonlinear Euler-Lagrange (EL) systems by employing H_∞ control techniques, in presence of parametric uncertainty and external disturbances by using only local information. Next, formal extension of the developed distributed adaptive state synchronization and set-point tracking control laws for nonlinear Euler-Lagrange (EL) systems for three types of FDI imperfections in actuator faults are discussed. It is shown that in presence of actuator faults, our proposed distributed control algorithm has the capability of compensating for the fault and taking proper controller reconfiguration actions.

Chapter 5

Constrained Synchronization

Control of Networked

Euler-Lagrange Systems

5.1 Introduction and Problem Statement

Our first main objective in this chapter is to design synchronization and set-point tracking control for a network of multi-agent EL systems by taking into account constraints on the control input and also by using partial state feedback. In actuality, there are always constraints on the maximum input an actuator can produce, and these constraints should ideally be taken into account in the design of control laws. Furthermore, availability of full state measurements and a fixed communication network topology cannot be guaranteed at all times for networked nonlinear EL systems. Therefore, we first develop a bounded distributed synchronization (or consensus seeking) and set-point tracking controllers with full state feedback. It is

shown that boundedness of the control effort is guaranteed independent of the initial conditions and for all times. Our next contribution in this chapter is concerned with the design of distributed output feedback (i.e. without full state feedback) controllers for synchronization and set-point tracking of networked EL systems.

Our third main objective is to design a reconfigurable controller for multi-agent EL system in presence of actuator saturation faults. Finally, our last objective of this chapter is to present a switching-based control reconfiguration strategy that is utilized in case of an actuator fault or an actuator saturation constraint to accomplish cooperative control of EL systems. Towards this end, we first introduce a class of distributed controllers (denoted as constrained *nominal* controller) that can be used for accomplishing cooperative state synchronization and set-point tracking control objectives. We then introduce a class of distributed constrained controllers (denoted as constrained *reconfigured* controller) that can be used to maintain the overall control objectives of the EL systems in presence of actuator faults and actuator constraints. Finally, we introduce a procedure that can be employed to switch between the two distributed constrained controllers (namely, the constrained *nominal* and the constrained *reconfigured* controllers). In presence of actuator faults and actuator saturations, a switching mechanism is introduced to provide a reconfigurable controller for the networked EL systems to ensure and maintain the overall mission objectives and requirements.

5.1.1 Communication Network Topology

The communication network topology considered in this chapter is defined according to Definition 3.1.1. In addition, we let the position synchronization error between the j -th and the n -th EL system agents be represented by (3.1). We assume

in this chapter that the desired constant position for the networked EL systems, \mathbf{q}^* , is available to only the first ‘ l ’ EL systems in the network, which are denoted as the *leaders*. The EL systems that do not receive the desired coordinates information are denoted as the *followers*, i.e. agent 1 to l are the leaders and agent ‘ $l + 1$ ’ to ‘ m ’ are followers. Consequently, the set-point tracking error for the leader is defined according to (3.3) and for the follower is defined according to (3.4).

5.1.2 Statement of the Problem

Consider a network of ‘ m ’ multiple heterogeneous nonlinear EL systems with a set of ‘ h ’ communication graphs as per Definition 3.1.1. The j -th EL system in the network, $j \in \mathcal{V}$, is governed by the dynamic equation (2.7) with $\delta(t) = 0$. Our objective is to design and develop distributed nonlinear control laws which can guarantee state synchronization of the networked EL systems as well as position tracking. In other words, we employ nonlinear control techniques to develop distributed control laws which guarantee the following requirements: (r1) stability of the closed-loop networked EL systems, (r2) synchronization of the EL system coordinates (which is also denoted as the consensus seeking or the formation-keeping), that is $\mathbf{q}_{jn} \rightarrow 0$ and $\dot{\mathbf{q}}_{jn} \rightarrow 0$ as $t \rightarrow \infty$, and (r3) tracking of the desired position by the networked EL systems (which is also denoted as the station-keeping), i.e. $\tilde{\mathbf{q}}_j \rightarrow 0$ and $\dot{\tilde{\mathbf{q}}}_j \rightarrow 0$ as $t \rightarrow \infty$. The above requirements will guarantee that the EL systems reach, at the steady-state, to the same relative posture. The controller that guarantees the requirements (r1) and (r2) is denoted as the *formation-keeping controller* and the controller that guarantees the requirements (r1) and (r3) is denoted as the *station-keeping controller*.

The constraints that we consider for the development of our control laws are

as follows: (c1) the communication network topology is *not* fixed and is *switching*, (c2) the EL systems parameters are not known, (c3) there exist actuator constraints on the maximum control efforts, i.e. $u_r|_j(t) \leq \bar{u}_r^{\max}|_j$, where $r = 1, \dots, k$, $j \in \mathcal{V}$ and $\bar{u}_r^{\max}|_j$, and (c4) velocity measurement is not available for feedback and exchange among the EL systems in the network.

We make the following assumption explicit in this chapter.

Assumption 5.1.1. We assume in this chapter that the weights of the adjacency matrix are the same for all the nodes of the communication graph, i.e. we have $\lambda_{jn} = \lambda_{j\bar{n}}$, where $j \in \mathcal{V}$ and $n, \bar{n} \in \mathcal{N}_j$.

5.2 Distributed Constrained Nonlinear Control

We introduce the following distributed nonlinear controller for the j -th EL system for the i -th communication network topology (as per Definition 3.1.1) to satisfy the objectives that are introduced in the previous section, while satisfying the constraints (c1) and (c2) simultaneously,

$$\begin{aligned}
\mathbf{u}_j^{\text{leader}} &= \mathbf{u}_j^0 + \mathbf{u}_j^s + \mathbf{u}_{j,i}^f \\
\mathbf{u}_j^{\text{follower}} &= \mathbf{u}_j^0 + \mathbf{u}_{j,i}^f, \quad \text{where} \\
\begin{cases} \mathbf{u}_j^0 = \mathbf{G}_j(\mathbf{q}_j) \\ \mathbf{u}_j^s = -\Lambda_j^p \chi(\tilde{\mathbf{q}}_j + \Lambda_j^d \dot{\mathbf{q}}_j) \\ \mathbf{u}_{j,i}^f = -\sum_{n \in \mathcal{N}_{j,i}} \Lambda_{jn,i}^p \chi(\mathbf{q}_{jn} + \Lambda_j^d \dot{\mathbf{q}}_j + \Lambda_j^d \dot{\mathbf{q}}_{jn}) \end{cases} & \quad (5.1)
\end{aligned}$$

where $\chi(\mathbf{x}) = \text{col}[\chi(x_1), \dots, \chi(x_n)]$ denotes a monotonically increasing odd function. The term \mathbf{u}_j^0 is denoted as the *feed-forward controller* and is added to compensate for the effects of the GFV. The term \mathbf{u}_j^s is denoted as the *station-keeping controller* and the term $\mathbf{u}_{j,i}^f$ is denoted as the *formation-keeping controller*. In addition, the controller gains Λ_j^p , Λ_j^d , $\Lambda_{jn,i}^p$ and $\Lambda_{jn,i}^d$ are positive definite diagonal matrices corresponding to proportional and derivative terms (the superscript ‘p’ denotes the proportional and the superscript ‘d’ denotes the derivative).

The following lemma is used subsequently in this chapter.

Lemma 5.2.1. *Consider the following algebraic equations that correspond to a strongly connected network of ‘m’ agents*

$$\Lambda_j^p \chi(\tilde{\mathbf{q}}_j) + \sum_{n \in \mathcal{N}_j} \Lambda_{jn}^p \chi(\mathbf{q}_{jn}) = 0, \quad j, n \in \{1, \dots, m\}, j \neq n \quad (5.2)$$

where $\tilde{\mathbf{q}}_j \in \mathbb{R}^k$, $\chi(x)$ is a monotonically increasing odd function, and $\Lambda_{jn}^p = \Lambda_{nj}^p$ are positive definite matrices. Furthermore, assume that Λ_j^p is a positive definite diagonal matrix for only $0 < l \leq m$ number of equations (corresponding to ‘l’ leaders) and is zero, otherwise. If we have $\sum_{j=1}^l \Lambda_j^p \chi(\tilde{\mathbf{q}}_j) = 0$, then the only solution to equation (5.2) is $\tilde{\mathbf{q}}_j = 0, \forall j \in \{1, \dots, m\}$.

Proof: We prove this lemma by contradiction. First note that equation (5.2) implies that if for the j -th algebraic equation we have $\Lambda_j^p = 0$ (corresponding to $m - l \geq 0$ followers), then $\sum_{n \in \mathcal{N}_j} \Lambda_{jn}^p \chi(\mathbf{q}_{jn}) = 0$. Therefore, equation (5.2) essentially reduces to $\Lambda_j^p \chi(\tilde{\mathbf{q}}_j) + \sum_{n \in \mathcal{N}_j} \Lambda_{jn}^p \chi(\mathbf{q}_{jn}) = 0, j, n \in \{1, \dots, l\}, j \neq n$. Now, let us assume that the claim does not hold, i.e. $\tilde{\mathbf{q}}_j \neq 0, \forall j \in \{1, \dots, l\}$. This in view of $\sum_{j=1}^l \Lambda_j^p \chi(\tilde{\mathbf{q}}_j) = 0$, implies that there exists at least one system (let’s say the l -th system, without loss of any generality) for which we have: $\sum_{j=1}^{l-1} \Lambda_j^p \chi(\tilde{\mathbf{q}}_j) =$

$-\Lambda_l^p \chi(\tilde{\mathbf{q}}_l) \equiv \Lambda_l^p \chi(-\tilde{\mathbf{q}}_l)$, which implies that the sign of the l -th system error is opposite to that of the others in the network. Without loss of generality, let us assume $\tilde{\mathbf{q}}_l = -\varepsilon_j \tilde{\mathbf{q}}_j$, $j = 1, \dots, l-1$, where $\varepsilon_j > 0$, and that $\tilde{\mathbf{q}}_j > 0$, $j = 1, \dots, l-1$. Thus, from equation (5.2) we have: $\Lambda_l^p \chi(\tilde{\mathbf{q}}_l) + \Lambda_{l,1}^p \chi(\tilde{\mathbf{q}}_l - \tilde{\mathbf{q}}_1) + \Lambda_{l,2}^p \chi(\tilde{\mathbf{q}}_l - \tilde{\mathbf{q}}_2) + \dots + \Lambda_{l,l-1}^p \chi(\tilde{\mathbf{q}}_l - \tilde{\mathbf{q}}_{l-1}) = 0$, which can be re-written as: $-\Lambda_l^p \chi(\varepsilon_1 \tilde{\mathbf{q}}_1) - \Lambda_{l,1}^p \chi[(\varepsilon_1 + 1)\tilde{\mathbf{q}}_1] - \dots - \Lambda_{l,l-1}^p \chi[(\varepsilon_{l-1} + 1)\tilde{\mathbf{q}}_{l-1}] = 0$. The statement above does not hold when $\tilde{\mathbf{q}}_j \neq 0$, $\forall j \in \{1, \dots, l\}$, which is a contradiction. Therefore, the only solution to the problem is to have $\tilde{\mathbf{q}}_j = 0$, $j = 1, \dots, l$. Consequently, from equation (5.2) we have $\sum_{n \in \mathcal{N}_j} \Lambda_{jn}^p \chi(\mathbf{q}_{jn}) = 0$, $\forall j, n \in \{1, \dots, m\}, j \neq n$, which by the strong connectivity of the communication graph, and the fact that $\chi(x)$ is a monotonically increasing odd function implies that $\mathbf{q}_{jn} = 0$, $\forall j, n \in \{1, \dots, m\}, j \neq n$. Therefore, in view of equation (3.1), one obtains $\tilde{\mathbf{q}}_j = 0$, $j = l+1, \dots, m$. Hence, we have: $\tilde{\mathbf{q}}_j = 0$, $\forall j \in \{1, \dots, m\}$. This completes the proof of the lemma. \blacksquare

Our first main result of this section is provided in the next subsection.

5.2.1 Distributed State Synchronization Control with Bounded Input

We present the following assumption which will be used subsequently.

Assumption 5.2.1. We assume the communication among the agents is a function of distances among the agents. Specifically, we assume when the communication link among two agents j and n are removed we have $\|\mathbf{q}_{jn}\| > r_0$, where r_0 is a positive constant. Furthermore, when the communication link among two agents j and n are established we have $\|\mathbf{q}_{jn}\| < r_0$. In addition, at each switching instant when a communication link among the j -th and the n -th agents is removed and a new communication link among the j -th and the \bar{n} -th agents is established one has

$$\|\mathbf{q}_{j\bar{n}}\| \leq \|\mathbf{q}_{jn}\|.$$

The above assumption implies that at the switching instant the distance among the j -th and the \bar{n} -th agents is less than the distance among the j -th and the n -th agents. We now present the first result of this chapter.

Theorem 5.2.1. *Consider a network of ‘ m ’ ($m > 1$) heterogeneous EL systems where each agent is governed by the dynamics (2.7) with $\delta = 0$. Without loss of generality, let the first ‘ l ’ agents ($l \geq 1$) denote the formation leaders and ‘ $l+1, \dots, m$ ’ denote the formation followers as per Definition 3.1.2. Let the j -th agent’s controller be given by (5.1). Then, under Assumptions 5.1.1 and 5.2.1 and in presence of an average dwell-time switching (refer to Definition 2.9.13) among the ‘ h ’ communication network topologies that satisfy Definition 3.1.1, the EL systems synchronize their states asymptotically and follow the desired set-point. The boundedness of the control efforts command (constraint (c3) in Subsection 5.1.2) is also guaranteed globally provided that one sets $\chi(x) \triangleq \text{Sat}(x)$ and one selects the controller gain matrices Λ_j^p and $\Lambda_{jn,i}^p$ such that the following inequalities are satisfied for all the EL systems,*

$$\begin{aligned} \bar{g}_r|_j + \lambda_r|_j^p + \sum_{n \in \mathcal{N}_{j,i}} \lambda_r|_{jn,i}^p &< \bar{u}_r^{\max}|_j, \quad r \in \{1, \dots, k\}, \quad j \in \{1, \dots, l\} \\ \bar{g}_r|_j + \sum_{n \in \mathcal{N}_{j,i}} \lambda_r|_{jn,i}^p &< \bar{u}_r^{\max}|_j, \quad r \in \{1, \dots, k\}, \quad j \in \{l+1, \dots, m\} \end{aligned} \quad (5.3)$$

where $\lambda_r|_j^p$ represents the r -th diagonal element of Λ_j^p and $\lambda_r|_{jn,i}^p$ represents the r -th diagonal element of $\Lambda_{jn,i}^p$.

Proof: We first show that the distributed control law (5.1) guarantees global

asymptotic state synchronization under switchings among the communication network topologies. Consider the following radially unbounded positive definite Lyapunov function candidate for the closed-loop system under the \bar{i} -th communication network topology ($\bar{i} \in \mathcal{H}$),

$$\mathcal{W}_{\bar{i}} = \frac{1}{2} \sum_{j=1}^m \left(\dot{\mathbf{q}}_j^T \mathbf{D}_j(\mathbf{q}_j) \dot{\mathbf{q}}_j + \sum_{n \in \mathcal{N}_{j,\bar{i}}} \sum_{r=1}^k \int_0^{\mathbf{q}_{jn}} \lambda_r |\Lambda_{jn,\bar{i}}^p \chi(x) dx \right) + \sum_{j=1}^l \sum_{r=1}^k \int_0^{\tilde{\mathbf{q}}_j} \lambda_r |\Lambda_j^p \chi(x) dx$$

Positive definiteness of the above function follows from the Property **2.1.1** and Lemma 2.6.1.

The time derivative of the above function along the trajectories of the closed-loop system (2.7) and (5.1) is obtained as

$$\begin{aligned} \dot{\mathcal{W}}_{\bar{i}} &= \sum_{j=1}^m \left[\dot{\mathbf{q}}_j^T \mathbf{D}_j(\mathbf{q}_j) \ddot{\mathbf{q}}_j + \frac{1}{2} \dot{\mathbf{q}}_j^T \dot{\mathbf{D}}_j(\mathbf{q}_j) \dot{\mathbf{q}}_j + \frac{1}{2} \sum_{n \in \mathcal{N}_{j,\bar{i}}} \dot{\mathbf{q}}_{jn}^T \Lambda_{jn,\bar{i}}^p \chi(\mathbf{q}_{jn}) \right] + \sum_{j=1}^l \dot{\mathbf{q}}_j^T \Lambda_j^p \chi(\tilde{\mathbf{q}}_j) \\ &= \sum_{j=1}^l \left\{ \dot{\mathbf{q}}_j^T \left[-\Lambda_j^p \chi(\tilde{\mathbf{q}}_j + \Lambda_j^d \dot{\mathbf{q}}_j) + \Lambda_j^p \chi(\tilde{\mathbf{q}}_j) \right] \right\} \\ &\quad + \sum_{j=1}^m \left\{ \dot{\mathbf{q}}_j^T \left[- \sum_{n \in \mathcal{N}_{j,\bar{i}}} \Lambda_{jn,\bar{i}}^p \chi(\mathbf{q}_{jn} + \Lambda_j^d \dot{\mathbf{q}}_j + \Lambda_j^d \dot{\mathbf{q}}_{jn}) \right] + \frac{1}{2} \sum_{n \in \mathcal{N}_{j,\bar{i}}} \dot{\mathbf{q}}_{jn}^T \Lambda_{jn,\bar{i}}^p \chi(\mathbf{q}_{jn}) \right\} \\ &= \sum_{j=1}^l \left\{ \dot{\mathbf{q}}_j^T \left[-\Lambda_j^p \chi(\tilde{\mathbf{q}}_j + \Lambda_j^d \dot{\mathbf{q}}_j) + \Lambda_j^p \chi(\tilde{\mathbf{q}}_j) \right] \right\} \\ &\quad + \sum_{j=1}^m \left\{ \dot{\mathbf{q}}_j^T \left[- \sum_{n \in \mathcal{N}_{j,\bar{i}}} \Lambda_{jn,\bar{i}}^p \chi(\mathbf{q}_{jn} + \Lambda_j^d \dot{\mathbf{q}}_j + \Lambda_j^d \dot{\mathbf{q}}_{jn}) \right] + \frac{1}{2} \sum_{n \in \mathcal{N}_{j,\bar{i}}} \dot{\mathbf{q}}_{jn}^T \Lambda_{jn,\bar{i}}^p \chi(\mathbf{q}_{jn}) \right\} \\ &= - \sum_{j=1}^l \left\{ \dot{\mathbf{q}}_j^T \left[\Lambda_j^p \chi(\tilde{\mathbf{q}}_j + \Lambda_j^d \dot{\mathbf{q}}_j) + \Lambda_j^p \chi(\tilde{\mathbf{q}}_j) \right] \right\} \\ &\quad - \sum_{j=1}^m \sum_{n \in \mathcal{N}_{j,\bar{i}}} \left\{ \dot{\mathbf{q}}_j^T \Lambda_{jn,\bar{i}}^p \left[\chi(\mathbf{q}_{jn} + \Lambda_j^d \dot{\mathbf{q}}_j + \Lambda_j^d \dot{\mathbf{q}}_{jn}) - \chi(\mathbf{q}_{jn}) \right] \right\} \end{aligned}$$

The definition of $\chi(x)$ implies that $\chi(x+y) - \chi(x) > 0 \Leftrightarrow y > 0$, and $\chi(x+y) -$

$\chi(x) < 0 \Leftrightarrow y < 0$. Therefore, the sign of $\dot{\mathcal{W}}_i$ is the same as the sign of the following expression,

$$\begin{aligned}\Xi_1 &= -\sum_{j=1}^l k_1 \dot{\mathbf{q}}_j^T \dot{\mathbf{q}}_j - k_2 \sum_{j=1}^m \sum_{n \in \mathcal{N}_{j,\bar{i}}} \dot{\mathbf{q}}_j^T (\dot{\mathbf{q}}_j + \dot{\mathbf{q}}_{jn}) \\ &= -\sum_{j=1}^l k_1 \dot{\mathbf{q}}_j^T \dot{\mathbf{q}}_j - k_2 \sum_{j=1}^m \sum_{n \in \mathcal{N}_{j,\bar{i}}} \dot{\mathbf{q}}_j^T \dot{\mathbf{q}}_j - \frac{k_2}{2} \sum_{j=1}^m \sum_{n \in \mathcal{N}_{j,\bar{i}}} \dot{\mathbf{q}}_{jn}^T \dot{\mathbf{q}}_{jn} \leq 0\end{aligned}\tag{5.4}$$

for some positive numbers k_1 and k_2 . Consequently, we have $\dot{\mathcal{W}}_i \leq 0$.

First, note that since the Lyapunov function is radially unbounded, all signals remain globally bounded. Without loss of generality, let the i -th network topology ($i \in \mathcal{H}$) has the maximum graph size, i.e. $|\mathcal{E}_i| < |\mathcal{E}_i|$, $\bar{i} \in \mathcal{H}$, $i \neq \bar{i}$. Therefore, under Assumption 5.1.1 we have $\dot{\mathcal{W}}_i(t) \leq \dot{\mathcal{W}}_i(t)$, $\forall t \geq 0$. Let t_{h_1}, t_{h_2}, \dots denote an infinite sequence of switching time to the i -th communication network topology, and $t_{h_1+1}, t_{h_2+1}, \dots$, denote another infinite sequence of switching times from the i -th communication network topology. It can be shown that at any switching times to the i -th communication network topology under Assumption 5.2.1 we have $\mathcal{W}_i(t_{h_1}) \geq \mathcal{W}_i(t_{h_2}) \geq \dots \geq \mathcal{W}_i(t_{h_e})$, with $e \rightarrow \infty$.

Note that Lemma 2.9.3 implies that there exist a non-vanishing dwell time $\bar{\tau} \in (0, \tau_{ad})$ among each switchings in the communication network topology. One can, therefore, invoke Lemma 2.9.5 to conclude that under non-vanishing dwell-time switching one has $\dot{\mathcal{W}}_i \rightarrow 0$ as $t \rightarrow \infty$. Now, from (5.4) and by noting strong connectivity of the communication graph (refer to Definition 3.1.1) we have $\dot{\mathbf{q}}_j \rightarrow 0$ and $\dot{\mathbf{q}}_{jn} \rightarrow 0$ as $t \rightarrow \infty$. Again, by invoking Lemma 2.9.5 one can show that we have $\ddot{\mathbf{q}}_j \rightarrow 0$ as $t \rightarrow \infty$, which by studying the closed-loop system dynamics and invoking Lemma 5.2.1 it implies that $\ddot{\mathbf{q}}_j \rightarrow 0$ and $\ddot{\mathbf{q}}_{jn} \rightarrow 0$ as $t \rightarrow \infty$. Therefore, the state

synchronization and set-point tracking are achieved globally under average dwell-time switchings. It is straightforward to show that by setting $\chi(x) \triangleq \text{Sat}(x)$, and by selecting the controller gains according to (5.3) the constraints on the control efforts are always satisfied globally, i.e. $u_r|_j(t) \leq \bar{u}_r^{\max}|_j$ for all times. This completes the proof of the theorem. \blacksquare

Corollary 5.2.2. *Consider a network of ‘m’ ($m > 1$) heterogeneous EL systems where each agent is governed by the dynamics (2.7). Let the j -th agent’s controller be given by $\mathbf{u}_j^{\text{follower}}$ in (5.1). Then, under Assumptions 5.1.1 and 5.2.1 and in presence of an average dwell-time switching (refer to Definition 2.9.13) among the ‘h’ communication network topologies that satisfy Definition 3.1.1, the EL systems synchronize their states asymptotically. The boundedness of the control efforts command (constraint (c3) in Subsection 5.1.2) is also guaranteed globally provided that one sets $\chi(x) \triangleq \text{Sat}(x)$ and one selects the controller gain matrix $\Lambda_{jn,i}^p$ such that the following inequalities are satisfied for all the EL systems,*

$$\bar{g}_r|_j + \sum_{n \in \mathcal{N}_{j,i}} \lambda_r|_{jn,i}^p < \bar{u}_r^{\max}|_j, \quad r \in \{1, \dots, k\}, \quad j \in \{1, \dots, m\} \quad (5.5)$$

where $\lambda_r|_{jn,i}^p$ represents the r -th diagonal element of $\Lambda_{jn,i}^p$.

Proof: It follows from Theorem 5.2.1.

5.3 Distributed Dynamic Output Feedback Constrained Nonlinear Control

The following distributed dynamic output feedback nonlinear controller for the j -th EL system is proposed to satisfy the objectives that are introduced in Subsection

5.1.2, while satisfying the three constraints (c1), (c2), and (c4) simultaneously,

$$\begin{aligned}
\mathbf{u}_j^{\text{leader}} &= \mathbf{u}_j^0 + \mathbf{u}_j^s + \mathbf{u}_{j,i}^f \\
\mathbf{u}_j^{\text{follower}} &= \mathbf{u}_j^0 + \mathbf{u}_{j,i}^f, \quad \text{where} \\
\left\{ \begin{array}{l} \mathbf{u}_j^0 = \mathbf{G}_j(\mathbf{q}_j) \\ \mathbf{u}_j^s = -\Lambda_j^p \chi(\tilde{\mathbf{q}}_j + \Lambda_j^d \vartheta_j) \\ \vartheta_j = \mathbf{z}_j + \bar{\mathbf{B}}\tilde{\mathbf{q}}_j, \dot{\mathbf{z}}_j = -\bar{\mathbf{A}}(\mathbf{z}_j + \bar{\mathbf{B}}\tilde{\mathbf{q}}_j) \end{array} \right. & \quad (5.6) \\
\left\{ \begin{array}{l} \mathbf{u}_{j,i}^f = -\sum_{n \in \mathcal{N}_{j,i}} \Lambda_{jn,i}^p \chi(\mathbf{q}_{jn} + \Lambda_j^d \vartheta_j + \Lambda_j^d \vartheta_{jn}) \\ \vartheta_{jn} = \bar{\mathbf{z}}_r + \bar{\mathbf{B}}\mathbf{q}_{jn}, \dot{\bar{\mathbf{z}}}_r = -\bar{\mathbf{A}}(\bar{\mathbf{z}}_r + \bar{\mathbf{B}}\mathbf{q}_{jn}) \end{array} \right.
\end{aligned}$$

where $r = 1, \dots, |\mathcal{N}_{j,i}|$, $\chi(\mathbf{x}) = \text{col}[\chi(x_1), \dots, \chi(x_n)]$ denotes a monotonically increasing odd function, $\bar{\mathbf{A}} \triangleq \text{diag}[\bar{a}_1, \dots, \bar{a}_k]$ and $\bar{\mathbf{B}} \triangleq \text{diag}[\bar{b}_1, \dots, \bar{b}_k]$ are positive definite diagonal matrices. The controller term \mathbf{u}_j^0 is denoted as the *feed-forward controller*, the controller term \mathbf{u}_j^s is denoted as the *velocity-free station-keeping controller*, and the controller term $\mathbf{u}_{j,i}^f$ is denoted as the *velocity-free formation-keeping controller*. In addition, the controller gains Λ_j^p , Λ_j^d , $\Lambda_{jn,i}^p$, and Λ_j^d are positive definite diagonal matrices representing the positive proportional and derivative terms (the superscript ‘ p ’ denotes the proportional and the superscript ‘ d ’ denotes the derivative).

5.3.1 Distributed Output Feedback Synchronization Control with Bounded Input

We now present the first result of this subsection.

Theorem 5.3.1. *Consider a network of m ($m > 1$) heterogeneous EL systems where*

each agent is governed by the dynamics (2.7) with $\delta = 0$ under the controller given in equation (5.6). Then, under the Assumptions 5.1.1 and 5.2.1 and in presence of an average dwell-time switching (refer to Definition 2.9.13) among the ‘h’ communication network topologies that satisfy Definition 3.1.1, there exist matrices $\bar{\mathbf{A}}$ and $\bar{\mathbf{B}}$ such that the EL systems globally synchronize their states and follow the desired set-point asymptotically. This is achieved under the constraints (c1), (c2) and (c4) given in Subsection 5.1.2. The boundedness of the control efforts command (constraint (c3)) is also guaranteed globally provided that one sets $\chi(x) \triangleq \text{Sat}(x)$ and one selects the controller gain matrices Λ_j^p and $\Lambda_{jn,i}^p$ such that the inequalities (5.3) are satisfied for all $j \in \mathcal{V}$.

Proof: We first show that under the distributed velocity-free control law (5.6) one can guarantee global asymptotic state synchronization and set-point tracking under average dwell-time switching. Consider the following radially unbounded positive definite Lyapunov function candidate for the closed-loop system under the \bar{i} -th communication network topology ($\bar{i} \in \mathcal{H}$),

$$\begin{aligned} \mathcal{W}_{\bar{i}} = & \frac{1}{2} \sum_{j=1}^m \dot{\mathbf{q}}_j^T \mathbf{D}_j(\mathbf{q}_j) \dot{\mathbf{q}}_j + \sum_{j=1}^l \sum_{r=1}^k \left[\int_0^{\tilde{\mathbf{q}}_j} \lambda_r |_{j}^p \chi(x) dx + \int_0^{\vartheta_r |_{j}} \frac{\lambda_r |_{j}^p}{\bar{b}_r} \chi(x) dx \right] \\ & + \frac{1}{2} \sum_{j=1}^m \sum_{n \in \mathcal{N}_{j,\bar{i}}} \sum_{r=1}^k \left[\int_0^{\mathbf{q}_{jn}} \lambda_r |_{jn,\bar{i}}^p \chi(x) dx + \int_0^{\vartheta_r |_{j} + \vartheta_r |_{jn}} \frac{\lambda_r |_{jn,\bar{i}}^p}{\bar{b}_r} \chi(x) dx \right] \end{aligned}$$

Positive definiteness of the above function follows from the Property 2.1.1 and Lemma 2.6.1.

The time derivative of this function along the trajectories of the closed-loop

system (2.7) and (5.6) is governed by

$$\begin{aligned}
\mathcal{W}_{\bar{i}} &= - \sum_{j=1}^l \dot{\mathbf{q}}_j^T \Lambda_j^p \chi \left(\tilde{\mathbf{q}}_j + \Lambda_j^d \vartheta_j \right) - \sum_{j=1}^m \sum_{n \in \mathcal{N}_{j,\bar{i}}} \dot{\mathbf{q}}_j^T \Lambda_{jn,\bar{i}}^p \chi \left(\mathbf{q}_{jn} + \Lambda_j^d \vartheta_j + \Lambda_j^d \vartheta_{jn} \right) \\
&\quad + \sum_{j=1}^l \dot{\mathbf{q}}_j^T \Lambda_j^p \chi \left(\tilde{\mathbf{q}}_j \right) \\
&\quad + \frac{1}{2} \sum_{j=1}^m \sum_{n \in \mathcal{N}_{j,\bar{i}}} \dot{\mathbf{q}}_{jn}^T \Lambda_{jn,\bar{i}}^p \chi \left(\mathbf{q}_{jn} \right) + \sum_{j=1}^l [-\bar{\mathbf{A}} \vartheta_j + \bar{\mathbf{B}} \dot{\mathbf{q}}_j]^T \Lambda_j^p \bar{\mathbf{B}}^{-1} \chi \left(\vartheta_j \right) \\
&\quad + \frac{1}{2} \sum_{j=1}^m \sum_{n \in \mathcal{N}_{j,\bar{i}}} [-\bar{\mathbf{A}} (\vartheta_j + \vartheta_{jn}) + \bar{\mathbf{B}} (\dot{\mathbf{q}}_j + \dot{\mathbf{q}}_{jn})]^T \Lambda_{jn,\bar{i}}^p \bar{\mathbf{B}}^{-1} \chi \left(\vartheta_j + \vartheta_{jn} \right) \\
&= - \sum_{j=1}^l \dot{\mathbf{q}}_j^T \Lambda_j^p \left[\chi \left(\tilde{\mathbf{q}}_j + \Lambda_j^d \vartheta_j \right) - \chi \left(\tilde{\mathbf{q}}_j \right) \right] \\
&\quad - \frac{1}{2} \sum_{j=1}^m \sum_{n \in \mathcal{N}_{j,\bar{i}}} \dot{\mathbf{q}}_{jn}^T \Lambda_{jn,\bar{i}}^p \left[\chi \left(\mathbf{q}_{jn} + \Lambda_j^d \vartheta_j + \Lambda_j^d \vartheta_{jn} \right) \right. \\
&\quad \left. - \chi \left(\mathbf{q}_{jn} \right) \right] + \sum_{j=1}^l [-\bar{\mathbf{A}} \vartheta_j + \bar{\mathbf{B}} \dot{\mathbf{q}}_j]^T \Lambda_j^p \bar{\mathbf{B}}^{-1} \chi \left(\vartheta_j \right) + \frac{1}{2} \sum_{j=1}^m \sum_{n \in \mathcal{N}_{j,\bar{i}}} [-\bar{\mathbf{A}} (\vartheta_j + \vartheta_{jn}) \\
&\quad + \bar{\mathbf{B}} (\dot{\mathbf{q}}_j + \dot{\mathbf{q}}_{jn})]^T \Lambda_{jn,\bar{i}}^p \bar{\mathbf{B}}^{-1} \chi \left(\vartheta_j + \vartheta_{jn} \right)
\end{aligned} \tag{5.7}$$

Consequently, by noting $\chi(x+y) - \chi(x) > 0 \Leftrightarrow y > 0$, and $\chi(x+y) - \chi(x) < 0 \Leftrightarrow y < 0$, one has

$$\begin{aligned}
\mathcal{W}_{\bar{i}} &\leq -k_1 \sum_{j=1}^l \dot{\mathbf{q}}_j^T \chi \left(\vartheta_j \right) - k_2 \sum_{j=1}^m \sum_{n \in \mathcal{N}_{j,\bar{i}}} \dot{\mathbf{q}}_{jn}^T \chi \left(\vartheta_j + \vartheta_{jn} \right) + k_3 \sum_{j=1}^l [-\bar{\mathbf{A}} \vartheta_j + \bar{\mathbf{B}} \dot{\mathbf{q}}_j]^T \bar{\mathbf{B}}^{-1} \chi \left(\vartheta_j \right) \\
&\quad + k_4 \sum_{j=1}^m \sum_{n \in \mathcal{N}_{j,\bar{i}}} [-\bar{\mathbf{A}} (\vartheta_j + \vartheta_{jn}) + \bar{\mathbf{B}} (\dot{\mathbf{q}}_j + \dot{\mathbf{q}}_{jn})]^T \Lambda_{jn,\bar{i}}^p \bar{\mathbf{B}}^{-1} \chi \left(\vartheta_j + \vartheta_{jn} \right)
\end{aligned}$$

for some positive constants k_1, k_2, k_3 and k_4 . One can re-write the above equation

as

$$\dot{\mathcal{W}}_i \leq -k_1 \sum_{j=1}^l \vartheta_j^T \bar{\mathbf{A}} \bar{\mathbf{B}}^{-1} \chi(\vartheta_j) - k_2 \sum_{j=1}^m \sum_{n \in \mathcal{N}_{j,\bar{i}}} (\vartheta_j + \vartheta_{jn})^T \bar{\mathbf{A}} \bar{\mathbf{B}}^{-1} \chi(\vartheta_j + \vartheta_{jn}) \leq 0$$

Consequently, $\dot{\mathcal{W}}_i$ is a negative semi-definite function $\forall \bar{i} \in \mathcal{H}$. First, note that since the Lyapunov function is radially unbounded and $\dot{\mathcal{W}}_i \leq 0$, all the signals remain globally bounded. Without loss of generality, let the i -th network topology ($i \in \mathcal{H}$) has the maximum graph size, i.e. $|\mathcal{E}_i^c| < |\mathcal{E}_{\bar{i}}^c|$, $\bar{i} \in \mathcal{H}$, $i \neq \bar{i}$. Therefore, under Assumption 5.1.1 we have $\dot{\mathcal{W}}_{\bar{i}}(t) \leq \dot{\mathcal{W}}_i(t)$, $\forall t \geq 0$. Let t_{h_1}, t_{h_2}, \dots denote an infinite sequence of switching time to the i -th communication network topology, and $t_{h_1+1}, t_{h_2+1}, \dots$ denote another infinite sequence of switching times from the i -th communication network topology. At any switching times to the i -th communication network topology under Assumption 5.2.1 we have $\mathcal{W}_i(t_{h_1}) \geq \mathcal{W}_i(t_{h_2}) \geq \dots \geq \mathcal{W}_i(t_{h_e})$, with $e \rightarrow \infty$.

Note that Lemma 2.9.3 implies that there exists a non-vanishing dwell time $\bar{\tau} \in (0, \tau_{ad})$ among each switchings in the communication network topology. One can invoke Lemma 2.9.5 to conclude that under non-vanishing dwell-time switching one has $\dot{\mathcal{W}}_i \rightarrow 0$ as $t \rightarrow \infty$.

From equation (5.7) and by noting strong connectivity of the communication graph (refer to Definition 3.1.1) it now follows that $\vartheta_j \rightarrow 0$ and $\vartheta_{jn} \rightarrow 0$ as $t \rightarrow \infty$ under non-vanishing dwell-time switching. This from (5.6) implies that $\mathbf{z}_j + \bar{\mathbf{B}}\tilde{\mathbf{q}}_j \rightarrow 0$ and $\bar{\mathbf{z}}_r + \bar{\mathbf{B}}\mathbf{q}_{jn} \rightarrow 0$ as $t \rightarrow \infty$. Therefore, by invoking Lemma 2.9.5 one obtains $\dot{\vartheta}_j \rightarrow 0$ and $\dot{\vartheta}_{jn} \rightarrow 0$ as $t \rightarrow \infty$. Consequently, we have $\dot{\mathbf{z}}_j + \bar{\mathbf{B}}\dot{\mathbf{q}}_j = 0$ and $\dot{\bar{\mathbf{z}}}_r + \bar{\mathbf{B}}\dot{\mathbf{q}}_{jn} = 0$ at steady-state. This from (5.6) implies that $-\bar{\mathbf{A}}\vartheta_j + \bar{\mathbf{B}}\dot{\mathbf{q}}_j \rightarrow 0$ and $-\bar{\mathbf{A}}\vartheta_{jn} + \bar{\mathbf{B}}\dot{\mathbf{q}}_{jn} \rightarrow 0$ as $t \rightarrow \infty$. Noting the fact that $\vartheta_j = \vartheta_{jn} = 0$ at steady-state we obtain $\dot{\mathbf{q}}_j \rightarrow 0$ and $\dot{\mathbf{q}}_{jn} \rightarrow 0$ as $t \rightarrow \infty$. This implies that $\mathbf{z}_j = \dot{\mathbf{z}}_j = \dot{\bar{\mathbf{z}}}_r = \bar{\mathbf{z}}_r = 0$ at steady-state and $\ddot{\mathbf{q}}_j \rightarrow 0$ as $t \rightarrow \infty$. Therefore, the state synchronization is achieved globally

with *only* position feedback and exchange among the agents under average dwell-time switching. It is straightforward to show that by using equation (5.6), setting $\chi(x) \triangleq \text{Sat}(x)$, and selecting the controller gains $\lambda_l|_j^p$ and $\lambda_l|_{jn,i}^p$ according to the inequalities (5.3) the constraints on the control efforts are always satisfied globally, i.e. $u_r|_j(t) \leq \bar{u}_r^{\max}|_j$ for all times. This completes the proof of the theorem. ■

Corollary 5.3.2. *Consider a network of m ($m > 1$) heterogeneous EL systems where each agent is governed by the dynamics (2.7) under the controller $\mathbf{u}_j^{\text{follower}}$ given in equation (5.6). Then, under the Assumptions 5.1.1 and 5.2.1 and in presence of an average dwell-time switching (refer to Definition 2.9.13) among the ‘h’ communication network topologies that satisfy Definition 3.1.1, there exist matrices $\bar{\mathbf{A}}$ and $\bar{\mathbf{B}}$ such that the EL systems globally synchronize their states. This is achieved under the constraints (c1), (c2) and (c4) given in Subsection 5.1.2. The boundedness of the control efforts command (constraint (c3)) is also guaranteed globally provided that one sets $\chi(x) \triangleq \text{Sat}(x)$ and one selects the controller gain matrix $\Lambda_{jn,i}^p$ such that the inequalities (5.5) are satisfied for all $j \in \mathcal{V}$.*

Proof: It follows from Theorem 5.3.1.

Remark 5.3.1. The distributed controller (5.6) requires no local velocity feedback, no velocity measurement exchanges, and no velocity estimation exchanges among the networked agents.

5.4 Cooperative Controller Reconfiguration under Actuator Saturation Constraints Faults

The objective of this section is to introduce a controller reconfiguration strategy which can be employed in presence of actuator faults. Specifically, we design two

control laws that are denoted as constrained *nominal* and constrained *reconfigured* controllers. In presence of an actuator fault, a stable switching mechanism is developed to reconfigure (switch from) the constrained nominal controller to the constrained reconfigured controller. Furthermore, once the fault is cleared or removed (that is corresponding to an intermittent actuator fault) the proposed mechanism will switch from the constrained reconfigured controller to the constrained nominal controller. This process can take place as often as applicable and stability of the networked EL systems is guaranteed by using the developed switching strategy.

We make the following assumptions explicit.

Assumption 5.4.1. The following conditions are assumed to hold for the considered EL systems:

- (a) In presence of actuator faults, the maximum control effort for the i -th actuator of the j -th EL system may fall below $\bar{u}_r^{\max}|_j$ and this maximum bound could be time-varying, in general, and is denoted by $u(t)_r^{\max}|_j$;
- (b) The maximum control effort available in presence of the worst-case actuator faults, $u(t)_r^{\max}|_j$, is bounded from below. Specifically, the least upper bound of the available control effort for the i -th actuator of the j -th EL system under all possible faults and constraints is known *a priori* and is denoted by $\underline{u}_r^{\max}|_j$;
- (c) The control bounds described above satisfy, $0 \leq \left\| M_j^{-1} \mathbf{G}_j(q_j) \right\| < \left\| \underline{u}_j^{\max} \right\| \leq \left\| u(t)_j^{\max} \right\|$. This implies that the actuators should maintain the j -th system at rest corresponding to all desired positions in presence of a fault.

We now present the formal definitions of the constrained controllers.

Definition 5.4.1. A distributed controller is called constrained *nominal* if the control law is given by

$$u_j^{\text{nom}} = -\bar{\Lambda}_j^p \chi_1(\tilde{\mathbf{q}}_j) - \bar{\Lambda}_j^d \chi_1(\dot{\mathbf{q}}_j) + \mathbf{G}_j(\mathbf{q}_j) - \sum_{n \in \mathcal{N}_j} \bar{\Lambda}_{jn}^p \chi_1(\mathbf{q}_{jn}) - \sum_{n \in \mathcal{N}_j} \bar{\Lambda}_{jn}^d \chi_1(\dot{\mathbf{q}}_{jn}) \quad (5.8)$$

where ‘nom’ stands for *nominal* with $\chi_1(x) \triangleq \text{Sat}(x)$. The controller gains are selected as

$$\bar{\Lambda}_j^p = \text{diag}(\bar{\lambda}_1^p|_j, \dots, \bar{\lambda}_k^p|_j)$$

$$\bar{\Lambda}_j^d = \text{diag}(\bar{\lambda}_1^d|_j, \dots, \bar{\lambda}_k^d|_j)$$

$$\bar{\Lambda}_{jn}^p = \text{diag}(\bar{\lambda}_1^p|_{jn}, \dots, \bar{\lambda}_k^p|_{jn})$$

$$\bar{\Lambda}_{jn}^d = \text{diag}(\bar{\lambda}_1^d|_{jn}, \dots, \bar{\lambda}_k^d|_{jn})$$

such that the following constrained conditions are satisfied

$$\bar{\lambda}_r^p|_j + \bar{\lambda}_r^d|_j + \sum_{n \in \mathcal{N}_j} \bar{\lambda}_r^p|_{jn} + \sum_{n \in \mathcal{N}_j} \bar{\lambda}_r^d|_{jn} + g_r|_j \leq \bar{u}_r^{\max}|_j, \quad r \in \{1, \dots, k\}, j \in \{1, \dots, m\} \quad (5.9)$$

corresponding to the *nominal* EL systems operation. Note that for the follower EL system we have $\bar{\Lambda}_j^p = \bar{\Lambda}_j^d = 0$. \square

Definition 5.4.2. A distributed controller is called constrained *reconfigured* if the control law is given by

$$u_j^{\text{rfg}} = -\underline{\Lambda}_j^p \chi_2(\tilde{\mathbf{q}}_j) - \underline{\Lambda}_j^d \chi_2(\dot{\mathbf{q}}_j) + \mathbf{G}_j(\mathbf{q}_j) - \sum_{n \in \mathcal{N}_j} \underline{\Lambda}_{jn}^p \chi_2(\mathbf{q}_{jn}) - \sum_{n \in \mathcal{N}_j} \underline{\Lambda}_{jn}^d \chi_2(\dot{\mathbf{q}}_{jn}) \quad (5.10)$$

where ‘rfg’ stands for *reconfigured* with $\chi_2(x) \triangleq \text{Sat}(x)$. The controller gains are

selected as

$$\underline{\Lambda}_j^p = \text{diag}(\underline{\lambda}_1^p|_j, \dots, \underline{\lambda}_k^p|_j)$$

$$\underline{\Lambda}_j^d = \text{diag}(\underline{\lambda}_1^d|_j, \dots, \underline{\lambda}_k^d|_j)$$

$$\underline{\Lambda}_{jn}^p = \text{diag}(\underline{\lambda}_1^p|_{jn}, \dots, \underline{\lambda}_k^p|_{jn})$$

$$\underline{\Lambda}_{jn}^d = \text{diag}(\underline{\lambda}_1^d|_{jn}, \dots, \underline{\lambda}_k^d|_{jn})$$

such that the following constrained conditions are satisfied

$$\underline{\lambda}_r^p|_j + \underline{\lambda}_r^d|_j + \sum_{n \in \mathcal{N}_j} \underline{\lambda}_r^p|_{jn} + \sum_{n \in \mathcal{N}_j} \underline{\lambda}_r^d|_{jn} + g_r|_j \leq \underline{u}_r^{\max}|_j, \quad r \in \{1, \dots, k\}, j \in \{1, \dots, m\} \quad (5.11)$$

corresponding to the *faulty* EL systems operation. Note that for the follower EL system we have $\bar{\Lambda}_j^p = \bar{\Lambda}_j^d = 0$. \square

Note that the above definitions allow the functions $\chi_1(x)$ and $\chi_2(x)$ to be different. In other words, the functions $\chi_1(x)$ and $\chi_2(x)$ given in Definitions 5.4.1 and 5.4.2 are saturation functions with possibly different structures, respectively.

In presence of actuator faults, the maximum control effort available to each actuator may change (as per Assumption 5.4.1, parts (a) and (b)). In this case, the *nominal* controller must be *reconfigured* in order to satisfy the constraints on the control effort due to the actuator fault. Note that the nominal and reconfigured controllers do not have the same structure and do not employ the same gains. The control reconfiguration is to be accomplished and achieved by *switchings* between the constrained *nominal* and the constrained *reconfigured* controllers.

In this section it is shown that by any number of switchings between these two controllers, it follows that: (A) a globally stable closed-loop EL system is obtained; (B) the synchronization errors asymptotically converge to zero; and (C) the

set-point tracking errors asymptotically converge to zero, provided that certain conditions are satisfied. These are very useful properties as they show that in case of a fault and presence of a subsequent actuator saturation constraint, one can switch from the constrained *nominal* controller to the constrained *reconfigured* controller while still ensuring desirable behavior of the overall networked EL system. Furthermore, when the injected actuator fault is removed (corresponding to an intermittent fault), one can safely switch back from the constrained *reconfigured* controller to the constrained *nominal* controller.

One of the advantages of the above switching strategy is that the only information that is required for controller reconfiguration is the knowledge of the fault occurrence, which can be determined through a large body of fault detection algorithms that are available in the literature (refer to recent works in [183, 185, 187] and references therein). The proposed reconfigurable approach does not rely and require exact knowledge of the severity of the fault (fault identification) as long as Assumption 5.4.1 parts (b) and (c) are satisfied. Furthermore, the requirements for the switching operation is rather straightforward to satisfy and implement in practice. We now state the following definition and assumption before presenting our main result of this section.

Definition 5.4.3. Let $\mathcal{W}_1(x)$ be represented by

$$\mathcal{W}_1 = \sum_{j=1}^m \left(\frac{1}{2} \dot{\mathbf{q}}_j^T \mathbf{D}_j(\mathbf{q}_j) \dot{\mathbf{q}}_j + \sum_{r=1}^k \bar{\lambda}_r^p |_{j} \int_0^{\tilde{\mathbf{q}}_{i,j}} \chi_1(x) dx + \frac{1}{2} \sum_{n \in \mathcal{N}_j} \sum_{r=1}^k \bar{\lambda}_r^p |_{jn} \int_0^{\mathbf{q}_{i,jn}} \chi_1(x) dx \right) \quad (5.12)$$

Furthermore, let $\mathcal{W}_2(x)$ be given by

$$\mathcal{W}_2 = \sum_{j=1}^m \left(\frac{1}{2} \dot{\mathbf{q}}_j^T \mathbf{D}_j(\mathbf{q}_j) \dot{\mathbf{q}}_j + \sum_{r=1}^k \underline{\lambda}_r^p |_{j} \int_0^{\tilde{\mathbf{q}}_{i,j}} \chi_2(x) dx + \frac{1}{2} \sum_{n \in \mathcal{N}_j} \sum_{r=1}^k \underline{\lambda}_r^p |_{jn} \int_0^{\mathbf{q}_{i,jn}} \chi_2(x) dx \right) \quad (5.13)$$

□

Assumption 5.4.2. The following conditions are assumed to hold:

- (a) The controller gains and the saturation functions are selected such that $\bar{\Lambda}_j^P \chi_1(x) \geq \underline{\Lambda}_j^P \chi_2(x)$, $\forall x$ and $\bar{\Lambda}_{jn}^P \chi_1(x) \geq \underline{\Lambda}_{jn}^P \chi_2(x)$, $\forall x$. This from Definition 5.4.3 implies that $\mathscr{W}_1(x) \geq \mathscr{W}_2(x)$, $\forall x$, where $x = [\dot{\mathbf{q}}_j^T, \tilde{\mathbf{q}}_j^T, \mathbf{q}_{jn}^T]^T$. We denote $[-\bar{b}, \bar{b}]$ as the region where $\bar{\Lambda}_j^P \chi_1(x) = \underline{\Lambda}_j^P \chi_2(x)$ and $\bar{\Lambda}_{jn}^P \chi_1(x) = \underline{\Lambda}_{jn}^P \chi_2(x)$.
- (b) At every switching instant from the constrained *reconfigured* controller to the constrained *nominal* controller (this instant is at the designer's disposal since the fault is no longer present) one needs to ensure that $\tilde{q}_{i,j}, q_{i,jn} \in [-\bar{b}, \bar{b}]$, $i = 1, \dots, k$, $j, n \in \{1, \dots, m\}$, $j \neq n$ (existence of such a region is guaranteed in part (a)), whereas at the switching instant from the constrained *nominal* controller to the constrained *reconfigured* controller (this instant is not at the designer's disposal since the fault detection time is unknown) one cannot guarantee the size of $q_{i,j}$ and $q_{i,jn}$.
- (c) The switchings between the nominal and the reconfigured controllers satisfy the requirement of an *average dwell-time* switching as per Definition 2.9.13.

We are now in a position to state the main result of this section.

Theorem 5.4.1. *Consider a network of 'm' ($m > 1$) EL systems where the j-th agent dynamics is governed by equation (2.7) and which is subject to the constrained nominal distributed control law that is given by Definition 5.4.1. Also consider the same network and communication topology which is subject to the constrained reconfigured distributed cooperative control law that is given by Definition 5.4.2. Any switchings between the constrained nominal and the constrained reconfigured closed-loop systems will yield a globally stable EL system, and moreover, the state*

synchronization and the set-point tracking errors globally asymptotically converge to the origin provided that the conditions of Assumptions 5.4.1 and 5.4.2 hold.

Proof: We can pick an infinite subsequence of switching times from the constrained *reconfigured* controlled system to the constrained *nominal* controlled system. One can show that the time derivative of the Lyapunov function candidate \mathcal{W}_1 along with the trajectories of the closed-loop system (2.7) and (5.8) is given by

$$\dot{\mathcal{W}}_1 = - \sum_{j=1}^l \dot{\mathbf{q}}_j^T \bar{\Lambda}_j^d \chi(\dot{\mathbf{q}}_j) - \sum_{j=1}^m \dot{\mathbf{q}}_j^T \frac{\partial \mathcal{F}_j(\dot{\mathbf{q}}_j)}{\partial \dot{\mathbf{q}}_j} - \sum_{j=1}^m \sum_{n \in \mathcal{N}_j} \dot{\mathbf{q}}_{jn}^T \bar{\Lambda}_{jn}^d \chi(\dot{\mathbf{q}}_{jn}) \leq 0 \quad (5.14)$$

which is a negative semi-definite decrescent function. In addition, one can show that the time derivative of the Lyapunov function candidate \mathcal{W}_2 along the trajectories of the closed-loop system (2.7) and (5.10) is given by

$$\dot{\mathcal{W}}_2 = - \sum_{j=1}^l \dot{\mathbf{q}}_j^T \underline{\Lambda}_j^d \chi(\dot{\mathbf{q}}_j) - \sum_{j=1}^m \dot{\mathbf{q}}_j^T \frac{\partial \mathcal{F}_j(\dot{\mathbf{q}}_j)}{\partial \dot{\mathbf{q}}_j} - \sum_{j=1}^m \sum_{n \in \mathcal{N}_j} \dot{\mathbf{q}}_{jn}^T \underline{\Lambda}_{jn}^d \chi(\dot{\mathbf{q}}_{jn}) \leq 0 \quad (5.15)$$

which is a negative semi-definite decrescent function.

Furthermore, from the condition (v) of Definition 2.6.1, and by using conditions (a) and (b) of Assumption 5.4.2, one can show that at each switching instant from the constrained *reconfigured* controller to the constrained *nominal* controller, we have $\bar{\lambda}_r^p|_j \int_0^{\tilde{q}_{r,j}} \chi_1(\xi) d\xi = \underline{\lambda}_r^p|_j \int_0^{\tilde{q}_{r,j}} \chi_2(\xi) d\xi$ and $\bar{\lambda}_r^p|_{jn} \int_0^{q_{r,jn}} \chi_1(\xi) d\xi = \underline{\lambda}_r^p|_{jn} \int_0^{q_{r,jn}} \chi_2(\xi) d\xi$. These properties along with Definition 5.4.3 imply that at each switching instant from the constrained *reconfigured* controller to the constrained *nominal* controller we have $\mathcal{W}_2(\bar{\mathbf{y}}) = \mathcal{W}_1(\bar{\mathbf{y}})$, where $\bar{\mathbf{y}} = [\dot{\mathbf{q}}_j^T, \tilde{\mathbf{q}}_j^T, \mathbf{q}_{jn}^T]^T$.

Additionally, from condition (v) of Definition 2.6.1, and by using conditions (a) and (b) of Assumption 5.4.2, one can show that at each switching instance from the constrained *nominal* controller to the constrained *reconfigured* controller, we have $\bar{\lambda}_r^p|_j \int_0^{\tilde{q}_{r,j}} \chi_1(\xi) d\xi \geq \underline{\lambda}_r^p|_j \int_0^{\tilde{q}_{r,j}} \chi_2(\xi) d\xi$ and $\bar{\lambda}_r^p|_{jn} \int_0^{q_{r,jn}} \chi_1(\xi) d\xi \geq \underline{\lambda}_r^p|_{jn} \int_0^{q_{r,jn}} \chi_2(\xi) d\xi$. These properties along with Definition 5.4.3 imply that at each switching instant from the constrained *nominal* controller to the constrained *reconfigured* controller, we have $\mathcal{W}_1(\bar{y}) \geq \mathcal{W}_2(\bar{y})$. From equations (5.12) and (5.13), we have $\text{sgn}(\dot{\mathcal{W}}_1(y)) = \text{sgn}(\dot{\mathcal{W}}_2(y))$, where $y = [\dot{\mathbf{q}}_j^T, \dot{\mathbf{q}}_{jn}^T]^T$. Consequently, when \mathcal{W}_1 is “non-increasing”, \mathcal{W}_2 is also “non-increasing”, and vice-versa. Therefore, it is guaranteed that the value of \mathcal{W}_1 (\mathcal{W}_2) at the beginning of each interval on which the constrained *nominal* controlled system (constrained *reconfigured* controlled system) is active does not exceed the value of \mathcal{W}_1 (\mathcal{W}_2) at the end of the previous such interval, if one exists.

Now by taking into account the strong connectivity of the communication graph, and invoking Lemma 2.9.5 under part (c) of Assumption 5.4.2 it follows from equations (5.14) and (5.15) that $\dot{\mathbf{q}}_j \rightarrow 0$ and $\dot{\mathbf{q}}_{jn} \rightarrow 0$, $\forall j, n \in \{1, \dots, m\}, j \neq n$ as $t \rightarrow \infty$. In addition, under part (c) of Assumption 5.4.2 and by invoking Lemma 2.9.5 one can conclude that $\ddot{\mathbf{q}}_j \rightarrow 0$, $\forall j \in \{1, \dots, m\}$ as $t \rightarrow \infty$. Therefore, the closed-loop dynamics of the j -th EL system can be written as $\mathbf{D}_j(\mathbf{q}_j)\ddot{\mathbf{q}}_j = -\Lambda_j^p \chi(\tilde{\mathbf{q}}_j) - \sum_{n \in \mathcal{N}_j} \Lambda_{jn}^p \chi(\mathbf{q}_{jn}) \rightarrow 0$, $\forall j, n \in \{1, \dots, m\}, j \neq n$ as $t \rightarrow \infty$. Given that $\Lambda_{jn}^p = \Lambda_{nj}^p$ and $\chi(\mathbf{q}_{jn}) = -\chi(\mathbf{q}_{nj})$, it is straightforward to show that $\sum_{j=1}^m \sum_{n \in \mathcal{N}_j} \Lambda_{jn}^p \chi(\mathbf{q}_{jn}) = 0$, which implies that $\sum_{j=1}^l \Lambda_j^p \chi(\tilde{\mathbf{q}}_j) = 0$. Therefore, the requirements of Lemma 4.2.1 are satisfied, and one can conclude that $\tilde{\mathbf{q}}_j \rightarrow 0$, $\mathbf{q}_{jn} \rightarrow 0$, $\forall j, n \in \{1, \dots, m\}, j \neq n$, as $t \rightarrow \infty$. In other words, (A) all the states and control signals of the closed-loop networked EL system will remain bounded, (B) the synchronization errors asymptotically converge to the origin, i.e., $\mathbf{q}_{jn} \rightarrow 0$ and $\dot{\mathbf{q}}_{jn} \rightarrow 0$ as $t \rightarrow \infty$, and

Table 5.1: Physical parameters for each manipulator in the network

Index	m_1 (kg)	m_2 (kg)	l_1 (m)	l_2 (m)	l_{c1} (m)	l_{c2} (m)
1	3	5	0.3	0.5	0.15	0.25
2	3.5	10.5	0.4	0.4	0.2	0.2
3	3.5	6.5	0.45	0.5	0.225	0.25
4	5.5	6.5	0.65	0.75	0.325	0.375
5	7.5	6.5	0.65	0.35	0.325	0.175
6	8.5	4.5	0.45	0.75	0.225	0.375

(C) the set-point tracking errors asymptotically converge to the origin, i.e., $\tilde{\mathbf{q}}_j \rightarrow 0$, $\dot{\mathbf{q}}_j \rightarrow 0$ as $t \rightarrow \infty$. This completes the proof of the theorem. ■

5.5 Simulation Results

We divide the simulation results into two parts. The first part discusses synchronization control with input constraints and in presence of switching in the communication network topology and absence of actuator faults. In the second part, we only discuss controller reconfiguration strategy in presence of actuator saturation faults.

5.5.1 Synchronization Control with Input Saturation Constraints

In simulations conducted in this subsection we consider a network of six 2-DOF *nonlinear* manipulators with revolute joints. Each manipulator dynamics is described by the EL model (2.7). Their inertia matrices, Coriolis and centrifugal matrices can be found in Section 2.3.1, where the gravity vectors are assumed to be zero. The physical parameters for each manipulator are provided in Table 5.1. We set $\chi(x) \triangleq \text{Sat}(x) = \frac{x}{\sqrt{\kappa^2 + x^2}}$, with $\kappa = 0.5$.

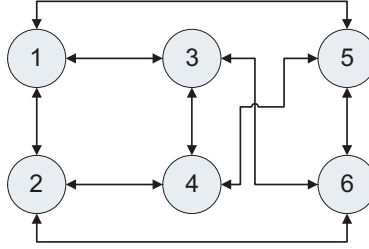


Figure 5.1: The communication network considered in the first two case study simulations.

In the first part of the simulations below, we consider the synchronization (formation-keeping) control (consensus control) objective with and without velocity feedback and exchange. We also compare the performance of our proposed constrained controllers with the constrained synchronization controller that is proposed in [63] (refer to equation (7) in [63]) with a fixed communication network topology. In the second part of the simulations in this subsection, we consider the synchronization and set-point tracking control objective in presence of switchings in the communication network topology.

Table 5.2: Performance of the state synchronization control strategies.

Performance measure	Controller (5.1)	Controller (5.6)	Controller in [63] (eq. 7)
$\sum_{j=1}^6 \sum_{n=1, n \neq j}^6 \int_0^{200} (q_1 _{jn})^2 dt$	61.91	95.30	299.57
$\sum_{j=1}^6 \sum_{n=1, n \neq j}^6 \int_0^{200} (q_2 _{jn})^2 dt$	5.48	3.98	21.82
$\sum_{j=1}^6 \sum_{n=1, n \neq j}^6 \int_0^{200} (\dot{q}_1 _{jn})^2 dt$	14.28	11.97	20.86
$\sum_{j=1}^6 \sum_{n=1, n \neq j}^6 \int_0^{200} (\dot{q}_2 _{jn})^2 dt$	3.06	3.98	7.73
$\sum_{j=1}^6 \int_0^{200} (u_1 _j)^2 dt$	14.67	18.76	6.10
$\sum_{j=1}^6 \int_0^{200} (u_2 _j)^2 dt$	2.07	3.44	0.70

State Synchronization Problem

In this part of simulations we only consider the problem of synchronization (formation-keeping) control (consensus control) with and without velocity feedback and exchange subject to input constraints. The communication network topology is depicted in Fig. 5.1. It is assumed that the maximum torque capacity of the i -th actuator for the j -th system is bounded by 1.2 [N.m], i.e. $\bar{u}_l^{\max}|_j = 1.2$, where $l \in \{1,2\}$, $j \in \{1, \dots, 6\}$ in this part of the simulations. Therefore, the controller gain matrices are selected as: $\Lambda_{jn}^p = \Lambda_{nj}^p = 0.4\mathfrak{J}_2$, $\Lambda_{jn}^d = \Lambda_{nj}^d = 0.8\mathfrak{J}_2$, where $j \in \mathcal{V}$, $n \in \mathcal{N}_j$. It is guaranteed according to the inequality (5.3) that the state synchronization (formation-keeping) control effort is bounded by 1.2 [N.m] for all times, with and without velocity feedback. Additionally, the initial conditions (both positions and velocities) are chosen randomly between 0 and 1 in the simulations.

We now compare the performance of our proposed distributed state synchronization controllers with the controller that is proposed in [63]. The gains of the constrained controller developed in [63] are selected such that the control efforts do not exceed the actuator limits. We have conducted 10 Monte Carlo simulation runs. The average time integral of the squared position and velocity synchronization errors as well as the average time integral of the squared control efforts are provided in Table 5.2 for the first 200 seconds. This table clearly shows that the performance of our proposed constrained distributed synchronization controllers (with velocity feedback and without velocity feedback) are considerably superior to that of the constrained controller that is proposed in [63] for both position and velocity synchronization objectives. Our improved results are admittedly accomplished with larger overall control efforts, however the available control effort is utilized more efficiently. Note that the bounds on the control efforts have not been violated during

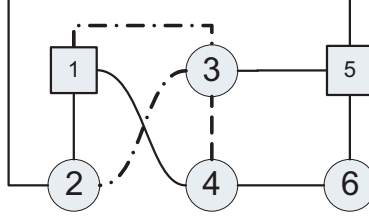


Figure 5.2: The communication network considered in the second part of the simulation studies in this subsection. The black vertices represent fixed communication links and the dashed and dashed-dotted vertices represent switching communication links. The agents shown with boxes are the leaders and agents shown by circles represent the followers.

the simulations. It also follows from Table 5.2 that when the velocity information is not available for feedback and exchange among the agents, the overall velocity synchronization performance has not been compromised and adversely affected significantly for the networked EL systems.

State Synchronization and Set-Point Tracking Control Problem with Switchings in the Communication Network Topology

In the last part of simulations in this subsection, we consider the problem of both synchronization (formation-keeping) control and set-point tracking (station-keeping) control with and without velocity feedback and exchange subject to input constraints *as well as* switchings in the communication network topology. The communication network is depicted in Fig. 5.2. The black vertices represent fixed communication links and the dashed and dashed-dotted vertices represent non-fixed (switching) communication links. Based on this figure, agent 3 always receives information from agent 5, it also receives information from agents 1 and 2, however, this depends on the distance among them with agent 3. Specifically, based on Assumption 5.2.1 if $\|\mathbf{q}_{13}\| \leq \|\mathbf{q}_{23}\|$ then agent 3 communicates with agent 1, otherwise, it communicates with agent 2. Similarly, agent 3 receives information from

agent 4, however, this depends on the distance among these two agents. Specifically, based on Assumption 5.2.1 if $\|\mathbf{q}_{34}\| \leq 0.01$, then agent 3 communicates with agent 4, otherwise, there will be no communication among these two agents. It is assumed that only agents 1 and 5 receive the desired set-point and are equipped with station-keeping and formation-keeping controllers. Other agents in the network are *only* equipped with formation-keeping controllers. The gains of the constrained controllers (5.1) and (5.6) are selected as: $\Lambda_j^p = 0.8\mathfrak{J}_2$, $\Lambda_j^d = 0.45\mathfrak{J}_2$, $\Lambda_{jn}^p = 0.4\mathfrak{J}_2$, $\Lambda_{jn}^d = 0.5\mathfrak{J}_2$, where $j \in \mathcal{V}$, $n \in \mathcal{N}_j$. It is guaranteed according to the inequality (5.3) that the control effort is bounded by 1.2 [N.m] for agents 2, 3 and 4 and it is bounded by 2.0 [N.m] for agents 1 and 5 and bounded by 0.8 [N.m] for agent 6, for all times, with and without velocity feedback. Additionally, the initial conditions (both positions and velocities) are chosen randomly between -0.5 and 0.5 in the simulations.

Figs. 5.3-5.5 show the angular positions, angular velocities, as well as control efforts for the six manipulators in the network, respectively, with velocity feedback for the first 250 seconds. From these figures one can observe that the synchronization is achieved before trajectory tracking, and also the desired set-point is followed. Fig. 5.8 also confirms that the limits on the control efforts are also satisfied. In simulations conducted we observed 35 switchings in the communication network topology, i.e. $N_{sw} = 35$. Consequently, one can show that $\tau_{ad} = 7.14$ seconds. This from Lemma 2.9.3 implies that there exists a non-vanishing dwell-time, $\bar{\tau}$, in the interval $(0, 7.14)$ for the switched networked system.

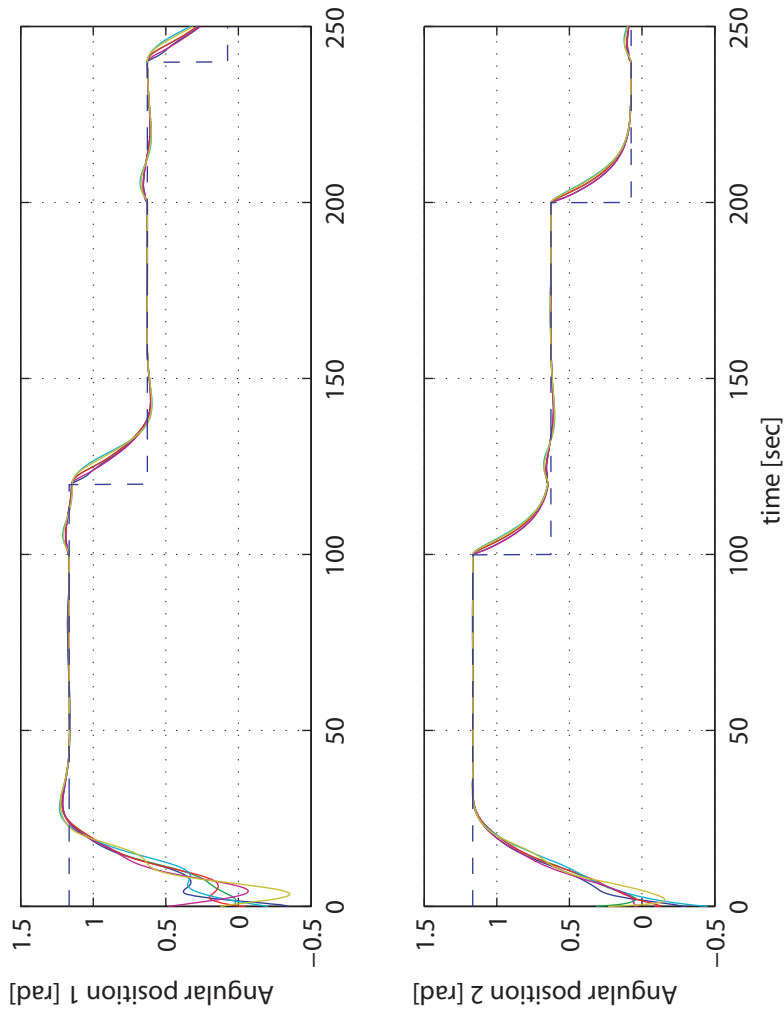


Figure 5.3: The angular positions of the six 2-DOF *nonlinear* manipulators in the network with velocity feedback and switchings in the communication network topologies. The dashed blue line represents the reference signal.

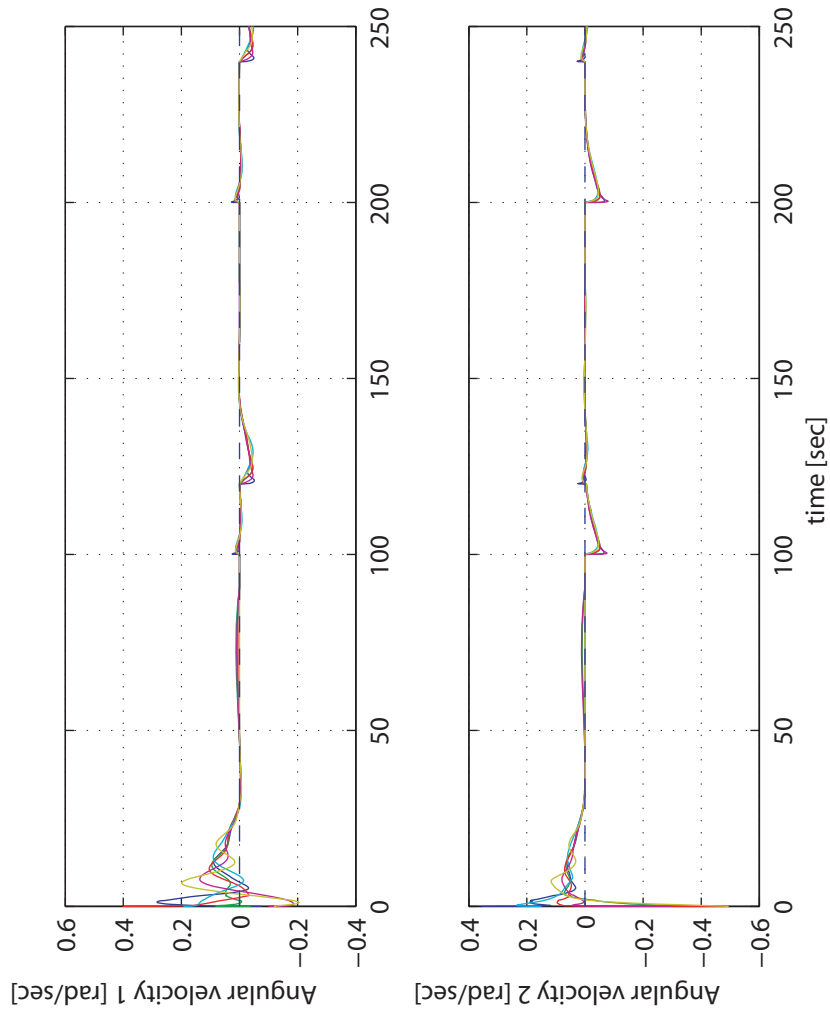


Figure 5.4: The angular velocities of the six 2-DOF *nonlinear* manipulators in the network with velocity feedback and switchings in the communication network topologies. The dashed blue line represents the reference signal.

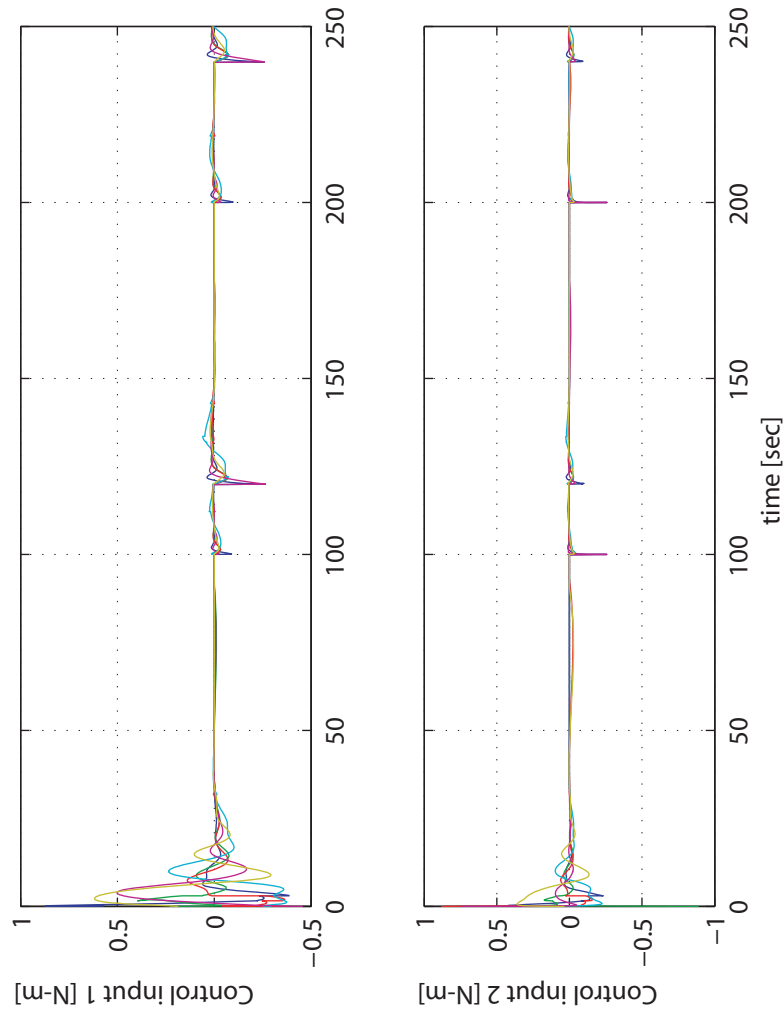


Figure 5.5: The control efforts of the six 2-DOF *nonlinear* manipulators in the network with velocity feedback and switchings in the communication network topologies.

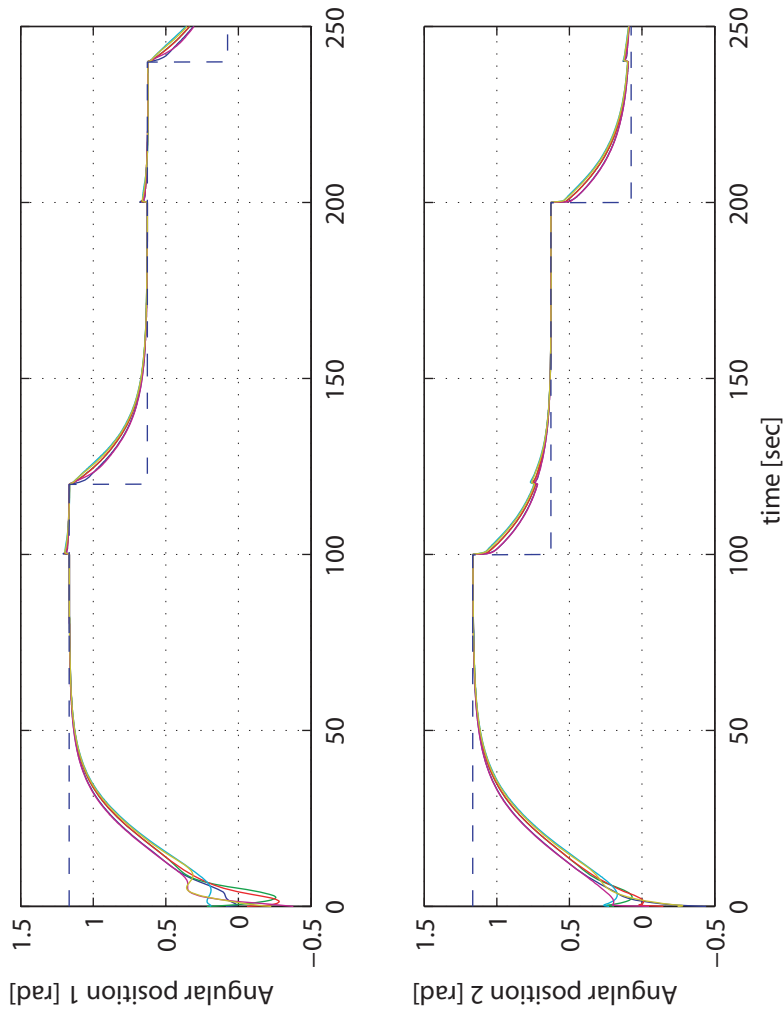


Figure 5.6: The angular positions of the six 2-DOF *nonlinear* manipulators in the network *without* velocity feedback and switchings in the communication network topologies. The dashed blue line represents the reference signal.

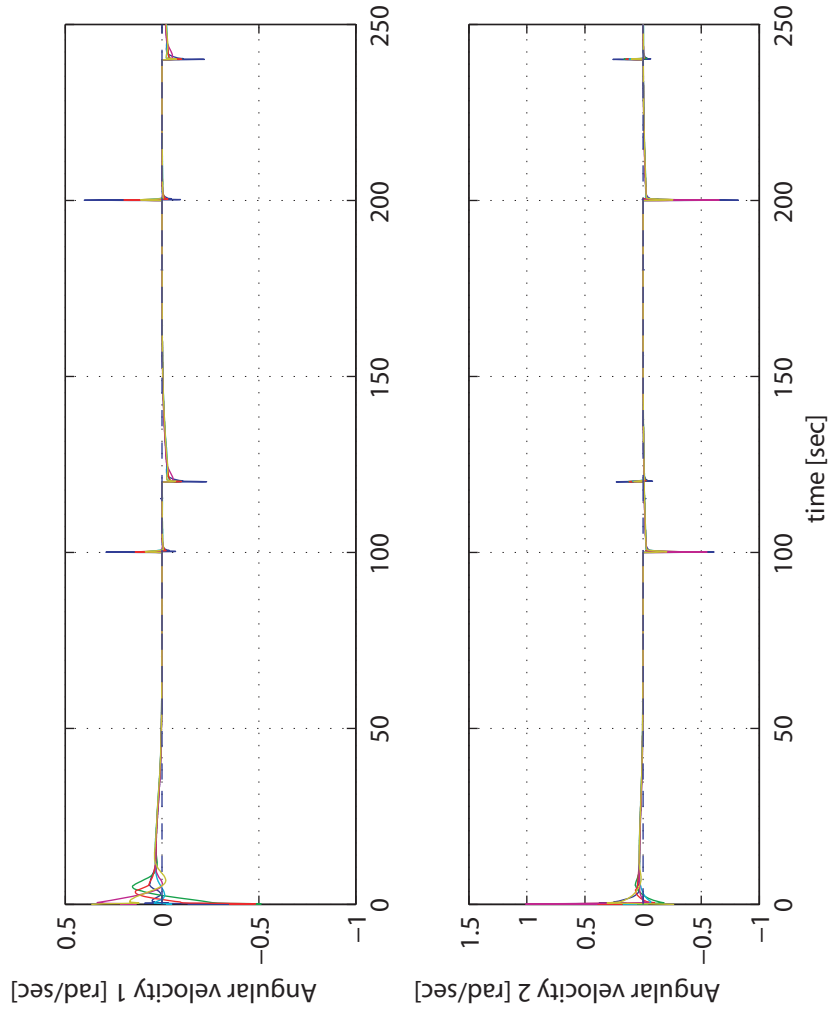


Figure 5.7: The angular velocities of the six 2-DOF *nonlinear* manipulators in the network *without* velocity feedback and switchings in the communication network topologies. The dashed blue line represents the reference signal.

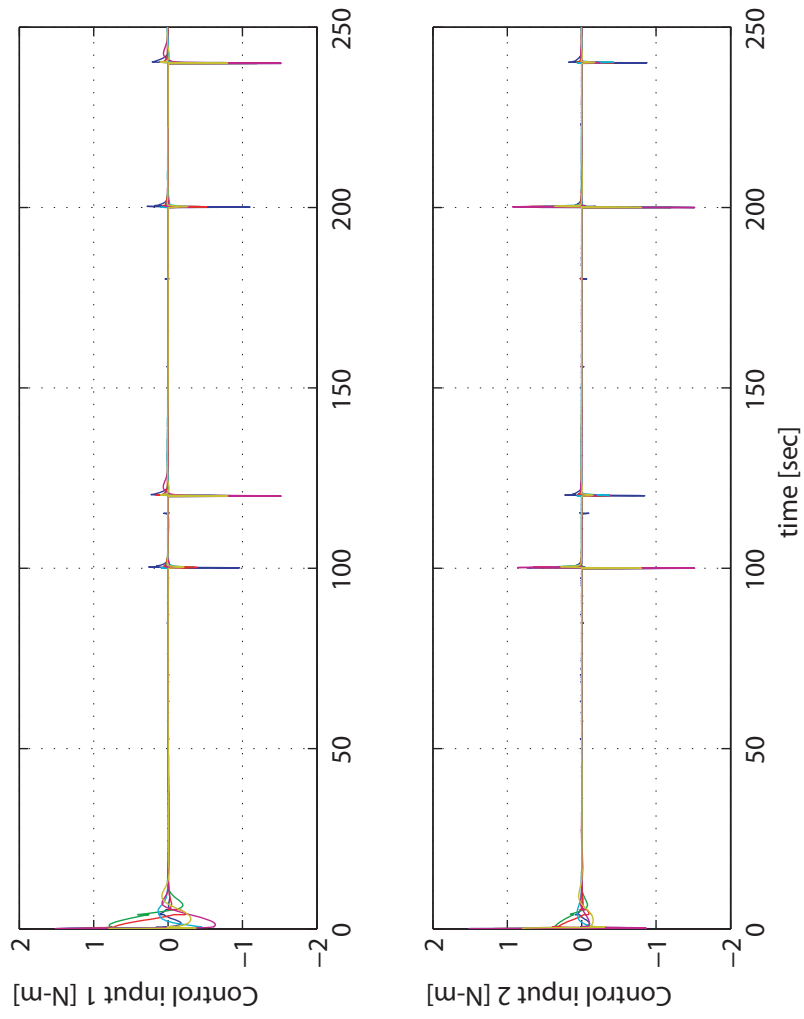


Figure 5.8: The control efforts of the six 2-DOF *nonlinear* manipulators in the network *without* velocity feedback and switchings in the communication network topologies.

The angular positions, angular velocities, and control efforts for the six manipulators in the network are depicted in Figs. 5.6-5.8, respectively, without velocity feedback for the first 250 seconds. From these figures one can observe that the synchronization is achieved before the trajectory tracking, and also the desired set-point is followed. In addition, one can observe that the limits on the control efforts are also satisfied. In simulations conducted we observed 11 switchings in the communication network topology, i.e. $N_{sw} = 11$. Consequently, one can show that $\tau_{ad} = 22.72$ seconds. This from Lemma 2.9.3 implies that there exists a non-vanishing dwell-time, $\bar{\tau}$, in the interval $(0, 22.72)$ for the switched networked system. These simulation results confirm our analytical results.

5.5.2 Cooperative Controller Reconfiguration

The reconfigurable control scheme that we have developed in the previous sections is now applied to the problem of cooperative control of a team of robot manipulators. The nonlinear dynamical models corresponding to the manipulators are developed in the Matlab SimMechanics toolbox. We consider three *non-identical* (heterogenous) manipulators ($m = 3$) with two rotational joints. We further consider a fully bidirectionally connected communication graph with two leaders (the manipulators #1 and #2, i.e. $l = 2$) and one follower (the manipulator #3). Note that providing the desired coordinate vector to only one single leader creates the possibility of a single point of failure in the network. Therefore, for the purpose of conducting simulations we consider a team having two leaders and one follower.

Through the use of our proposed control approach, we will illustrate subsequently that synchronization errors do indeed asymptotically converge to zero

for the manipulators in the network while following the desired coordinate vector which is assumed to be identical for the three manipulators. It is assumed that the torques that are applied to the joints are initially constrained during the normal operation of the actuators with $\bar{u}_j^{\max} = 30$ N-m, $j \in \{1, 2, 3\}$. However, due to an intermittent actuator fault in the manipulator #1, the maximum torque that is available to the first joint is reduced to $\underline{u}_1^{\max}|_1 = 6$ N-m. This intermittent fault is injected at $t_{\text{fault}} = 370$ sec and is *cleared* at $t = 550$ sec. The constrained *nominal* controller gains for the manipulator #1 are selected as follows, namely, $\bar{\Lambda}_1^p = 4\mathfrak{J}_2$, $\bar{\Lambda}_1^d = 6\mathfrak{J}_2$, $\bar{\Lambda}_{12}^p = 4\mathfrak{J}_2$, $\bar{\Lambda}_{12}^d = 6\mathfrak{J}_2$, $\bar{\Lambda}_{13}^p = 4\mathfrak{J}_2$, $\bar{\Lambda}_{13}^d = 6\mathfrak{J}_2$. The constrained *reconfigured* controller gains for the manipulator #1 are selected as follows, namely, $\underline{\Lambda}_1^p = \mathbf{Diag}(0.5, 4)$, $\underline{\Lambda}_1^d = \mathbf{Diag}(0.5, 6)$, $\underline{\Lambda}_{12}^p = \mathbf{Diag}(2, 4)$, $\underline{\Lambda}_{12}^d = \mathbf{Diag}(1, 6)$, $\underline{\Lambda}_{13}^p = \mathbf{Diag}(1, 4)$, $\underline{\Lambda}_{13}^d = \mathbf{Diag}(1, 6)$. The constrained controllers (nominal and reconfigured) gains for the manipulator #2 are selected as follows, namely, $\bar{\Lambda}_2^p = \underline{\Lambda}_2^p = 4\mathfrak{J}_2$, $\bar{\Lambda}_2^d = \underline{\Lambda}_2^d = 6\mathfrak{J}_2$, $\bar{\Lambda}_{21}^p = 4\mathfrak{J}_2$, $\bar{\Lambda}_{21}^d = 6\mathfrak{J}_2$, $\bar{\Lambda}_{23}^p = \underline{\Lambda}_{23}^p = 4\mathfrak{J}_2$, $\bar{\Lambda}_{23}^d = \underline{\Lambda}_{23}^d = 6\mathfrak{J}_2$, $\underline{\Lambda}_{21}^p = \mathbf{Diag}(2, 4)$, $\underline{\Lambda}_{21}^d = \mathbf{Diag}(1, 6)$. The constrained controllers (nominal and reconfigured) gains for the manipulator #3 are selected as follows, namely, $\bar{\Lambda}_3^p = \underline{\Lambda}_3^p = 0$, $\bar{\Lambda}_3^d = \underline{\Lambda}_3^d = 0$, $\bar{\Lambda}_{31}^p = 4\mathfrak{J}_2$, $\bar{\Lambda}_{31}^d = 6\mathfrak{J}_2$, $\bar{\Lambda}_{32}^p = \underline{\Lambda}_{32}^p = 4\mathfrak{J}_2$, $\bar{\Lambda}_{32}^d = \underline{\Lambda}_{32}^d = 6\mathfrak{J}_2$, $\underline{\Lambda}_{31}^p = \mathbf{Diag}(2, 4)$, $\underline{\Lambda}_{31}^d = \mathbf{Diag}(1, 6)$.

We use the linear saturation function, i.e., $\chi_1(x) = \begin{cases} x & \text{if } -1 \leq x \leq 1 \\ \text{sgn}(x) & \text{otherwise} \end{cases}$,

for the constrained *nominal* controller and $\chi_2(x) = \frac{x}{\sqrt{\kappa^2 + x^2}}$ for the constrained *reconfigured* controller in our simulations with $\kappa = 0.2$. The closed-loop responses of the manipulators under the proposed nominal and reconfigured control strategies are depicted in Fig. 5.9(a). The associated control efforts of the manipulator #1 for joints 1 and 2 are depicted in Fig. 5.9(b). It follows from Fig. 5.9(a) that prior to the injection of the fault, the angular positions settle down to their desired set-points by

using the constrained *nominal* controller.

At $t = 400$ sec while the fault is still present the set-point of the joint 1 of all the manipulators is changed. Due to the coupling effects, the change in the set-point of joint 1 causes a change in the angular position of joint 2. It can be observed from Fig. 5.9(b) that from $t = 370$ sec to $t = 400$ sec the control efforts do not exceed the saturation limit of 6 N-m. However, the required torque to maintain the manipulator #1 joint 1 at its desired angular position becomes higher than that of its actuator limit as seen from Fig. 5.9(b). Consequently, this leads to the actuator saturation and *instability* of the network of manipulators (from $t = 400$ sec to $t = 430$ sec). It is now assumed that the control reconfiguration is implemented and invoked at $t_{\text{reconf.}} = 430$ sec, that is the controller is switched from the constrained *nominal* to the constrained *reconfigured* module.

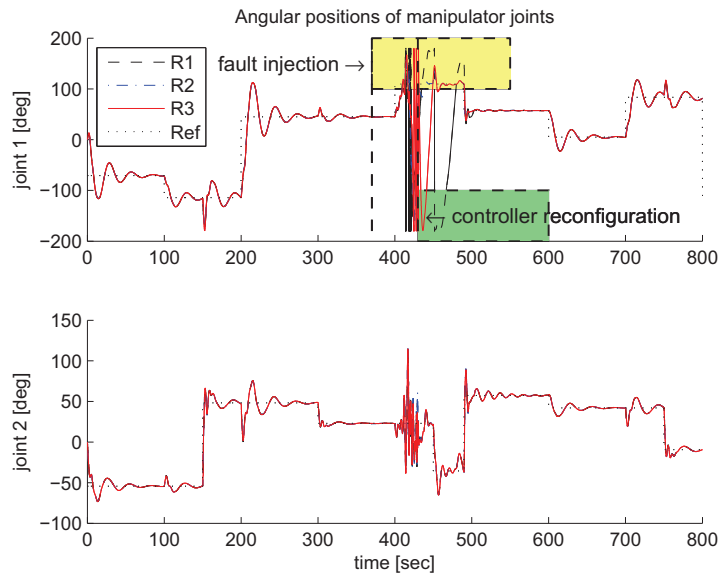
Fig. 5.9(a) shows that after the controller reconfiguration at $t = 430$ sec, the closed-loop networked system is stabilized and the angular position errors converge to zero by utilizing the constrained control effort of 6 N-m in the first joint of manipulator #1. Moreover, to further demonstrate the stability of our switched system, at time $t = 550$ sec the fault is *removed* or *cleared* from the actuator of the manipulator #1. Subsequently, following the conditions of Assumption 5.4.2 we switch from the constrained *reconfigured* controller to the constrained *nominal* controller at time $t = 600$ sec (the top yellow boxes in Fig. 5.9(a) and Fig. 5.9(b) show the duration when the fault is present and the bottom green boxes show the duration when the constrained *reconfigured* control is active). It can be observed from Fig. 5.9(a) that after $t = 600$ sec the tracking errors converge to zero as required.

For providing a more descriptive explanation on the behavior of the synchronization error, in Fig. 5.10(a) the closed-loop EL system responses before and after the controller reconfiguration are provided. One can observe from Fig. 5.10(b) that

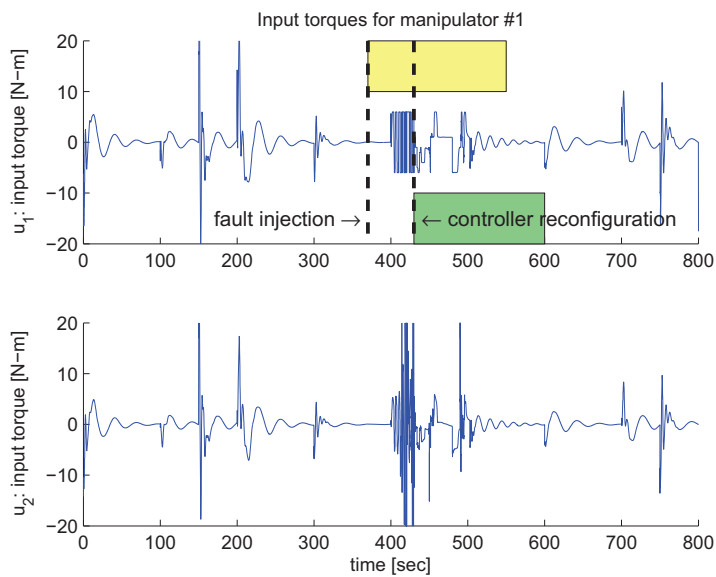
the synchronization errors are smaller when the constrained *nominal* controllers are used as compared to the constrained *reconfigured* controllers. This is obviously due to the fact that while the control effort constraints on the constrained *nominal* system are satisfied, nevertheless, degradations in the performance of the faulty system are unavoidable due to the reduction of the control effort. Therefore, it is highly recommended that one switches to the constrained *reconfigured* controller only when a fault is present in the system. On the other hand, when the fault is removed or cleared and during the healthy operation of the EL system agents, the constrained *nominal* controller should be used exclusively.

5.6 Concluding Remarks

In this chapter, we provided two distributed bounded and nonlinear controllers for state synchronization and set-point tracking of networked Euler-Lagrange systems in presence of input constraints and switchings in the communication network topology. The first controller requires velocity feedback and exchange among the agents, whereas the second controller does not require velocity measurements and exchange among the agents. This considerably reduces the required communication load among the agents without sacrificing the overall networked system performance. Our second contribution is development of a reconfiguration strategy for cooperative control of a network of nonlinear EL systems subject to actuator faults. The proposed nonlinear *nominal* and *reconfigured* constrained control strategies each individually guarantee stability of the EL networked agents states and control signals and guarantee global convergence of set-point tracking errors and state

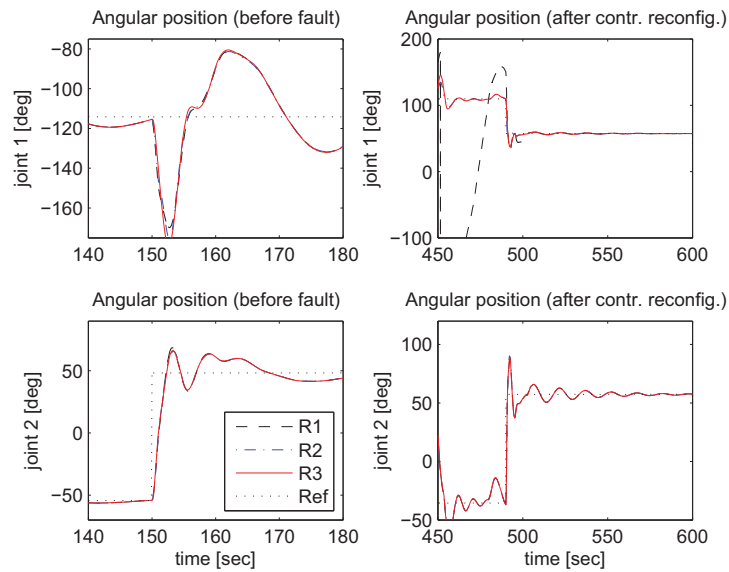


(a) Angular positions of the three manipulators.

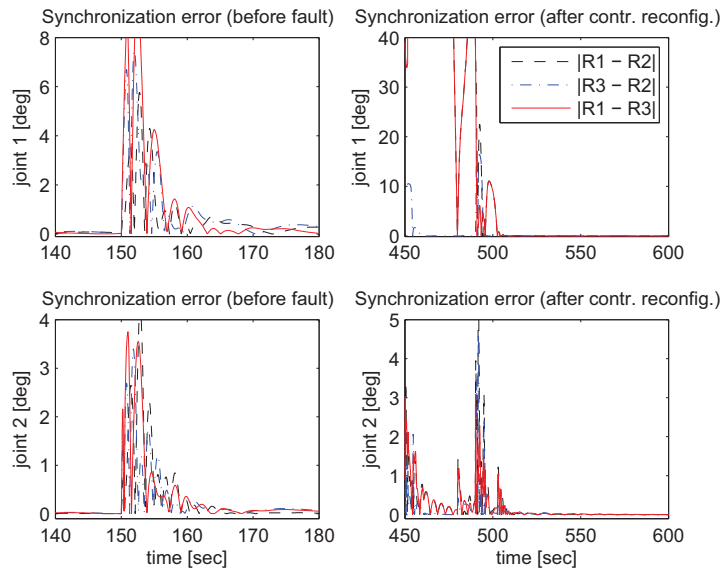


(b) Zoomed control efforts of the robotic manipulator # 1 for clarity (the actual bounds of the actuators are ± 30 N-m).

Figure 5.9: Reconfigurable control of three robotic manipulators (R1 to R3) when an intermittent fault is injected at $t = 370$ sec and cleared at $t = 550$ sec *only* in the actuator # 1 of manipulator # 1.



(a) Closed-loop angular position responses.



(b) Synchronization errors in angular positions.

Figure 5.10: Scaled responses before an intermittent fault is injected only in the joint #1 of manipulator #1 and after the control reconfiguration.

synchronization errors to the origin despite the presence of actuator saturation constraints and intermittent or permanent actuator faults. The performance of our proposed reconfigurable control strategy is demonstrated by simulation of networked manipulators subject to an actuator fault and actuators saturation constraints.

Chapter 6

Quaternion-Based Attitude

Synchronization and Tracking for Spacecraft Formation

6.1 Introduction and Problem Statement

We propose two quaternion-based attitude synchronization and set-point tracking for networked spacecraft (SC) in this chapter. Our proposed algorithms guarantee boundedness of the control effort for all initial conditions. Furthermore, by using our proposed control law, the desired attitude coordinates are only provided to a subset of SC in the formation called the formation leaders. This essentially increases flexibility in the design of the formation structure which increases robustness of the formation to component faults. Our second proposed control law does not require exchange of spacecraft angular velocities (or their estimates) among the spacecraft in the network. Furthermore, we have used bidirectional communication between the agents, which increases robustness of the formation to component

faults. In the simulations presented our proposed constrained attitude controllers are compared to the controller proposed recently in the literature and it is shown in the simulations that our proposed controllers have a better performance.

6.1.1 Spacecraft Attitude Error Dynamics

For a SC in a formation we define two error measures. These measures are the *station-keeping* and the *formation-keeping* attitude state errors. The station-keeping error is defined as the attitude state error of an individual SC with respect to its absolute desired attitude state. The station-keeping error, $\delta\vec{q}_j$, is defined as:

$$\delta\vec{q}_j = \mathcal{Q}(\vec{q}_j^*{}^{-1})\vec{q}_j \quad (6.1)$$

where \vec{q}_j^* is the desired attitude of the SC formation and the matrix $\mathcal{Q}(\vec{q})$ is defined as:

$$\mathcal{Q}(\vec{q}) = \begin{bmatrix} \bar{E}(\vec{q}) & \bar{q} \\ -\bar{q}^T & \hat{q}_4 \end{bmatrix}$$

where $\bar{E}(\vec{q}) = q_4\mathcal{I}_{3 \times 3} + \bar{q}^\times$. One can decompose the station-keeping error into a vector and a scalar part, namely, $\delta\vec{q}_j = [\delta\bar{q}_j^T, \delta\hat{q}_{j,4}]^T$.

The station-keeping angular velocity error, $\delta\omega_j$, is defined as:

$$\delta\omega_j = \omega_j - \Omega_j \quad (6.2)$$

where $\Omega_j = \mathbf{R}(\delta\vec{q}_j)\omega^*$, and $\omega^* \in C^1$ is the absolute desired angular velocity vector

expressed in the absolute desired reference frame. The first derivative of the station-keeping angular velocity error is obtained as [93]:

$$\delta \dot{\omega}_j = \dot{\omega}_j - \mathbf{R}(\delta \vec{q}_j) \dot{\omega}^* + \omega_j^\times \Omega_j \quad (6.3)$$

We can now express the governing equations for the attitude error $\delta \vec{q}_j$ and the angular velocity error $\delta \omega_j$ as follows:

$$\delta \dot{\vec{q}}_j = \frac{1}{2} E(\delta \vec{q}_j) \delta \omega_j \quad (6.4)$$

$$\mathbf{J}_j \delta \dot{\omega}_j = \mathbf{u}_j - \omega_j^\times \mathbf{J}_j \omega_j + \mathbf{J}_j \left(\omega_j^\times \Omega_j - \mathbf{R}(\delta \vec{q}_j) \dot{\omega}^* \right) \quad (6.5)$$

where the matrix $E(\vec{q})$ is given by

$$E(\vec{q}) = \begin{bmatrix} q_4 \tilde{\mathcal{J}}_{3 \times 3} + \vec{q}^\times \\ -\vec{q}^T \end{bmatrix} \equiv \begin{bmatrix} \bar{E}(\vec{q}) \\ -\vec{q}^T \end{bmatrix} \quad (6.6)$$

Formation-keeping error, for the j -th SC is the attitude state error of the j -th SC with respect to the other SC in the formation. The relative attitude error between the j -th and the n -th SC is defined as:

$$\vec{q}_{jn} = \mathcal{Q}(\vec{q}_n^{-1}) \vec{q}_j \equiv \mathcal{Q}(\delta \vec{q}_n^{-1}) \delta \vec{q}_j \quad (6.7)$$

The relative angular velocity vector of the j -th SC with respect to the n -th SC, ω_{jn} , can be written in terms of $\delta \omega_j$ and $\delta \omega_n$, as follows

$$\omega_{jn} = \delta \omega_j - \mathbf{R}(\vec{q}_{jn}) \delta \omega_n \quad (6.8)$$

Consequently, the dynamics of the relative attitude error, $\vec{\mathbf{q}}_{jn}$ is obtained as

$$\dot{\vec{\mathbf{q}}}_{jn} = \frac{1}{2}E(\vec{\mathbf{q}}_{jn})\boldsymbol{\omega}_{jn} \quad (6.9)$$

The following equations corresponding to the relative states of the j -th and the n -th SC will be used subsequently [85], namely

$$\mathbf{R}(\vec{\mathbf{q}}_{jn}) = \mathbf{R}^T(\vec{\mathbf{q}}_{nj}) \text{ and } \bar{\mathbf{q}}_{nj} = -\bar{\mathbf{q}}_{jn} = -\mathbf{R}(\vec{\mathbf{q}}_{nj})\bar{\mathbf{q}}_{jn} \quad (6.10)$$

We define two objectives in this chapter. Our first objective is to design a distributed controller for each SC which commands the actuators in order guarantee coordinated SC attitude and angular velocity alignment, i.e. $\mathbf{q}_j \rightarrow \mathbf{q}_n$ (or equivalently, $\vec{\mathbf{q}}_{jn} \rightarrow 0$) and $\boldsymbol{\omega}_{jn} \rightarrow 0$. This objective is designated as the *formation-keeping*. Our second objective is to ensure that the designed controllers guarantee that each SC attitude converges to the commanded attitude, i.e. $\delta\vec{\mathbf{q}}_j \rightarrow 0$ and $\delta\boldsymbol{\omega}_j \rightarrow 0$. This objective is designated as the *station-keeping*. Note that in the development of the control laws it is assumed that the final angular velocity for the spacecraft network is *zero*. We impose two constraints in the design, which are (1) there should be no information exchange regarding the angular velocities of the SC in the formation, and (2) there exist actuator constraints on the maximum control efforts, i.e. $u_r|_j(t) \leq \bar{u}_r^{\max}|_j$, where $f = 1, 2, 3$, $j \in \mathcal{V}$ and $\bar{u}_r^{\max}|_j$ is a known positive scalar.

6.2 Formation Attitude Synchronization and Tracking with Bounded Input

Our first result is provided in the following theorem.

Theorem 6.2.1. Consider a network of ‘ m ’ ($m > 1$) SC with the dynamic and kinematic equation (2.17). It is assumed that the desired coordinates are provided to only ‘ l ’ agents ($l \leq m$) SC in the network that are designated as the network leaders. Let the error dynamics and kinematics of the j -th SC be governed by (6.4) and (6.5). Consider the following control law for the j -th leader SC,

$$\mathbf{u}_j^{leader} = -\Delta_j \delta \bar{\mathbf{q}}_j - \sum_{n=1}^m \lambda_{jn} \text{Sat} \left(\bar{\mathbf{q}}_{jn} + \beta_{jn} \delta \boldsymbol{\omega}_j + \frac{\beta_{jn}}{2} \boldsymbol{\omega}_{jn} \right) \quad (6.11)$$

and the following control law for the j -th follower SC (which does not receive the desired coordinates),

$$\mathbf{u}_j^{follower} = - \sum_{n=1}^m \lambda_{jn} \text{Sat} \left(\bar{\mathbf{q}}_{jn} + \beta_{jn} \delta \boldsymbol{\omega}_j + \frac{\beta_{jn}}{2} \boldsymbol{\omega}_{jn} \right) \quad (6.12)$$

where $\Delta_j \in \mathbb{R}^{3 \times 3}$ is a positive definite matrix and β_{jn} is a positive constant that satisfy the equality $\beta_{jn} = \beta_{nj}$. Furthermore, we assume the communication network is bidirectional and connected, where λ_{jn} is defined in Section 2.7. The application of the control laws (6.11) and (6.12) will guarantee that the spacecraft synchronize their state and the set-point tracking error is asymptotically stable, i.e. $\bar{\mathbf{q}}_{jn} \rightarrow 0$ and $\boldsymbol{\omega}_{jn} \rightarrow 0$ as $t \rightarrow \infty$, in addition, $\delta \bar{\mathbf{q}}_j \rightarrow 0$ and $\delta \boldsymbol{\omega}_j \rightarrow 0$ as $t \rightarrow \infty$ for all spacecraft in the network (both leaders and followers).

Additionally, the j -th control effort is bounded for all time and for all initial conditions, i.e. $\|\mathbf{u}_j(t)\| \leq \|\mathbf{u}_j^{\max}\|$, provided that the controller gains Δ_j , λ_{jn} and β_{jn} for the leader SC are selected such that $\|\Delta_j\| + \sum_{n=1}^m \lambda_{jn} \leq \|\mathbf{u}_j^{\max}\|$, and for the follower SC are selected such that $\sum_{n=1}^m \lambda_{jn} \leq \|\mathbf{u}_j^{\max}\|$.

Proof: Consider the following radially unbounded decrescent Lyapunov function candidate for the SC formation,

$$\begin{aligned} \mathcal{U} = & \sum_{j=1}^m \frac{1}{2} \beta_{jn} \delta \omega_j^T \Delta_j^{-1} \mathbf{J}_j \delta \omega_j + \sum_{j=1}^l \beta_{jn} \left[\delta \bar{\mathbf{q}}_j^T \delta \bar{\mathbf{q}}_j + (1 - \delta q_{j,4})^2 \right] \\ & + \frac{1}{2} \sum_{j=1}^m \sum_{n=1}^m \beta_{jn} \lambda_{jn} \left(\bar{\mathbf{q}}_{jn}^T \bar{\mathbf{q}}_{jn} + (1 - q_{jn,4})^2 \right) \end{aligned} \quad (6.13)$$

Note that Δ^{-1} is a positive definite matrix and $\lambda_{jn} \geq 0$, this essentially implies that the above function is positive definite. The time derivative of the Lyapunov function candidate along the trajectories of the closed-loop system (6.4), (6.5), (6.11) and (6.12) is given by

$$\begin{aligned} \dot{\mathcal{U}} = & \sum_{j=1}^l \beta_{jn} \left(-\delta \omega_j^T \delta \bar{\mathbf{q}}_j + \delta \omega_j^T \delta \bar{\mathbf{q}}_j \right) + \frac{1}{2} \sum_{j=1}^m \sum_{n=1}^m \beta_{jn} \lambda_{jn} \omega_{jn}^T \bar{\mathbf{q}}_{jn} \\ & - \sum_{j=1}^m \sum_{n=1}^m \beta_{jn} \lambda_{jn} \delta \omega_j^T \text{Sat} \left(\bar{\mathbf{q}}_{jn} + \beta_{jn} \delta \omega_j + \frac{\beta_{jn}}{2} \omega_{jn} \right) \end{aligned}$$

which can be re-written as

$$\begin{aligned}
\dot{\mathcal{W}} &= - \sum_{j=1}^m \sum_{n=1}^m \beta_{jn} \lambda_{jn} \delta \omega_j^T \left[\text{Sat} \left(\bar{\mathbf{q}}_{jn} + \beta_{jn} \delta \omega_j + \frac{\beta_{jn}}{2} \omega_{jn} \right) - \text{Sat}(\bar{\mathbf{q}}_{jn}) \right] \\
&= - \frac{1}{2} \sum_{j=1}^m \sum_{n=1}^m \beta_{jn} \lambda_{jn} \delta \omega_j^T \left[\text{Sat} \left(\bar{\mathbf{q}}_{jn} + \beta_{jn} \delta \omega_j + \frac{\beta_{jn}}{2} \omega_{jn} \right) - \text{Sat}(\bar{\mathbf{q}}_{jn}) \right] \\
&\quad - \frac{1}{2} \sum_{j=1}^m \sum_{n=1}^m \beta_{jn} \lambda_{jn} \delta \omega_j^T \left[\text{Sat} \left(\bar{\mathbf{q}}_{jn} + \beta_{jn} \delta \omega_j + \frac{\beta_{jn}}{2} \omega_{jn} \right) - \text{Sat}(\bar{\mathbf{q}}_{jn}) \right] \\
&= - \frac{1}{2} \sum_{j=1}^m \sum_{n=1}^m \beta_{jn} \lambda_{jn} \delta \omega_j^T \left[\text{Sat} \left(\bar{\mathbf{q}}_{jn} + \beta_{jn} \delta \omega_j + \frac{\beta_{jn}}{2} \omega_{jn} \right) - \text{Sat}(\bar{\mathbf{q}}_{jn}) \right] \\
&\quad - \frac{1}{4} \sum_{j=1}^m \sum_{n=1}^m \beta_{jn} \lambda_{jn} \omega_{jn}^T \left[\text{Sat} \left(\bar{\mathbf{q}}_{jn} + \beta_{jn} \delta \omega_j + \frac{\beta_{jn}}{2} \omega_{jn} \right) - \text{Sat}(\bar{\mathbf{q}}_{jn}) \right] \\
&= - \frac{1}{2} \sum_{j=1}^m \sum_{n=1}^m \lambda_{jn} \left(\beta_{jn} \delta \omega_j + \frac{\beta_{jn}}{2} \omega_{jn} \right)^T \left[\text{Sat} \left(\bar{\mathbf{q}}_{jn} + \beta_{jn} \delta \omega_j + \frac{\beta_{jn}}{2} \omega_{jn} \right) - \text{Sat}(\bar{\mathbf{q}}_{jn}) \right]
\end{aligned}$$

Consequently, by noting $\chi(x+y) - \chi(x) > 0 \Leftrightarrow y > 0$, and $\chi(x+y) - \chi(x) < 0 \Leftrightarrow y < 0$, one concludes that $\dot{\mathcal{W}}$ is negative semi-definite, i.e. $\dot{\mathcal{W}} \leq 0$.

This by invoking Lemma 2.9.2 (where $\alpha \triangleq \dot{\mathcal{W}}$) essentially implies that $\omega_{jn} \rightarrow 0$ and $\delta \omega_j \rightarrow 0, j, n \in \mathcal{V}, j \neq n$ as $t \rightarrow \infty$. Consequently, by studying the closed-loop dynamics and invoking Lemma 5.2.1 one can now conclude that $\bar{\mathbf{q}}_{jn} \rightarrow 0$ and $\delta \bar{\mathbf{q}}_j \rightarrow 0$ as $t \rightarrow \infty$.

Now we show that the control effort is bounded under the control laws (6.11) and (6.12). First note that $\|\delta \bar{\mathbf{q}}_j\| \leq 1$ for all times. Consequently, one can show that for all the leader SC one has $\|\mathbf{u}_j(t)\| \leq \|\mathbf{u}_j^{\max}\|$ provided the controller gains are selected such that $\|\Delta_j\| + \sum_{n=1}^m \lambda_{jn} (1 + \bar{\beta}_{jn}) \leq \|\mathbf{u}_j^{\max}\|$. Similarly, one can show that for all the follower SC one has $\|\mathbf{u}_j(t)\| \leq \|\mathbf{u}_j^{\max}\|$ provided the controller gains are selected such that $\sum_{n=1}^m \lambda_{jn} \leq \|\mathbf{u}_j^{\max}\|$. This completes the proof of the theorem. ■

Corollary 6.2.2. *Consider a network of ‘m’ ($m > 1$) SC with the dynamic and*

kinematic equation (2.17). Consider the control law (6.12) for the j -th SC, where we set $\beta_{jn} = \beta_{nj}$. Furthermore, we assume the communication network is bidirectional and connected, where λ_{jn} is defined in Section 2.7. The application of the control law (6.12) will guarantee that the SC synchronize their states and the formation-keeping objective is achieved and the final angular velocity of the spacecraft in the network is zero. Additionally, the j -th control effort is bounded for all time and for all initial conditions, i.e. $\|\mathbf{u}_j(t)\| \leq \|\bar{\mathbf{u}}_j^{\max}\|$, provided that the controller gains λ_{jn} for the j -th SC are selected such that $\sum_{n=1}^m \lambda_{jn} \leq \|\bar{\mathbf{u}}_j^{\max}\|$.

Proof: It follows from Theorem 6.2.1.

6.3 Formation Attitude Synchronization and Tracking with Bounded Input without Velocity Feedback

Our last result is provided in the following theorem.

Theorem 6.3.1. Consider a network of ‘ m ’ ($m > 1$) SC with the dynamic and kinematic equation (2.17). It is assumed that the desired coordinates are provided to only ‘ l ’ ($l \leq m$) SC in the formation that are designated as the leaders. Consider

the following control law for the j -th leader SC,

$$\left\{ \begin{array}{l} \mathbf{u}_j^{leader} = -\Delta_j \delta \bar{\mathbf{q}}_j \\ \quad - \sum_{n=1}^m \lambda_{jn} \text{Sat} \left[\bar{\mathbf{q}}_{jn} + \beta_{jn} \left(\bar{E}^T (\delta \mathbf{q}_j) (-\gamma \mathbf{z}_j + \gamma \delta \bar{\mathbf{q}}_j) \right. \right. \\ \quad \left. \left. + \bar{E}^T (\mathbf{q}_{jn}) (-\gamma \mathbf{z}_{jn} + \gamma \bar{\mathbf{q}}_{jn}) \right) \right] \\ \dot{\mathbf{z}}_j = -\gamma \mathbf{z}_j + \gamma \delta \bar{\mathbf{q}}_j \\ \dot{\mathbf{z}}_{jn} = -\gamma \mathbf{z}_{jn} + \gamma \bar{\mathbf{q}}_{jn} \end{array} \right. \quad (6.14)$$

and the following control law for the j -th follower SC (which does not receive the desired attitude coordinates),

$$\left\{ \begin{array}{l} \mathbf{u}_j^{follower} = - \sum_{n=1}^m \lambda_{jn} \text{Sat} \left[\bar{\mathbf{q}}_{jn} + \beta_{jn} \left(\bar{E}^T (\delta \mathbf{q}_j) (-\gamma \mathbf{z}_j + \gamma \delta \bar{\mathbf{q}}_j) \right. \right. \\ \quad \left. \left. + \bar{E}^T (\mathbf{q}_{jn}) (-\gamma \mathbf{z}_{jn} + \gamma \bar{\mathbf{q}}_{jn}) \right) \right] \\ \dot{\mathbf{z}}_j = -\gamma \mathbf{z}_j + \gamma \delta \bar{\mathbf{q}}_j \\ \dot{\mathbf{z}}_{jn} = -\gamma \mathbf{z}_{jn} + \gamma \bar{\mathbf{q}}_{jn} \end{array} \right. \quad (6.15)$$

where $\Delta_j \in \mathbb{R}^{3 \times 3}$ is a positive definite matrix, $\beta_{jn} = \beta_{nj} > 0$ and $\gamma > 0$. Furthermore, we assume the communication network is bidirectional and connected, where λ_{jn} is defined in Section 2.7.

The application of the control laws (6.14) and (6.15) will guarantee that all spacecraft in the network synchronize their states and set-point tracking error is asymptotically stable, i.e. $\bar{\mathbf{q}}_{jn} \rightarrow 0$, $\mathbf{z}_{jn} \rightarrow 0$ and $\omega_{jn} \rightarrow 0$ as $t \rightarrow \infty$, in addition, $\delta \bar{\mathbf{q}}_j \rightarrow 0$, $\mathbf{z}_j \rightarrow 0$ and $\delta \omega_j \rightarrow 0$ as $t \rightarrow \infty$ for all spacecraft in the network (both leaders and followers). Furthermore, the control effort is bounded for all time and for all initial conditions, i.e. $\|\mathbf{u}_j(t)\| \leq \|\mathbf{u}_j^{\max}\|$, provided that the controller gains

Δ_j , λ_{jn} and β_{jn} for the leader SC are selected such that $\|\Delta_j\| + \sum_{n=1}^m \lambda_{jn} \leq \|\mathbf{u}_j^{\max}\|$, and for the follower SC are selected such that $\sum_{n=1}^m \lambda_{jn} \leq \|\mathbf{u}_j^{\max}\|$.

Proof: Consider the following positive-definite radially unbounded Lyapunov function candidate for the SC formation,

$$\begin{aligned}
\tilde{\mathcal{U}} = & \sum_{j=1}^l \left[\frac{1}{2} \delta \omega_j^T \Delta_j^{-1} \mathbf{J}_j \delta \omega_j + \frac{1}{2} \delta \bar{\mathbf{q}}_j^T \delta \bar{\mathbf{q}}_j + \frac{1}{2} (1 - \delta q_{j,4})^2 \right] \\
& + \sum_{j=1}^m \frac{\beta_{jn}}{\gamma} \sum_{k=1}^3 \int_0^{-\gamma z_{k,j} + \gamma \delta q_{k,j}} x \, dx \\
& + \sum_{j=1}^m \sum_{n=1}^m \lambda_{jn} \left(\frac{1}{4} \left[\bar{\mathbf{q}}_{jn}^T \Lambda_{jn}^p \bar{\mathbf{q}}_{jn} + (1 - q_{jn,4})^2 \right] + \frac{\beta_{jn}}{2\gamma} \sum_{k=1}^3 \int_0^{-\gamma z_{k,jn} + \gamma q_{k,jn}} x \, dx \right)
\end{aligned} \tag{6.16}$$

The time derivative of this function along the trajectories of the closed-loop system

can be computed as:

$$\begin{aligned}
\dot{\mathcal{U}} &= - \sum_{j=1}^l \delta \omega_j^T \delta \bar{\mathbf{q}}_j + \sum_{j=1}^l \delta \omega_j^T \delta \bar{\mathbf{q}}_j + \sum_{j=1}^m \frac{\beta_{jn}}{\gamma} (-\gamma \dot{\mathbf{z}}_j + \gamma \delta \dot{\bar{\mathbf{q}}}_j)^T \dot{\mathbf{z}}_j \\
&\quad - \sum_{j=1}^m \sum_{n=1}^m \lambda_{jn} \left\{ \delta \omega_j^T \text{Sat} \left[\bar{\mathbf{q}}_{jn} + \beta_{jn} \left(\bar{\mathbf{E}}^T (\delta \mathbf{q}_j) \dot{\mathbf{z}}_j + \bar{\mathbf{E}}^T (\mathbf{q}_{jn}) \dot{\mathbf{z}}_{jn} \right) \right] \right. \\
&\quad \left. - \frac{1}{2} \bar{\mathbf{q}}_{jn}^T \omega_{jn} + \frac{\beta_{jn}}{2\gamma} (-\gamma \dot{\mathbf{z}}_{jn} + \gamma \dot{\bar{\mathbf{q}}}_{jn})^T \dot{\mathbf{z}}_{jn} \right\} \\
&= \sum_{j=1}^m \frac{\beta_{jn}}{\gamma} (-\gamma \dot{\mathbf{z}}_j + \gamma \delta \dot{\bar{\mathbf{q}}}_j)^T \dot{\mathbf{z}}_j \\
&\quad - \sum_{j=1}^m \sum_{n=1}^m \lambda_{jn} \left\{ \delta \omega_j^T \text{Sat} \left[\bar{\mathbf{q}}_{jn} + \beta_{jn} \left(\bar{\mathbf{E}}^T (\delta \mathbf{q}_j) \dot{\mathbf{z}}_j + \bar{\mathbf{E}}^T (\mathbf{q}_{jn}) \dot{\mathbf{z}}_{jn} \right) \right] \right. \\
&\quad \left. - \frac{1}{2} \bar{\mathbf{q}}_{jn}^T \omega_{jn} + \frac{\beta_{jn}}{2\gamma} (-\gamma \dot{\mathbf{z}}_{jn} + \gamma \dot{\bar{\mathbf{q}}}_{jn})^T \dot{\mathbf{z}}_{jn} \right\} \\
&= \sum_{j=1}^m \frac{\beta_{jn}}{\gamma} (-\gamma \dot{\mathbf{z}}_j + \gamma \delta \dot{\bar{\mathbf{q}}}_j)^T \dot{\mathbf{z}}_j \\
&\quad - \sum_{j=1}^m \sum_{n=1}^m \lambda_{jn} \delta \omega_j^T \left\{ \text{Sat} \left[\bar{\mathbf{q}}_{jn} + \beta_{jn} \left(\bar{\mathbf{E}}^T (\delta \mathbf{q}_j) \dot{\mathbf{z}}_j + \bar{\mathbf{E}}^T (\mathbf{q}_{jn}) \dot{\mathbf{z}}_{jn} \right) \right] \right. \\
&\quad \left. - \text{Sat}(\bar{\mathbf{q}}_{jn}) \right\} + \sum_{j=1}^m \sum_{n=1}^m \lambda_{jn} \left[\frac{\beta_{jn}}{2\gamma} (-\gamma \dot{\mathbf{z}}_{jn} + \gamma \dot{\bar{\mathbf{q}}}_{jn})^T \dot{\mathbf{z}}_{jn} \right]
\end{aligned}$$

which essentially has the same sign as the following expression,

$$\begin{aligned}
\Xi_2 &= k_1 \sum_{j=1}^m \frac{\beta_{jn}}{\gamma} (-\gamma \dot{\mathbf{z}}_j + \gamma \delta \dot{\bar{\mathbf{q}}}_j)^T \dot{\mathbf{z}}_j - k_1 \sum_{j=1}^m \sum_{n=1}^m \lambda_{jn} \left[\beta_{jn} \delta \omega_j^T \left(\bar{\mathbf{E}}^T (\delta \mathbf{q}_j) \dot{\mathbf{z}}_j + \bar{\mathbf{E}}^T (\mathbf{q}_{jn}) \dot{\mathbf{z}}_{jn} \right) \right. \\
&\quad \left. - \frac{\beta_{jn}}{2\gamma} (-\gamma \dot{\mathbf{z}}_{jn} + \gamma \dot{\bar{\mathbf{q}}}_{jn})^T \dot{\mathbf{z}}_{jn} \right]
\end{aligned}$$

for some positive constant k_1 . By noting the facts that $\omega_{jn}^T \bar{\mathbf{E}}^T (\mathbf{q}_{jn}) = \dot{\bar{\mathbf{q}}}_{jn}^T$, $\delta \omega_j^T \bar{\mathbf{E}}^T (\delta \mathbf{q}_j) = \delta \dot{\bar{\mathbf{q}}}_j^T$ and $\beta_{jn} = \beta_{nj}$ one can show that

$$\sum_{j=1}^n \sum_{n=1}^m \lambda_{jn} \left[\delta \omega_j^T \left(\bar{\mathbf{E}}^T (\mathbf{q}_{jn}) \dot{\mathbf{z}}_{jn} \right) - \frac{1}{2} \dot{\bar{\mathbf{q}}}_{jn}^T \dot{\mathbf{z}}_{jn} \right] = 0$$

and

$$\delta \omega_j^T \left(\bar{E}^T (\delta \mathbf{q}_j) \dot{\mathbf{z}}_j \right) - \delta \dot{\mathbf{q}}_j^T \dot{\mathbf{z}}_j = 0$$

Therefore, we can further simplify Ξ_2 as follows,

$$\Xi_2 = -k_1 \sum_{j=1}^m \beta_{jn} \dot{\mathbf{z}}_j^T \dot{\mathbf{z}}_j - k_1 \sum_{j=1}^m \sum_{n=1}^m \frac{\beta_{jn}}{2} \dot{\mathbf{z}}_{jn}^T \dot{\mathbf{z}}_{jn} \leq 0 \quad (6.17)$$

This by invoking Lemma 2.9.2 essentially implies that $\dot{\mathbf{z}}_{jn} \rightarrow 0$ as $t \rightarrow \infty$, which by noting strong connectivity of the communication graph implies $\dot{\mathbf{z}}_j \rightarrow 0$ as $t \rightarrow \infty$. One can show, by noting (6.14) and (6.15), that when $\dot{\mathbf{z}}_{jn} = \ddot{\mathbf{z}}_{jn} \equiv 0$ we have $\dot{\mathbf{q}}_{jn} \equiv 0$. This result can be used along with (6.9) to show that $\omega_{jn} \equiv 0$. Furthermore, when $\ddot{\mathbf{z}}_j \equiv 0$ and $\dot{\mathbf{z}}_j \equiv 0$, $j \in \mathcal{V}$ one can use (6.14) to show that $\delta \dot{\mathbf{q}}_j \equiv 0$. This from (6.4) implies that $\delta \omega_j \equiv 0$, $j \in \mathcal{V}$. Consequently, by studying the closed-loop dynamics and invoking Lemma 5.2.1 one can now conclude that $\bar{\mathbf{q}}_{jn} \rightarrow 0$ and $\delta \bar{\mathbf{q}}_j \rightarrow 0$ as $t \rightarrow \infty$. Therefore, since γ is positive, (6.14) and (6.15) also imply that $\mathbf{z}_{jn} \equiv 0$ and $\mathbf{z}_j \equiv 0$. Consequently, all the spacecraft in the network synchronize their state and set-point tracking error is asymptotically stable.

Now we show that the control effort is bounded under the control laws (6.14) and (6.15). Note that $\|\delta \bar{\mathbf{q}}_j\| \leq 1$ for all times. Consequently, one can show that for all the leader SC one has $\|\mathbf{u}_j(t)\| \leq \|\mathbf{u}_j^{\max}\|$ provided the controller gains are selected such that $\|\Delta_j\| + \sum_{n=1}^m \lambda_{jn} \leq \|\mathbf{u}_j^{\max}\|$. Similarly, one can show that for all the follower SC one has $\|\mathbf{u}_j(t)\| \leq \|\mathbf{u}_j^{\max}\|$ provided the controller gains are selected such that $\sum_{n=1}^m \lambda_{jn} \leq \|\mathbf{u}_j^{\max}\|$. This completes the proof of the theorem. ■

Corollary 6.3.2. *Consider a network of ‘m’ ($m > 1$) SC with the dynamic and kinematic equation (2.17). Consider the control law (6.15) for the j-th SC, where we set $\beta_{jn} = \beta_{nj}$. Furthermore, assume that the communication network is bidirectional*

and connected, where λ_{jn} is defined in Section 2.7. The application of the control law (6.15) will guarantee that the SC synchronize their states and the formation-keeping objective is achieved and the final angular velocity of the spacecraft in the network is zero. Additionally, the j -th control effort is bounded for all time and for all initial conditions, i.e. $\|\mathbf{u}_j(t)\| \leq \|\bar{\mathbf{u}}_j^{\max}\|$, provided that the controller gains λ_{jn} for the j -th SC are selected such that $\sum_{n=1}^m \lambda_{jn} \leq \|\bar{\mathbf{u}}_j^{\max}\|$.

Proof: It follows from Theorem 6.3.1.

6.4 Simulation Studies

In this section, the performance of our proposed control algorithms for distributed synchronization and set-point tracking control of multiple spacecraft with saturation constraints in the network with and without velocity feedback is evaluated and compared to the performance of the velocity-free controller proposed in [94]. We consider four spacecraft in the network in the ring topology and we assume the desired spacecraft coordinates are provided to the first spacecraft. The initial conditions for the spacecraft in the network are set the same as the initial conditions in [94], i.e. we set $\delta \mathbf{q}_1(0) = [0, 0, 1, 0]^T$, $\mathbf{q}_2(0) = [1, 0, 0, 0]^T$, $\mathbf{q}_3(0) = [0, 1, 0, 0]^T$, $\mathbf{q}_4(0) = [0, 0, \sin(-\pi/4), \cos(-\pi/4)]^T$, $\delta \boldsymbol{\omega}_1(0) = [-0.5, 0.5, -0.45]^T$, $\delta \boldsymbol{\omega}_2(0) = [0.5, -0.3, 0.1]^T$, $\delta \boldsymbol{\omega}_3(0) = [0.1, 0.6, -0.1]^T$, and $\delta \boldsymbol{\omega}_4(0) = [0.4, 0.4, -0.5]^T$. The moment of inertia matrices are set as $\mathbf{J}_j = \mathbf{Diag}(20, 20, 30)kg - m^2$, $j = \{1, \dots, 4\}$. The desired attitude is set to be $\bar{\mathbf{q}}_j^* = [0, 0, 0, -1]^T$.

Two sets of controller gains are considered in the simulations, which are provided in Table 6.1. The bounds on maximum control efforts for the leader and the followers for the controller gain set #1 is ten times larger than the maximum control efforts for the leader and the followers for the controller gain set #2. It is

Table 6.1: The two sets of selected controller gains

Set #	Δ_j	λ_{jn}	β_{jn}	$\ \mathbf{u}_1^{\max}\ $	$\ \mathbf{u}_j^{\max}\ , j = 1, 2, 3$
1	20	30	0.6	80	60
2	2	3	0.6	8	6

important to note that by selection of the controller gains, more emphasis is placed on formation-keeping rather than station-keeping, since this is more important in networked spacecraft control missions. Additionally, the gain γ is set to 20 for the velocity-free control scheme.

The response of the closed-loop networked spacecraft using the controller gains set #1 *with* velocity feedback and exchange among the agents are depicted in Figs. 6.1–6.3. These figures imply that attitude and angular velocity synchronization and set-point tracking are achieved and the bounds on the control efforts are respected. Figs. 6.4–6.6 depict the response of the closed-loop networked spacecraft using the controller gains set #1 *without* velocity feedback and exchange among the agents. One can observe from these figures that attitude and angular velocity synchronization and set-point tracking are achieved and the bounds on the control efforts are respected.

The response of the closed-loop networked spacecraft using the controller gains set #2 *with* velocity feedback and exchange among the agents are depicted in Figs. 6.7–6.9. These figures imply that attitude and angular velocity synchronization and set-point tracking are achieved and the bounds on the control efforts are respected. Figs. 6.10–6.12 depict the response of the closed-loop networked spacecraft using the controller gains set #2 *without* velocity feedback and exchange among the agents. One can observe from these figures that attitude and angular velocity synchronization and set-point tracking are achieved and the bounds on the

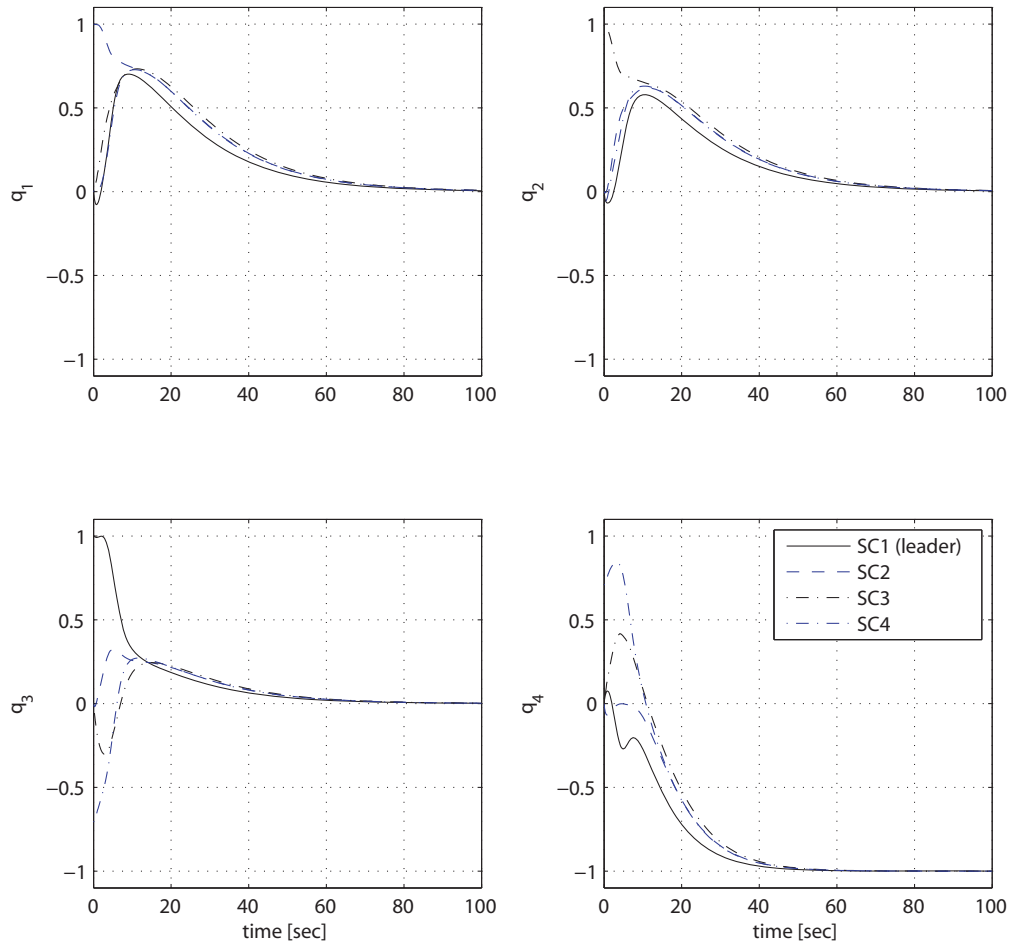


Figure 6.1: The quaternions of the four spacecraft in the network *with* velocity feedback with the controller gains set #1. Spacecraft #1 receives the desired attitude.

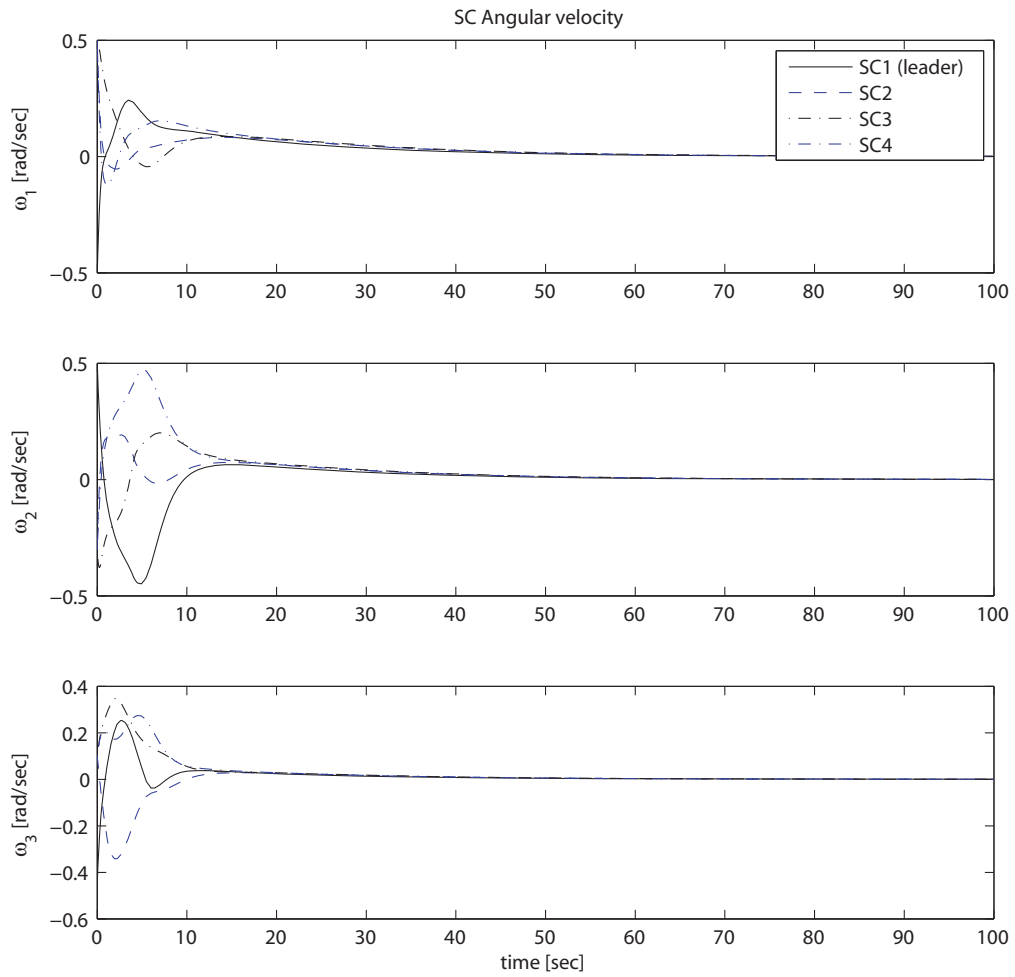


Figure 6.2: The angular velocities of the four spacecraft in the network *with* velocity feedback with the controller gains set #1. Spacecraft #1 receives the desired attitude.

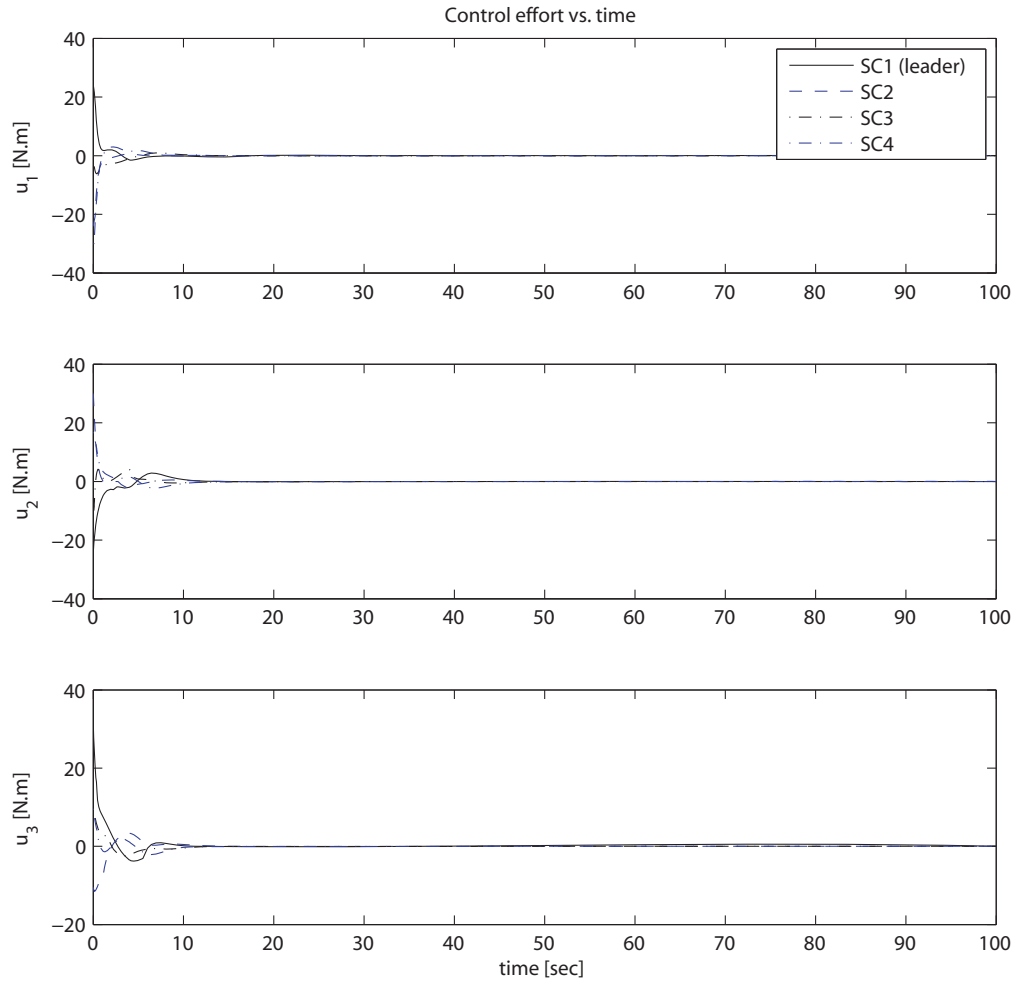


Figure 6.3: The control efforts of the four spacecraft in the network *with* velocity feedback with the controller gains set #1. Spacecraft #1 receives the desired attitude.

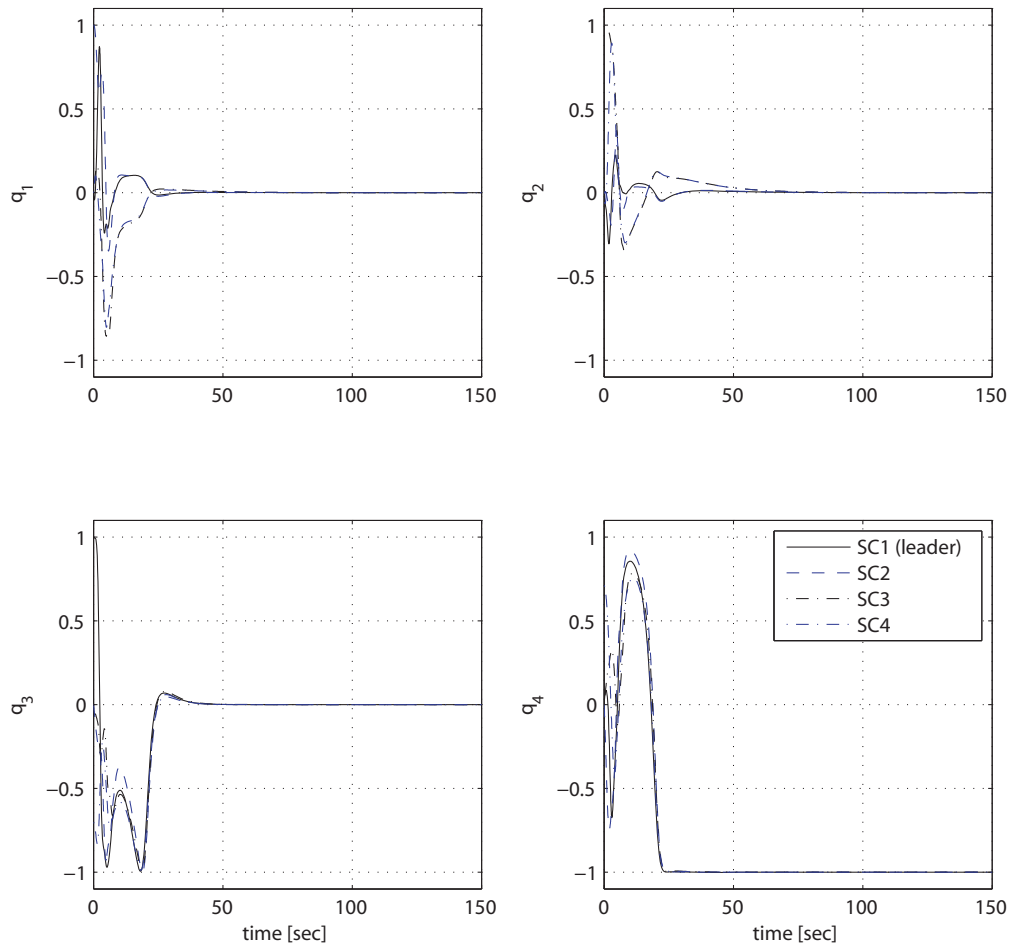


Figure 6.4: The quaternions of the four spacecraft in the network *without* velocity feedback with the controller gains set #1. Spacecraft #1 receives the desired attitude.

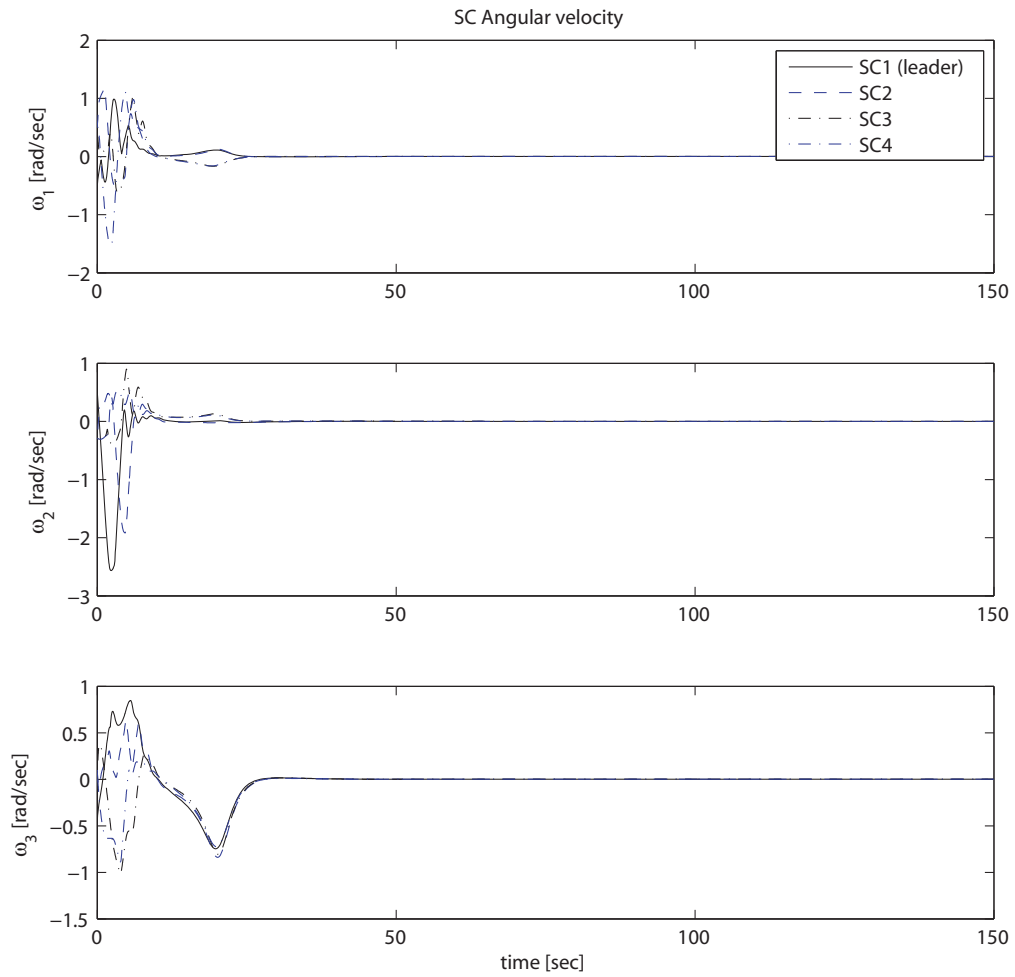


Figure 6.5: The angular velocities of the four spacecraft in the network *without* velocity feedback with the controller gains set #1. Spacecraft #1 receives the desired attitude.

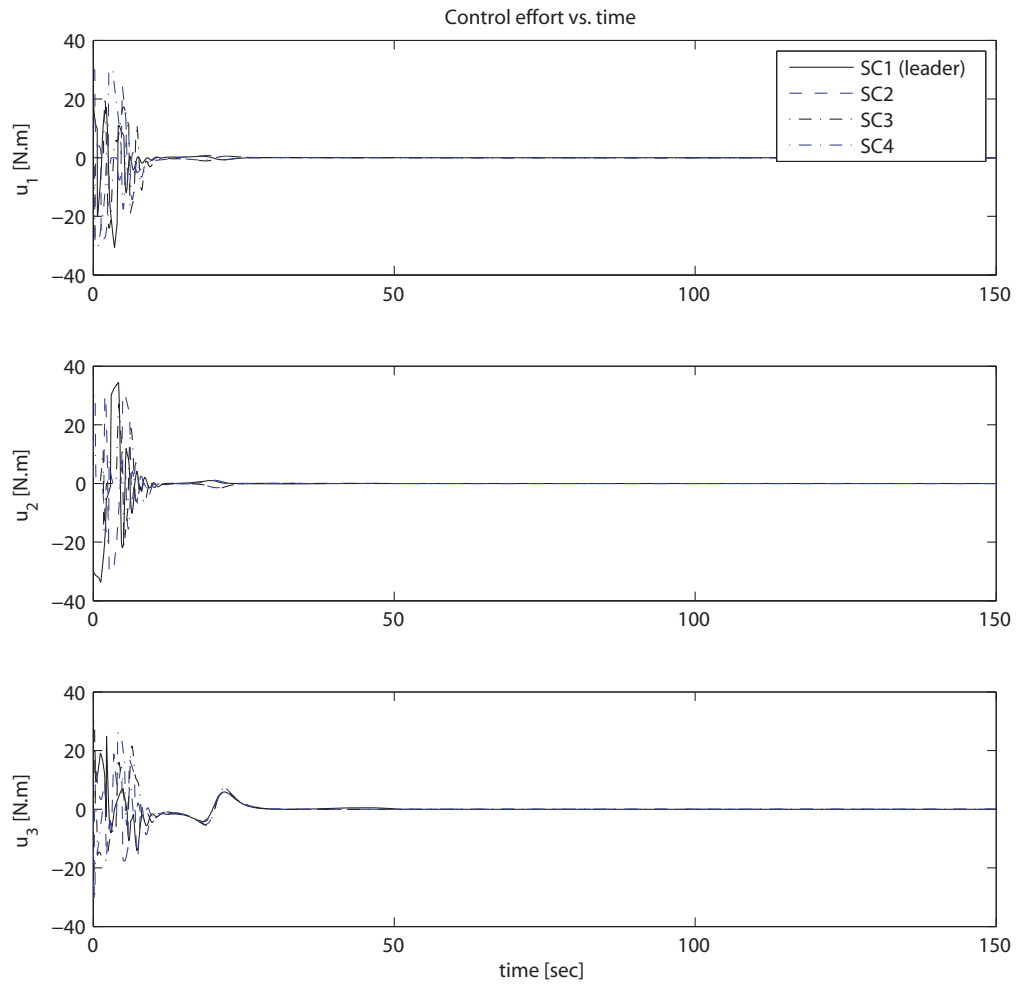


Figure 6.6: The control efforts of the four spacecraft in the network *without* velocity feedback with the controller gains set #1. Spacecraft #1 receives the desired attitude.

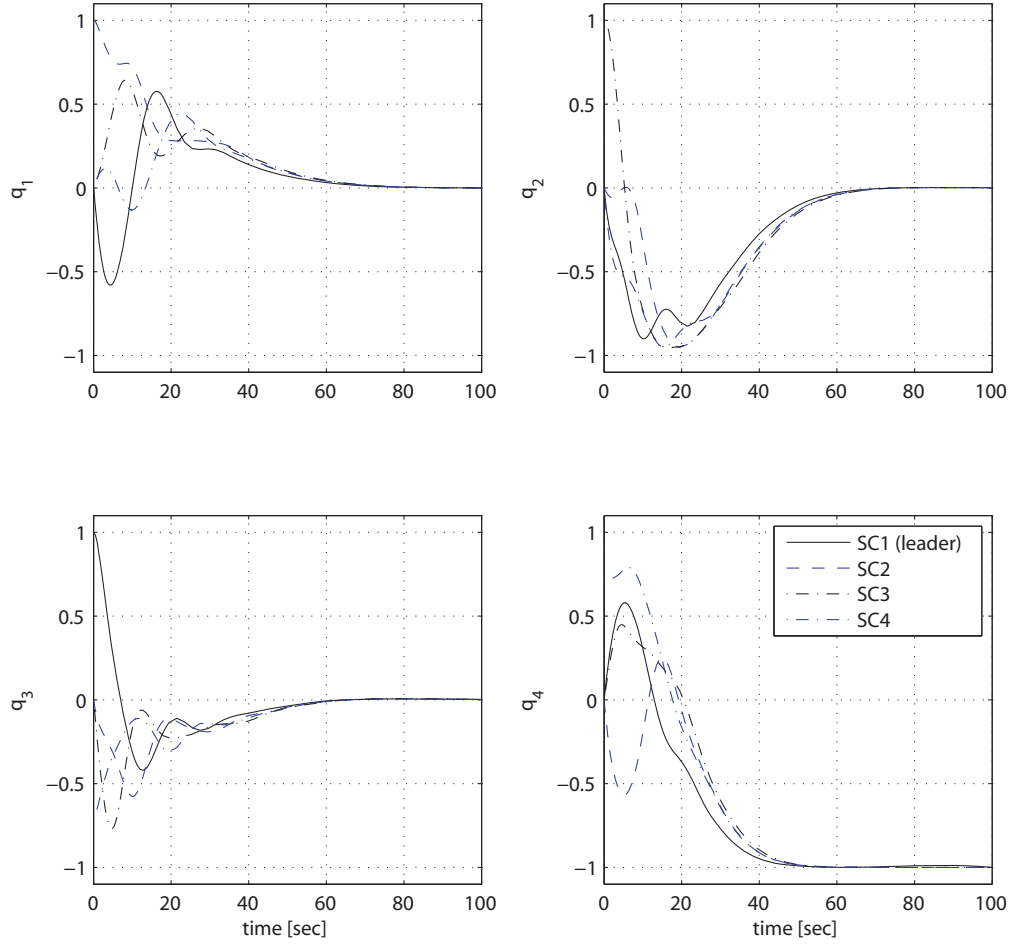


Figure 6.7: The quaternions of the four spacecraft in the network *with* velocity feedback with the controller gains set #1. Spacecraft #1 receives the desired attitude.

control efforts are respected.

Next, we compare the performance of our proposed constrained controllers with controller gain sets #1 and #2 to study the effects of changing the maximum control effort on the performance of the networked spacecraft. We execute ten Monte-Carlo simulation studies. The initial conditions are selected such that $\delta q_{r,j}(0) \in [0, 0.5]$ and $\delta \omega_{r,j}(0) \in [-0.5, 0.5]$, where $r \in \{1, 2, 3\}$ and $j \in \{1, \dots, 4\}$. We consider five performance measures, which are provided in Table 6.2. Table 6.2 summarizes the results that are obtained by using velocity-feedback controller

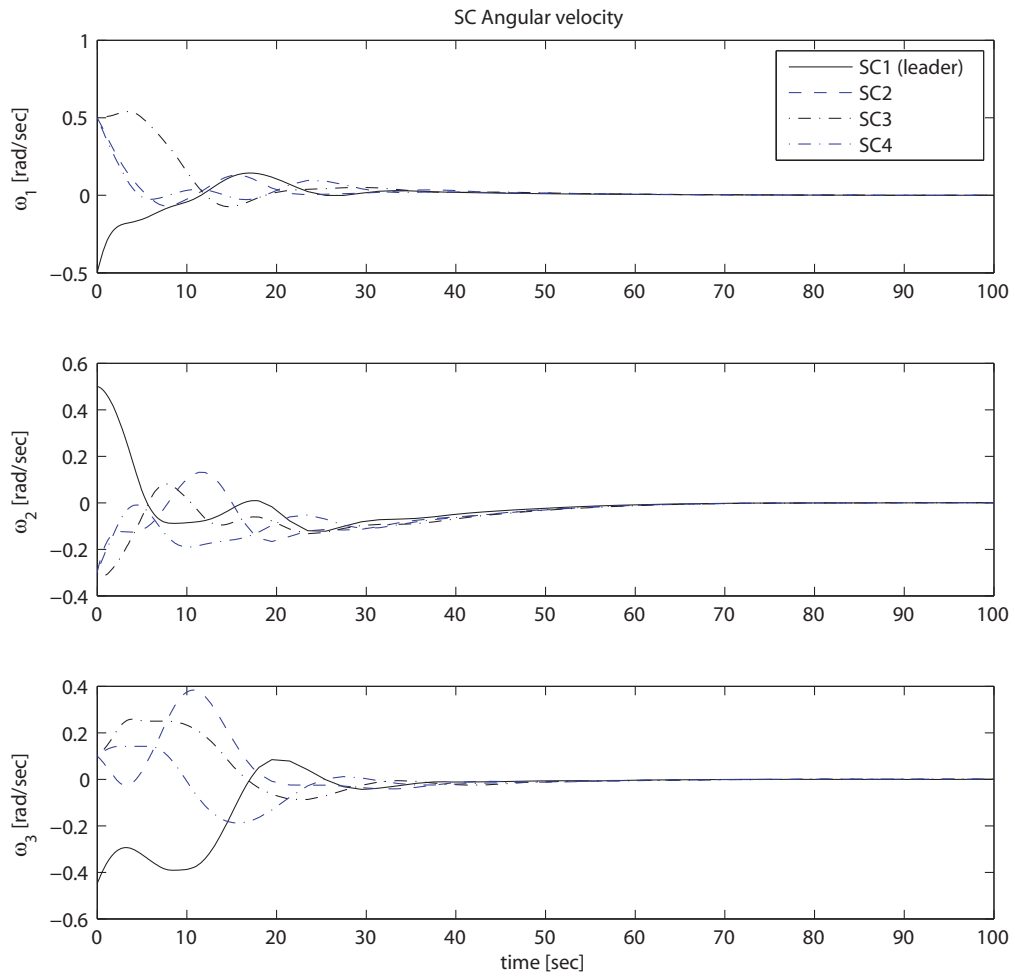


Figure 6.8: The angular velocities of the four spacecraft in the network *with* velocity feedback with the controller gains set #1. Spacecraft #1 receives the desired attitude.

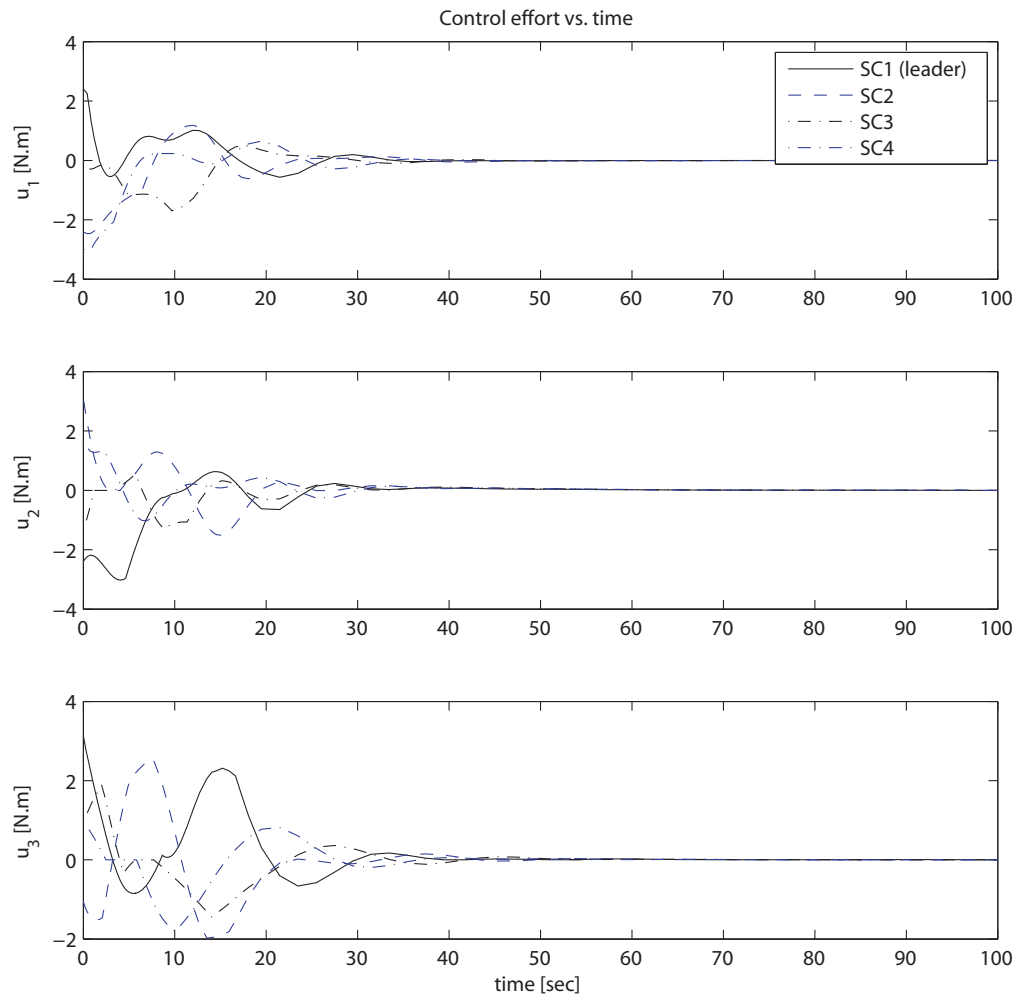


Figure 6.9: The control efforts of the four spacecraft in the network *with* velocity feedback with the controller gains set #1. Spacecraft #1 receives the desired attitude.

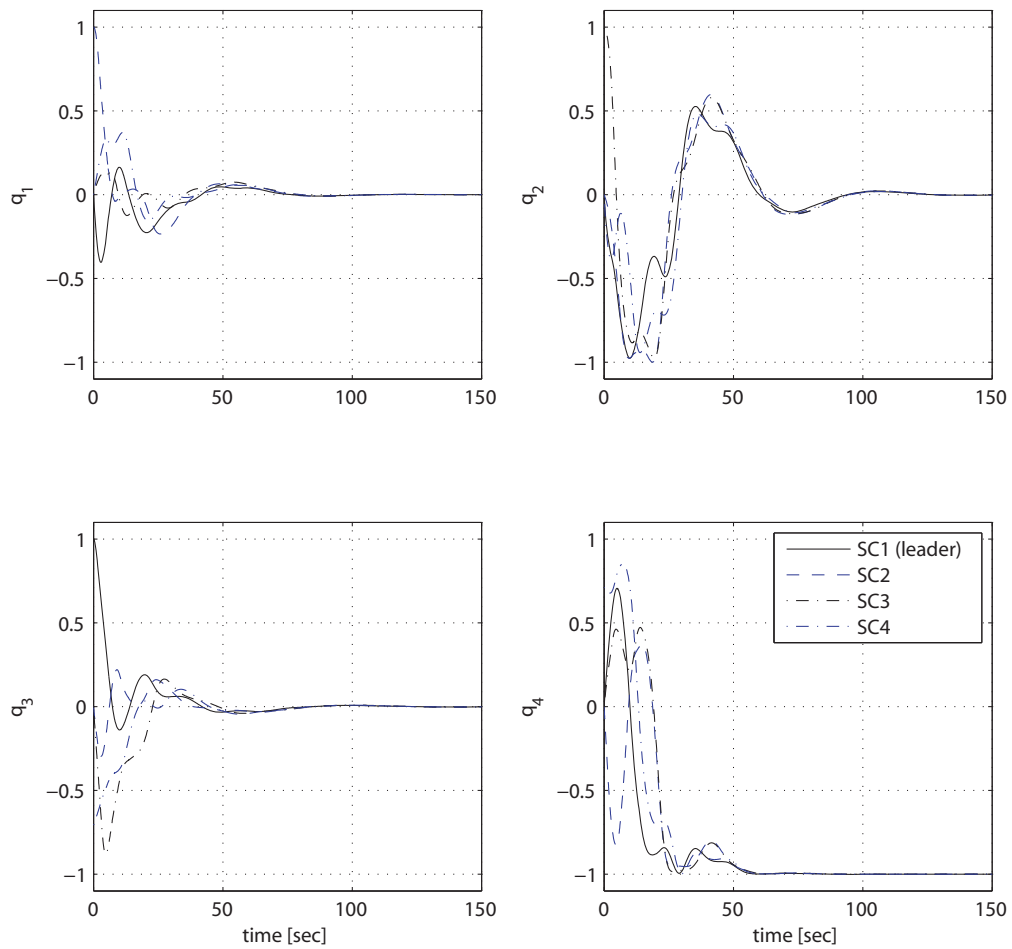


Figure 6.10: The quaternions of the four spacecraft in the network *without* velocity feedback with the controller gains set #2. Spacecraft #1 receives the desired attitude.

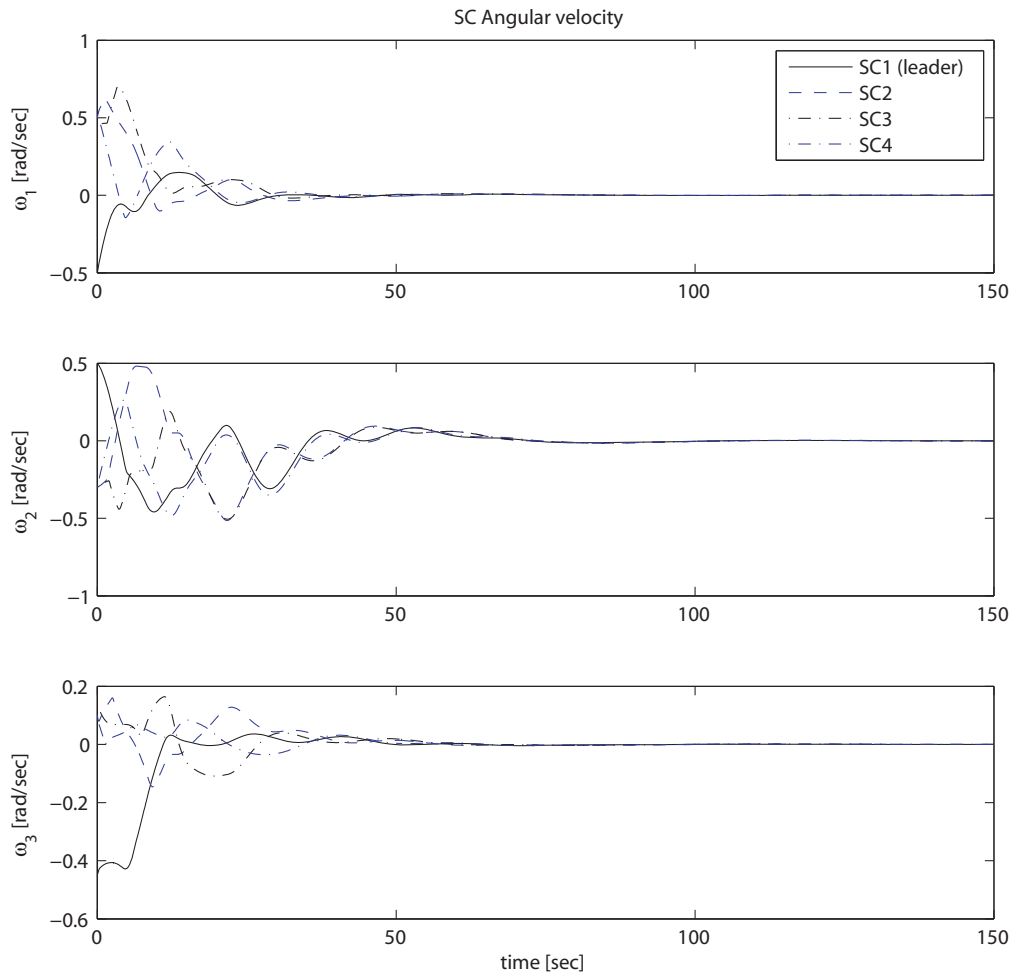


Figure 6.11: The angular velocities of the four spacecraft in the network *without* velocity feedback with the controller gains set #2. Spacecraft #1 receives the desired attitude.

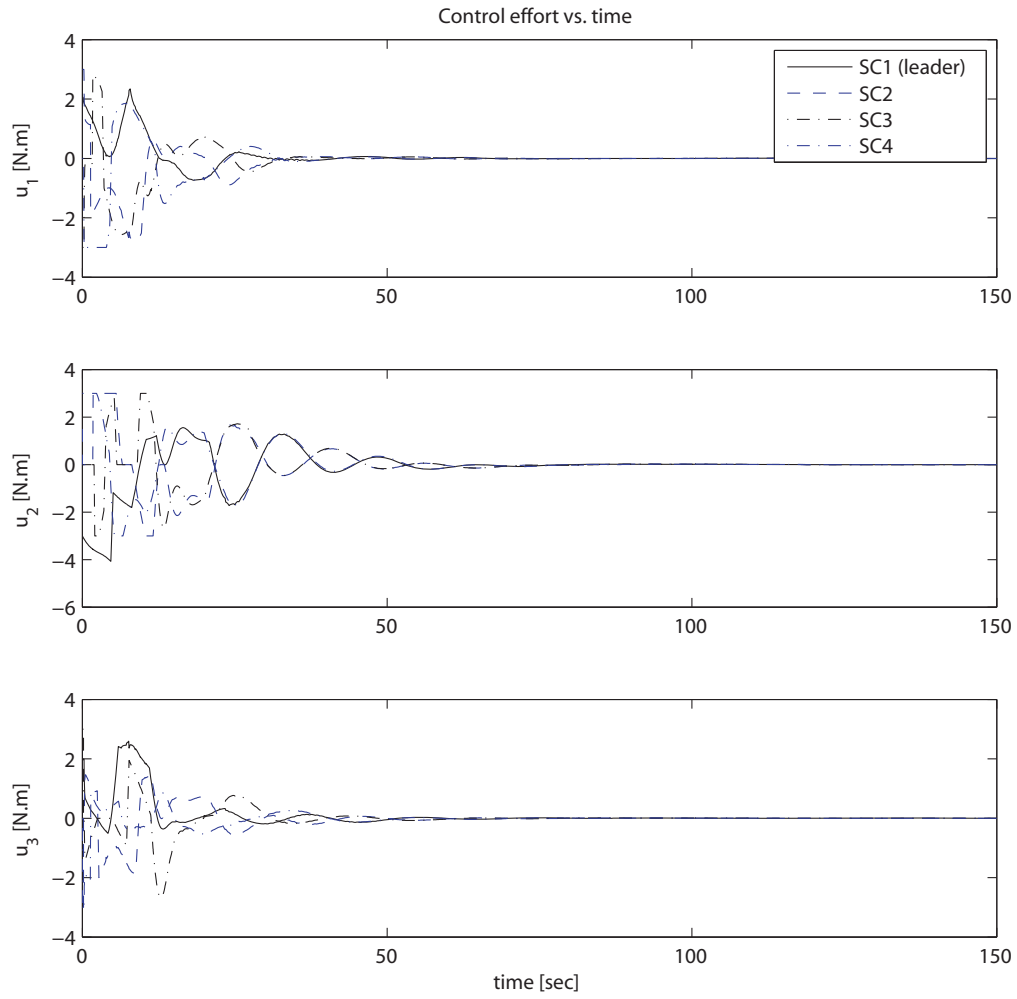


Figure 6.12: The control efforts of the four spacecraft in the network *without* velocity feedback with the controller gains set #2. Spacecraft #1 receives the desired attitude.

and Table 6.3 summarizes the results obtained by using the velocity-free controller. One can conclude from Table 6.2 that by using a higher control effort the error in the attitude and angular velocity synchronization as well as the error in the angular velocity set-point tracking are reduced. However, the attitude set-point tracking error has increased. This change in the performance comes with a high price, which is the increase in the overall spacecraft control effort by more than 640% for the controller with the gain set #1. From the results provided in Table 6.3 one can conclude that by increasing the bound on the control effort and by using our distributed velocity-free controllers one can improve the attitude synchronization and set-point tracking performance. However, one can note degradations in the angular velocity synchronization and set-point tracking performance. This change in the performance comes with a significant (more than 4400%) increase in the overall control effort by spacecraft in the network.

Table 6.2: Performance of our proposed constrained controllers *with* angular velocity feedback

Performance measure	Controller with gain set #1	Controller with gain set #2	Performance change of the gain set #1 with respect to gain set #2
$\sum_{i=1}^3 \sum_{j=1}^4 \int_0^{3000} q_{i,j}^2(t) dt$	111.93	90.49	-23.7%
$\sum_{i=1}^3 \sum_{j=1}^4 \int_0^{3000} \omega_{i,j}^2(t) dt$	2.43	4.82	98.35%
$\sum_{i=1}^3 \sum_{j=2}^4 \int_0^{3000} q_{j1,i}^2(t) dt$	6.45	10.29	59.52%
$\sum_{i=1}^3 \sum_{j=2}^4 \int_0^{3000} \omega_{j1,i}^2(t) dt$	0.6	3.31	455.3%
$\sum_{i=1}^3 \sum_{j=1}^4 \int_0^{3000} u_{i,j}^2(t) dt$	770.36	103.43	-644.78%

Table 6.3: Performance of our proposed constrained controllers *without* angular velocity feedback

Performance measure	Controller with gain set #1	Controller with gain set #2	Performance change of the gain set #1 with respect to gain set #2
$\sum_{i=1}^3 \sum_{j=1}^4 \int_0^{3000} q_{i,j}^2(t) dt$	27.67	165.88	499.57%
$\sum_{i=1}^3 \sum_{j=1}^4 \int_0^{3000} \omega_{i,j}^2(t) dt$	161.81	39.27	-312.09%
$\sum_{i=1}^3 \sum_{j=2}^4 \int_0^{3000} q_{j1,i}^2(t) dt$	4.315	29.32	579.42%
$\sum_{i=1}^3 \sum_{j=2}^4 \int_0^{3000} \omega_{j1,i}^2(t) dt$	19.817	16.67	-18.88%
$\sum_{i=1}^3 \sum_{j=1}^4 \int_0^{3000} u_{i,j}^2(t) dt$	25312	555.49	-4456.7%

Table 6.4: Performance loss in absence of angular velocity feedback

Performance measure	Performance change in absence of velocity feedback
$\sum_{i=1}^3 \sum_{j=1}^4 \int_0^{3000} q_{i,j}^2(t) dt$	-83.33%
$\sum_{i=1}^3 \sum_{j=1}^4 \int_0^{3000} \omega_{i,j}^2(t) dt$	-714.41%
$\sum_{i=1}^3 \sum_{j=2}^4 \int_0^{3000} q_{j1,i}^2(t) dt$	-185.04%
$\sum_{i=1}^3 \sum_{j=2}^4 \int_0^{3000} \omega_{j1,i}^2(t) dt$	-404.03%
$\sum_{i=1}^3 \sum_{j=1}^4 \int_0^{3000} u_{i,j}^2(t) dt$	-437.05%

Now, we study the performance degradation when the velocity feedback is not available for our proposed constrained control algorithms. Table 6.4 summarizes the results. This table shows that the performance of the networked spacecraft considerably degrades when the velocity information is not available for feedback and exchange. Absence of the velocity feedback mainly reduces the angular velocity synchronization and set-point tracking performance of the system, and it also results in an increase in the overall control effort of the spacecraft in the network.

Finally, we compare the performance of our proposed attitude synchronization controllers with the velocity-free controller proposed in [94]. We consider the network with the same setup and let the maximum control effort for the leader be bounded by $8 N - m$ and the follower control effort be bounded by $6 N - m$. The results of ten Monte-Carlo simulation studies are provided in Table 6.5. This table clearly shows that our proposed constrained velocity-free controller outperforms the velocity-free controller proposed in [94] in terms of attitude and angular velocity synchronization and attitude set-point tracking performance with a significant margin. In addition, our proposed velocity-free controller consumes much less energy, 437% less than the controller proposed in [94], which is critically important for networked spacecraft missions as the thruster fuel is limited. It should be noted

that the controller proposed in [94] produced lower angular velocity set-point error when compared to our proposed velocity-free controller. However, this should not be seen as a drawback for our proposed algorithm since in network spacecraft control, attitude and velocity synchronization errors are considerably more important than the single spacecraft angular velocity set-point tracking error.

6.5 Concluding Remarks

In this chapter we consider controller development for attitude synchronization for spacecraft formation flying missions. The control laws are developed subject to four constraints, namely, (1) constraints on the maximum control effort available to each SC in the network, (2) unavailability of velocity measurements, and, (3) unavailability of information about the SC moment of inertia matrix. The closed-loop performance of the control strategies proposed in this chapter are evaluated extensively through numerical simulations.

Table 6.5: Performance comparison and analysis.

Performance measure	Velocity-free controller [87]	Performance change when compared with our velocity-free controller
$\sum_{i=1}^3 \sum_{j=1}^4 \int_0^{3000} q_{i,j}^2(t) dt$	423.55	+155.33%
$\sum_{i=1}^3 \sum_{j=1}^4 \int_0^{3000} \omega_{i,j}^2(t) dt$	32.62	-20.37%
$\sum_{i=1}^3 \sum_{j=2}^4 \int_0^{3000} q_{j,1,i}^2(t) dt$	123.22	+320.31%
$\sum_{i=1}^3 \sum_{j=2}^4 \int_0^{3000} \omega_{j,1,i}^2(t) dt$	34.00	+103.97%
$\sum_{i=1}^3 \sum_{j=1}^4 \int_0^{3000} u_{i,j}^2(t) dt$	707.32	+27.33%

Chapter 7

Conclusions and Future Work

Directions

7.1 Conclusions

In this thesis we considered control of networked Euler-Lagrange (EL) systems with nonlinear dynamics. We focused on development of distributed control laws with several practical constraints. Specifically, in Chapter 3 optimal control techniques are developed for a network of nonlinear EL systems subject to communication topology switchings and parametric uncertainties. A formal design methodology for selection of distributed controllers for tackling the state synchronization and set-point tracking requirements for a team of multi-agent nonlinear EL systems is introduced. Additionally, when parametric uncertainties are taken into account explicitly, adaptive as well as robust distributed control techniques are proposed and developed to compensate for the adverse effects of these uncertainties in the networked EL systems. Moreover, additive actuator faults are considered and a

controller reconfiguration mechanism is introduced to recover stability and performance of the networked EL systems. Simulation studies corresponding to the attitude control of a network of eight spacecraft are conducted to demonstrate the merits, performance, and capabilities of our proposed control algorithms and also to conduct comparative studies of their performances.

In Chapter 4 formal development of distributed state synchronization and set-point tracking control laws for nonlinear EL systems by employing H_∞ control technique is discussed. To be precise, in presence of parametric uncertainty and external disturbances, H_∞ optimal control techniques are utilized to formally design a distributed control law which addresses state synchronization and set-point tracking of a team of multi-agent nonlinear EL systems given that the agents have access to only local information. In addition, we formally show that our proposed distributed control algorithm for EL systems is input-to-state stable (ISS) when the input is considered as the parameter uncertainty and external disturbances for *both* fixed and switching communication network topologies. The second main contribution of this chapter is formal extension of the developed distributed adaptive state synchronization and set-point tracking control law for nonlinear EL systems to FDI imperfections in the actuator faults. Specifically, in presence of actuator faults, our proposed distributed control algorithm has the capability of compensating for the fault and taking proper controller reconfiguration actions. We consider three main types of imperfections in the FDI algorithm, namely, (1) *fault detection imperfection* that arises when fault is not detected by the FDI algorithm, (2) *fault isolation imperfection* that arises when the fault is detected in the wrong channel or in the wrong agent, and (3) *fault identification imperfection* that arises when the fault estimation is not accurate. We show that our proposed distributed controller can maintain the closed-loop networked EL systems' stability under all these scenarios,

and can moreover improve the performance of the resulting closed-loop networked EL systems corresponding to the last scenario. Simulation results for the attitude control of a network of eight spacecraft demonstrate effectiveness and capabilities of our proposed distributed control algorithms.

In Chapter 5 two distributed bounded and nonlinear controllers are proposed for state synchronization and set-point tracking of networked EL systems in presence of input saturation constraints. The communication network is considered to be undirected and switching. The first controller requires velocity feedback and exchange among the agents, whereas the second controller does not require velocity measurements and exchange among the agents. This considerably reduces the required communication load among the agents without sacrificing the overall networked system performance. The performance of our proposed state synchronization and set-point tracking controllers are verified through simulations as well as comparisons with other synchronization and set-point tracking controllers that are available in the literature. It was shown that our proposed constrained distributed controllers yield a considerably improved performance for the closed-loop networked nonlinear EL systems. Furthermore, a reconfiguration strategy for cooperative control of a network of nonlinear EL systems subject to actuator faults and constraints is also developed in this Chapter. The proposed nonlinear *nominal* and *reconfigured* constrained control strategies each individually guarantee stability of the EL networked agents states and control signals and guarantee global convergence of the set-point tracking errors and state synchronization errors to the origin despite the presence of actuator saturation constraints and intermittent or permanent actuator faults. By using the proposed switching strategy between the constrained *nominal* and the constrained *reconfigured* controllers, global stability

of the closed-loop networked EL system states and control signals as well as convergence of the synchronization errors and the tracking errors to origin can still be ensured. In addition, the proposed control laws require minimum knowledge of the system's dynamics. The performance of our proposed reconfigurable control strategy is demonstrated by simulations to three heterogenous 2-DOF networked manipulators subject to an actuator fault and actuators saturation constraints.

The contribution of Chapter 6 is in the development of two constrained control algorithms for attitude synchronization for spacecraft formation flying missions. We used unit-quaternion to represent the spacecraft attitude dynamics as it does not have singularities and therefore enable execution of large attitude maneuvers. Our proposed constrained velocity-free attitude spacecraft controllers do not require availability of spacecraft angular velocities for feedback and exchange among the spacecraft in the network, which considerably reduces communication load in the formation. Simulation studies are reported to demonstrate the merits of our proposed control algorithms.

7.2 Suggestions for Future Research

Some suggestions for the future research are listed in followings as:

- Extension of the proposed control algorithms to distributed trajectory tracking problem: In the development of trajectory controllers for multi-agents EL systems (see for example [64]) it is assumed that the desired trajectory is available to all the agents in the network. However, this cannot be guaranteed in the formation control problem for all times. It is, therefore, important to develop a distributed control algorithm that enables development of distributed

trajectory tracking problem when the desired trajectory is not available to all the agents in the network.

- Extension of the proposed distributed control algorithms to general passive nonlinear systems: Euler-Lagrange systems can be seen as a subset of passive nonlinear systems. It is interesting and useful to extend the developed control algorithms in this thesis to a more general class of nonlinear systems, i.e. passive nonlinear systems.
- Robustness analysis of the developed constrained controllers in Chapter 5 to external disturbances: Mechanical systems in their daily operation are subject to external disturbances. It is, therefore, interesting and very useful to study robustness of the control developed in Chapter 5.
- Analysis and extension of the proposed control laws for directed communication networks: In several practical applications, the communication graph is *directed*. Extension of the present work to directed communication graphs will enhance applicability of the developed control algorithms.
- Extension of proposed control algorithms to EL systems with non-holonomic constraints: Many robotic applications, like mobile wheeled robots, are subject to non-holonomic constraints. This constraint needs to be considered in the development of the control law, specially, when full state measurement is not available.
- Development of distributed velocity-free fault tolerant controllers: As discussed in this thesis, velocity measurements are not always available. It is, therefore, practically useful to extend the results in this thesis for development of the velocity-free fault tolerant controllers for multi-agent nonlinear

EL systems.

Appendix A

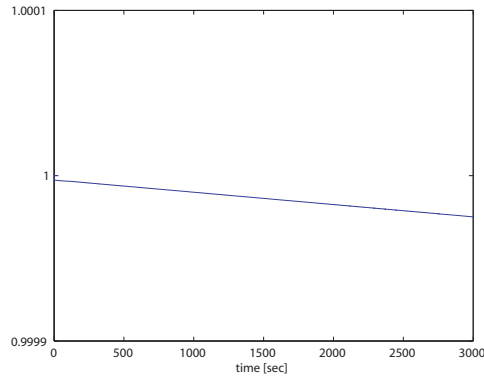
Simulation Validation

In this thesis we use Matlab/Simulink to for simulation purposes and to validate our analytical results. MATLAB (MATrix LABoratory) is a numerical computing environment and fourth-generation programming language. Developed by MathWorks, MATLAB allows matrix manipulations, plotting of functions and data, implementation of algorithms, creation of user interfaces, and interfacing with programs written in other languages, including C, C++, Java, and Fortran [192].

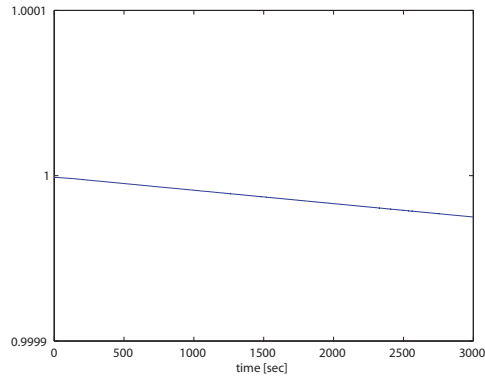
Simulink, developed by MathWorks, is a data flow graphical programming language tool for modeling, simulating and analyzing multidomain dynamic systems. Its primary interface is a graphical block diagramming tool and a customizable set of block libraries. It offers tight integration with the rest of the MATLAB environment and can either drive MATLAB or be scripted from it. Simulink is widely used in control theory and digital signal processing for multidomain simulation and model-based design [193].

A.1 Simulation Validation

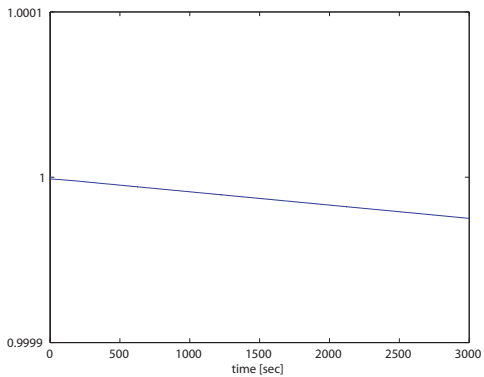
In this subsection we validate our simulation results presented in Section 6.4. We verify the results by showing that constraint (2.15) is always satisfied for all four spacecraft in the formation. The Following four figures show that this constraint is satisfied within an acceptable tolerance for all the four spacecraft in the formation.



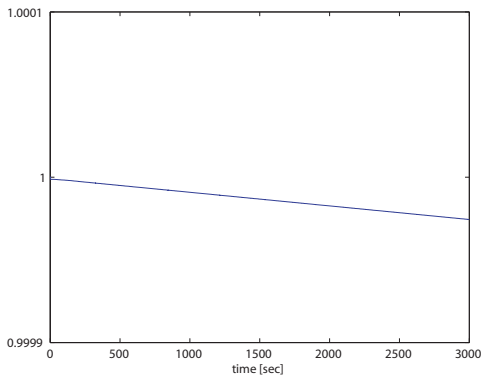
(a) Validation of constraint (2.15) for spacecraft #1 in the formation.



(b) Validation of constraint (2.15) for spacecraft #2 in the formation.



(c) Validation of constraint (2.15) for spacecraft #3 in the formation.



(d) Validation of constraint (2.15) for spacecraft #4 in the formation.

Figure A.1: Simulation software validation by checking satisfaction of constraint (2.15) for the four spacecraft in the formation.

Bibliography

- [1] M. Brunnermeier, *Asset Pricing under Asymmetric Information: Bubbles, Crashes, Technical Analysis, and Herding*. Oxford University Press, 2001.
- [2] L. Rook, “An economic psychological approach to herd behavior,” *J. Economic Issues*, vol. 40, no. 1, pp. 75–95, 2006.
- [3] I. Couzin, “Collective cognition in animal groups,” *Trends in Cognitive Sciences*, vol. 13, no. 1, pp. 36–43, 2009.
- [4] B. Lemassona, J. Andersona, and R. Goodwi, “Collective motion in animal groups from a neurobiological perspective: The adaptive benefits of dynamic sensory loads and selective attention,” *J. Theoret. Bio.*, vol. 261, no. 4, pp. 501–510, 2009.
- [5] J. Kennedy and R. Eberhart, “Particle swarm optimization,” *IEEE Int. Conf. on Neural Net.*, vol. 4, pp. 1942–1948, 1995.
- [6] D. Karaboga and B. Akay, “A comparative study of artificial bee colony algorithm,” *Appl. Math. and Comput.*, vol. 214, no. 1, pp. 108–132, 2009.
- [7] A. Mehrabian and C. Lucas, “A novel numerical optimization algorithm inspired from weed colonization,” *Ecolog. Inform.*, vol. 1, no. 4, pp. 355–366, 2006.

- [8] W. Ren and R. Beard, "Formation feedback control for multiple spacecraft via virtual structures," *IEE Contr. Theory & Appl.*, vol. 151, no. 3, pp. 357–368, 2004.
- [9] D. M. Stipanovic, G. Inalhan, R. Teo, and C. J. Tomlin, "Decentralized overlapping control of a formation of unmanned aerial vehicles," *Automatica*, vol. 40, no. 8, pp. 1285–1296, 2004.
- [10] V. Gazi, *Stability analysis of swarms*. The Ohio State University, USA: Ph.D. dissertation, 2002.
- [11] F. Xiao and L. Wang, "Consensus problems for high-dimensional multiagent systems," *IET Contr. Theory & Appl.*, vol. 1, no. 3, pp. 830–837, 2007.
- [12] E. Semsar-Kazerooni, *Cooperative Control of a Network of Multi-Vehicle Unmanned Systems*. Concordia University, Canada: Ph.D. dissertation, 2009.
- [13] M. Alighanbari and J. How, "Decentralized task assignment for unmanned aerial vehicles," *IEEE Conf. Deci. Contr. and Euro. Contr. Conf.*, pp. 5668–5673, 2005.
- [14] E. Nett and S. Schemmer, "Reliable real-time communication in cooperative mobile applications," *IEEE Trans. Comput.*, vol. 52, no. 2, pp. 166–180, 2003.
- [15] S. Jinyan, W. Long, and Y. Junzhi, "Cooperative control of multiple robotic fish in a disk-pushing task," *Amer. Contr. Conf.*, pp. 2730–2735, 2006.

- [16] R. Beard, J. Lawton, and F. Y. Hadaegh, "A coordination architecture for spacecraft formation control," *IEEE Trans. Contr. Syst. Tech.*, vol. 9, no. 6, pp. 777–789, 2001.
- [17] R. Olfati-Saber and R. M. Murray, "Consensus problems in networks of agents with switching topology and time-delays," *IEEE Trans. on Auto. Contr.*, vol. 49, no. 9, pp. 1520–1533, 2004.
- [18] D. Scharf and S. P. F.Y. Hadaegh, "A survey of spacecraft formation flying guidance and control (part ii): Control," *Amer. Contr. Conf.*, pp. 2976–2985, 2004.
- [19] A. Jadbabaie, J. Lin, and A. S. Morse, "Coordination of groups of mobile autonomous agents using nearest neighbor rules," *IEEE Trans. on Auto. Contr.*, vol. 48, no. 6, pp. 988–1001, 2003.
- [20] M. Mesbahi and F. Hadaegh, "Formation flying control of multiple spacecraft via graphs, matrix inequalities and switching," *AIAA J. Guid., Contr., and Dyn.*, vol. 24, no. 2, pp. 369–377, 2001.
- [21] H. Tanner, A. Jadbabaie, and G. J. Pappas, "Flocking in fixed and switching networks," *IEEE Trans. on Auto. Contr.*, vol. 52, no. 5, pp. 863–868, 2007.
- [22] P. Wang, "Navigation strategies for multiple autonomous mobile robots moving in formation," *J. Robotic Syst. Tech.*, vol. 8, no. 2, pp. 177–195, 1991.
- [23] J. Marschak, "Elements for a theory of teams," *Management Science*, vol. 1, no. 2, pp. 127–137, 1955.

- [24] Y. Ho and K. Chu, “Team decision theory and information structures in optimal control problems-part i,” *IEEE Trans. on Auto. Contr.*, vol. 17, no. 1, pp. 15–22, 1972.
- [25] —, “Team decision theory and information structures in optimal control problems-part ii,” *IEEE Trans. on Auto. Contr.*, vol. 17, no. 1, pp. 22–28, 1972.
- [26] R. Radner, “Team decision problems,” *Annals of Mathematical Statistics*, vol. 33, no. 3, pp. 857–881, 1962.
- [27] W. Ren and R. Beard, “Consensus seeking in multiagent systems under dynamically changing interaction topologies,” *Syst. & Contr. Lett.*, vol. 50, no. 5, pp. 655–661, 2005.
- [28] W. Ren, “Consensus strategies for cooperative control of vehicle formations,” *IET Contr. Theory & Appl.*, vol. 1, no. 2, pp. 505–512, 2007.
- [29] J. Fax and R. Murray, “Information flow and cooperative control of vehicle formations,” *IEEE Trans. Auto. Contr.*, vol. 49, no. 9, pp. 1465–1476, 2004.
- [30] J. Qin, W. X. Zheng, and H. Gao, “Coordination of multiple agents with double-integrator dynamics under generalized interaction topologies,” *IEEE Transactions on Systems, Man, & Cybernetics, Part B – Cybernetics*, vol. 42, no. 1, pp. 44–57, 2012.
- [31] J. Qin, H. Gao, and W. X. Zheng, “Second-order consensus for multi-agent systems with switching topology and communication delay,” *Syst. and Contr. Lett.*, vol. 60, no. 6, pp. 390–397, 2011.

- [32] Y. Zhao, G. Wen, Z. Duan, X. Xu, and G. Chen, "A new observer-type consensus protocol for linear multi-agent dynamical systems," *Asian J. Control*, no. DOI: 10.1002/asjc.572, forthcoming.
- [33] Q. Li and Z.-P. Jiang, "Asynchronous distributed algorithms for heading consensus of multi-agent systems with communication delay," *Asian J. Control*, no. DOI: 10.1002/asjc.551, forthcoming.
- [34] G. Wen, Z. Duan, W. Yu, and G. Chen, "Consensus of multi-agent systems with nonlinear dynamics and sampled-data information: A delayed-input approach," *Int. J. Robust & Nonlinear Contr.*, no. DOI: 10.1002/rnc.2779, forthcoming.
- [35] J. Qin and H. Gao, "A sufficient condition for convergence of sampled-data consensus for double-integrator dynamics with nonuniform and time-varying communication delays," *IEEE Trans. on Auto. Contr.*, vol. 57, no. 9, pp. 2417–2422, 2012.
- [36] Y. Su and J. Huang, "Stability of a class of linear switching systems with applications to two consensus problems," *IEEE Trans. on Auto. Contr.*, vol. 57, no. 6, pp. 1420–1430, 2007.
- [37] Z.-W. Liu, Z.-H. Guan, T. Li, X.-H. Zhang, and J.-W. Xiao, "Quantized consensus of multi-agent systems via broadcast gossip algorithms," *Asian J. Control*, no. DOI: 10.1002/asjc.525, forthcoming.
- [38] H. Zhao, S. Xu, and D. Yuan, "Consensus of data-sampled multi-agent systems with markovian switching topologies," *Asian J. Control*, no. DOI: 10.1002/asjc.444, forthcoming.

- [39] L. Fang, P. J. Antsaklis, and A. Tzimas, "Asynchronous consensus protocols: Preliminary results, simulations, and open questions," *IEEE Conf. Deci. Contr. and Euro. Contr. Conf.*, pp. 2194–2199, 2005.
- [40] M. Arcak, "Passivity as a design tool for group coordination," *IEEE Trans. on Auto. Contr.*, vol. 52, no. 8, pp. 1380–1390, 2007.
- [41] S. Hirche and S. Hara, "Stabilizing interconnection characterization for multi-agent systems with dissipative properties," *IFAC World Congress*, vol. 52, no. 8, pp. 1571–1577, 2008.
- [42] L. Moreau, "Stability of continuous time distributed consensus algorithms," *IEEE Conf. Deci. Contr.*, pp. 3998–4003, 2004.
- [43] F. Y. Hadaegh, A. Ghavimi, G. Singh, and M. Quadrelli, "A centralized optimal controller for formation flying spacecraft," *Int. conf. intel. tech.*, 2000.
- [44] R. Raffard, C. Tomlin, and S. Boyd, "Distributed optimization for cooperative agents: application to formation flight," *IEEE Conf. Deci. Contr.*, pp. 2453–2459, 2004.
- [45] G. Inalhan, D. Stipanovic, and C. J. Tomlin, "Decentralized optimization, with application to multiple aircraft coordination," *IEEE Conf. Deci. Contr.*, pp. 1147–1155, 2002.
- [46] J. Fax, *Optimal and cooperative control of vehicle formations*. California Institute of Technology, USA: Ph.D. dissertation, 2002.
- [47] V. Gupta, B. Hassibi, and R. Murray, "On the synthesis of control laws for a network of autonomous agents," *Amer. Contr. Conf.*, pp. 4927–4932, 2004.

- [48] G. A. Decastro and F. Paganini, "Convex synthesis of controllers for consensus," *Amer. Contr. Conf.*, pp. 4933–4938, 2004.
- [49] D. Bauso, L. Giarre, and R. Pesenti, "Mechanism design for optimal consensus problems," *IEEE Conf. Deci. Contr.*, pp. 3381–3386, 2006.
- [50] Q. Hui and W. M. Haddad, " h_2 optimal semistable stabilization for linear discrete-time dynamical systems with applications to network consensus," *IEEE Conf. Deci. Contr.*, pp. 2315–2320, 2007.
- [51] J. C. Delvenne, R. Carli, and S. Zampieri, "Optimal strategies in the average consensus problem," *IEEE Conf. Deci. Contr. and Euro. Contr. Conf.*, pp. 2498–2503, 2007.
- [52] V. Gupta, B. Hassibi, and R. M. Murray, "A sub-optimal algorithm to synthesize control laws for a network of dynamic agents," *Int. J. Contr.*, vol. 78, no. 16, pp. 1302–1313, 2005.
- [53] D. Bauso, L. Giarre, and R. Pesenti, "Non-linear protocols for optimal distributed consensus in networks of dynamic agents," *Syst. and Contr. Lett.*, vol. 55, no. 11, pp. 918–928, 2006.
- [54] Y. Kim and M. Mesbahi, "On maximizing the second smallest eigenvalue of a state-dependent graph laplacian," *IEEE Trans. on Auto. Contr.*, vol. 51, no. 1, pp. 116–120, 2006.
- [55] Y. Cao and W. Ren, "Optimal linear-consensus algorithms: An lqr perspective," *IEEE Trans. on Syst. Man & Cyber. - Part B*, vol. 40, no. 3, pp. 819–830, 2010.

- [56] J. Tsitsiklis, *Problems in decentralized decision making and computation*. Massachusetts Institute of Technology, USA: Ph.D. dissertation, 1984.
- [57] D. B. J. Tsitsiklis and M. Athans, “Distributed asynchronous deterministic and stochastic gradient optimization algorithms,” *IEEE Trans. on Auto. Contr.*, vol. 31, no. 9, pp. 803–812, 1986.
- [58] G. Xie and L. Wang, “Consensus control for a class of networks of dynamic agents: Switching topology,” *Amer. Contr. Conf.*, pp. 1382–1387, 2006.
- [59] L. Wang and F. Xiao, “A new approach to consensus problems for discrete-time multiagent systems with time-delays,” *Amer. Contr. Conf.*, pp. 2118–2123, 2006.
- [60] D. Kingston and R. Beard, “Discrete-time average-consensus under switching network topologies,” *Amer. Contr. Conf.*, pp. 3551–3556, 2006.
- [61] L. W. Y. Sun and G. Xie, “Average consensus in directed networks of dynamic agents with time-varying communication delays,” *Amer. Contr. Conf.*, pp. 3393–3398, 2006.
- [62] N. Chopra, *Output Synchronization of Networked Passive Systems*. University of Illinois at Urbana-Champaign, USA: Ph.D. dissertation, 2006.
- [63] W. Ren, “Distributed leaderless consensus algorithms for networked euler-lagrange systems,” *Int. J. Contr.*, vol. 82, no. 11, pp. 2137–2149, 2009.
- [64] S.-J. Chung and J.-J. Slotine, “Cooperative robot control and concurrent synchronization of lagrangian systems,” *IEEE Trans. on Robot.*, vol. 25, no. 3, pp. 1–15, 2009.

- [65] J. Mei, W. Ren, and G. Ma, “Containment control for multiple euler-lagrange systems with parametric uncertainties in directed networks,” *Amer. Contr. Conf.*, pp. 2186–2191, 2011.
- [66] A. Pereira, L. Hsu, and R. Ortega, “Globally stable adaptive formation control of euler-lagrange agents via potential functions,” *Amer. Contr. Conf.*, pp. 2606–2611, 2009.
- [67] Y. Miyasato, “Adaptive h_∞ formation control for euler-lagrange systems,” *IEEE Conf. Deci. Contr.*, pp. 2614–2619, 2010.
- [68] H. Yu and P. Antsaklis, “Passivity-based output synchronization of networked euler-lagrange systems subject to nonholonomic constraints,” *Amer. Contr. Conf.*, pp. 208–213, 2010.
- [69] A. R. Angeles, *Synchronization of Mechanical Systems*. Technical University of Eindhoven, Netherlands: Ph.D. dissertation, 2002.
- [70] A. Pereira and L. Hsu, “Adaptive formation control using artificial potentials for euler-lagrange agents,” *IFAC World Congress*, pp. 10 788–10 793, 2008.
- [71] E. Nuno, R. Ortega, L. Basanez, and D. Hill, “Synchronization of networks of nonidentical euler-lagrange systems with uncertain parameters and communication delays,” *IEEE Trans. on Auto. Contr.*, vol. 56, no. 4, pp. 935–941, 2011.
- [72] H. Min, F. Sun, S. Wang, and H. Li, “Distributed adaptive consensus algorithm for networked euler-lagrange systems,” *IET Contr. Theory & Appl.*, vol. 5, no. 1, pp. 145–154, 2011.

- [73] Y.-C. Liu and N. Chopra, "Synchronization of networked robotic systems on strongly connected graphs," *IEEE Conf. Deci. Contr.*, pp. 3194–3199, 2010.
- [74] I. Chang, S.-J. Chung, and L. Blackmore, "Cooperative control with adaptive graph laplacians for spacecraft formation flying," *IEEE Conf. Deci. Contr.*, pp. 4926–4933, 2010.
- [75] J.-J. S. C.-C. Cheah, S. Hou, "Region-based shape control for a swarm of robots," *Automatica*, vol. 45, no. 10, pp. 2406–2411, 2009.
- [76] S. Unwin and C. Beichman, "Terrestrial planet finder: science and technology overview," *SPIE Astronomical Telescopes and Instrumentation*, 2004.
- [77] B. Mennesson, "Expected science capabilities of the tpf interferometer," *SPIE Astronomical Telescopes and Instrumentation*, 2004.
- [78] L. Kaltenegger, *Search for Extra-Terrestrial planets: The DARWIN mission - Target Stars and Array Architectures*. Karl Franzens University, Graz, Austria: Ph.D. dissertation, 2004.
- [79] P. Wang and F. Hadaegh, "Coordination and control of multiple microspacecraft moving in formation," *J. Astro. Sci.*, vol. 44, no. 3, pp. 315–355, 1996.
- [80] P. Wang, F. Hadaegh, and K. Lau, "Synchronized formation rotation and attitude control of multiple free-flying spacecraft," *J. Guid., Contr., and Dynamics*, vol. 22, no. 1, pp. 28–35, 1999.
- [81] V. Kapilal, A. G. Sparks, J. M. Buffington, and D. P. Q. Yan, "Spacecraft formation flying: Dynamics and control," *Amer. Contr. Conf.*, vol. 6, pp. 4137–4141, 1999.

- [82] H.-H. Y. W. Kang and A. Sparks, "Coordinated control of relative attitude for satellite formation," *AIAA Guid., Nav., and Cont. Conf.*, 2001.
- [83] W. Ren and R. Beard, "Decentralized scheme for spacecraft formation flying via the virtual structure approach," *AIAA J. Guid., Contr., and Dyn.*, vol. 27, no. 1, pp. 73–82, 2004.
- [84] R. B. J. Lawton and F. Hadaegh, "Elementary attitude formation maneuvers via leader-following and behavior-based control," *AIAA Guid., Nav., and Cont. Conf.*, 2000.
- [85] M. VanDyke and C. D. Hall, "Decentralized coordinated attitude control within a formation of spacecraft," *J. Guid., Contr., and Dyn.*, vol. 29, no. 5, pp. 1101–1109, 2006.
- [86] R. B. J.R. Lawton, "Synchronized multiple spacecraft rotations," *Automatica*, vol. 38, no. 8, pp. 1359–1364, 2002.
- [87] A. Abdessameud and A. Tayebi, "Attitude synchronization of a group of spacecraft without velocity measurements," *IEEE Trans. on Auto. Contr.*, vol. 54, no. 11, pp. 2642–2648, 2009.
- [88] W. Ren, "Distributed cooperative attitude synchronization and tracking for multiple rigid bodies," *IEEE Trans. on Contr. Syst. Techno.*, vol. 18, no. 2, pp. 383–392, 2010.
- [89] R. Kristiansena, A. Loria, A. Chailletc, and P.-J. Nicklasson, "Spacecraft relative rotation tracking without angular velocity measurements," *Automatica*, vol. 45, no. 3, pp. 750–756, 2009.

- [90] W. Kang and H.-H. Yeh, “Co-ordinated attitude control of multi-satellite systems,” *Int. J. Robu. & Nonlinear Contr.*, vol. 12, no. 2–3, pp. 185–205, 2002.
- [91] W. Kang and A. Sparks, “Coordinated attitude and formation control of multisatellite systems,” *AIAA Guid., Nav., and Cont. Conf.*, 2002.
- [92] F. Lizarralde and J. Wen, “Attitude control without angular velocity measurements: A passivity approach,” *IEEE Trans. Auto. Contr.*, vol. 41, no. 3, pp. 468–472, 1996.
- [93] M. R. Akella, “Rigid body attitude tracking without velocity feedback,” *Syst. and Contr. Lett.*, vol. 42, pp. 321–326, 2001.
- [94] A. Tayebi, “Unit quaternion-based output feedback for the attitude tracking problem,” *IEEE Trans. Auto. Contr.*, vol. 53, no. 6, pp. 1516–1520, 2008.
- [95] Q. H. Bing Xiao and Y. Zhang, “Fault-tolerant attitude control for flexible spacecraft without angular velocity magnitude measurement,” *AIAA J. Guid., Contr., and Dyn.*, vol. 34, no. 5, pp. 1556–1561, 2011.
- [96] ———, “Fault-tolerant attitude control for spacecraft under loss of actuator effectiveness,” *AIAA J. Guid., Contr., and Dyn.*, vol. 34, no. 3, pp. 927–932, 2011.
- [97] W. Ren and R. Beard, “Virtual structure based spacecraft formation control with formation feedback,” *AIAA Guid., Nav., and Cont. Conf.*, 2002.
- [98] M. VanDyke and C. Hall, “Decentralized coordinated attitude control within a formation of spacecraft,” *AIAA J. Guid., Contr., and Dyn.*, vol. 29, no. 5, pp. 1101–1109, 2006.

- [99] J. Erdonga, J. Xiaoleib, and S. Zhaoweia, “Robust decentralized attitude coordination control of spacecraft formation,” *Syst. & Contr. Lett.*, vol. 57, no. 7, pp. 567–577, 2008.
- [100] D. V. Dimarogonas, P. Tsiotras, and K. J. Kyriakopoulos, “Leaderfollower cooperative attitude control of multiple rigid bodies,” *Syst. & Contr. Lett.*, vol. 58, no. 6, pp. 429–435, 2009.
- [101] Z. Meng, W. Ren, and Z. You, “Decentralized cooperative attitude tracking using modified rodriguez parameters,” *IEEE Conf. Deci. Contr.*, pp. 853–858, 2009.
- [102] B. Halder and N. Sarkar, “Robust fault detection of a robotic manipulator,” *Int. J. of Robotics Research*, vol. 26, no. 3, pp. 273–285, 2007.
- [103] E. Y. Chow and A. S. Willsky, “Analytical redundancy and the design of robust failure detection systems,” *IEEE Trans. on Auto. Contr.*, vol. AC-29, no. 27, pp. 603–614, 1984.
- [104] E. C. Wu, J. C. Hwang, and J. T. Chladek, “Fault-tolerant joint development for the space shuttle remote manipulator system: Analysis and experiment,” *IEEE Trans. on Robot. Auto.*, vol. 9, no. 5, pp. 675–684, 1993.
- [105] A. D. Luca and R. Mattone, “Actuator failure detection isolation using generalized momenta,” *IEEE Int. Conf. on Robotics and Automation*, 2003.
- [106] ———, “An adapt-and-detect actuator fdi scheme for robot manipulators,” *IEEE Int. Conf. on Robotics and Automation*, 2004.

- [107] W. E. Dixon, I. D. Walker, D. M. Dawson, and J. P. Hartranft, "Fault detection for robot manipulators with parametric uncertainty: A prediction-error-based approach," *IEEE Trans. on Robot. Auto.*, vol. 16, no. 6, pp. 689–699, 2000.
- [108] M. L. McIntyre, W. E. Dixon, D. M. Dawson, and I. D. Walker, "Fault identification for robot manipulators," *IEEE Trans. on Robot. Auto.*, vol. 21, no. 5, pp. 1028–1034, 2005.
- [109] A. D. Luca and R. Mattone, "An identification scheme for robot actuator faults," *IEEE/RSJ Int. Conf. Intell. Robots Syst.*, 2005.
- [110] D. Brambilla, L. M. Capisani, A. Ferrara, and P. Pisu, "Fault detection for robot manipulators via second-order sliding modes," *IEEE Trans. on Indust. Elec.*, vol. 55, no. 11, pp. 3954–3963, 2008.
- [111] B. Freyermuth, "An approach to model based fault diagnosis of industrial robots," *IEEE Int. Conf. on Robotics and Automation*, 1991.
- [112] A. Pouliezios, S. Tzafestas, and G. Stavrakakis, "Fault detection and location in mrac robotic systems," in *System Fault Diagnostics, Reliability and Related Knowledge-Based Approaches*, M. S. S. Tzafestas and G. Schmidt, Eds. Dordrecht, The Netherlands, 1986, pp. 203–217.
- [113] M. L. Visinsky, I. D. Walker, and J. R. Cavallaro, "A dynamic fault tolerance framework for remote robots," *IEEE Trans. Robot. Autom.*, vol. 11, no. 4, pp. 477–490, 1995.
- [114] J. J. Gertler, *Fault Detection and Diagnosis in Engineering Systems*. Marcel Dekker, 1998.

- [115] H. Schneider and P. M. Frank, "Observer-based supervision and fault detection in robots using nonlinear and fuzzy logic residual evaluation," *IEEE Trans. Contr. Syst. Technol.*, vol. 4, no. 3, pp. 274–282, 1996.
- [116] C. Chan, K. Cheung, Y. Wang, and W. Chan, "On-line fault detection and isolation of nonlinear systems," *American Control Conf.*, pp. 3980–3984, 1999.
- [117] A. T. Vemuri and M. M. Polycarpou, "Neural-network-based robust fault diagnosis in robotic systems," *IEEE Trans. Neural Networks*, vol. 8, no. 6, pp. 1410–1419, 1997.
- [118] M. Terra and R. Tinos, "Fault detection and isolation in robotic manipulators via neural networks: a comparison among three architectures for residual analysis," *J. Rob. Syst.*, vol. 18, no. 7, pp. 357–374, 2001.
- [119] T. Yuksel and A. Sezgin, "Two fault detection and isolation schemes for robot manipulators using soft computing techniques," *Applied Soft Computing*, vol. 10, no. 1, pp. 125–134, 2010.
- [120] G. Paviglianiti, F. Pierri, F. Caccavale, and M. Mattei, "Robust fault detection and isolation for proprioceptive sensors of robot manipulators," *Mechatronics*, vol. 20, no. 1, pp. 162–170, 2010.
- [121] R. A. Carrasco, F. Nunez, and A. Cipriano, "Fault detection and isolation in cooperative mobile robots using multilayer architecture and dynamic observers," *Robotica*, 2010.

- [122] S. I. Roumeliotis, G. S. Sukhatme, and G. A. Bekey, "Fault detection and identification in a mobile robot using multiple-model estimation," *Int. Conf. on Robotics and Auto.*, pp. 2223–2228, 1998.
- [123] ———, "Sensor fault detection and identification in a mobile robot," *IEEE/RSJ Int. Conf. Intelligent Robots and Syst.*, pp. 1383–1386, 1998.
- [124] P. Goel, G. Dedeoglu, S. I. Roumeliotis, and G. S. Sukhatme, "Fault detection and identification in a mobile robot using multiple model estimation and neural network," *Int. Conf. on Robotics and Auto.*, pp. 2302–2309, 2000.
- [125] H. K. Nikkhoo, *Fault detection in trajectory tracking of wheeled mobile robots*. Concordia University: M.A.Sc. dissertation, 2008.
- [126] R. Washington, "On-board real-time state and fault identification for rovers," *Int. Conf. on Robotics and Auto.*, pp. 1175–1181, 2000.
- [127] E. N. Skoundrianos and S. G. Tzafestas, "Finding fault - fault diagnosis on the wheels of a mobile robot using local model neural networks," *IEEE Robotics & Automation Magazine*, vol. 11, no. 3, pp. 83–90, 2004.
- [128] Y. Lu, E. G. Collins, and M. F. Selekwa, "Parity relation based fault detection, isolation and reconfiguration for autonomous ground vehicle localization sensors," *Proceedings for the Army Science Conference (24th)*, 2004.
- [129] W. E. Dixon, I. D. Walker, and D. Dawson, "Fault detection for wheeled mobile robots with parametric uncertainty," *IEEE/ASME Int. Conf. Adv. Intelligent Mechatro.*, pp. 1245–1250, 2001.

- [130] P. Sundvall and P. Jensfelt, "Fault detection for mobile robots using redundant positioning systems," *Int. Conf. on Robotics and Auto.*, pp. 3781–3786, 2006.
- [131] J. Lin and J. Jiang, "Fault detection and analysis of control software for a mobile robot," *Int. Conf. on Intelligent Syst. Design and Apps.*, 2006.
- [132] O. Pettersson, L. Karlsson, and A. Saffiotti, "Model-free execution monitoring in behavior-based robotics," *IEEE Trans. on Syst., Man, and Cyber.–part B: Cyber.*, vol. 37, no. 4, pp. 890–901, 2007.
- [133] M. A. K. Jaradat and R. Langari, "A hybrid intelligent system for fault detection and sensor fusion," *Applied Soft Computing*, vol. 9, no. 1, pp. 415–422, 2009.
- [134] D. G. Michaelson and J. Jiang, "Modeling of redundancy in multiple mobile robots," *American Control Conf.*, pp. 28–30, 2000.
- [135] L. Parker, "Alliance: An architecture for fault tolerant multirobot cooperation," *IEEE Trans. Robot. Autom.*, vol. 14, no. 2, pp. 220–240, 1998.
- [136] R. Tinos, L. E. Navarro-Serment, and C. J. J. Paredis, "Fault tolerant localization for teams of distributed robots," *IEEE/RSJ Int. Conf. Intelligent Robots and Syst.*, pp. 1061–1066, 2001.
- [137] G. Heredia, F. Caballero, I. Maza, L. Merino, A. Viguria, and A. Ollero, "Multi-uav cooperative fault detection employing vision based relative position estimation," *17th IFAC World Congress*, pp. 12 093–12 098, 2008.

- [138] ———, “Multi-unmanned aerial vehicle (uav) cooperative fault detection employing differential global positioning (dgps), inertial and vision sensors,” *Sensors*, vol. 9, 2009.
- [139] M. L. Visinsky, I. D. Walker, and J. R. Cavallaro, “Layered dynamic fault detection and tolerance for robots,” *Int. Conf. on Robotics and Auto.*, pp. 180–187, 1993.
- [140] X. Li and L. E. Parker, “Distributed sensor analysis for fault detection in tightly-coupled multi-robot team tasks,” *Int. Conf. on Robotics and Auto.*, pp. 3103–3110, 2009.
- [141] M. J. Daigle, M. Xenofon D. Koutsoukos, and G. Biswas, “Distributed diagnosis in formations of mobile robots,” *IEEE Trans. on Robot.*, vol. 23, no. 2, pp. 353–369, 2007.
- [142] V. Verma and R. Simmons, “Scalable robot fault detection and identification,” *Robotics and Autonomous Systems*, vol. 54, no. 2, pp. 184–191, 2006.
- [143] D. Zhuo-hua, F. Ming, C. Zi-xing, and Y. Jin-xia, “An adaptive particle filter for mobile robot fault diagnosis,” *J. Cent. South Univ. Technol.*, vol. 13, no. 6, pp. 689–693, 2006.
- [144] D. Zhuohua, C. Zixing, and Y. Jinxia, “Fuzzy adaptive particle filter algorithm for mobile robot fault diagnosis,” *Neural Inf. Proc., Lecture Notes in Computer Science*, vol. 4234/2006, 2006.
- [145] C. Plagemann, D. Fox, and W. Burgard, “Efficient failure detection on mobile robots using particle filters with gaussian process proposals,” *20th Int. Conf. on Artificial intelligence*, pp. 28–30, 2007.

- [146] V. Verma, G. Gordon, and R. Simmons, "Efficient monitoring for planetary rovers," *Int. Symp. on Artificial Intelligence and Robotics in Space (iSAIRAS)*, 2003.
- [147] V. Verma and G. Gordon, "Bayesian methods for identifying faults on robots for planetary exploration," *Int. Society for Bayesian Analysis*, 2004.
- [148] R. Dearden and D. Clancy, "Particle filters for real-time fault detection in planetary rovers," *Proceedings of DX*, 2002.
- [149] S. Tafazoli and X. Sun, "Hybrid system state tracking and fault detection using particle filters," *IEEE Trans. Contr. Syst. Tech.*, vol. 14, no. 6, pp. 1078–1087, 2006.
- [150] N. de Freitas, R. Dearden, F. Hutter, R. Morales-Menendez, J. Mutch, and D. Poole, "Diagnosis by a waiter and a mars explorer," *Proceedings of the IEEE*, 2004.
- [151] M. Namvar and F. Aghili, "Failure detection and isolation in robotic manipulators using joint torque sensors," *Robotica*, vol. 28, no. 4, pp. 549–561, 2010.
- [152] X. Li and L. E. Parker, "Fault-tolerant and high reliability space robot design and research," *IEEE World Congress on Computational Intelligence*, pp. 2413–2417, 2008.
- [153] L. Portinale and P. Torasso, "Diagnosis as a variable assignment problem: A case study in space robot fault diagnosis," *Int. Conference on Artificial Intelligence*, pp. 1087–1093, 1999.

- [154] L. Portinale, P. Torasso, and G. Correndo, “Knowledge representation and reasoning for fault identification in a space robot arm,” *5th Int. Sympo. on AI, Robotics and Autonomy in Space*, pp. 539–546, 1999.
- [155] D. Tesar, J. Chladek, R. Hooper, D. Sreevijayan, C. Kapoor, J. Geisinger, M. Meaney, G. Browning, and K. Rackers, “Advanced development for space robotics with emphasis on fault tolerance,” *29th Aerospace Mechanisms Symposium*, pp. 30–44, 1995.
- [156] S.-J. Chung, *Nonlinear Control and Synchronization of Multiple Lagrangian Systems with Application to Tethered Formation Flight Spacecraft*. MIT, USA: Ph.D. dissertation, 2007.
- [157] M. Huang, P. Caines, and R. Malhame, “Large-population costcoupled lqg problems with nonuniform agents: Individual-mass behavior and decentralized ϵ -nash equilibria,” *IEEE Trans. on Auto. Contr.*, vol. 52, no. 9, pp. 1560–1571, 2007.
- [158] R. Ortega, P. J. Nicklasson, and H. Sira-Ramirez, *Passivity-Based Control of Euler-Lagrange Systems: Mechanical, Electrical, and Electromechanical Applications*. New York, NY: Springer-Verlag, 1998.
- [159] C. Lanczos, *The Variational Principles of Mechanics*. Mineola, NY: Courier Dover Publications, 1986.
- [160] M. Spong and M. Vidyasagar, *Robot Dynamics and Control*. New York, NY: John Wiley and Sons, 1989.

- [161] S. A. A. Moosavian and E. Papadopoulos, "Explicit dynamics of space free-flyers with multiple manipulators via spacemaple," *J. of Adv. Robot.*, vol. 18, no. 2, pp. 223–244, 2004.
- [162] M. W. Spong, "On the robust control of robot manipulators," *IEEE Trans. on Auto. Contr.*, vol. 37, no. 11, pp. 1782–1786, 1992.
- [163] H. Schaub and J. L. Junkins, *Analytical mechanics of aerospace systems*. AIAA, 2002.
- [164] B. Wie, *Space Vehicle Dynamics and Control*. Reston, VA: AIAA Education Series, 1998.
- [165] J. Ahmed, V. T. Coppola, and D. Bernstein, "Adaptive asymptotic tracking of spacecraft attitude motion with inertia matrix identification," *AIAA J. Guid. Navig. and Contr.*, vol. 21, no. 5, pp. 684–691, 1998.
- [166] T. Krogstad and J. Gravdahl, "6-dof mutual synchronization of formation flying spacecraft," *IEEE Conf. Deci. Contr.*, pp. 5706–5711, 2006.
- [167] S.-J. Chung, U. Ahsun, and J.-J. Slotine, "Application of synchronization to formation flying spacecraft: Lagrangian approach," *AIAA J. of Guid., Contr. and Dyn.*, vol. 32, no. 2, pp. 512–526, 2009.
- [168] R. Horn and C. Johnson, *Topics in Matrix Analysis*. Cambridge University Press, 1991.
- [169] W. Rudin, *The Principles of Mathematical Analysis*. McGraw-Hill, 1976.
- [170] C. Godsil and G. Royle, *Algebraic Graph Theory*. New York, NY: Springer-Verlag, 2001.

- [171] C. Wu, “Agreement and consensus problems in groups of autonomous agents with linear dynamics,” *IEEE Int. Symp. Circui. and Syst.*, pp. 292–295, 2005.
- [172] T. Basar and G. Olsder, *Dynamic Noncooperative Game Theory*. New York, NY: Academic Press Inc., 1982.
- [173] J. C. Engwerda, *LQ Dynamic Optimization and Differential Games*. New York, NY: John Wiley & Sons, 2005.
- [174] H. K. Khalil, *Nonlinear Systems*. Upper Saddle River, NJ: Prentice Hall, 2002.
- [175] D. Liberzon, *Switching in Systems and Control*. New York, NY: Birkhauser, 2003.
- [176] J. Hespanha, D. Liberzon, D. Angeli, and E. Sontag, “Nonlinear norm-observability notions and stability of switched systems,” *IEEE Trans. on Auto. Contr.*, vol. 50, no. 2, pp. 154–168, 2005.
- [177] Z. Sun and S. S. Ge, *Stability Theory of Switched Dynamical Systems*. London: Springer-Verlag, 2011.
- [178] R. Bartle and D. Sherbert, *Introduction to real analysis*, 2nd ed. New York, NY: John Wiley & Sons, 1992.
- [179] S. S. Ge and Y. J. Cui, “New potential functions for mobile robot path planning,” *IEEE Trans. on Robo. Auto.*, vol. 16, no. 5, pp. 615–620, 2000.
- [180] Y. Choi and W. K. Chung, *PID Trajectory Tracking Control for Mechanical Systems*. New York, NY: Springer, 2004.

- [181] H. Alwi and C. Edwards, "Fault detection and fault-tolerant control of a civil aircraft using a sliding-mode-based scheme," *IEEE Trans. on Contr. Syst. Tech.*, vol. 16, no. 3, pp. 499–510, 2008.
- [182] —, "Fault tolerant control of a civil aircraft using a sliding mode based scheme," *IEEE Conf. on Deci. and Contr., and the Euro. Contr. Conf.*, pp. 1011–1016, 2005.
- [183] N. Meskin, K. Khorasani, and C. A. Rabbath, "A hybrid fault detection and isolation strategy for a network of unmanned vehicles in presence of large environmental disturbances," *IEEE Trans. on Contr. Syst. Tech.*, vol. 18, no. 6, pp. 1422–1429, 2010.
- [184] —, "Hybrid fault detection and isolation strategy for non-linear systems in the presence of large environmental disturbances," *IET Contr. Theory & Appl.*, vol. 4, no. 12, pp. 2879–2895, 2010.
- [185] N. Meskin and K. Khorasani, "Actuator fault detection and isolation for a network of unmanned vehicles," *IEEE Trans. on Auto. Contr.*, vol. 54, no. 4, pp. 835–840, 2009.
- [186] A. Valdes and K. Khorasani, "A pulsed plasma thruster fault detection and isolation strategy for formation flying of satellites," *App. Soft Comput.*, vol. 10, no. 3, pp. 746–758, 2010.
- [187] H. Talebi, K. Khorasani, and S. Tafazoli, "A recurrent neural-network-based sensor and actuator fault detection and isolation for nonlinear systems with application to the satellite's attitude control subsystem," *IEEE Trans. on Neural Networks*, vol. 20, no. 1, pp. 45–60, 2009.

- [188] R. Patton, P. Frank, and R. Clark, *Issues of Fault Diagnosis for Dynamic Systems*. London, UK: Springer-Verlag, 2000.
- [189] S. Simani, C. Fantuzzi, and R. Patton, *Model-based Fault Diagnosis in Dynamic Systems Using Identification Techniques*. New York, NY: Springer-Verlag, 2003.
- [190] A. J. van der Schaft, “L2-gain analysis of nonlinear systems and nonlinear state-feedback h_∞ control,” *IEEE Trans. on Auto. Contr.*, vol. 37, no. 6, pp. 770–784, 1992.
- [191] L. Vu, D. Chatterjee, and D. Liberzon, “Input-to-state stability of switched systems and switching adaptive control,” *Automatica*, vol. 43, no. 4, pp. 639–646, 2007.
- [192] WikipediaUsers. (2013, Feb.) Matlab - wikipedia, the free encyclopedia. [Online]. Available: <http://en.wikipedia.org/wiki/MATLAB>
- [193] ——. (2013, Feb.) Simulink - wikipedia, the free encyclopedia. [Online]. Available: <http://en.wikipedia.org/wiki/Simulink>